Synthesis and Properties of Amino Acid-derived Optically Active π-Conjugated Polymers

Hiromitsu Sogawa

Department of Polymer Chemistry

Graduate School of Engineering

Kyoto University

2013

Contents

General Introduction

Research Background

Amino Acid. α-Amino acids are simple molecules with the structure of $H_2NCHRCOOH$, where R are substituents including alkyl, aryl, amino, carboxy, hydroxy and mercapto groups, which enable them to be transformed into a wide variety of optically active materials. Amino acids are building blocks of polypeptides and proteins, and they are indispensable compounds for living organisms. Polypeptides form higher order structures such as α-helix, β-sheet, and random coil dependent on the constituent amino acids and environment. Proteins store and transport electrons and molecules, transmit information between cells and organs, control the passage of molecules across membranes that compartmentalize cells and organelles, and keep acid-base balance in the body in ranges that allow organisms to stay alive. Amino acids are also regarded as useful resources for organic chemistry because of low cost, high optical purity and reactivity. They find a wide range of applications such as waste oil treatment agents, antioxidant agents, pharmaceutical drugs, cosmetic, food, and surfactants.[1–7]

Polymers containing amino acids in the main or side chains are advantageous in reactivity, biodegradability and biocompatibility in a fashion similar to naturally derived biopolymers.[8–18] Amino acid-derived polymers showing high performance and multifunction have been developed based on the transformation of their higher order structures in response to external stimuli

such as temperature, pH and light. π-Conjugated polymers with regulated higher order structures show useful properties including molecular recognition, chiral catalysis and chemical sensing together with electronic and optical properties. This doctoral thesis concerns amino acid based π-conjugated helical polymers including poly(phenyleneethynylene)s and substituted polyacetylenes.

Helical Polymers. The helix is one of the most common higher-order structures of macromolecules, and is molecularly asymmetric; hence, polymers that take a predominantly one-handed helical structure are optically active. Representative helical structures exist in biomolecules; α-, 3_{10}-, π- and β-helices of proteins, helix of amylose, double helix of DNA, and triple helix of collagen.[19,20] Many sophisticated and intricate functions for the process of living organisms such as *in vivo* exquisite reactions, molecular recognition and replication largely depend on these well-defined helical structures. The study of artificial helical polymers are important not only from the viewpoints of fundamental study but also potential of practical application of these polymers.

The history of artificial helical polymers dates back to the discovery of isotactic polypropylene by Natta in 1955.[21] They found that the polymer formed a helical structure in the crystalline state, though it was unstable in solution due to the lack of the steric repulsion between methyl side groups, and was transformed into random coil structure instantly. Since then, various types of artificial helical polymers have been synthesized, some of which adopt helical

conformations even in solution.[22] There are mainly two types of artificial polymers that are classified by their properties and characters, namely, static and dynamic helical polymers.

Polyisocyanide **1**,[23–28] polychloral **2**[29–35] and poly(triarylmethyl methacrylate)s **3**[36–39] having very bulky substituents are categorized as stable helices. Polyisocyanide **1** is prepared by the polymerization of isocyanides using Ni, Pd–Pt and Rh catalysts, and form a 4/1 helix stabilized by steric repulsion between the side chains. The pendant groups are located at four directions around the 4/1 helical backbone in order to minimize the steric repulsion between the side chains.[28] Polychloral **2** is synthesized by the asymmetric anionic polymerization of trichloroacetaldehyde (chloral) using an optically active lithium alkoxide, and forms a stable 4/1 helical structures. Polychloral **2** is used as a chiral stationary separation phase (CSP) for high performance liquid chromatography (HPLC), and can resolve the racemates of poly(methylbenzyl methacrylate)[41] and various aromatic compounds.[42] As the first example for poly(triarylmethylmethacrylate)s **3**, Okamoto synthesized an optically active poly(triphenylmethyl metharylate) **4** by the helix-sense-selective polymerization of an achiral monomer, triphenylmethyl methacrylate, using chiral anionic initiator. Polymer **4** adopts a completely isotactic helical conformation exhibiting a large optical rotation.[43,44] Polymer **4** recognizes the chirality of a wide variety of racemic compounds, and is also applied to a CSP for HPLC.[45,46] This was a significant breakthrough regarding synthetic helical

polymers for practical use. Perfectly isotactic polymethacrylamide was synthesized by the asymmetric radical polymerization using optically active menthol as a composition of polymerization solvents.[47] Modification of ester linkage to amide one dramatically improved the durability for solvolysis. Helix-helix and/or helix-coil transformations are suppressed in these polymers, because of the rigidity of the main chains and/or steric repulsion between the bulky side chains.

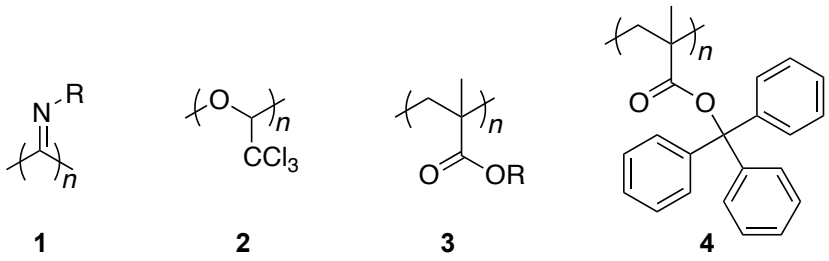

1 **2** **3** **4**

In contrast to static helical polymers, dynamic helical polymers quickly undergo helix-helix interconversion in solution due to the low helix inversion barriers. Polyisocyanates **5**–**7** are composed of an *N*-substituted amide repeating unit and adopt an 8/3 helical conformation rather than a restricted coplanar conformation. Goodman and Chen have discovered helical polyisocyanates carrying chiral pendant groups.[48,49] Green has reported that poly(*n*-hexyl isocyanate) **5** is a mixture of equivalent amounts of right- and left-handed helices that readily move along the polymer backbone.[50] It should be noted that **6**, whose chirality is only based on the difference between H and D in the pendant groups, forms a predominantly one-handed helical structure.[51,52]

Moreover, due to the extremely low helix inversion barrier, an excess one-handedness of helical polyisocyanates can be obtained by *R*-*S* copolymerization of **7** with a small enantiomeric excess (majority rule),[53] and also by chiral-achiral copolymerization with only a small amount of chiral units such as 99% of **5** and 1% of **7** (sergeants-and-soldiers rule).[54] Polysilanes **8**–**10** are also a typical class of dynamic helical polymers, which have Si σ-conjugating main chains, allowing the conformational study by means of photo-physical analysis.[55–62] Fujiki has reported that **9** consists of two diastereomeric helical structures, tight 7/3 helix that has a absorption maximum (λ_{max}) around 320 nm and loose 2/1 helix that has λ_{max} around 370 nm, while **10** consists of a single helix.[56,57] There is a proportional relationship between the viscosity index of Mark-Houwink-Sakurada plot (α) and λ_{max} of the polymer.[58] The rigidity of the polymer backbones depends particulary on the structures of the pendant groups the chain length and position of the branching methyl group at the chiral center. The chiroptical properties of the helical polysilanes also obey the sergeants and soldiers, and the majority rule.[61,62]

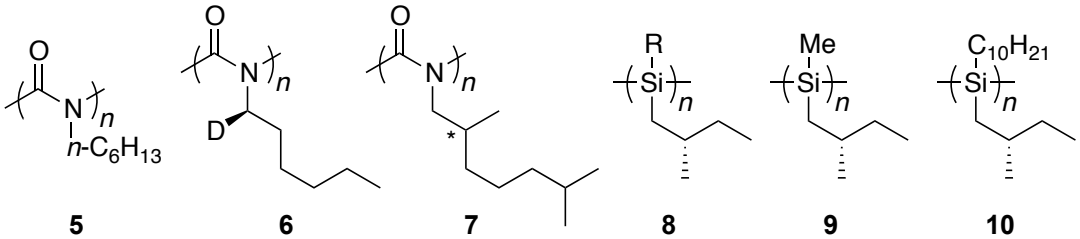

5 **6** **7** **8** **9** **10**

Helical Oligo- and Poly(phenyleneethynylene) Derivatives. Helical oligo(*m*-phenyleneethynylene) **11** is developed by Moore and coworkers in 1997.[63] Oligomer **11** folds into a helical conformation in polar solvents based on the amphiphilicity originating from the hydrophilic side chains and hydrophobic main chains. The *meta*-connectivity of monomer units also plays an important role for the oligomer to fold into a helix. *para*-Linked poly(phenyleneethynylene)s bearing chiral side chains exhibit strong CD signals as a result of aggregation.[64–66] Unlike these cases, **11** shows unimolecular chirality. Oligo(*m*-phenyleneethynylene) **12** containing chiral side groups adopts a predominantly one-handed folded helical conformation.[67–71] Optically active polymers **13**–**15** that possess analogous main chains also adopt a helical conformation with biased screw sense.[72–74] Sanda and coworkers have revealed

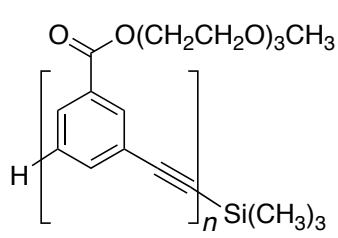

11

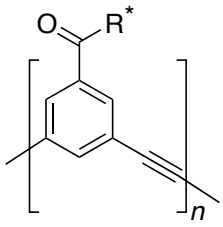

12

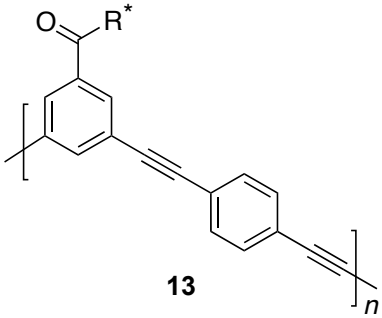

13

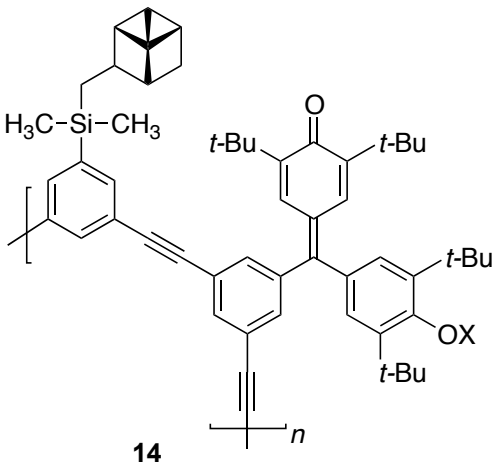

14

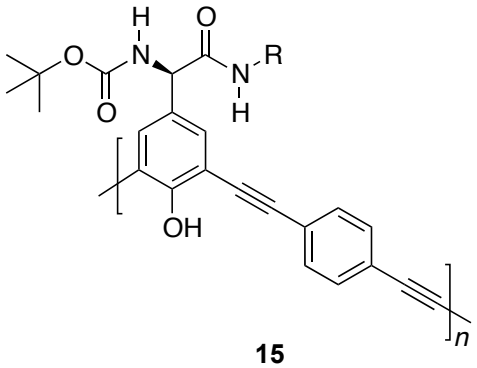

15

that **15** forms folded helical structures with an excess of one-handed screw sense in nonpolar solvents. The helix formation of this polymer is based on the amphiphilic balance opposite from that of previously reported poly(*m*-phenyleneethynylene) derivatives.

Oligo(*m*-phenyleneethynylene)s **16** and **17** containing short amide sequence and azobenzene moieties are also able to form folded helical conformations.[75–77] The introduction of an optically active binaphtol and tartrate moieties into the backbone of oligo(*m*-phenyleneethynylene)s **18** and **19** imparts a bias on the folded helical structure.[78,79] They undergo a solvent-dependent conformational transition from a random coil to a helix. As another approach to induce the twist sense bias, Tew and coworkers have successfully induced chirality in **20** by the addition of chiral mandelic acid.[80] Moore and coworkers have found that various chiral terpenes including (+)-β-pinene induce an excess helicity in achiral **11** by forming a complex preferentially with a right- or left-handed helical structure.[81,82] This phenomenon is regarded as chiral recognition by the helical phenyleneethynylene derivatives. Inouye and coworkers have reported that poly(*m*-ethynylpyridine) **21** adopts a helical conformation by binding various chiral saccharides inside of the cavity via hydrogen bonding both in nonpolar and polar solvents.[83,84] Recently, they have also found that poly(*m*-ethynylpyridine) **22** containing chiral pendant groups also form a predominantly one-handed helical structure, and changes its structure depending on saccharide recognition.[85]

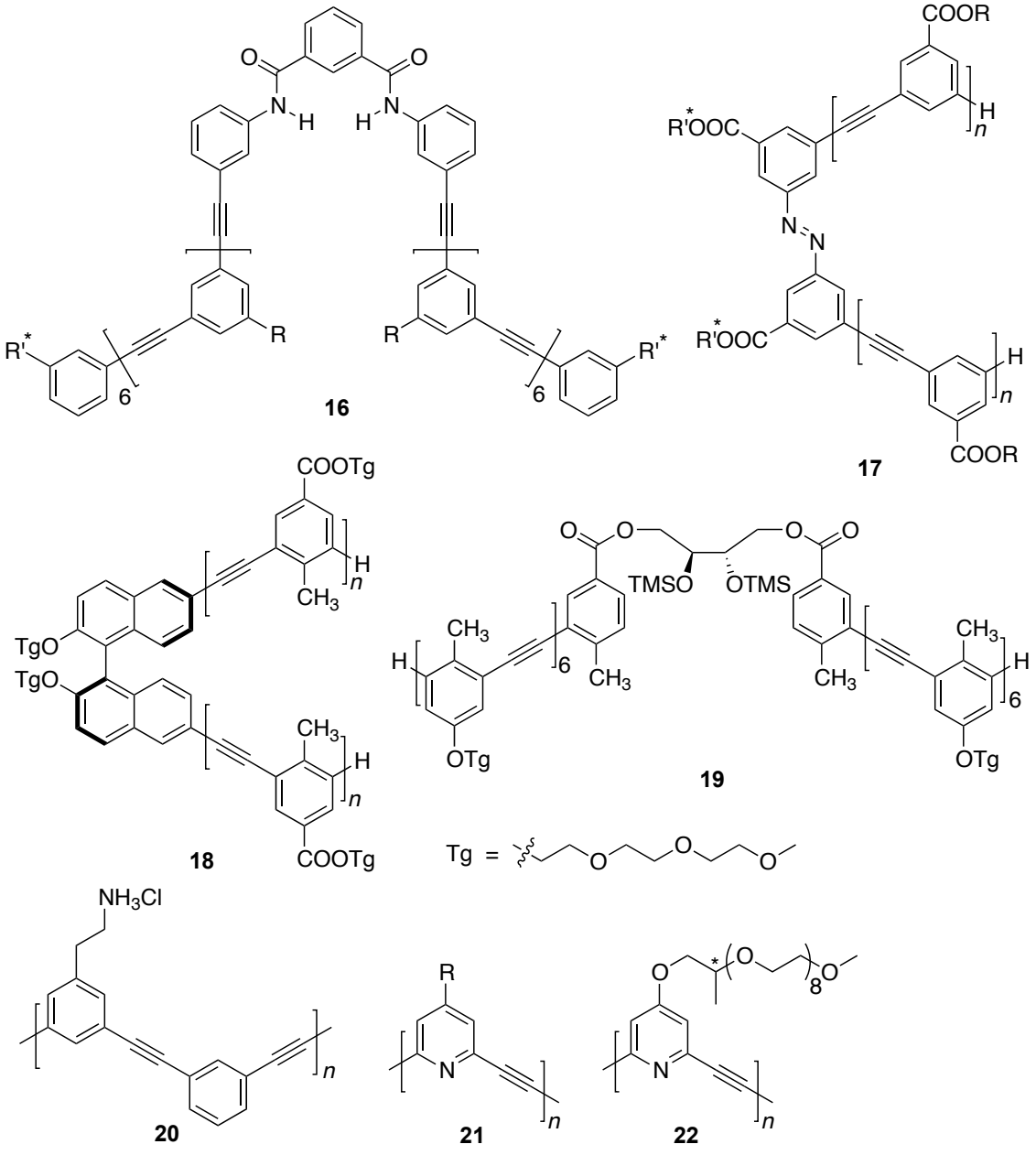

Helical Substituted Polyacetylenes. Helical polyacetylene derivatives **23** bearing chiral side chains have been first reported by Ciardelli.[86] Since this pioneering work, a large number of optically active monosubstituted acetylene polymers have been prepared by the polymerization of chiral monomers. Although some polyacetylenes equipped with chiral appendages are prepared by

ring-opening metathesis polymerization using tungsten[87] and ruthenium catalyst,[88] most chiral polyacetylenes are synthesized by the polymerization using rhodium (Rh) catalysts such as $[Rh(nbd)Cl]_2$ (nbd: 2,5-norbornadiene), due to the high functional group tolerance and *cis*-stereoregularity featured by late transiton metals.[89] Polyphenylacetylene **24** bearing chiral groups is the most widely examined polyacetylene that forms a helical structure. [90–106] The representative examples include **25** synthesized by Aoki in 1993[90] and **26** synthesized by Yashima and Okamoto in 1994 using Rh catalysts.[91,92] These polymers exhibit large optical rotations and intense CD signals at the absorption region of the main chain, indicating that the polymers adopt predominantly one-handed helical conformations. Various helical poly(phenylacetylene) derivatives carrying amino acid moieties have been reported, which show pH-dependent conformational transformation,[93,101] catalytic activity to asymmetric reactions,[98,102,104] anion sensing[99,100] and so on, demonstrating the possibility for practical applications. There are also several achiral polyphenylacetylene derivatives that induce a predominantly one-handed helical conformation by the addition of small molecules such as amines, acids and

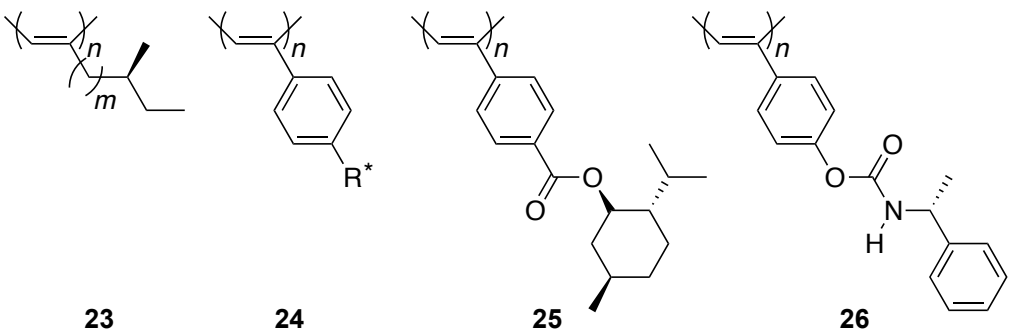

23 **24** **25** **26**

amino acids,[107–111] as well as by the polymerization of corresponding monomers in the presence of a chiral amine.[112–114]

Masuda and coworkers have reported a series of helical polyacetylenes featuring chiral side groups. Optically active poly(propiolic ester)s **27** exhibit large Cotton effects originating from a helical conformation.[115–118] The *cis*-stereoregular poly(*N*-propargylamide)s **28**,[119–123] poly(*N*-propargylcarbamate)s **29**[124,125] and poly(*N*-butynylamide)s **30**[126,127] biomimetically form helices stabilized by intramolecular hydrogen bonding along with steric repulsion between the side chains. The screw sense of a poly(*N*-propargylamide) carrying porphyrin moieties is determined by the exciton chirality method; the porphyrin units in the side chains form right-handed helical strands, while the main chain forms a left-handed one. Poly(1-methylpropargyl alcohol) **31** and poly(1-methylpropargyl ester) **32** also form a stable helical structure due to the steric repulsion between the side groups.[128,129] The copolymers of alanine-based *N*-propargylamides obey the sergeants and soldiers, and majority rule.[123]

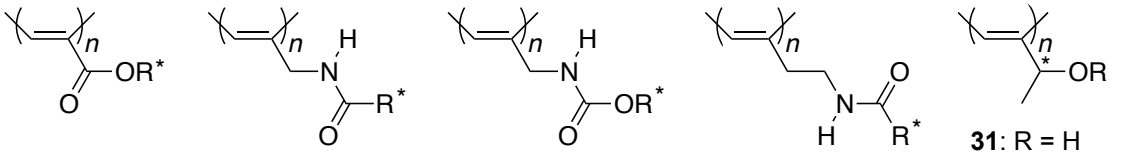

27 **28** **29** **30**

31: R = H
32: R = OCR'

As well as monosubstituted acetylene polymers, disubstituted acetylene polymers carrying bulky chiral pendant groups are also synthesized by the

polymerization using catalysts based on early transition metals such as niobium, tantalum and molybdenum. The polymers form predominantly one-handed helical structures in solution.[130–132]

Azobenzene. Azobenzene is the most widely used photo-responsive molecule

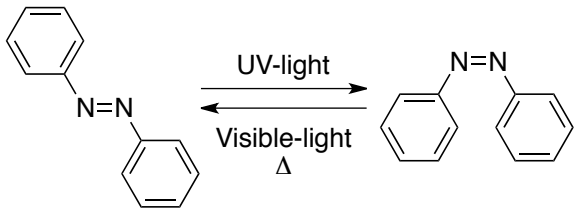

undergoing reversible photo-isomerization between *trans* and *cis* forms upon UV- and visible-light irradiation.[133] *trans*-Azobenzene shows a strong π–π^* transition band around 320 nm and a weak n–π^* band around 440 nm, while *cis*-azobenzene has a stronger n–π^* band also around 440 nm and shorter wavelength bands at 280 nm and 250 nm. *trans*-Azobenzene is near planar and has a dipole moment near zero. In contrast, *cis*-azobenzene adopts a twisted bent conformation and has a dipole moment of 3 Debye. Among the tremendous unique photo-responsive systems, Shinkai and coworkers have synthesized photo-responsive crown ether **33** and its derivatives, and developed them as ion-extraction and transport materials controllable by photo-irradiation.[134,135] Kinbara and Aida have reported light driven chiral molecular scissors **34**, where the open–close motion of the blade parts is interlocked by the handle parts strapped by a photo-isomerizable azobenzene unit, due to the pivotal motion of the connecting ferrocene unit.[136–141] An extension of this molecule might allow the remote control of molecular events in larger

interlocked molecular systems.[142–147] Ikeda and coworkers have demonstrated various photo-mobile polymer films. The liquid-crystalline elastomers films, which are composed of liquid-crystal azobenzene monomer **35** with a diarylate crosslinker **36**, are able to bend and rotate upon UV- and visible-light irradiation as a result of the cooperative movement of the liquid-crystal moieties and polymer segments. A light-driven plastic motor is assembled by the films upon continuous irradiation of UV and visible light. This motor can convert light energy directly into mechanical work without the aid of batteries, electric wires and/or gears.

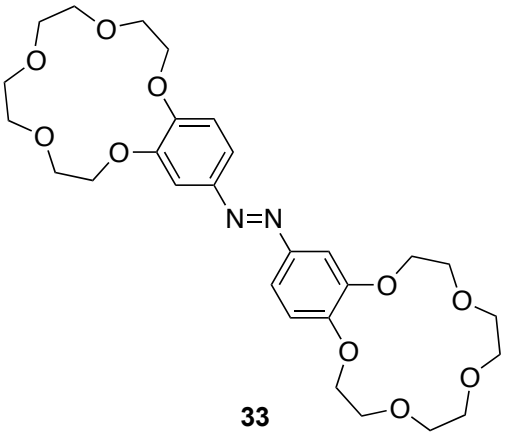

33

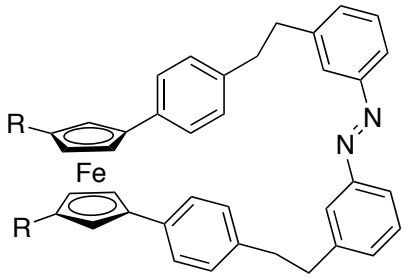

34

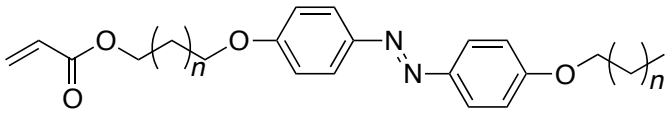

35

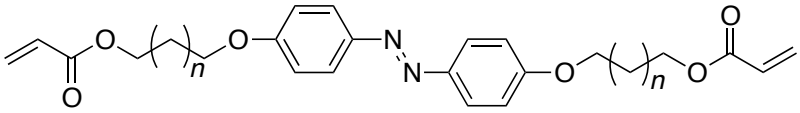

36

Various examples have been reported regarding π-conjugated polymers containing azobenzene units. Optically active poly(*N*-propargylamide) **37**

arranges azobenzene chromophores in a helical geometry with predominantly one-handed screw sense, and exhibits lyotropic liquid crystalline property.[148] The helical arrangement of azobenzene moieties becomes disordered upon photo-isomerization without affecting the helical polyacetylene backbone. This is a rare example for switching of helical orientation of the side chains keeping the helical conformation of the main chain intact.

The chirality of limonenes is successfully transferred to azobenzene-*alt*-fluorene copolymers **38** in the *trans* form, which allows the formation of optically active aggregates.[149] The reversible chiroptical response is achieved upon alternating photo-irradiation. A supramolecular complex is formed from an azobenzene-containing polymer and single-walled carbon nanotubes (SWNTs).[150] The *trans–cis* isomerization of the azobenzene moieties enables the selective dispersal of individual SWNTs in solvents.

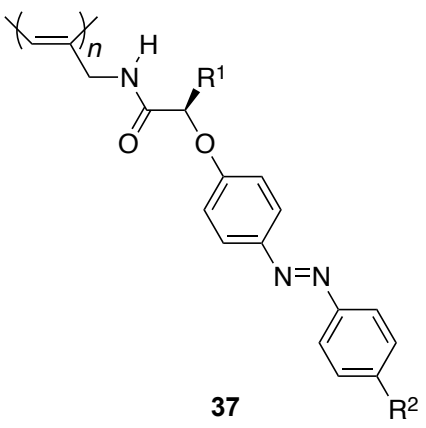

37

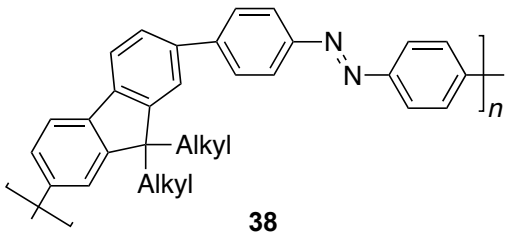

38

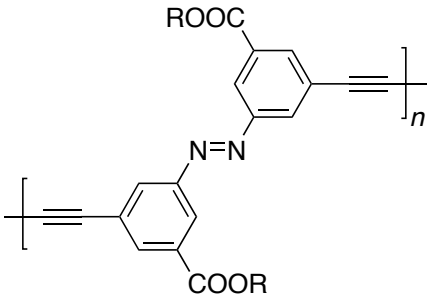

R = –Tg or –$CHCH_3CH_2OTg$

39

Hecht and coworkers have designed a new family of photo-switchable foldamers **39** composed of azobenzene and ethynylene units.[151,152] Polymer **39** is completely folded under the light rapidly and quantitatively, and reversibly unfolded upon UV-light irradiation.

Objectives of This Thesis

As demonstrated above, helical polymers have attracted considerable attention as stimuli-responsive, sensing and chiral recognition materials. Combination of natural amino acids into synthetic polymers is expected to contribute to develop peptide-mimetic functional materials with regulated higher-order structures. It is desirable to control the conformation of the polymers in response to external stimuli such as temperature, polarity of solvents, pH and light for the creation of materials with sophisticated functions.

In this thesis, the author designs and synthesizes novel chiral amino acid containing poly(phenyleneethynylene)s and polyacetylenes, and examines the chiroptical properties, their higher order structures, and responsiveness to external stimuli.

Outline of This Thesis

The present thesis consists of three parts: **Part I** (Chapters 1–3), **Part II** (Chapters 4–5) and **Part III** (Chapter 6).

In **Part I**, the author designs and synthesizes novel amino acid-based

polyphenyleneethynylenes containing hydroxy groups and studies the chiroptical properties based on the helical conformation, together with the effects of conjugation lengths for the formation of the helical structures, and helix stabilization utilizing the metathesis reactions at the polymer side chains.

Chapter 1 demonstrates the synthesis and properties of alanine-derived novel helical polyphenyleneethynylenes possessing various arylene units. CD, UV–vis and fluorescence spectroscopic data reveal that the polymers adopt predominantly one-handed helical conformation stabilized by hydrogen bonding between the amide groups, excepts for the polymers bearing phenylene units substituted with long alkyl chains. The polymers exhibit strong Cotton effects in $CHCl_3$ and THF. The formation of aggregate is confirmed by DLS measurement in THF/H_2O mixture. Molecular mechanics (MM) calculations give information on the helical conformation. Tube-like structures are observed by the AFM measurements of the polymers, presumably originate from perpendicular aggregation of the helical polymers.

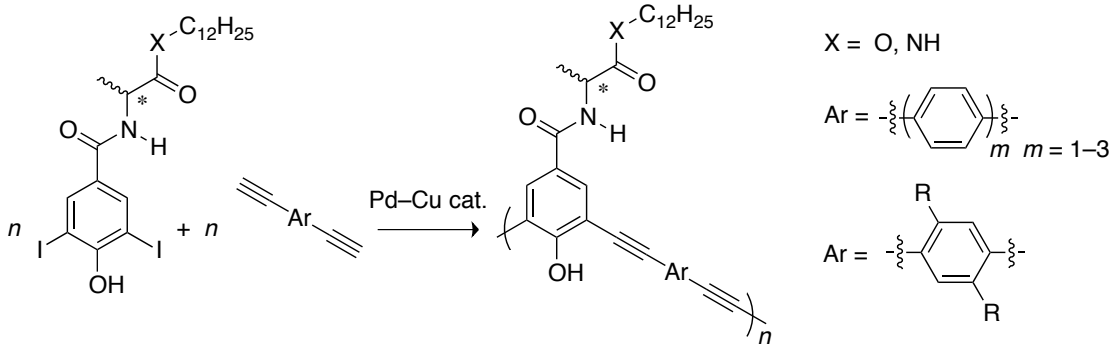

Chapter 2 deals with the synthesis of amino acid-derived polyphenyleneethynylene containing naphthalene and pyrene units. All the polymers exhibit strong Cotton effects in THF at the absorption regions of the main chains. Introduction of naphthalene and pyrene units leads to extension of conjugation of the polymers, which is confirmed by the TD-DFT calculations of the model compounds. The polymers show variously colored fluorescence such as blue, green and yellow.

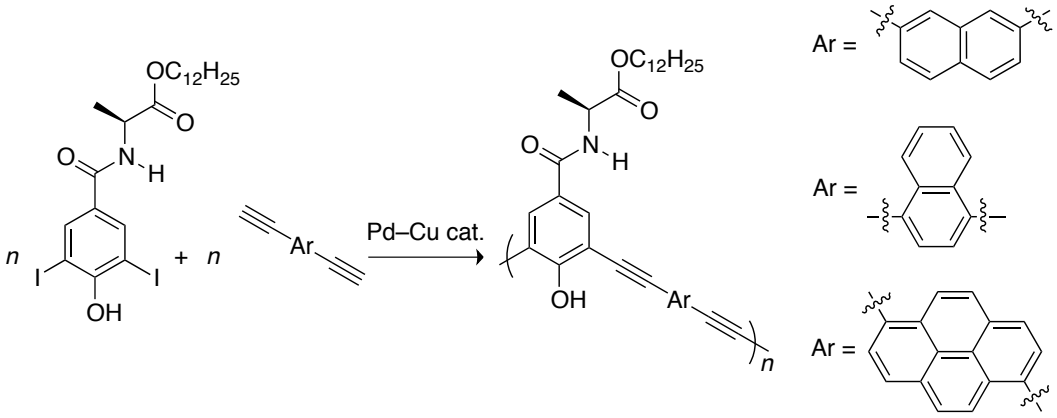

Chapter 3 discusses the synthesis of hydroxyphenylglycine-based polyphenyleneethynylenes containing diene and norbornene moieties at the side chains, and examines intramolecular acyclic diene and ring-opening metathesis reactions at the side chains to stabilize the secondary structures. CD and UV–vis spectroscopic analysis reveals that the polymers keep predominantly one-handed helical structures even in polar solvents such as DMF after the metathesis reactions.

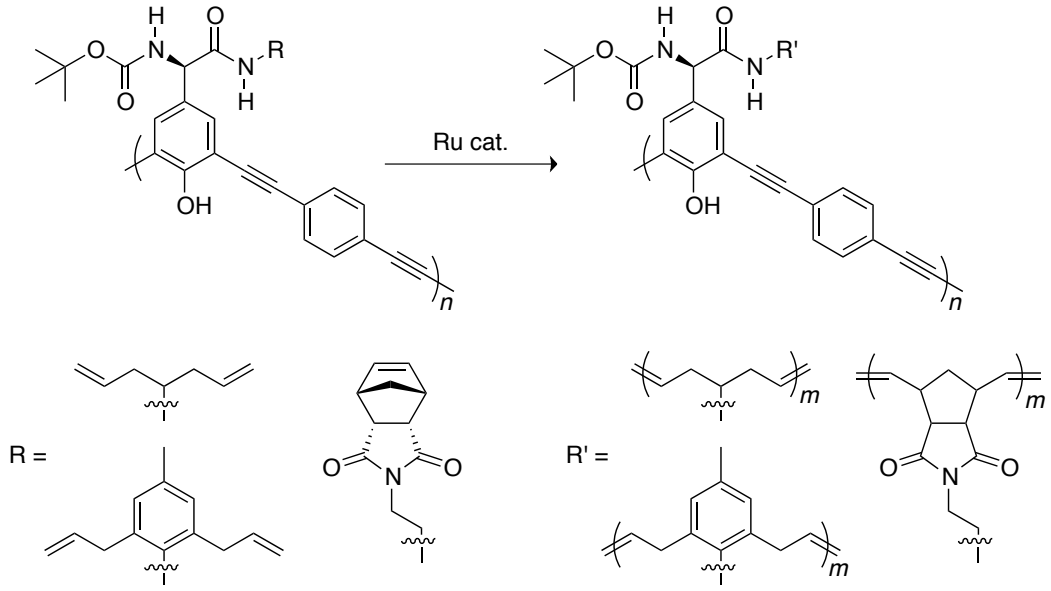

In **Part II**, the author synthesizes hydroxyphenylglycine-based optically active poly(phenyleneethynylene)s containing the azobenzene moieties, and examines the chiroptical properties, together with the photo-responsiveness of the higher order structures.

Chapter 4 describes the synthesis and properties of hydroxyphenylglycine-based optically active poly(phenyleneethynylene)s containing azobenzene moieties at the side chains. The formation of chiral aggregates is determined by CD and UV–vis spectroscopic measurements in CH_2Cl_2, together with filtration experiments and DLS measurements. A slight CD spectral change is observed upon UV-light irradiation, according to photo-isomerization of azobenzene moieties from *trans* to *cis*-form.

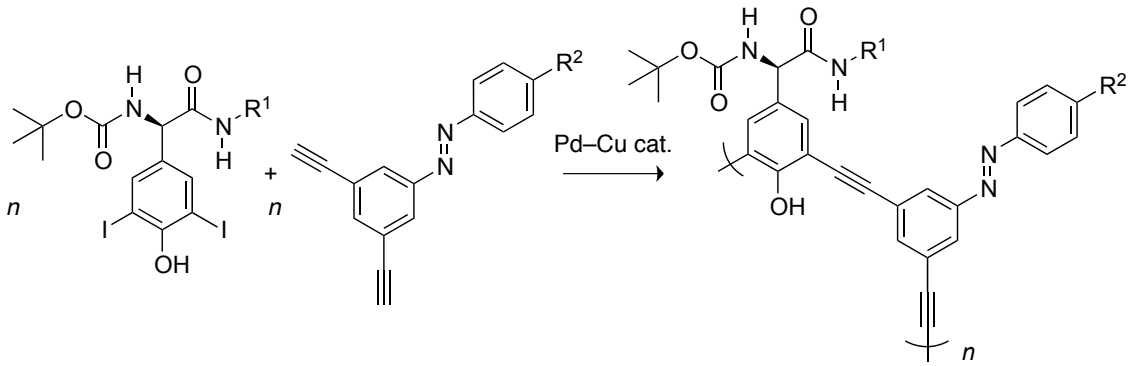

Chapter 5 delineates the synthesis of hydroxyphenylglycine-based poly(phenyleneethynylene)s containing azobenzene moieties at the main chains, examines the secondary structures and photo-responsiveness of the formed polymers, and analyzes the conformation by the DFT method. CD and UV–vis spectroscopic data suggest that both polymers form predominantly one-handed helical structures in nonpolar solvents such as $CHCl_3$. The azobenzene moieties of the *m*-linked polymers are isomerized from *trans* to *cis* by UV-light irradiation, which leads to the collapse of the helical structures. This photo-induced conformational transformation is highly reversible.

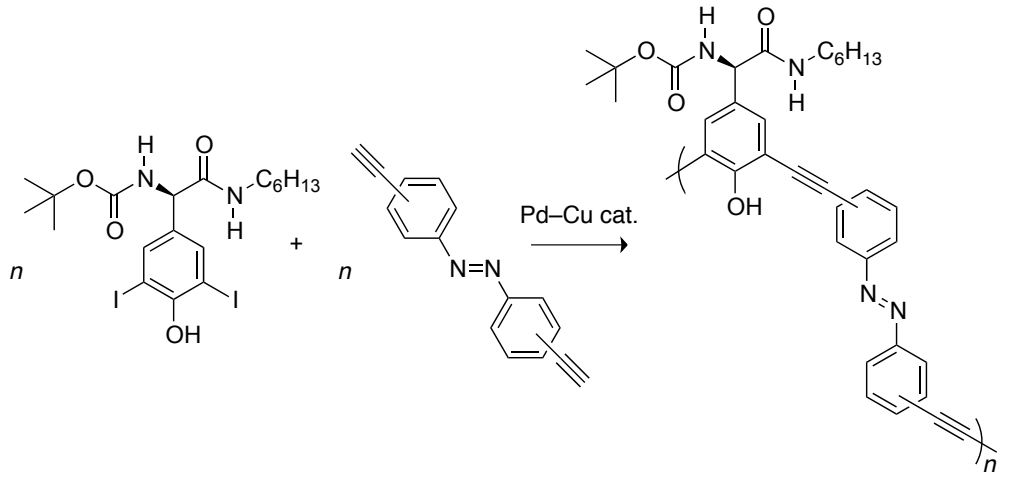

In **Part III**, the author describes the synthesis of α-propargyl amino acid derived polyacetylenes, and examination of the secondary structures, together with the external stimuli-responsiveness.

Chapter 6 deals with the synthesis and polymerization of monosubstituted acetylenes derived from α-propargyl amino acids. The formation of helical structures stabilized hydrogen bonding is confirmed by the CD and UV–vis spectroscopy and solution state IR measurement. The conformation is analyzed by MM calculations. The polymer containing unprotected carboxy groups changes its conformation by the addition of alkali hydroxides and THF. The changes of the solution color are detectable by naked eye.

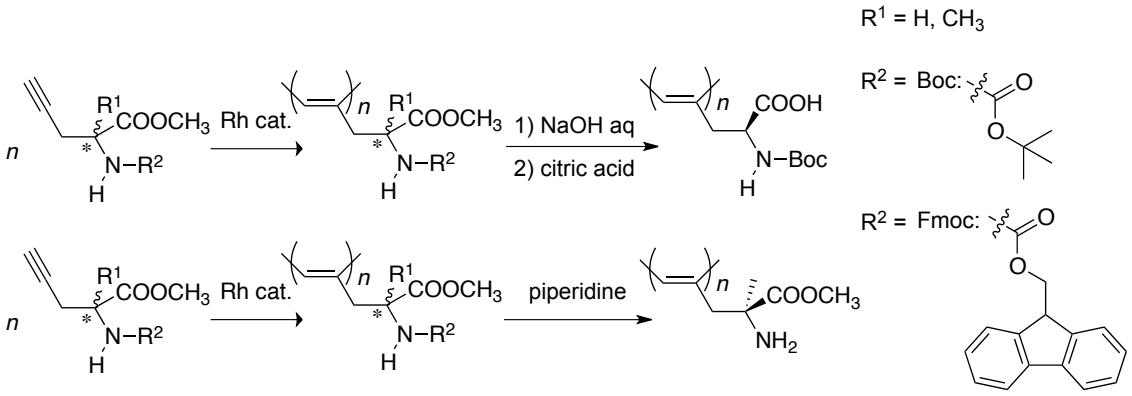

References

(1) Takehara, M. *Cosmet. Toiletries* **1983**, *98*, 51.

(2) Xia, J.; Qian, J.; Nnanna, I. A. *J. Agric. Food Chem.* **1996**, *44*, 975.

(3) Clapés, P.; Infante, M. R. *Biocatal. Biotransform.* **2002**, *20*, 215.

(4) Oldfield, E. *Annu. Rev. Phys. Chem.* **2002**, *53*, 349.

(5) Martínez, V.; Sánchez, L.; Busquets, M. A.; Infante, M. R.; Vinardell, M.

P.; Mitjans, M. *Amino Acids* **2007**, *33*, 459.

(6) Marques, E. F.; Brito, R. O.; Silva, S. G.; Rodríguez-Borges, J. E.; Vale, M. L. d.; Gomes, P.; Araújo, M. J.; Söderman, O. *Langmuir* **2008**, *24*, 11009.

(7) Trabocchi, A.; Scarpi, D.; Guarna, A. *Amino Acids* **2008**, *34*, 1.

(8) Mepherson, D. T.; Morrow, C.; Minehan, D. S.; Wu, J.; Hunter, E.; Urry, D. W. *Biotechnol. Prog.* **1992**, *8*, 347.

(9) Krejchi, M. T.; Atkins, E. D. T.; Waddon, A. J.; Fournier, M. J.; Mason, T. L.; Tirrell, D. A. *Science* **1994**, *265*, 1427.

(10) Prince, J. T.; McGrath, K. P.; Digirolamo, C. M.; Kaplan, D. L. *Biochemistry* **1995**, *34*, 10879.

(11) Petka, W. A.; Harden, J. L.; Negrath, K. P.; Wirtz, D.; Tirrell, D. A. *Science* **1998**, *281*, 389.

(12) Sanda, F.; Endo, T. *Macromol. Chem. Phys.* **1999**, *200*, 2651.

(13) Panitch, A.; Yamaoka, T.; Fournier, M. J.; Mason, T. L.; Tirrell, D. A. *Macromolecules* **1999**, *32*, 1701.

(14) Chilkoti, A.; Dreher, M. R.; Meyer, D. E. *Adv. Drug Delivery Rev.* **2002**, *54*, 1093.

(15) Beter, H.; Setton, L. A.; Meyer, D. E.; Chilkoti, A. *Biomacromolecules* **2002**, *3*, 910.

(16) Heilshorn, S. C.; Dizio, K. A.; Tirrell, D. A. *Macromolecules* **2003**, *36*, 1553.

(17) Schlaad, H.; Antonietti, M. *Eur. Phys. J. E.* **2003**, *10*, 17. (k) Katsarava, R. *Macromol, Symp.* **2003**, *199*, 419.

(18) Löwik, D. W. P. N.; van Hest, J. C. M. *Chem. Soc. Rev.* **2004**, *33*, 234.

(19) Branden, C.; Tooze, J. *Introduction to Protein Structure, 2nd ed.*; Garland Publishing: New York, 1999.

(20) Voet, D.; Voet, J. G.; Prett, C. W. *Fundamentals of Biochemistry*; Wiley: New York, 1999.

(21) Natta, G.; Pino, P.; Corradini, P.; Danusso, F.; Mantitca, E.; Nazzanti, G.; Moraglio, G. *J. Am. Chem. Soc.* **1955**, *77*, 1708.

(22) For a review, see: (a) Wuff, G. *Angew. Chem. Int. Ed.* **1989**, *28*, 21. (b) Okamoto, Y.; Nakano, T. *Chem. Rev.* **1994**, *94*, 349. (c) Choi, S.-K.; Gal,

Y.-S.; Jin, S.-H.; Kim, H. K. *Chem. Rev.* **2000**, *100*, 1645–1681. (d) Nagai, K.; Masuda, T.; Nakagawa, T.; Freeman, B. D.; Pinnau, I. *Prog. Polym. Sci.* **2001**, *26*, 721. (e) Nakano, T.; Okamoto, Y. *Chem. Rev.* **2001**, *101*, 4013. (f) Aoki, T.; Kaneko, T.; Teraguchi, M. *Polymer* **2006**, *47*, 4867. (g) Masuda, T. *J. Polym. Sci., Part A: Polym. Chem.* **2007**, *45*, 165. (h) Yashima, E.; Maeda, K.; Iida, H.; Furusho, Y.; Nagai, K. *Chem. Rev.* **2009**, *109*, 6102. (i) Akagi, K. *Chem. Rev.* **2009**, *109*, 5354. (j) Liu, J.; Lam, J. W. Y.; Tang, B. Z. *Chem. Rev.* **2009**, *109*, 5799. (k) Shiotsuki, M.; Sanda, F.; Masuda, T. *Polym. Chem.* **2011**, *2*, 1044.

(23) Millich, F.; Baker, G. K. *Macromolecules* **1969**, *2*, 122.

(24) van Beijinen, A. J. M.; Nolte, R. J. M.; Drenth, W.; Hezemans, A. M. K. *Tetrahedron* **1976**, *32*, 2017.

(25) Kamer, P. C.; Nolte, R. J. M.; Drenth, W. *J. Am. Chem. Soc.* **1988**, *110*, 6828.

(26) Deming, T. J.; Novak, B. M. *J. Am. Chem. Soc.* **1992**, *114*, 7926.

(27) Mayer, S.; Zentel, R. *Prog. Polym. Sci.* **2001**, *26*, 1973.

(28) Schwartz, E.; Koepf, M.; Kitto, H. J.; Nolte, R. J. M.; Rowan, A. E. *Polym. Chem.* **2011**, *2*, 33.

(29) Vogl, O.; Miller, H. C.; Sharky, W. H. *Macromolecules* **1972**, *5*, 658.

(30) Corley, L. S.; Vogl, O. *Polym. Bull.* **1980**, *3*, 211.

(31) Vogl, O.; Corley, L. S.; Harris, W. J.; Jaycox, G. D.; Zhang, J. *Macromol. Chem. Suppl.* **1985**, *13*, 1.

(32) Zhang, J.; Jaycox, G. D.; Vogl, O. *Polym. J.* **1987**, *19*, 603.

(33) Vogl, O.; Xi, F.; Vass, F.; Ute, K.; Nishimura, T.; Hatada, K. *Macromolecules* **1989**, *22*, 4658.

(34) Jaycox, G. D.; Vogl, O. *Macromol. Chem. Rapid Commun.* **1990**, *11*, 61.

(35) Ute, K.; Hirose, K.; Kashimoto, H.; Nakayama, K.; Hatada, K.; Vogl, O. *Polym. J.* **1993**, *25*, 1175.

(36) Nakano, T.; Taniguchi, K. Okamoto, Y. *Polym J.* **1997**, *29*, 540.

(37) Ren, C.; Chen, F.; Xi, F.; Nakano, T.; Okamoto, Y. *J. Polym. Sci., Part A.: Polym. Chem.* **1993**, *31*, 2721.

(38) Nakano, T.; Masuda, A.; Mori, M.; Okamoto, Y. *Polym. J.* **1996**, *28*, 300.

(39) Okamoto, Y.; Mohri, H.; Hatada, K. *Chem. Lett.* **1988**, 1879.
(40) Okamoto, Y.; Mohri, H.; Nakano, T.; Hatada, K. *Chirality* **1991**, *3*, 277.
(41) Hatada, K.; Shimizu, S.-I.; Yuki, H.; Harris, W.; Vogl, O. *Polym. Bull.* **1981**, *4*, 179.
(42) Hatada, K.; Kitayama, T.; Shimizu, S.-I.; Yuki, H. *J. Chromatogr.* **1982**, *248*, 63.
(43) Okamoto, Y.; Suzuki, K.; Ohta, K.; Hatada, K.; Yuki, H. *J. Am. Chem. Soc.* **1979**, *101*, 4763.
(44) Okamoto, Y.; Suzuki, K.; Yuki, H. *J. Polym. Sci., Polym. Chem. Ed.* **1980**, *18*, 3043.
(45) Yuki, H.; Okamoto, Y.; Okamoto, I. *J. Am. Chem. Soc.* **1980**, *102*, 6358.
(46) Okamoto, Y.; Honda, S.; Okamoto, I.; Yuki, H.; Murata, S.; Noyori, R.; Takaya, H. *J. Am. Chem. Soc.* **1981**, *103*, 6971.
(47) Hoshikawa, N.; Hotta, Y.; Okamoto, Y. *J. Am. Chem. Soc.* **2003**, *125*, 12380.
(48) Goodman, M.; Chen, S.-C. *Macromolecules* **1970**, *3*, 398.
(49) Goodman, M.; Chen, S.-C. *Macromolecules* **1971**, *4*, 625.
(50) Green, M. M.; Gross, R. A.; Crosby, C., III; Schilling, R. C. *Macromolecules* **1987**, *20*, 992.
(51) Green, M. M.; Andreola, C.; Munoz, B.; Reidy, M. P.; Zero, K. *J. Am. Chem. Soc.* **1988**, *110*, 4063.
(52) Green, M. M.; Peterson, N. C.; Sato, T.; Teramoto, A.; Cook, R.; Lifson, S. *Science* **1995**, *268*, 1860.
(53) Green, M. M.; Reidy, M. P.; Johnson, R. D.; Darling, G.; Oleary, D. J.; Willson, G. *J. Am. Chem. Soc.* **1989**, *111*, 6452.
(54) Green, M. M.; Garetz, B. A.; Munoz, B.; Chang, H.; Hoke, S.; Cooks, R. G. *J. Am. Chem. Soc.* **1995**, *117*, 4181.
(55) Frey, H.; Möller, M.; Matyjaszewski, K. *Macromolecules* **1994**, *27*, 1814.
(56) Fujiki, M. *J. Am. Chem. Soc.* **1994**, *116*, 6017.
(57) Fujiki, M. *J. Am. Chem. Soc.* **1994**, *116*, 11976.
(58) Fujiki, M. *J. Am. Chem. Soc.* **1996**, *118*, 7424.
(59) Fujiki, M. *J. Am. Chem. Soc.* **2000**, *122*, 3336.

(60) Fujiki, M.; Koe, J. R.; Motonaga,M.; Nakashima, H.; Terao, K.; Teramoto, A. *J. Am. Chem. Soc.* **2001**, *123*, 6253.
(61) Fujiki, M. *Macromol. Rapid Coommun.* **2001**, *22*, 539–563.
(62) Fujiki, M.; Koe, J. R.; Terao, K.; Sato, T.; Teramoto, A. Watanabe, J. *Polym. J.* **2003**, *35*, 297.
(63) Nelson, J. C.; Saven, J. G.; Moore, J. S.; Wolynes, P. G. *Science*, **1997**, *277*, 1793.
(64) Fiesel, R.; Scherf, U. *Macromol. Rapid Commun.* **1998**, *19*, 427.
(65) Fiesel, R.; Halkyard, C. E.; Rampey, M. E.; Kloppenburg, L.; Studer-Martinez, S. L.; Scherf, S.; Bunz, U. H. F. *Macromol. Rapid Commun*. **1999**, *20*, 107.
(66) Wilson, J. N.; Steffen, W.; McKenzie, T. G.; Lieser, G.; Oda, M.; Neher, D.; Bunz, U. H. F. *J. Am. Chem. Soc.* **2002**, *124*, 6830.
(67) Prince, R. B.; Brunsveld, L.; Meijer, E. W.; Moore, J. S. *Angew. Chem., Int. Ed.* **2000**, *39*, 228.
(68) Brunsveld, L.; Prince, R. B.; Meijer, E. W.; Moore, J. S. *Org. Lett.* **2000**, *2*, 1525.
(69) Tan, C.; Pinto, M. R.; Kose, M. E.; Ghiviriga, I.; Schanze, K. S. *Adv. Mater.* **2004**, *16*, 1208.
(70) Inoue, M.; Teraguchi, M.; Aoki, T.; Hadano, S.; Namikoshi, T.; Marwanta, E.; Kaneko, T. *Synths. Met.* **2009**, *159*, 854.
(71) Banno, M.; Yamaguchi, T.; Nagai, K.; Kaiser, C.; Hecht, S.; Yashima, E. *J. Am. Chem. Soc.* **2012**, *134*, 8718–8728.
(72) Zhao, X. Y.; Schanze, K. S. *Langmuir* **2006**, *22*, 4856–4862.
(73) Kaneko, T.; Yoshimoto, S.; Hadano, S.; Teraguchi, M.; Aoki, T. *polyhedron* **2007**, *26*, 1825.
(74) Liu, R.; Shiotsuki, M.; Masuda, T.; Sanda, F. *Macromolecules* **2009**, *42*, 6115–6122.
(75) Goto, K.; Moore, J. S. *Org. Lett.* **200**5, *7*, 1683.
(76) Khan, A.; Kaiser, C.; Hecht, S. *Angew. Chem. Int. Ed.* **2006**, *45*, 1878.
(77) Khan, A.; Hecht, S. *Chem. Eur. J.* **2006**, *12*, 4764.
(78) Gin, M. S.; Yokozawa, T.; Prince, R. B.; Moore, J. S. *J. Am. Chem. Soc.* **1999**, *121*, 2643.

(79) Gin, M. S.; Moore, J. S. *Org. Lett.* **2000**, *2*, 135.
(80) Arnt, L; Tew, G. N. *Macromolecules* **2004**, *37*, 1283.
(81) Prince, R. B.; Barnes, S. A.; Moore, J. S. *J. Am. Chem. Soc.* **2000**, *122*, 2758.
(82) Tatanami, A.; Mio, M. J.; Moore, J. S. *J. Am. Chem. Soc.* **2001**, *123*, 1792.
(83) Inouye, M.; Waki, M.; Abe, H. *J. Am. Chem. Soc.* **2004**, *126*, 2022.
(84) Waki, M.; Abe, H.; Inouye, M. *Chem. Eur. J.* **2006**, *12*, 7839.
(85) Abe, H.; Okada, K.; Makida, H.; Inouye, M. *Org. Bioorg. Chem.* **2012**, *10*, 6930.
(86) Ciardelli, F.; Lanzillo, S; Pieroni, O. *Macromolecules* **1974**, *7*, 174.
(87) Moore, J. S.; Gorman, C. B.; Grubbs, R. H. *J. Am. Chem. Soc.* **1991**, *113*, 1704.
(88) Katsumata, T.; Shiotsuki, M.; Sanda, F.; Sauvage, X.; Delaude, L.; Masuda, T. *Macromol. Chem. Phys.* **2009**, *210*, 1891.
(89) Tabata, M.; Yang, W.; Yokota, K. *Polym. J.* **1990**, *22*, 1105–1107.
(90) Aoki, T.; Kokai, M.; Shinohara, K.; Oikawa, E. *Chem. Lett.* **1993**, 2009.
(91) Yashima, E.; Huang, S.; Okamoto, Y. *J. Chem. Soc., Chem. Commun.* **1994**, 1811.
(92) Yashima, E.; Huang, S.; Matsushima, T.; Okamoto, Y. *Macromolecules* **1995**, *28*, 4184.
(93) Li, B. S.; Cheuk, K. K. L.; Yang, D.; Lam, J. W. Y.; Wan, L. J.; Bai, C.; Tang, B. Z. *Macromolecules* **2003**, *36*, 5447.
(94) Maeda, K.; Kamiya, N.; Yashima, E. *Chem. Eur. J.* **2004**, *10*, 4000–4010.
(95) Okoshi, K.; Sakajiri, K.; Kumaki, J.; Yashima, E. *Macromolecules* **2005**, *38*, 745.
(96) Zhao, H.; Sanda, F.; Masuda, T. *Macromol. Chem. Phys.* **2006**, *207*, 1921.
(97) Zhao, H.; Sanda, F.; Masuda, T. *J. Polym. Sci., Part A: Polym. Chem.* **2007**, *45*, 1691.
(98) Maeda, K.; Tanaka, K.; Morino, K.; Yashima, E. *Macromolecules* **2007**, *40*, 6783.

(99) Otsuka, I.; Hongo, T.; Nakade, H.; Narumi, A.; Sakai, R.; Satoh, T.; Kaga, H.; Kakuchi, T. *Macromolecules* **2007**, *40*, 8930.
(100) Kakuchi, R.; Nagata, S.; Sakai, R.; Otsuka, I.; Nakade, H.; Satoh, T.; Kakuchi T. *Chem. Eur. J.* **2008**, *14*, 10259.
(101) Chan, K. H.; Lam, J. W.; Wong, K. M.; Tang, B. Z.; Yam, V. W. W. *Chem. Eur. J.* **2009**, *15*, 2328.
(102) Terada, K.; Masuda, T.; Sanda, F. *J. Polym. Sci., Part A: Polym. Chem.* **2009**, *47*, 4971.
(103) Ohsawa, S.; Sakurai, S.; Nagai, K.; Banno, M.; Maeda, K.; Kumaki, J.; Yashima, E. *J. Am. Chem. Soc.* **2011**, *133*, 108.
(104) Ikeda, A.; Terada, K. Shiotsuki, M.; Sanda, F. *J. Polym. Sci., Part A: Polym. Chem.* **2011**, *49*, 3783.
(105) Terada, K.; Masuda, T.; Sanda, F. *Macromolecules* **2009**, *42*, 913.
(106) Tang, Z.; Iida, H.; Hu, H. Y.; Yashima, E. *ACS Macro Lett.* **2012**, *1*, 261.
(107) Yashima, E.; Matsushima, T.; Okamoto, Y. *J. Am. Chem. Soc.* **1995**, *117*, 11596.
(108) Yashima, E.; Maeda, K.; Okamoto, Y. *J. Am. Chem. Soc.* **1996**, *118*, 9800.
(109) Yashima, E.; Matsushima, T.; Okamoto, Y. *J. Am. Chem. Soc.* **1997**, *119*, 6345.
(110) Yashima, E.; Maeda, K.; Onouchi, K. *Nature* **1999**, *399*, 449.
(111) Nonokawa, R. and Yashima, E. *J. Am. Chem. Soc*. **2003**, *125*, 1278.
(112) Aoki, T.; Kaneko, T.; Maruyama, N.; Sumi, A.; Takahashi, M.; Sato, T.; Teraguchi, M. *J. Am. Chem. Soc.* **2003**, *125*, 6346.
(113) Kaneko, T.; Umeda, Y.; Yamamoto, T.; Teraguchi, M.; Aoki, T. *Macromolecules* **2005**, *38*, 9420.
(114) Hadano, S.; Kishimoto, T.; Hattori, T.; Tanioka, D.; Teraguchi, M.; Aoki, T.; Kaneko, T.; Namikoshi, T.; Marwanta, E. *Macromol. Chem. Phys.* **2009**, *210*, 717.
(115) Nakako, H.; Nomura, R.; Tabata, M.; Masuda, T. *Macromolecules* **1999**, *32*, 2861.
(116) Nakako, H.; Mayahara, Y.; Nomura, R.; Tabata, M.; Masuda, T. *Macromolecules* **2000**, *33*, 3978.

(117) Nomura, R.; Fukishima, Y.; Nakako, H.; Masuda, T. *J. Am. Chem. Soc.* **2000**, *122*, 8830.
(118) Nakako, H.; Nomura, R.; Masuda, T. *Macromolecules* **2001**, *34,* 1496.
(119) Nomura, R.; Tabei, J.; Masuda, T. *J. Am. Chem. Soc.* **2001**, *123*, 8430.
(120) Tabei, J.; Nomura, R.; Masuda, T. *Macromolecules* **2002**, *35*, 2955.
(121) Tabei, J.; Nomura, R.; Masuda, T. *Macromolecules* **2002**, *35*, 5405.
(122) Tabei, J.; Nomura, R.; Sanda, F.; Masuda, T. *Macromolecules* **2003**, *36*, 8603.
(123) Gao, G.; Sanda, F.; Masuda, T. *Macromolecules*, **2003**, *36*, 3938.
(124) Nomura, R.; Nishiura, S.; Tabei, J.; Sanda, F.; Masuda, T. *Macromolecules* **2003**, *36*, 5076.
(125) Sanda, F.; Nishiura, S.; Shiotsuki, M.; Masuda, T. *Macromolecules* **2005**, *38*, 3075.
(126) Tabei, J.; Shiotsuki, M.; Sanda, F.; Masuda, T. *Macromolecules* **2005**, *38*, 9448.
(127) Suzuki, Y.; Tabei, J.; Shiotsuki, M.; Inai, Y.; Sanda, F.; Masuda, T. *Macromolecules* **2008**, *41*, 1086.
(128) Suzuki, Y.; Shiotsuki, M.; Sanda, F.; Masuda, T. *Macromolecules* **2007**, *40*, 1864.
(129) Suzuki, Y.; Shiotsuki, M.; Sanda, F.; Masuda, T. *Chem. Asian J.* **2008**, 3, 2075.
(130) Aoki, T.; Kobayashi, Y.; Kaneko, T.; Oikawa, E.; Yamamura, Y.; Fujita, Y.; Teraguchi, M.; Nomura, T.; Masuda, *Macromolecules* **1999**, *32*, 79.
(131) Lam, J. W. Y.; Dong, Y. P.; Cheuk, K. K. L.; Law, C. C. W.; Lai, L. M.; Tang, B. Z. *Macromolecules* **2004**, *37*, 6695.
(132) Zhang, X. A.; Qin, A.; Tong, L.; Zhao, H.; Zhao, Q.; Sun, J. Z.; Tang, B. Z. *ACS Macro Lett.* **2012**, *1*, 75.
(133) For a review, see: (a) Tamai, N.; Miyasaka, H. *Chem. Rev.* **2000**, *100*, 1875. (b) Natansohn, A.; Ronchon, P. *Chem. Rev.* **2002**, *102*, 4139. (c) Seki, T. *Bull. Chem. Soc. Jpn.* **2007**, *80*, 2084. (d) Russew, M.; Hecht, S. *Adv. Mater.* **2010**, *22*, 3348. (e) Beharry, A. A.; Woolley, G. A. *Chem. Soc. Rev.* **2011**, *40*, 4422.
(134) Shinkai, S.; Nakaji, T.; Nishida, Y.; Ogawa, T.; Manabe, O. *J. Am. Chem.*

Soc. **1980**, *102*, 5860.
(135) Shinkai, S.; Nakaji, T.; Ogawa, T.; Shigematsu, K.; Manabe, O. *J. Am. Chem. Soc.* **1981**, *103*, 111.
(136) Muraoka, T.; Kinbara, K.; Kobayashi, Y.; Aida, T. *J. Am. Chem. Soc.* **2003**, *125*, 5612.
(137) Muraoka, T.; Kinbara, K.; Aida, T. *Nature* **2006**, *440*, 512.
(138) Muraoka, T.; Kinbara, K.; Aida, T.; *J. Am. Chem. Soc.* **2006**, *128*, 11600.
(139) Muraoka, T.; Kinbara, K.; Aida, T. *Chem. Commun.* **2007**, 1441.
(140) Kinbara, K.; Muraoka, T.; Aida, T. *Org. Biomol. Chem.* **2008**, 1871.
(141) Kai, H.; Nara, S.; Kinbara, K.; Aida, T. *J. Am. Chem. Soc.* **2008**, *130*, 6725.
(142) Yu, Y; Nakano, M.; Ikeda, T. *Nature*, **2003**, *425*, 145.
(143) Ikeda, T.; Nakano, M.; Yu, Y.; Tsutsumi, O.; Kanazawa, A. *Adv. Mater.* **2003**, *15*, 201.
(144) Yu, Y.; Nakano, M.; Shishido, A.; Shiono, T.; Ikeda, T. *Chem. Mater.* **2004**, *16*, 1637.
(145) Kondo, M.; Yu, Y.; Ikeda, T. *Angew. Chem. Int. Ed.* **2006**, *45*, 1378.
(146) Yu, Y.; Maeda, T.; Mamiya, J.; Ikeda, T. *Angew. Chem. Int. Ed.* **2007**, *46*, 881.
(147) Yamada, M.; Kondo, M.; Mamiya, J.; Yu, Y.; Kinoshita, M.; Barrett, C. J.; Ikeda, T. *Angew. Chem. Int. Ed.* **2008**, *47*, 4986.
(148) Fujii, T.; Shiotsuki, M.; Inai, Y.; Sanda, F.; Masuda, T. *Macromolecules* **2007**, *40*, 7079.
(149) Zhang, W.; Yoshida, K.; Fujiki, M.; Zhu, X. *Macromolecules* **2011**, *44*, 5105.
(150) Imin, P.; Lmit, M.; Adronov, A. *Macromolecules* **2012**, *45*, 5045.
(151) Yu, Z.; Hecht, S. *Angew. Chem. Int. Ed.* **2011**, *50*, 1640.
(152) Yu, Z.; Hecht, S. *Chem. Eur. J.* **2012**, *18*, 10519.

Part I

Synthesis and Properties of Amino Acid-derived Helical Poly(*m*-phenyleneethynylene-aryleneethynylene)s

Chapter 1

Synthesis of Optically Active Poly(*m*-phenyleneethynylene-aryleneethynylene)s Bearing Hydroxy Groups and Exmaination of the Higher Order Structures

Abstract

Novel optically active poly(*m*-phenyleneethynylene-aryleneethynylene)s bearing hydroxy groups with various arylene units {poly[(*S*)- / (*R*)-**1**–**3a**]–poly[(*R*)-**1**–**3e**] and poly[(*S*)-**2**–**3a**]} were synthesized by the Sonogashira–Hagihara coupling polymerization of 3,5-diiodo-4-hydroxy-$C_6H_4CONHCH(CH_3)COXC_{12}H_{25}$ [(*S*)- / (*R*)-**1** (X = O), (*S*)-**2** (X = NH)] with HC≡C-Ar-C≡CH [**3a** (Ar = 1,4-C_6H_4), **3b** (Ar = 1,4-C_6H_4-1,4-C_6H_4-), **3c** (Ar = 1,4-C_6H_4-1,4-C_6H_4-1,4-C_6H_4-), **3d** (Ar = 2,5-dihexyl-1,4-C_6H_2), **3e** (Ar = 2,5-didodecyl-1,4-C_6H_2)]. The yields and number-average molecular weights of the polymers were 60–94% and 7,000–29,500. CD, UV–vis, and fluorescence spectroscopic analyses indicated that poly[(*S*)-**1**–**3a**]–poly[(*S*)-**1**–**3c**] and poly[(*S*)-**2**–**3a**] formed predominantly one-handed helical structures in THF, while poly[(*S*)-**1**–**3d**] and poly[(*S*)-**1**–**3e**] showed no evidence for forming chirally ordered structures. The all polymers emitted blue fluorescence.

Introduction

Biomacromolecules such as proteins and DNA exhibit sophisticated and intricate functions largely depending on their well-defined higher order structures. For the decade, the artificial helical polymers including polymethacrylates,[1] polyisocyanides,[2] polysilanes,[3] poly(phenyleneethynylene)s[4] and polyacetylenes[5] have been extensively synthesized by imitating naturally derived helical polymers. Artificial helical polymers are important not only from the viewpoint of fundamental study but also potentiality for practical applications such as molecular recognition,[6–9] chiral catalysis[10–14] and chemical sensing[15–18] based on their electronic and optical properties. Moore and coworker reported that *m*-linked oligophenyleneethynylene bearing tetraethylene glycol moieties at the side chains folded into intramolecularly p-stacked helical structure in polar solvents such as acetonitrile based on the amphiphilicity originating from the hydrophilic side chains and hydrophobic main chains.[19] Since then, many efforts have been made concerning synthesis of polymers that possess phenyleneethynylene and the analogous main chain, and investigation on the conformation and optical activity.[4,6,7,20–29] Recently, the synthesis and chiroptical properties of various novel D-hydroxyphenylglycine-/L-tyrosine-derived poly(*m*-phenyleneethynylene-*p*-phenyleneethynylene)s,[30–33] photo-responsiveness,[32] stabilization of the conformation by intramolecular crosslinking at the side chains have been reported. The key importance for helix formation for these polymers is

amphiphilicity caused by hydrophobic exterior (alkyl groups and phenyleneethynylene main chain) and hydrophilic interior (hydroxy groups). It should be noteworthy that the amphiphilic balance of formed helix is opposite from that of typical poly(*m*-phenyleneethynylene) derivatives. p-Stacking between the phenylene moieties at the main chain and intramolecular hydrogen bonding between the amide/carbamate groups at the side chains also play important roles for helix formation. It is expected that the polymers may recognize molecules utilizing the cavity inside of the helical structures.

UV–vis absorption maxima of oligo-/poly-*p*-phenylenes increase according the increase of degree of polymerization, and get saturated at certain regions.[34] The optoelectronic properties of oligo-/poly-*p*-phenylenes follows a so called 1/*n* relationship, where *n* represents a degree of polymerization.[35,36] This trend is commonly observed for conjugated polymers representatively for *trans*-[37] and *cis*-polyacetylenes.[38] On the other hand, no clear result has been reported concerning the effect of repeating number of phenylene moiety [*n* of –C≡C–(1,4-C_6H_4)$_n$–C≡C–] on the chiroptical properties of phenyleneethynylene-based polymers. Herein the author discusses the synthesis of novel alanine-derived poly(*m*-pheyleneethynylene-aryleneethynylene)s containing hydroxy groups by the Sonogashira–Hagihara coupling polymerization of the corresponding monomers (Scheme 1). The author further discusses the effects of repeating number of phenylene moiety and substituents on the chiroptical properties,

conjugation length of the polymers, and secondary structures based on DFT and MM calculations.

Scheme 1. Sonogashira–Hagihara Coupling Polymerization of Monomers (*S*)-/(*R*)-**1** and (*S*)-**2** with **3a**–**3e**

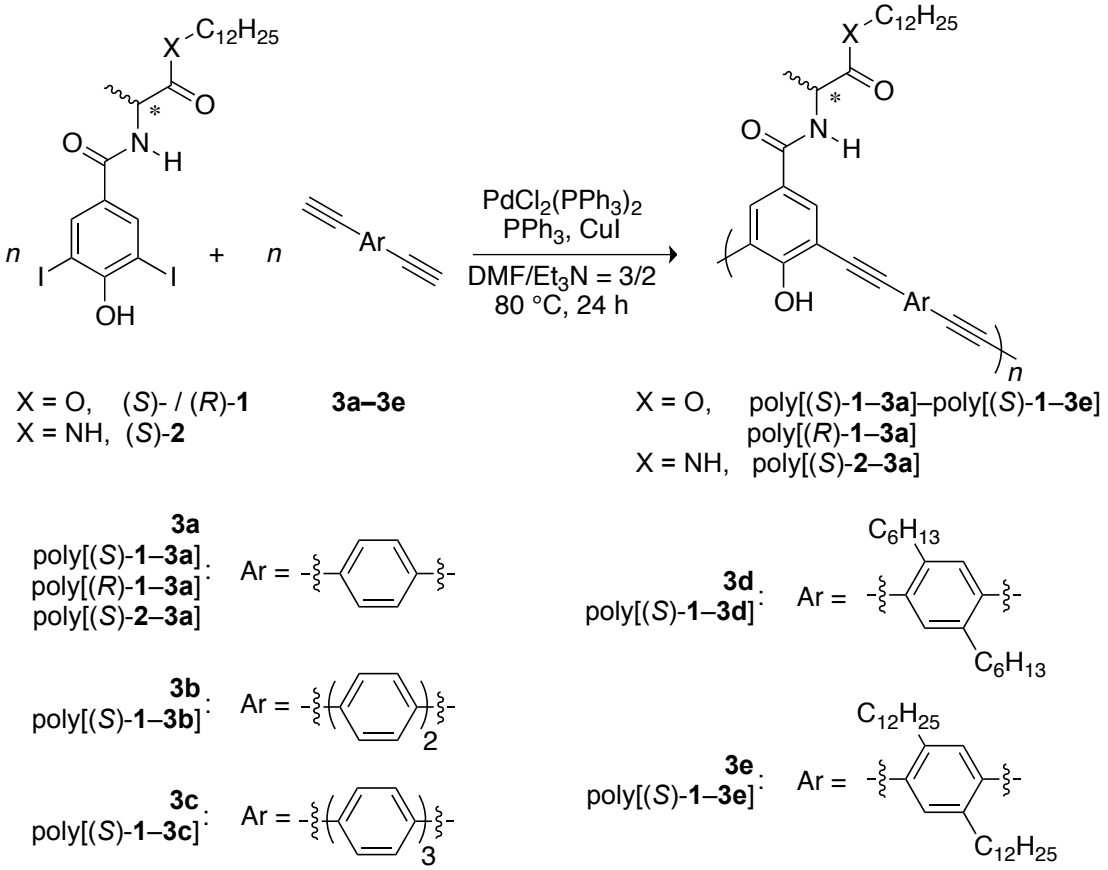

Result and Discussion

Polymerization. The Sonogashira–Hagihara coupling polymerization of (*S*)-/(*R*)-**1** or (*S*)-**2** with various diethynyl monomers (**3a**–**3e**) were carried out in DMF at 80 °C for 24 h. The formed polymers were isolated as insoluble parts in MeOH/acetone = 9/1 (v/v) mixture. As listed in Table 1,

poly[(*S*)-/(*R*)-**1–3a**]–poly[(*S*)-**1–3e**] and poly[(*S*)-**2**–**3a**] with moderate number average molecular weights (M_n) in the range of 7,000–29,500 were obtained in good yields. The solubility of poly[(*S*)-**1–3c**] was comparatively low. It was insoluble in DMSO, and partly insoluble in $CHCl_3$ and THF. The other polymers were soluble in common organic solvents such as $CHCl_3$, THF, DMSO, and DMF. Poly[(*S*)-**1–3d**] and poly[(*S*)-**1–3e**] containing phenylene units with long alkyl chains were highly soluble in spite of their high M_n's compared to the other polymers. The two polymers were even soluble in toluene. Introduction of long alkyl chains certainly improves the solubility as often observed for conjugated polymers with stiff main chains.

Table 1. Sonogashira–Hagihara coupling polymerization of (*S*)-/(*R*)-**1** with **3a**–**e** and (*S*)-**1** with **3a**[a]

monomer	polymer			
		yield[b] (%)	M_n[c]	M_w/M_n[c]
(*S*)-**1** + **3a**	poly[(*S*)-**1**–**3a**]	88	8,900	1.9
(*R*)-**1** + **3a**	poly[(*R*)-**1**–**3a**]	88	7,000	1.6
(*S*)-**1** + **3b**	poly[(*S*)-**1**–**3b**]	94	9,600	1.9
(*S*)-**1** + **3c**	poly[(*S*)-**1**–**3c**]	87	9,700[d]	1.5[d]
(*S*)-**1** + **3d**	poly[(*S*)-**1**–**3d**]	60	13,200	2.1
(*S*)-**1** + **3e**	poly[(*S*)-**1**–**3e**]	86	29,500	1.5
(*S*)-**2** + **3a**	poly[(*S*)-**2**–**3a**]	91	9,400	1.4

[a] conditions: $[\mathbf{1}]_0 = [\mathbf{2}]_0 = [\mathbf{3a}–\mathbf{e}]_0 = 0.10$ M, $[PdCl_2(PPh_3)_2] = 0.0050$ M, [CuI] = 0.0025, $[PPh_3] = 0.0010$ M, DMF/Et_3N = 3/2 (v/v), 80 °C, 24 h. [b] Insoluble part in MeOH/acetone = 9/1 (v/v). [c] Estimated by SEC measured in THF, polystyrene calibration. [d] THF-soluble part.

Chiroptical Properties of the Polymers. The CD and UV–vis spectra of the polymers were measured in THF to obtain information on the secondary

structures. As shown in Figure 1, poly[(*S*)-**1–3a**] exhibited split CD signals at the absorption region of the main chain chromophore around 300–400 nm in THF. The CD and UV–vis signals did not change after membrane filtration (pore size = 0.45 mm) of the sample solutions,[39] and the sample concentration did not affect the signal intensity at a range of 0.03–0.30 mM. These results indicate that the CD signals originate from unimolecular folded helical conformations of the polymers with predominantly one-handed screw sense, unlike the cases of chirally substituted poly(thiophene)s[40–42] and poly(*p*-phenylenevinylene)s[40,43,44] that form chiral aggregates. Poly[(*S*)-**1–3a**] and poly[(*R*)-**1–3a**], having side chains with opposite absolute configurations, exhibited mirror-image CD signals at 250–500 nm. These polymers form helical structures with opposite screw sense mutually, and the helix sense is determined by the amino acid chirality.

Interestingly, the λ_{max}'s of poly[(*S*)-**1–3b**] and poly[(*S*)-**1–3c**], having biphenylene and terphenylene units, were observed at almost the same wavelengths (342–344 nm) as poly[(*S*)-**1–3a**] (342 nm) having monophenylene units. The two polymers also exhibited split CD signals around the main chain absorption region in THF (Figure 2). This result provides support for the formation of predominantly one-handed helical structures as well. The CD intensities of the polymers varied depending on the phenylene repeating units, and poly[(*S*)-**1–3c**] exhibited the largest CD signals. Although the presence of rotatable single bonds at the *p*-terphenylene backbone, the conformation of

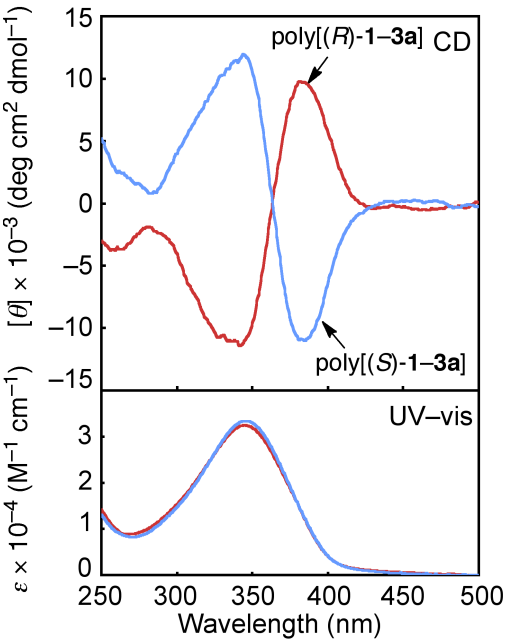

Figure 1. CD and UV–vis spectra of poly[(*S*)-**1**–**3a**] and poly[(*R*)-**1**–**3a**] measured in THF (c = 0.03 mM) at 20 °C.

poly[(*S*)-**1**–**3c**] seems to be constrained presumably by π-stacking interactions.[45] Since poly[(*S*)-**1**–**3c**] has the most extended conjugation units (terphenylene) among the three polymers, it is likely that intramolecular π-stacking interaction between the polymer backbones is largest, resulting in the most stabilized helically folded structure.[46] It should be noted that poly[(*S*)-**1**–**3d**] and[(*S*)-**1**–**3e**] tethering long alkyl chains exhibited no intense CD signals in THF (Figure 2) and neither in $CHCl_3$ and toluene (not shown). The two polymers do not form chirally ordered structures in the solvents. On the other hand, poly[(*S*)-**2**–**3a**] showed intense CD signals at the absorption area of the main chains, and its intensity was twice as high as that of poly[(*S*)-**1**–**3a**] in spite of almost the same molar absorbance. The both two amide groups seem to form regulated

intramolecular hydrogen-bonding strands, leading to high predominance of one-handed screw sense.

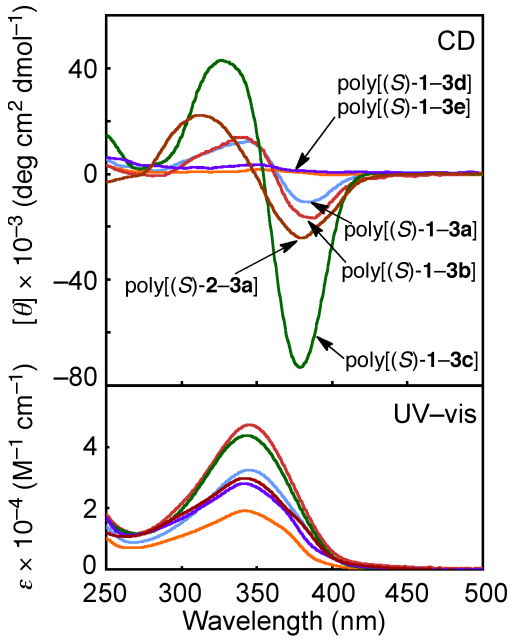

Figure 2. CD and UV–vis spectra of poly[(*S*)-**1–3a**]–poly[(*S*)-**1–3e**] and poly[(*S*)-**2–3a**] measured in THF (c = 0.03 mM) at 20 °C.

Poly[(*S*)-**1–3a**] exhibited almost the same CD and UV–vis spectroscopic patterns at the absorption region of the main chain chromophore around 300–400 nm in $CHCl_3$ and THF/MeOH mixtures. The intensity of CD signals increased as increasing the MeOH content in THF/MeOH mixtures accompanying a slight blue shift of the absorption maximum (λ_{max}). This results indicates the increase of one-handed helicity upon addition of MeOH, which is different from the case previously reported.[30] The possibility of increase of helix content is also present, because the l_{max} of a helical structure of poly(*m*-phenyleneethynylene) is observed at a shorter wavelength than that of trans-zigzag structure.[24,47]

Figure 4 shows the plot of the Kuhn dissymmetry factor ($g = \Delta\varepsilon/\varepsilon$, in

which $\Delta\varepsilon$ = $[\theta]$/3,298) at the $[\theta]_{max}$ of poly[(*S*)-**1–3a**]–poly[(*S*)-**1–3c**] and poly[(*S*)-**2–3a**] in THF/MeOH mixtures at various compositions. No aggregation took place, because the CD and UV–vis spectra showed no difference between and after membrane filtration in all cases. The *g* values give quantitative information associated with the degree of preferential screw sense.[48] Poly[(*S*)-**1–3b**] and poly[(*S*)-**1–3c**] show similar behavior to poly[(*S*)-**1–3a**]. The existence of a certain amount of MeOH may lead to an amphiphilic balance that is suitable for forming folded structures for these polymers. On the other hand, the *g* value of poly[(*S*)-**2–3a**] remarkably decreased as increasing the MeOH composition. The disruption of predominantly one-handed helical structure took place by the addition of MeOH in this case. The folded helical structure of poly[(*S*)-**2–3a**] is more sensitive toward MeOH addition. The collapse of regulated hydrogen-bonding strands between the dodecyl amide groups probably causes large conformational irregularity whole of the molecules.

On the contrary to addition of MeOH, addition of DMF to a THF solution of poly[(*S*)-**1–3a**] resulted in decrease of CD intensity. Aggregation is deniable because no difference was observed in the CD and UV–vis spectra before and after membrane filtration. When H_2O was added to a THF solution of poly[(*S*)-**1–3a**], the CD signals became more intense. In this case, H_2O-induced aggregation was confirmed. Namely, filtration of sample solutions in THF/H_2O = 6/4 by a membrane filter (pore size = 0.45 mm) resulted in disappearance of CD and UV–vis signals as shown Figure 5. Judging from

the almost same CD signal patterns of the aggregated and non-aggregated states, poly[(*S*)-**1**–**3a**] seems to keep its folded helical structure upon aggregation as observed in oligo(*o*-phenyleneethynylene-*p*-phenyleneethynylene) tethering oligo ethylene glycol units.[49] It should be noted that no blue shift was observed in the UV–vis spectra, differently from the case of THF/MeOH. The DLS measurement revealed the existence of the some aggregates, whose R_h is around 82 nm, in THF/H_2O = 6/4 mixture at as same concentration as CD spectroscopic measurements (Figure 6). No such aggregates were observed in THF/MeOH and THF/DMF mixture. These results also suggest that some chiral aggregates were observed only by the addition of H_2O. At the moment, the author cannot explain the reason for the different responsiveness of poly[(*S*)-**1**–**3a**] in THF solution upon addition of MeOH, DMF and H_2O.

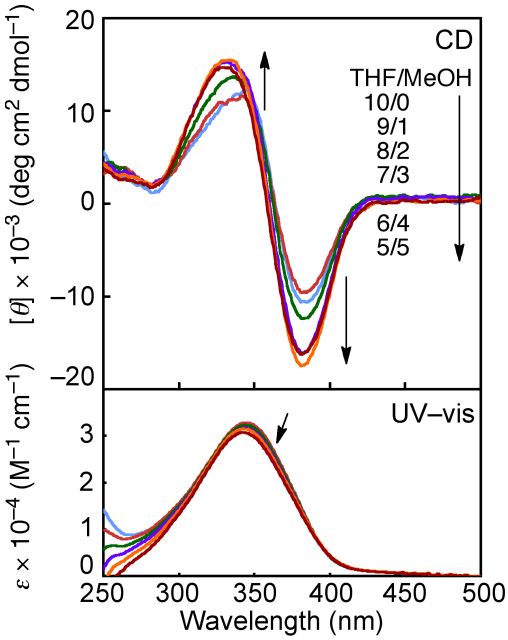

Figure 3. CD and UV–vis spectra of poly[(*S*)-**1**–**3a**] measured in THF/MeOH mixture with various compositions (c = 0.03 mM) at 20 °C.

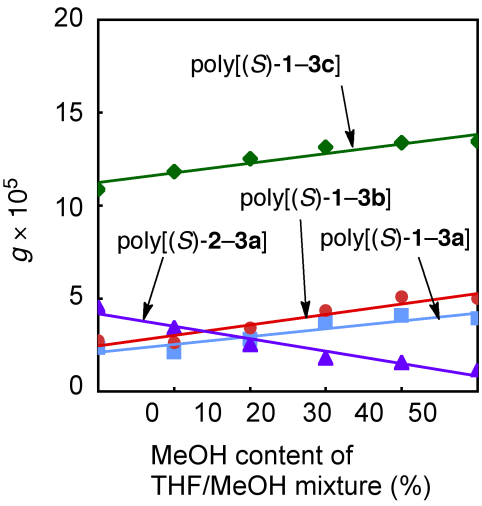

Figure 4. Plot of g value of poly[(*S*)-**1**-**3a**]–poly[(*S*)-**1**-**3c**] and poly[(*S*)-**2**-**3a**] at $[\theta]_{max}$ measured in THF/MeOH mixture at 20 °C versus MeOH content of THF/MeOH mixture (c = 0.03 mM).

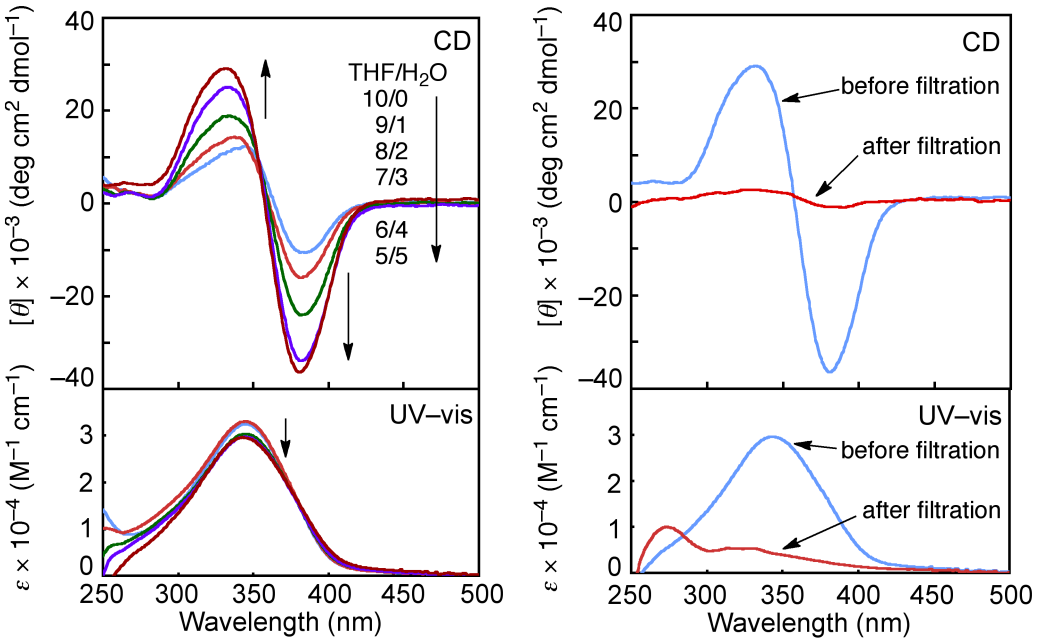

Figure 5. CD and UV–vis spectra of poly[(*S*)-**1**–**3a**] measured in various component of THF/H_2O mixture (top) and in THF/H_2O = 6/4 before and after filtration using a membrane with 0.45 μm pore size (bottom) (c = 0.03 mM) at 20 °C.

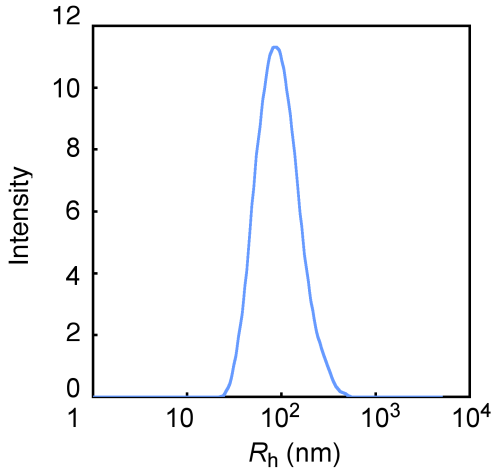

Figure 6. Distribution of R_h of poly[(*S*)-**1**–**3a**] in THF/H_2O = 6/4 mixture measured by dynamic light scattering (c = 0.03 mM).

Some of helical poly(phenyleneethnylene)s stabilize the conformation by intramolecular hydrogen bonds between the pendent side chains.[29,30,32,50,51] Solution-state IR spectra of poly[(*S*)-**1**–**3a**], poly[(*S*)-**1**–**3e**] and the corresponding monomer [(*S*)-**1**] were measured in $CHCl_3$ under diluted conditions (3 mM)[52] to determine the presence/absence of intramolecular hydrogen bonding (Table 2). Poly[(*S*)-**1**–**3a**] and monomer (*S*)-**1** exhibited two strong absorption peaks assignable to C=O stretching of amide and ester groups. The ester C=O peaks of poly[(*S*)-**1**–**3a**] and (*S*)-**1** were observed at same wavenumber (1728 cm^{-1}). The amide C=O peak positions of poly[(*S*)-**1**–**3a**] were observed at same wavenumber and 17 cm^{-1} lower wavenumber compared with that of (*S*)-**1**. Both ester and amide C=O peaks of poly[(*S*)-**1**–**3a**] appeared as same wavelengths as that of (*S*)-**1.** It is assumed that poly[(*S*)-**1**–**3a**] partially forms intramolecular hydrogen bonds between the amide groups to stabilize the helical structure in $CHCl_3$. The solution state IR spectrum of poly[(*S*)-**2**–**3a**]

was also measured and compared with that of (*S*)-**2**. Poly[(*S*)-**2–3a**] exhibited somewhat complicated peaks at C=O stretching absorption regions, indicating the presence of hydrogen bonding but the regularity is not high enough to show a simple absorption pattern.

Table 2. Solution-state IR spectroscopic data (C=O absorption peaks) of the monomers and polymers[a]

compound	wavenumber (cm^{-1}) C=O	
	ester	amide
(*S*)-**1**	1728	1659
poly[(*S*)-**1**–**3a**]	1727	1659, 1642
poly[(*S*)-**1**–**3e**]	1728	1659

[a] Measured in $CHCl_3$ (c = 3 mM).

Figure 7 depicts the fluorescence spectra of poly[(*S*)-**1–3a**]–poly[(*S*)-**1–3e**] and poly[(*S*)-**2–3a**] measured in THF excited at the main chain-based absorption maxima. The fluorescence spectroscopic data of polymers are listed in Table 3. Poly[(*S*)-**1–3a**]–poly[(*S*)-**1–3c**] and poly[(*S*)-**2–3a**] emitted blue-light fluorescence around 445 nm in quantum yields ranging from 28 to 59%.[53] Poly[(*S*)-**1–3d**] and Poly[(*S*)-**1–3e**] emitted purplish fluorescence and the peak tops existed 29–34 nm shorter than poly[(*S*)-**1–3a**]–poly[(*S*)-**1–3c**] and poly[(*S*)-**2–3a**]. Oligo(*m*-phenyleneethynylene)s emit two sets of fluorescence peaks assignable to non-excimer and excimer type conformations.[19,20] Helically folded oligo(*m*-phenyleneethynylene)s show intramolecular excimer-type fluorescence bands at longer wavelengths in low quantum yields compared with the *trans*-zigzag conformational isomers. Together with the results of CD

spectroscopy mentioned above, poly[(*S*)-**1**–**3a**]–poly[(*S*)-**1**–**3c**] and poly[(*S*)-**2**–**3a**] adopt helically folded conformations, while poly[(*S*)-**1**–**3d**] and poly[(*S*)-**1**–**3e**] adopt *trans*-zigzag conformations. It is speculated that poly[(*S*)-**1**–**3d**] and poly[(*S*)-**1**–**3e**] do not have abilities to form folded structure due to the steric effects and change of suitable amphiphilic balance to form helix.

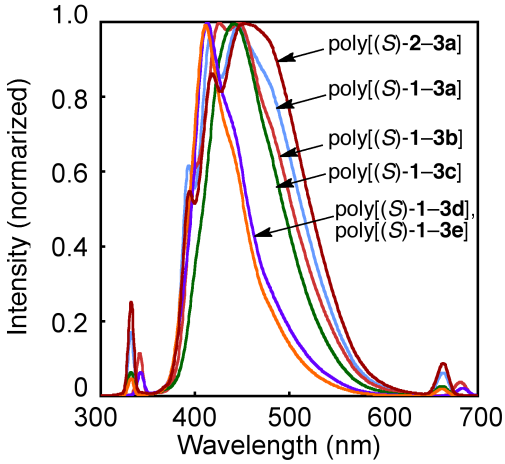

Figure 7. Fluorescence spectra of poly[(*S*)-**1**–**3a**]–poly[(*S*)-**1**–**3e**], and poly[(*S*)-**2**–**3a**] measured in THF at room temperature excited at λ_{max} (*c* = 0.6–3.0 mM)

Table 3. Optical data of the polymers[a]

polymer	λ_{abs} (nm)	λ_{emi} (nm)	Φ_{emi}[b]
poly[(*S*)-**1**–**3a**]	342	446	0.31
poly[(*S*)-**1**–**3b**]	344	427, 446	0.28
poly[(*S*)-**1**–**3c**]	342	442	0.59
poly[(*S*)-**1**–**3d**]	342	413	0.86
poly[(*S*)-**1**–**3e**]	344	412	0.77
poly[(*S*)-**2**–**3a**]	344	452	0.29

[a] Measured in THF. [b] Measured using anthracene as a standard in EtOH (Φ_{emi} = 0.27).

Poly[(*S*)-**1**–**3d**] and poly[(*S*)-**1**–**3e**] exhibited almost the same CD, UV–vis and fluorescence spectra in THF. The polymer films of these two were fabricated from THF solutions (1 wt %) on quartz glass plates by solvent-casting

and spin-coating methods. As shown Figure 8, the green- and blue-light emissions were observed from poly[(*S*)-**1–3d**] and poly[(*S*)-**1–3e**], respectively.[54] Red-shifted UV–vis signals appeared only in poly[(*S*)-**1–3d**], probably originating from aggregated structures. It is likely that the dodecyl groups of poly[(*S*)-**1–3e**] are long enough to prevent the molecules from p-stacking each other even in the film state, while the hexyl groups of poly[(*S*)-**1–3d**] are not.[55] No evidence for forming higher structures was obtained in the film states.

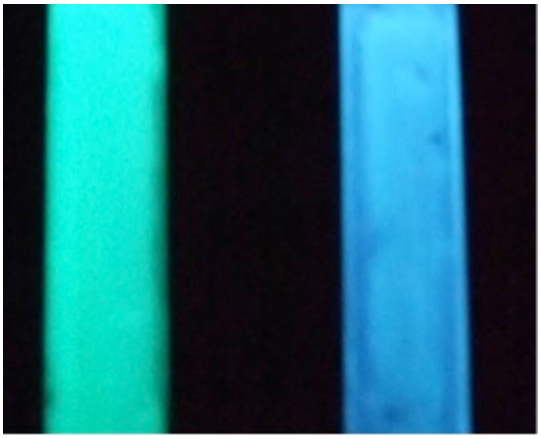

Figure 8. Photograph of poly[(*S*)-**1**–**3d**] (left) and poly[(*S*)-**1**–**3e**] (right) films fabricated from THF solutions (1 wt%) on quartz glass plates under irradiation of light (365 nm).

Conformational Analysis. As mentioned above, poly[(*S*)-**1**–**3a**]–poly[(*S*)-**1**–**3c**] show the λ_{max} at nearly the same wavelengths (343–344 nm) in spite of the difference of the phenylene repeating units. To gain knowledge for this result, TD-DFT-based simulations of the model compounds (**M1**–**M3** in Chart 1) were performed at the B3LYP/6-31+G* level. Figure 9 shows the velocity-based oscillator strength (*f*) values and UV–vis spectra predicted from

the *f* values and their positions, where a half Gaussian (1/e)-bandwidth ($\Delta/2$) was assumed to be 40 nm. Unimodal peaks were predicted in any case, and the calculated λ_{max} of **M1**–**M3** positioned at 399, 398, and 396 nm for **M1**, **M2** and **M3**, respectively. The energy levels of the highest occupied molecular orbital (HOMO) and lowest unoccupied molecular orbital (LUMO) were different in every case, but the energy band gaps between HOMO and LUMO were almost identical. Consequently, the λ_{max} values of **M1**–**M3** were predicted at almost the same wavelengths as observed in poly[(*S*)-**1**–**3a**]–poly[(*S*)-**1**–**3c**], verifying the results of TD-DFT calculations. It is likely that the torsion between the phenylene rings (35° both for **M2** and **M3** in average) prevents the phenylene moieties from extending the conjugation. Several attempts have been made to analyze the conformation of poly(phenyleneethynylene)s so far including molecular dynamics simulation of amine-[56,57] and ester-functionalized[58] poly(*m*-phenyleneethynylene)s. These polymers have a nature to adopt helical conformations that are energetically favorable rather than extended ones in water, wherein water molecules play an important role to fold the polymer chains into compacted structures. Such helical structures are preferred because they minimize unfavorable contacts between the hydrocarbon backbone and polar solvents, and maximize the interactions between the polar side chains and solvents as well.[4] Judging from the nature of poly(phenyeleneethynylene)s, poly[(*S*)-**1**–**3a**]–poly[(*S*)-**1**–**3c**], and poly[(*S*)-**2**–**3a**] in the present chapter also seem to adopt helical conformations stabilized by π-stacking interaction between

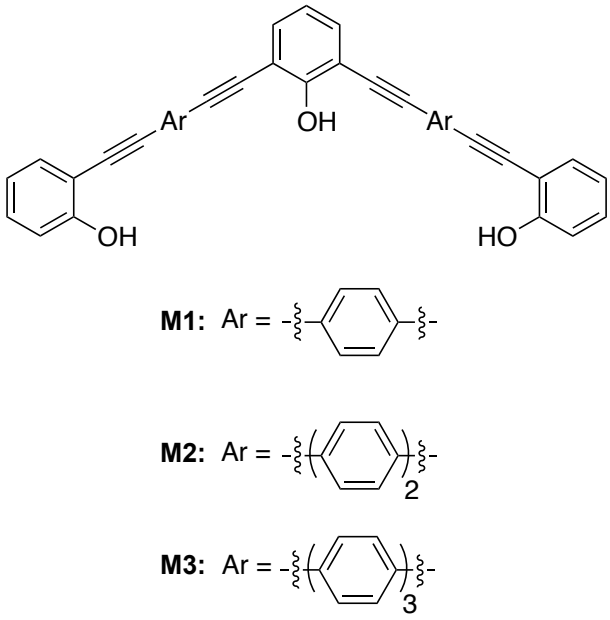

Chart 1. Structures of Model Compounds **M1**–**M3**

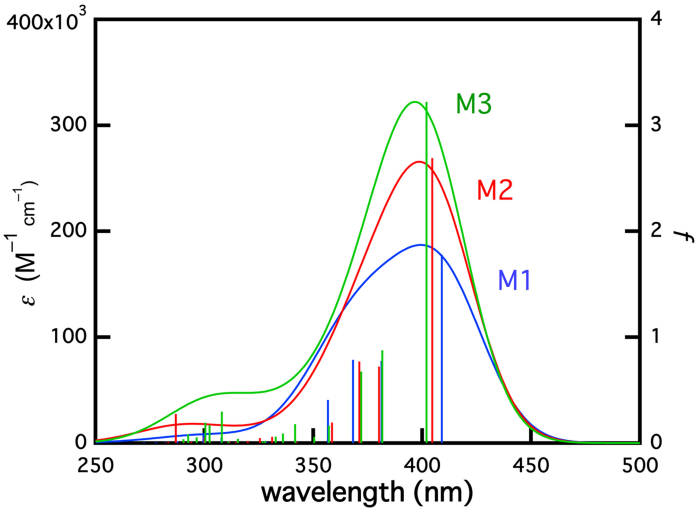

Figure 9. Excited-state parameters and UV–vis spectra simulated for **M1–M3.** The *f* values are predicted at the B3LYP/6–31+G* level in velocity form.

the phenylene moieties. The author examined the conformation of the polymers based on the molecular mechanics method (MMFF94).[59] The right- and left-handed helical conformations of a 24-mer of poly[(*S*)-**1**–**3a**] were constructed. The both chain ends were terminated with hydrogen atoms. The

torsional angles of main chains were set to –1° and +1° per phenylene unit for left- and right-handed helices at the initial geometries, respectively. After geometry optimization, the left-handed helical 24-mer was estimated to be 5.7 kJ/mol•unit more stable than the right-handed counterpart. Figure 10 shows the part of the optimized conformation of poly[(*S*)-**1**–**3a**] (left-handed helices). The amide of a monomer unit formed regulated intramolecular hydrogen bonds between *i*th and (*i* + 6)th units. The existence of intramolecular hydrogen bonds in this way agrees with the results of the solution state IR spectroscopic analysis, and the sign of the exciton coupling pattern[67] observed for poly[(*S*)-**1**–**3a**] in THF (first negative and second positive) agree with the favorability of left-handed helices compared with right-handed one. These results support the possibility of this conformation. The diameters of the pore (between inner edge carbon atoms at diagonal positions) is 25 Å and the helical pitch is 3.8 Å.

Morphological Analysis. As discussed above, the present polymers adopt stiff helical conformations in solution. They likely to keep regulated structures at the solid state as well in a fashion similar to some helical polymers such as poly(phenylacetylene)s[60,61] and poly(phenyleneethynylene)s.[29] A solid state sample of poly[(*R*)-**1**–**3a**] was analyzed by AFM to obtain morphological information (Figure 11).[62] Samples for AFM measurements were prepared by spin coating from the stock solutions of poly[(*R*)-**1**–**3a**] (0.5 mg mL^{-1}) in chloroform on freshly cleaved HOPG. After the polymers had been deposited on

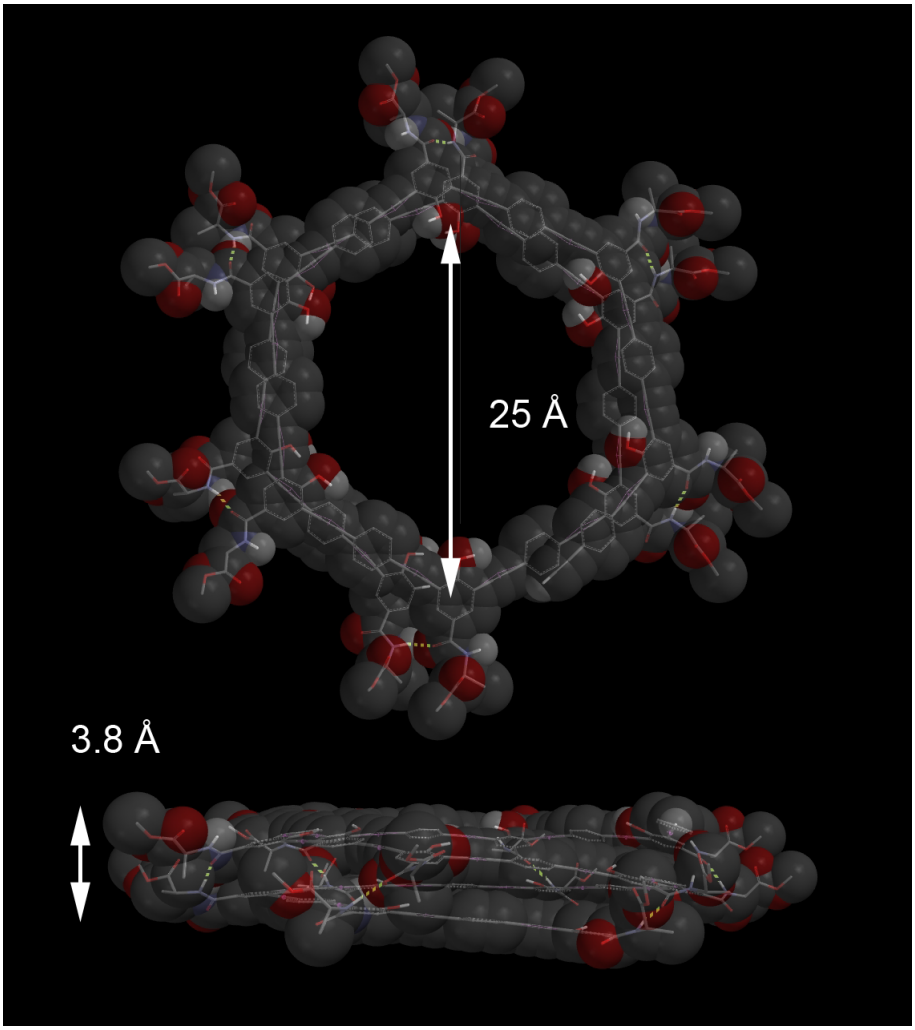

Figure 10. Side and top views of a possible conformation (left-handed helix) of poly[(*S*)-**1**–**3a**]-24-mer. CH_3 groups were employed in place of $C_{12}H_{25}$ groups to save CPU time.

the HOPG, the substrates were dried under reduced pressure for 2 h. Tube-like structures were observed together with periodic stripe patterns here and there. The diameters of the tubes were 4–5 nm, which approximately agree with the outside diameter: ca. 6.8 nm estimated by conformational analysis mentioned above. Judging from the M_n (= 7,000) of poly[(*R*)-**1**–**3a**], one polymer

molecule forms a helix with 2 turns. It is therefore considered that the helical polymer molecules are aggregated perpendicularly to form the tube-like structures. The driving force is considered to be intermolecular hydrogen bonding between the amide groups at the helix edges. Thus, the AFM observation provided support for the formation of folded helical structures of poly[(*R*)-**1**–**3a**], though the direct determination of screw sense was difficult.

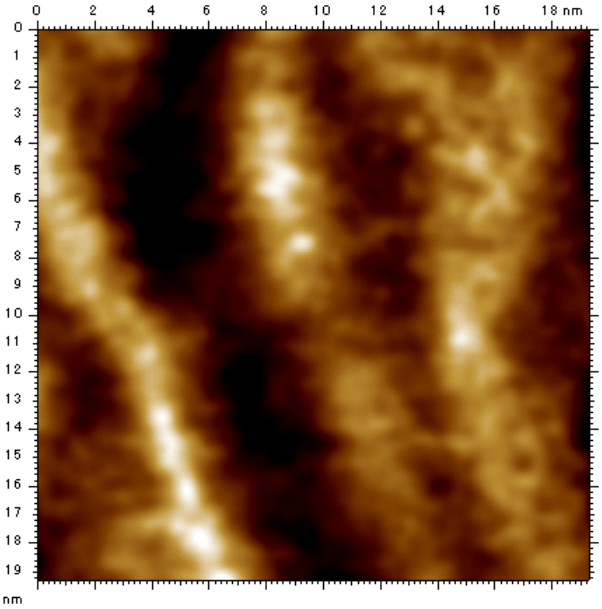

Figure 11. AFM phase image of poly[(*R*)-**1**–**3a**] on HOPG (scale 20 × 20 nm) prepared by spin coating from the stock polymer solutions (0.5 mg mL–1) in chloroform.

Conclusions

The author has demonstrated the synthesis of novel poly(*m*-phenyeleneethynylene-aryleneethynylene)s containing hydroxy groups {poly[(*S*)-/(*R*)-**1**–**3a**]–poly[(*S*)-**1**–**3e**] and poly[(*S*)-**2**–**3a**]} by the Sonogashira–

Hagihara coupling polymerization. Poly[(*S*)-/(*R*)-**1–3a**]–poly[(*S*)-**1–3c**] and poly[(*S*)-**2–3a**] exhibited intense CD signals at the absorption region of the conjugated main chains in THF both before and after membrane filtration, indicating that these polymers adopt predominantly one-handed helical structures in the solvent. Poly[(*S*)-**1–3a**] and poly[(*R*)-**1–3a**] exhibited mirror image Cotton effects, which means that the predominance of the helical structure were determined by the chirality of the amino acids. The CD signal patterns of poly[(*S*)-**1–3a**] in THF changed in different manners by the addition of MeOH, DMF and H_2O, presumably depends on the subtle hydrophobic/hydrophilic balance that are affected by interaction with solvent molecules. The formation of the aggregated structures in THF/H_2O mixture was confirmed by the DLS measurement. The solution state IR spectra revealed the presence of intramolecular hydrogen bonding between the amide groups of poly[(*S*)-**1–3a**], and the absence of intramolecular hydrogen bonding in poly[(*S*)-**1–3e**]. Poly[(*S*)-**1–3a**]–poly[(*S*)-**1–3c**] and poly[(*S*)-**2–3a**] showed blue fluorescence, while poly[(*S*)-**1–3d**] and poly[(*S*)-**1–3e**] showed excimer-base purplish fluorescence. Together with the results of CD spectroscopic analysis, it is concluded that poly[(*S*)-**1–3a**]–poly[(*S*)-**1–3c**] and poly[(*S*)-**2–3a**] preferably adopt helically folded conformations, and poly[(*S*)-**1–3d**] and poly[(*S*)-**1–3e**] preferably adopt *trans*-zigzag conformations. This is reasonably explained by the presence of long alkyl chains in the latter two polymers, which disturbs folding into compacted helical structures by the steric repulsion, and suitable

amphiphilic balance for helix formation. The different effect of alkyl chain length in poly[(*S*)-**1–3d**] and poly[(*S*)-**1–3e**] was apparently observed in the film states. Hexyl-group tethering poly[(*S*)-**1–3d**] emitted eximer-based fluorescence, but dodecyl-group tethering poly[(*S*)-**1–3e**] did not.

Further information about conjugation lengths of the polymers were obtained from the TD-DFT calculation of the **M1**–**M3**, which is the model compounds of the poly[(*S*)-**1**–**3a**]–poly[(*S*)-**1**–**3c**]. The Stimulated λ_{max} of **M1**–**M3** appears at as same wavelengths as observed one. The energy band gaps between HOMO and LUMO were almost identical, though the energy levels of HOMO and LUMO were different in every case. The conformational analysis of poly[(*S*)-**1**–**3a**] was performed using MM calculation. The results that left-handed helices were more stable than light-handed coincide with the sign of the exciton coupling pattern observed in THF. The existence of the hydrogen bonding between amide groups was also confirmed.

The tube-like structures of the polymer were observed by the AFM measurements. It is estimated that this tube-like structures were formed by the perpendicular aggregation of the helical polymers. AFM observation also provided support for the formation of folded helical structures of poly[(*R*)-**1**–**3a**].

Experimental Sections

Measurements. ^{1}H (400 MHz) and ^{13}C (100 MHz) NMR spectra were recorded on a JEOL EX-400 or a JEOL AL-400 spectrometer. IR spectra were

measured on a JASCO FT/IR-4100 spectrophotometer. Melting points (mp) were measured on a Yanaco micro melting point apparatus. Mass spectra were measured on a Thermo Scientific Exactive mass spectrometer. Specific rotations ($[\alpha]_D$) were measured on a JASCO DIP-1000 digital polarimeter. Number- and weight-average molecular weights (M_n and M_w) of polymers were determined by SEC (Shodex columns KF805 × 3) eluted with tetrahydrofuran (THF) calibrated by polystyrene standards at 40 °C. CD, UV–vis absorption, and fluorescence spectra were recorded on a JASCO J-820 and FP-750 spectropolarimeter. Dynamic light scattering (DLS) measurement were performed at 25°C using a Zetasizer Nano ZS (Malvern Instrunments Ltd., Worcestershire, UK) instrument to determine the size. The measured autocorrelation function was analyzed using a cumulant method. The hydrodynamic radius (R_h) of the polymer was calculated from the Stokes-Einstein equations. The AFM measurements were performed by using an Agilent 5100 microscope in air at ambient temperature with standard silicon cantilevers (NCH, NanoWorld, NeuchFtel, Switzerland) in the tapping mode. The Pico Image processing program was used for the image analysis.

Materials. Unless stated otherwise, reagents and solvents were purchased and used without purification. 4-[4,6-Dimethoxy-1,3,5-triazin-2-yl]-4-methylmorpholinium chloride (TRIAZIMOCH) and trimethylsilylacetylene were gifted from Tokuyama and Shin-Etsu Chemical. 4-Hydroxy-3,5-diiodobenzoic acid,[63]

p-diethynylbenzene (**3a**),[64] 4,4'-diethynylbiphenyl (**3b**), 4,4'-diiodo-*p*-terphenyl,[65] 1,4-dihexyl-2,5-diethnynylbenzene (**3d**),[66] 1,4-didodecyl-2,5-diiodobenzene[67] were synthesized according to the literature. Et_3N and *N,N*-dimethylformamide (DMF) used for polymerization were distilled prior to use.

Monomer Synthesis. *N-tert*-Butoxycarbonyl-L-alanine dodecyl ester. EDC•HCl (11.5 g, 60.0 mmol), 4-dimethylaminopyridine (DMAP) (0.732 g, 6.00 mmol), and 1-dodecanol (11.2 g, 60.0 mmol) were added to a solution of *N-tert*-butoxycarbonyl-L-alanine (9.45 g, 50.0 mmol) in CH_2Cl_2 (80ml) at 0 °C, and then the resulting mixture were stirred at room temperature overnight. It was washed with 0.5 M HCl, saturated $NaHCO_3$ aq., and saturated NaCl aq., dried over anhydrous $MgSO_4$, and then filtrated to afford *N-tert*-butoxycarbonyl-L-alanine dodecyl ester in quantitatively. The product was used in the next step without purification. ^{1}H NMR (400 MHz, $CDCl_3$): δ 0.88 (t, J = 7.2 Hz, 3H, –CH_2CH_3), 1.23–1.41 [m, 21H, –$OCH_2(CH_2)_9$–, –CH_3], 1.44 [s, 9H, –$C(CH_3)_3$], 1.63–1.65 (m, 2H, –CH_2CH_3), 4.06–4.18 [m, 2H, –$OCH_2(CH_2)_9$–], 4.26–4.29 (m, 1H, –CH–), 5.31 (br, 1H, –NH–). ^{13}C NMR (100 MHz, $CDCl_3$): δ 13.76 (–$CH_2CH_2CH_3$), 18.21 (–CH_3), 22.39 (–$CH_2CH_2CH_3$), 25.54 (–$CH_2CH_2CH_3$), 27.99 [–$C(CH_3)_3$], 28.94, 29.06, 29.22, 29.28, 29.34, 29.36, 29.40 [–$(CH_2)_7$–], 31.63 (–OCH_2CH_2–), 53.12 (–CH–), 62.31 (–OCH_2CH_2–), 79.18 [–$C(CH_3)_3$], 163.18 [–COOC$(CH_3)_3$], 173.11 (–COOCH_2–).

Dodecyl (*S*)-2-(4-hydroxy-3,5-diiodobenzamido)propanoate [(*S*)-1].

Trifluoroacetic acid (TFA, 10 mL, 135 mmol) was added to a solution of *N*-*tert*-butoxycarbonyl-L-alanine dodecyl ester (13.2 g, 35.5 mmol) in THF (15 mL) at 0 °C, and then the resulting mixture were stirred at room temperature overnight. The resulting solution was concentrated in vacuo to obtain L-alanine dodecyl ester trifluoroacetate salt as a viscous liquid. Triethylamine (7.00 mL, 50.2 mmol) was added to a solution of L-alanine dodecyl ester trifluoroacetate salt (3.71 g, 10.0 mmol) in THF, and then the resulting mixture was stirred at room temperature for 2 h. 4-Hydroxy-3,5-diiodobenzoic acid (3.89 g, 10.0 mmol) and TRIAZIMOCH (3.24 g, 10.0 mmol) were added to the solution subsequently, and the resulting mixture was stirred at room temperature overnight. It was washed with 1.0 M HCl, saturated $NaHCO_3$ aq., and saturated NaCl aq., dried over anhydrous $MgSO_4$, and then filtered. The filtrate was concentrated, and the residual mass was purified by silica gel column chromatography eluted with $CHCl_3$/hexane = 4/1 (v/v), followed by recrystallization to obtain dodecyl (*S*)-2-(4-hydroxy-3,5-diiodobenzamido)propanoate as a white solid in 26%. Mp 104–105 °C. $[\alpha]_D$ +14° (*c* = 0.10 g/dL, THF). IR (KBr): 3445, 3058, 2918, 1740, 1625, 1537, 1447, 1389, 1349, 1315, 1173, 1127, 765, 703 cm^{-1}. ^1H NMR (400 MHz, $CDCl_3$): δ 0.88 (t, *J* = 7.2 Hz, 3H, $–CH_2CH_3$), 1.23–1.52 [m, 21H, $–OCH_2(CH_2)_9–$, $–CH_3$], 1.63–1.65 (m, 2H, $–CH_2CH_3$), 4.14–4.20 [m, 2H, $–OCH_2(CH_2)_9–$], 4.71–4.75 (m, 1H, –C*H*–), 6.05 (br, 1H, –N*H*–), 6.58 (s, 1H, –O*H*), 8.12 (s, 2H, Ar). ^{13}C NMR (100 MHz, $CDCl_3$): δ 14.04 ($–CH_2CH_2CH_3$),

18.34 (–*C*H_3), 22.58 (–CH_2*C*H_2CH_3), 25.72 (–*C*$H_2CH_2CH_3$), 28.43, 29.10, 29.24, 29.28, 29.40, 29.46, 29.52 [–(*C*H_2)$_7$–], 31.81 (–OCH_2*C*H_2–), 48.61 (–*C*H–), 65.87 (–O*C*H_2CH_2–), 82.11, 129.48, 138.39, 156.39 (Ar), 163.44, (–NH*C*O–), 173.39 (–*C*$OOCH_2$–). Anal. Calcd for $C_{22}H_{33}I_2NO_4$: C, 41.99; H, 5.29; N, 2.23. Found: C, 41.71; H, 5.28; N, 2.19.

***N-tert*-Butoxycarbonyl-D-alanine dodecyl ester**. The title compound was synthesized from *N-tert*-butoxycarbonyl-D-alanine in a manner similar to *N-tert*-butoxycarbonyl-L-alanine. Quantitative yield (viscous liquid). ^{1}H NMR (400 MHz, $CDCl_3$): δ 0.88 (t, *J* = 7.2 Hz, 3H, –CH_2C*H*$_3$), 1.27–1.41 [m, 21H, –OCH_2(C*H*$_2$)$_9$–, –C*H*$_3$], 1.44 [s, 9H, –C(C*H*$_3$)$_3$], 1.63–1.65 (m, 2H, –C*H*$_2CH_3$), 4.10–4.14 [m, 2H, –OC*H*$_2$(CH$_2$)$_9$–], 4.26–4.29 (m, 1H, –C*H*–), 5.30 (br, 1H, –N*H*–). ^{13}C NMR (100 MHz, $CDCl_3$): δ 13.76 (–CH_2CH_2*C*H_3), 18.21 (–*C*H_3), 22.39 (–CH_2*C*H_2CH_3), 25.54 (–*C*$H_2CH_2CH_3$), 27.99 [–C(*C*H_3)$_3$], 28.94, 29.05, 29.21, 29.27, 29.33, 29.35, 29.41 [–(*C*H_2)$_7$–], 31.62 (–OCH_2*C*H_2–), 53.11 (–*C*H–), 62.10 (–O*C*H_2CH_2–), 79.03 [–*C*(CH$_3$)$_3$], 164.73 [–*C*OOC(CH$_3$)$_3$], 172.89 (–*C*$OOCH_2$–).

Dodecyl (*R*)-2-(4-hydroxy-3,5-diiodobenzamido)propanoate [(*R*)-1]. The title compound was synthesized from *N-tert*-butoxycarbonyl-D-alanine dodecyl ester in a manner similar to *N-tert*-butoxycarbonyl-L-alanine dodecyl ester**.** Yield 38% (white solid). Mp 104–106 °C. $[\alpha]_D$ –18° (*c* = 0.10 g/dL, THF). IR (KBr): 3445, 3057, 2918, 1740, 1625, 1537, 1446, 1389, 1348, 1315, 1173, 1127, 764, 702 cm^{-1}. ^{1}H NMR (400 MHz, $CDCl_3$): δ 0.87 (t, *J* = 6.8 Hz,

3H, –CH_2CH_3), 1.23–1.52 [m, 21H, –$OCH_2(CH_2)_9$–, –CH_3], 1.64–1.67 (m, 2H, –CH_2CH_3), 4.16–4.20 [m, 2H, –$OCH_2(CH_2)_9$–], 4.71–4.75 (m, 1H, –CH–), 6.12 (br, 1H, –NH–), 6.68 (s, 1H, –OH), 8.12 (s, 2H, Ar). ^{13}C NMR (100 MHz, $CDCl_3$): δ 14.17 (–$CH_2CH_2CH_3$), 18.71 (–CH_3), 22.27 (–$CH_2CH_2CH_3$), 25.86 (–$CH_2CH_2CH_3$), 28.57, 29.24, 29.38, 29.53, 29.59, 29.66, 29.67 [–$(CH_2)_7$–], 31.94 (–OCH_2CH_2–), 48.75 (–CH–), 65.96 (–OCH_2CH_2–), 81.98, 129.73, 138.24, 156.22 (Ar), 163.18 (–NHCO–), 173.14 (–$COOCH_2$–). Anal. Calcd for $C_{22}H_{33}I_2NO_4$: C, 41.99; H, 5.29; N, 2.23. Found: C, 41.71; H, 5.16; N, 2.15.

***N*-*tert*-Butoxycarbonyl-L-alanine dodecyl amide**. *N*-*tert*-Butoxycarbonyl- L-alanine (4.73 g, 25.0 mmol), dodecylamine (6.9 mL, 30.0 mmol) and TRIAZIMOCH (9.72 g, 30.0 mmol) were added to EtOAc (100 mL) subsequently, and the resulting mixture was stirred at room temperature overnight. It was washed with 1.0 M HCl, saturated $NaHCO_3$ aq., and saturated NaCl aq., dried over anhydrous $MgSO_4$, and then filtered. The filtrate was concentrated, and the residual mass was purified by silica gel column chromatography eluted with $CHCl_3$/hexane = 9/1 (v/v) to obtain *N*-*tert*-butoxycarbonyl- L-alanine dodecyl amide as a white solid in 53%. ^{1}H NMR (400 MHz, $CDCl_3$): δ 0.88 (t, *J* = 6.8 Hz, 3H, –CH_2CH_3), 1.23–1.36 [m, 21H, –$NHCH_2(CH_2)_9$–, –CH_3], 1.44 [s, 9H, –$C(CH_3)_3$], 1.48–1.59 (m, 2H, –CH_2CH_3), 3.15–3.23 [m, 2H, –$NHCH_2(CH_2)_9$–], 4.16–4.21 (m, 1H, –CH–), 5.42 (br, 1H, –NH–), 6.70 (br, 1H, –NH–). ^{13}C NMR (100 MHz, $CDCl_3$): δ 13.97 (–$CH_2CH_2CH_3$), 18.59 (–CH_3), 22.54 (–$CH_2CH_2CH_3$), 26.76 (–$CH_2CH_2CH_3$),

28.21 [–C(*C*H_3)$_3$], 29.19, 29.30, 29.42, 29.43, 29.47, 29.49, 29.52 [–(*C*H_2)$_7$–], 31.77 (–NHCH$_2$*C*H$_2$–), 39.36 (–NH*C*H$_2$CH$_2$–), 49.92 (–*C*H–), 79.63 [–*C*(CH$_3$)$_3$], 155.48 (–*C*ONH–), 172.63 [–*C*OOC(CH$_3$)$_3$].

(*S*)-*N*-(1-(dodecylamino)-1-oxopropan-2-yl)-4-hydroxy-3,4-diiodoben zamide [(*S*)-2]. The title compound was synthesized from *N*-*tert*-butoxycarbonyl-L-alanine dodecyl amide in a manner similar to *N*-*tert*-butoxycarbonyl-L-alanine dodecyl ester**.** Yield 26% (white solid). Mp 159–162 °C. $[\alpha]_D$ +4° (*c* = 0.10 g/dL, THF). IR (KBr): 3288, 3101, 2919, 1651, 1609, 1536, 1452, 1363, 1292, 1238, 1119, 686 cm^{-1}. (400 MHz, $CDCl_3$): δ 0.88 (t, *J* = 6.8 Hz, 3H, –CH$_2$C*H*$_3$), 1.24–1.28 [m, 21H, –NHCH$_2$(C*H*$_2$)$_9$–, –C*H*$_3$], 1.44–1.52 (m, 2H, –C*H*$_2$CH$_3$), 3.24–3.30 [m, 2H, –NHC*H*$_2$(CH$_2$)$_9$–], 4.58–4.62 (m, 1H, –C*H*–), 6.35 (br, 1H, –N*H*–). 7.00 (br, 1H, –N*H*–), 8.11 (s, 2H, Ar). ^{13}C NMR (100 MHz, $CDCl_3$): δ 14.03 (–CH$_2$CH$_2$*C*H$_3$), 18.79 (–*C*H$_3$), 22.64 (–CH$_2$*C*H$_2$CH$_3$), 26.89 (–*C*H$_2$CH$_2$CH$_3$), 29.27, 29.31, 29.48, 29.52, 29.56, 29.61, 29.62 [–(*C*H$_2$)$_7$–], 31.90 (–NHCH$_2$*C*H$_2$–), 39.83 (–NH*C*H$_2$CH$_2$–), 49.53 (–*C*H–), 82.09, 129.75, 138.46, 156.57 (Ar), 163.70 (–NH*C*O–), 172.14 (–*C*ONH–). High-resolution mass spectra (HRMS, *m*/*z*): [M – H]$^-$ calcd for $C_{22}H_{33}I_2N_2O_3$, 627.0581; found, 627.0594.

4,4'-Diethynyl-*p*-terphenyl (3c). 4,4'-Diiodo-*p*-terphenyl (5.79 g, 12.0 mmol), $PdCl_2(PPh_3)_2$ (0.842 g, 1.20 mmol), PPh_3 (1.36 g, 7.20 mmol), and CuI (1.37 g, 7.20 mmol) were fed into a two-neck flask, ant it was flushed with dry nitrogen. THF (40 mL) and triethylamine (15 mL) were added to the

solution, and then trimethylsilylacetylene (8.20 mL, 60.0 mmol) was added dropwise to the solution. The mixture was stirred at room temperature overnight. The resulting mixture was concentrated in vacuo and the residual mass was washed with Et_2O to extract the product. The organic phase was washed with 1.0 M HCl, and saturated NaCl aq., dried over anhydrous $MgSO_4$, and then filtered. The filtrate was concentrated, and the residual mass was purified by silica gel column chromatography eluted with hexane/$CHCl_3$ = 9/1 (v/v) to obtain 4,4'-bis(trimethylsilylethnyl)-*p*-terphenyl. After that, it was dissolved in $CHCl_3$ (60 mL) and a suspension of K_2CO_3 (6.63 g, 48.0 mmol) in MeOH (20 mL) was added to the solution. The resulting mixture was concentrated in vacuo, and the residual mass was dispersed in dispersed in $CHCl_3$ and water. The organic layer was washed with 1.0 M HCl, and saturated NaCl aq., dried over anhydrous $MgSO_4$, and then filtered. The filtrate was concentrated, and the residual mass was purified by preparative HPLC to obtain **3c** as a white solid in 2%. ^{1}H NMR (400 MHz, $CDCl_3$): δ 3.14 (s, 2H, –C≡C*H*), 7.57–7.68 (m, 12H, Ar). ^{13}C NMR (100 MHz, $CDCl_3$): δ 77.91 (–C≡*C*H), 83.50 (–*C*≡CH), 121.23, 126.88, 127.50, 132.65, 139.60, 140.87 (Ar).

1,4-Didodecyl-2,5-diethynylbenzene (3e). The title compound was synthesized from 1,4-didodecyl-2,5-diiodobenzene and trimethylsilylacetylene in a manner similar to **3c**. Yield 37% (white solid). Mp 54–56 °C. ^{1}H NMR (400 MHz, $CDCl_3$): δ 0.88 (t, *J* = 6.8 Hz, 6H, –CH_2CH_3), 1.27–1.41 [m, 36H, $CH_2(CH_2)_9$–], 1.59–1.61 (m, 4H, –CH_2CH_3), 2.70, [t, *J* = 7.2 Hz, 4H,

C*H*$_2$(CH$_2$)$_9$–], 3.27 (s, 2H, –C≡C*H*), 7.28 (s, 2H, Ar). ^{13}C NMR (100 MHz, $CDCl_3$): δ 14.19 (–CH$_2$*C*H$_3$), 22.76 (–*C*H$_2$CH$_3$), 29.41, 29.48, 29.50, 29.62, 29.71, 29.73, 29.75, 30.51, 31.98, 33.83 [–(*C*H$_2$)$_{10}$–], 81.49 (–C≡*C*H), 82.27 (–*C*≡CH), 121.86, 132.86, 142.62 (Ar).

Polymerization. All the polymerizations were carried out in a glass tube equipped with a three-way stopcock under nitrogen. A typical experimental procedure for polymerization **(*S*)-1** with **2a** is given as follows: A solution of **(*S*)-1** (188 mg, 0.300 mmol), **2a** (37.8 mg, 0.300 mmol), Pd(PPh$_3$)$_2$Cl$_2$ (10.5 mg, 0.015 mmol), CuI (11.8 mg, 0.045 mmol), PPh_3 (5.70 mg, 0.030 mmol), and Et_3N (1.2 mL) in DMF (1.8 mL) was stirred at 80 °C for 24 h. The resulting mixture was poured into MeOH/acetone [9/1 (v/v), 300 mL] to precipitate a polymer. It was separated by filtration using a membrane filter (ADVANTEC H100A047A) and dried under reduced pressure.

Spectroscopic Data of the Polymers. Poly[(*S*)-1–3a]: $[\alpha]_D$ +55° (*c* = 0.100 g/dL, THF). IR (KBr): 3338, 3064, 2925, 2852, 2208, 1735, 1654, 1509, 115, 838, 753, 518 cm^{-1}. ^{1}H NMR (400 MHz, $CDCl_3$): δ 0.81–0.90 (br, 3H, –CH$_2$C*H*$_3$), 1.21–1.34 [br, 21H, –OCH$_2$(C*H*$_2$)$_9$–, –C*H*$_3$], 1.58–1.73 (br, 2H, –C*H*$_2$CH$_3$), 4.10–4.31 [br, 2H, –OC*H*$_2$(CH$_2$)$_9$–], 4.70–4.95 (br, 1H, –C*H*–), 6.50–8.07 (br, 8H, –N*H*–, –O*H*, Ar). **Poly[(*R*)-1–3a]**: $[\alpha]_D$ –98° (*c* = 0.096 g/dL, THF). IR (KBr): 3423, 3339, 2923, 2852, 2208, 1736, 1654, 1509, 1455, 1262, 1176, 1092, 838, 753 cm^{-1}. ^{1}H NMR (400 MHz, $CDCl_3$): δ 0.78–0.87 (br, 3H, –CH$_2$C*H*$_3$), 1.15–1.34 [br, 21H, –OCH$_2$(C*H*$_2$)$_9$–, –C*H*$_3$], 1.50–1.65 (br, 2H, –

C*H*$_2$CH$_3$), 4.13–4.28 [br, 2H, –OC*H*$_2$(CH$_2$)$_9$–], 4.72–4.92 (br, 1H, –C*H*–), 6.39–8.10 (br, 8H, –N*H*–, –O*H*, Ar). **Poly[(*S*)-1–3b]**: $[\alpha]_D$ –27° (*c* = 0.098 g/dL, THF). IR (KBr): 3422, 3034, 2923, 2852, 2208, 1735, 1654, 1509, 1175, 821, 754 cm^{-1}. ^{1}H NMR (400 MHz, $CDCl_3$): δ 0.78–0.90 (br, 3H, –CH$_2$C*H*$_3$), 1.15–1.34 [br, 21H, –OCH$_2$(C*H*$_2$)$_9$–, –C*H*$_3$], 1.51–1.72 (br, 2H, –C*H*$_2$CH$_3$), 4.13–4.28 [br, 2H, –OC*H*$_2$(CH$_2$)$_9$–], 4.72–4.92 (br, 1H, –C*H*–), 6.45–8.08 (br, 12H, –N*H*–, –O*H*, Ar). **Poly[(*S*)-1–3c]**: IR (KBr): 3422, 3031, 2922, 2211, 1735, 1654, 1509, 1489, 1457, 1174, 1003, 815, 754 cm^{-1}. ^{1}H NMR (400 MHz, $CDCl_3$): δ 0.80–0.90 (br, 3H, –CH$_2$C*H*$_3$), 1.15–1.31 [br, 21H, –OCH$_2$(C*H*$_2$)$_9$–, –C*H*$_3$], 1.61–1.73 (br, 2H, –C*H*$_2$CH$_3$), 4.13–4.26 [br, 2H, –OC*H*$_2$(CH$_2$)$_9$–], 4.72–4.92 (br, 1H, –C*H*–), 6.46–8.19 (br, 16H, –N*H*–, –O*H*, Ar). **Poly[(*S*)-1–3d]**: $[\alpha]_D$ +33° (*c* = 0.094 g/dL, THF). IR (KBr): 3339, 2923, 2853, 2208, 1736, 1646, 1526, 1457, 1176, 1090, 899, 754 cm^{-1}. ^{1}H NMR (400 MHz, $CDCl_3$): δ 0.71–0.88 (br, 9H, –CH$_2$C*H*$_3$), 1.20–1.44 [br, 33H, –OCH$_2$(C*H*$_2$)$_9$–, –CH$_2$(C*H*$_2$)$_3$–, –C*H*$_3$], 1.54–1.72 (br, 6H, –C*H*$_2$CH$_3$), 2.87–3.00 [br, 4H, –C*H*$_2$(CH$_2$)$_3$–], 4.12–4.27 [br, 2H, –OCH$_2$(C*H*$_2$)$_9$–], 4.76–4.90 (br, 1H, –C*H*–), 6.80–7.02 (br, 2H, –N*H*–, –O*H*), 7.35–7.55, 7.60–7.70, 8.07–8.13, 8.17–8.19 (br, 4H, Ar). **Poly[(*S*)-1–3e]**: $[\alpha]_D$ +23° (*c* = 0.097 g/dL, THF). IR (KBr): 3348, 2923, 2208, 1736, 1654, 1603, 1527, 1176, 1091, 898, 754 cm^{-1}. ^{1}H NMR (400 MHz, $CDCl_3$): δ 0.67–0.88 (br, 9H, –CH$_2$C*H*$_3$), 1.05–1.37 [br, 57H, –OCH$_2$(C*H*$_2$)$_9$–, –CH$_2$(C*H*$_2$)$_9$–, –C*H*$_3$], 1.54–1.78 (br, 4H, –C*H*$_2$CH$_3$), 2.85–3.02 [br, 4H, –C*H*$_2$(CH$_2$)$_3$–], 4.15–4.23 [br, 2H, –OCH$_2$(C*H*$_2$)$_9$–], 4.80–4.87 (br, 1H, –C*H*–), 6.82–7.02 (br, 2H, –N*H*–, –O*H*),

7.40–7.58, 7.68–7.78, 7.91–7.99, 8.06–8.14 (br, 4H, Ar). **Poly[(*S*)-2–3a]**: $[\alpha]_D$ –150° (*c* = 0.090 g/dL, THF). IR (KBr): 3298, 2922, 2851, 2208, 1639, 1509, 1456, 1342, 1177, 1098, 837, 753 cm^{-1}. ^1H NMR (400 MHz, $CDCl_3$): δ 0.78–0.96 (br, 3H, $–CH_2CH_3$), 1.15–1.34 [br, 21H, $–NHCH_2(CH_2)_9–$, $–CH_3$], 1.57–1.66 (br, 2H, $–CH_2CH_3$), 3.13–3.48 [br, 2H, $–NHCH_2(CH_2)_9–$], 4.56–4.78 (br, 1H, –CH–), 6.09–8.21 [br, 9H, –NH–, $–NHCH_2(CH_2)_9–$, –OH, Ar].

References and Notes

(1) For a review, see: Yahima, E.; Maeda, K.; Iida, H.; Furusho, Y.; Nagai, K. *Chem. Rev.* **2009**, *109*, 6102–6211.

(2) For a review, see: Schwartz, E.; Koepf, M.; Kitto, H. J.; Nolte, R. J. M.; Rowan, A. E. *Polym. Chem.* **2011**, *2*, 33–47.

(3) For a review, see: Sato, T.; Terao, K.; Teramoto, A.; Fujiki, M. *Polymer* **2003**, *44*, 5477–5495.

(4) For a review, see: Hill, D. J.; Mio, M. J.; Prince, R. B.; Hughes, T. S.; Moore, J. S. *Chem Rev* **2001**, *101*, 4013–4018.

(5) For a review, see: Masuda, T. *J. Polym. Sci., Part A: Polym. Chem.* **2007**, *45*, 165–180.

(6) Abe, H.; Okada, K.; Makida, H.; Inouye, M. *Org. Biomol. Chem.* **2012**, *10*, 6930–6936.

(7) Smaldone, R. A.; Moore, J. S. *J. Am. Chem. Soc.* **2007**, *129*, 5444–5450.

(8) Ferrand, Y.; Chandramouli, N.; Kendhale, A. M.; Aube, C.; Kauffmann, B.; Grelard, A.; Laguerre, M.; Dubreuil, D.; Huc, I. *J. Am. Chem. Soc.* **2012**, *134*, 11282–11288.

(9) Tamura, K.; Miyabe, T.; Iida, H.; Yashima, E. *Polym. Chem.* **2011**, *2*, 91–98.

(10) Terada, K.; Masuda, T.; Sanda, F. *J. Polym. Sci., Part A: Polym. Chem.* **2009**, *47*, 2596–2602.

(11) Ikeda, A; Terada, K.; Shiotsuki, M.; Sanda, F. *J. Polym. Sci., Part A: Polym.*

Chem. **2011**, *49*, 3783–3796.
(12) Yu, A.; Yamamoto, T.; Nagata, Y.; Ohmura, T.; Suginome, M. *J. Am. Chem. Soc.* **2012**, *134*, 11098–11095.
(13) Tang, Z.; Iida, H.; Hu, H.; Yahima, E. *ACS Macro Lett.* **2012**, *1*, 261–265.
(14) Zhang, D.; Ren, C.; Yang, W.; Deng, J. *Macromol. Rapid Commun.* **2012**, 1, 261–265.
(15) Goto, H.; Furusho, Y.; Yashima E. *Chem Commun.* **2009**, 1650–1652.
(16) Peter, K.; Nilsson, R; Inganäs, O. *Nat. Mater.* **2003**, *6*, 419–424.
(17) Sogawa, H.; Shiotsuki, M.; Sanda, F. *J. Polym. Sci., Part A: Polym. Chem.* **2012**, *50*, 2008–2018.
(18) Suk, J.; Kim, D. A.; Jeong, K. *Org. Lett.* Doi: 10.1021/ol31022148.
(19) Nelson, J. C.; Saven, J. G.; Moore, J. S.; Wolynes, P. G. *Science*, **1997**, *277*, 1793–1796.
(20) Prince, R. B; Saven, J. G.; Wolynes, P. G.; Moore, J. S. *J. Am. Chem. Soc.* **1999**, *121*, 3114–3121.
(21) Matsuda, K.; Stone, M. T.; Moore, J. S. *J. Am. Chem. Soc.* **2002**, *124*, 11836–11837.
(22) Khan, A.; Hecht, S. *Chem. Eur. J.* **2006**, *12*, 4764–4774.
(23) Wackerly, J. W.; Moore, J. S. *Macromolecules* **2006**, *39*, 7269–7276.
(24) Zhao, X.; Schanze, K. S. *Langmuir* **2006**, *22*, 4856–4862.
(25) Balbo Block, M. A.; Hecht, S. *Macromolecules* **2008**, *41*, 3219–3227.
(26) Zhang, Z.; Che, Y.; Smaldone, R. A.; Xu, M.; Bunes, B. R.; Moore, J. S.; Zang, L. *J. Am. Chem. Soc.* **2010**, *132*, 14113–14117.
(27) Takashima, S.; Abe, H.; Inouye, M. *Chem. Commun.* **2012**, 48, 3330–3332.
(28) Chen, Y.; Malkovskiy, A.; Wang, X.; Lebron-Colon, M.; Sokolov, A. P.; Perry, K.; More, K.; Pang, Y. *ACS Macro Lett.* **2012**, *1*, 246–251.
(29) Banno, M.; Yamaguchi, T.; Nagai, K.; Kaiser, C.; Hecht, S.; Yashima, E. *J. Am. Chem. Soc.* **2012**, *134*, 8718–8728.
(30) Liu, R.; Shiotsuki, M.; Masuda, T.; Sanda, F. *Macromolecules* **2009**, *42*, 6115–6122.
(31) Liu, R.; Sogawa, H.; Shiotsuki, M.; Masuda, T.; Sanda, F. *Polymer* **2010**, *51*, 2255–2263.
(32) Sogawa, H.; Shiotsuki, M.; Matsuoka, H.; Sanda, F. *Macromolecules* **2011**,

44, 3338–3345.

(33) Hashimoto, A.; Sogawa, H.; Shiotsuki, M.; Sanda, F. *Polymer* **2012**, *53*, 2559–2566.

(34) Meier, H.; Stalmach, U.; Kolshorn, H. *Acta Polym.* **1997**, *48*, 379–384.

(35) Grimme, J.; Kreyenschmidt, M.; Uckert, F.; Müllen, K.; Scherf, U. *Adv. Mater.* **1995**, *7*, 292–295.

(36) Banerjee, M.; Shukla, R.; Rathore, R. *J. Am. Chem. Soc.* **2009**, *131*, 178–1786.

(37) Harada, I.; Tasumi, M.; Shirakawa, H.; Ikeda, S. *Chem. Lett.* **1978**, 1411–1414.

(38) Shiotsuki, M.; Kumazawa, S.; Onishi, N.; Sanda, F. *J. Polym. Sci., Part A: Polym. Chem.* **2011**, *49*, 4921–4925.

(39) The membrane filtration of solutions of conjugated polymers is effective to remove aggregate. See Yamamoto, T.; Komarudin, D.; Arai, M.; Lee, B. L.; Suganuma, H.; Asakawa, N.; Inoue, Y.; Kubota, K.; Sasaki, S.; Fukuda, T.; Matsuda, H. *J. Am. Chem. Soc.* **1998**, *120*, 2047–2058.

(40) Langeveld-Voss, B. M. W.; Peeters, E.; Janssen, R. A. J.; Meijer, E. W. *Synth. Met.* **1997**, *84*, 611–614.

(41) Van den Bergh, K.; Cosemans, I.; Verbiest, T.; Koeckelberghs, G. *Macromolecules* **2010**, *43*, 3794–3800.

(42) Goto, H.; Yokochi, Y.; Yashima, E. *Chem. Commun.* **2012**, *48*, 3291–3293.

(43) Satrijio, A.; Meskers, S. C. J.; Swager, T. M. *J. Am. Chem. Soc.* **2006**, *128*, 9030–9031.

(44) Traiphol, R.; Charoenthai, N.; Srikhirin, T.; Kerdcharoen, T.; Osotchan, T.; Maturos, T. *Polymer* **2007**, *48*, 813–826.

(45) Chen, Y.; Lv, Y.; Han, Y.; Zhu, B.; Zhang, F.; Bo, Z.; Liu, C. *Lungmuir* **2009**, *25*, 8548–8555.

(46) The author also tried unsuccessfully to synthesize relevant polymers containing *p*-quoterphenylene units, because of the low solubility of the monomer. 4,4’’’-Diiodo-*p*-quoterphenyl, a precursor of the diyne monomer, was insoluble in common organic solvents and difficult to handle.

(47) Tan, C.; Pinto, M. R.; Kose, M. E.; Ghiviriga, I.; Schanze, K. S. *Adv. Mater.* **2004**, *14*, 1208–1212.

(48) Fujiki, M. *Macromol. Rapid Commun.* **2001**, *22*, 539–563.
(49) Zhu, N.; Yan, Q.; Luo, Z.; Zhai, Y.; Zhao, D. *Chem. Asian J.* **2012**, *7*, 2386–2393.
(50) Cary, J. M.; Moore, J. S. *Org. Lett.* **2002**, *4*, 4663–4666.
(51) Yang, X.; Brown, A. L.; Furukawa, M.; Li, S.; Gardinier, W. E.; Bukowski, E. J.; Bright, F. V.; Zheng, C.; Zeng, X. C.; Gong, B. *Chem. Commun.* **2003**, 56–57.
(52) This concentration is low enough to eliminate the effect of intermolecular hydrogen bonding.
(53) The fluorescence intensity of poly[(*S*)-**1–3a**] only slightly decreased as increasing the MeOH composition in THF/MeOH mixtures. No excimer-based fluorescence appeared.
(54) The same fluorescent colors were observed from spin-coated films.
(55) Wide-angle X-ray diffraction (WAXD) measurements of the polymer films were performed to unsuccessfully obtain evidence for structural difference between poly[(*S*)-**1–3e**] and poly[(*S*)-**1–3d**].
(56) Adisa, B.; Bruce, D. A. *J. Phys. Chem. B* **2005**, *109*, 7548–7556.
(57) Adisa, B.; Bruce, D. A. *J. Phys. Chem. B* **2005**, *109*, 19952–19959.
(58) Lee, O. S.; Saven, J. G. *J. Phys. Chem. B* **2004**, *108*, 11988–11994.
(59) Halgre, T. A. *J. Comput. Chem.* **1996**, *17*, 490–519. The molecular mechanics calculations were carried out with Wavefunction, Inc., Spartan ’10 Macintosh.
(60) *Circular Dichronism Principles and Applications*, 2nd ed.; Beroya, N., Nakanishi, K. Woody, R. W., Eds.; Wiley-VCH: New York, 2000; Chapter 12.
(61) Sakurai, S.; Ohsawa, S.; Nagai, K.; Okoshi, K.; Kumaki, J.; Yashima, E. *Angew. Chem. Int. Ed.* **2007**, *46*, 7605–7608.
(62) Ohsawa, S.; Sakurai, S.; Nagai, K.; Banno, M.; Maeda, K.; Kumaki, J.; Yashima, E. *J. Am. Chem. Soc.* **2011**, *133*, 108–114.
(63) Li, C.; Guo, Y.; Lv, J.; Xu, J.; Li, Y.; Wang, S.; Liu, H.; Zhu, D. *J. Polym. Sci., Part A: Polym. Chem.* **2006**, *45*, 1403–1412.
(64) Takahashi, S.; Kuroyama, Y.; Sonogashira, K.; Hagihara, N. *Synthesis* **1980**, *8*, 627–629.

(65) Iwamoto, T.; Watanabe, Y.; Sakamoto, Y.; Suzuki, T.; Yamago, S. *J. Am. Chem. Soc.* **2011**, *133*, 8354–8361.

(66) Mössinger, D.; Jester, S.; Sigmund, E.; Müller, U.; Höger, S. *Macromolecules* **2009**, *42*, 7974–7978.

(67) Schaate, A.; Roy, P.; Preuβe, T.; Lohmeier, S. J.; Godt, A.; Behrens, P. *Chem. Eur. J.* **2011**, *17*, 9320–9325.

Chapter 2

Synthesis of Optically Active Poly(*m*-phenyleneethynylene-aryleneethynylene)s Bearing Hydroxy Groups with Various Conjugation Lengths and Examination of the Higher Order Structure

Abstract

Novel optically active poly(phenyleneethynylene-aryleneethynylene)s bearing hydroxy groups with various arylene units [poly(**1**–**2a)**, poly(**1**–**2b**) and poly(**1**–**3**)] were synthesized by the Sonogashira–Hagihara coupling polymerization of (*S*)-3,5-diiodo-4-hydroxy-$C_6H_4CONHCH(CH_3)COOC_{12}H_{25}$ (**1**) with HC≡C-Ar-C≡CH [**2a** (Ar = 2,7-naphthylene), **3b** (Ar = 1,4-naphthylene), **3** (Ar = 1,6-pyrenylene), and the optical properties were compared with those of 1,4-phenylene counterpart [poly(**1**–**4**)]. Polymers with number-average molecular weights (M_n) of 5,300–11,300 were obtained in 88–94% yields. CD and UV–vis spectroscopic analysis revealed that all the polymers formed predominantly one-handed helical structures in THF. The order of absorption maxima (λ_{max}) of the polymers was poly(**1**–**2a)** < poly(**1**–**4**) < poly(**1**–**2b**) < poly(**1**–**3**). Poly(**1**–**2a),** poly(**1**–**2b**) and poly(**1**–**3**) emitted blue, green and yellow fluorescence, respectively.

Introduction

Conjugated polymers with regulated higher order structures show useful properties including molecular recognition, chiral catalysis and chemical sensing together with electronic and optical properties.[1] Poly(phenyleneethynylene) is one of typical conjugated polymers that have a nature to adopt a folded helical conformation. *m*-Linked oligo(phenyleneethynylene)s bearing tetraethylene glycol moieties at the side chains are folded into helices in polar solvents such as acetonitrile/water based on the amphiphilicity originating from the hydrophilic side chains and hydrophobic main chains.[2] Many efforts have been made to synthesize such helical phenyleneethynylene polymers, and to investigate the chiroptical properties.[3–15] It has recently revealed that D-hydroxyphenylglycine- and L-tyrosine-derived poly(*m*-phenyleneethynylene-*p*-phenyleneethynylene)s form helically folded structures due to p-stacking between phenylene moieties, intramolecular hydrogen bonding between the amide groups at the side chains, and amphiphilicity caused by hydrophobic exterior (alkyl groups and phenyleneethynylene main chain) and hydrophilic interior (hydroxy groups).[16–19] It is noteworthy that the amphiphilic balance of these polymers is opposite from that of typical helically folded poly(*m*-phenyleneethynylene) derivatives reported so far.

Naphthalene[20,21] and pyrene[22,23] are flat-shaped aromatic molecules that gather much interest because of their photoelectric functions. Extension of

conjugation length is expected by introducing these condensed aromatic rings into the main chains of π-conjugated polymers, when the aromatics are linked at proper positions.[24–29] For instance, 1,4-naphthylene and 1,6-pyrenylene linkages are effective for this purpose,[25,26,28,29] while 2,7-naphthylene linkage is not because of its kinked structure and inefficient resonance.[30] There are several reports on the synthesis of π-conjugated polymers containing pyrene moieties at the main chains,[27–29] and also optically active helical polymers containing pyrene moieties at the side chains.[31–35] Nevertheless, there is no report concerning chiral conjugated polymers containing pyrene moieties at the main chains as far as the author knows.

In this chapter, the author discusses synthesis of novel optically active poly(phenyleneethynylene-napthyleneethynylene)s and poly(pheyleneethynylene-pyrenyleneethynylene)s containing hydroxy groups by the Sonogashira–Hagihara coupling polymerization of the corresponding monomers (Scheme 1). The author further discusses the effects of naphthylene and pyrenylene units on the chiroptical and fluorescence properties, conjugation length of the polymers, and secondary structures based on CD, UV–vis and fluorescence spectroscopic analysis together with DFT calculations.

Scheme 1. Sonogashira–Hagihara Coupling Polymerization of Diiodophenylene Monomer **1** with Diethynylarylene Monomers **2a**, **2b** and **3**.

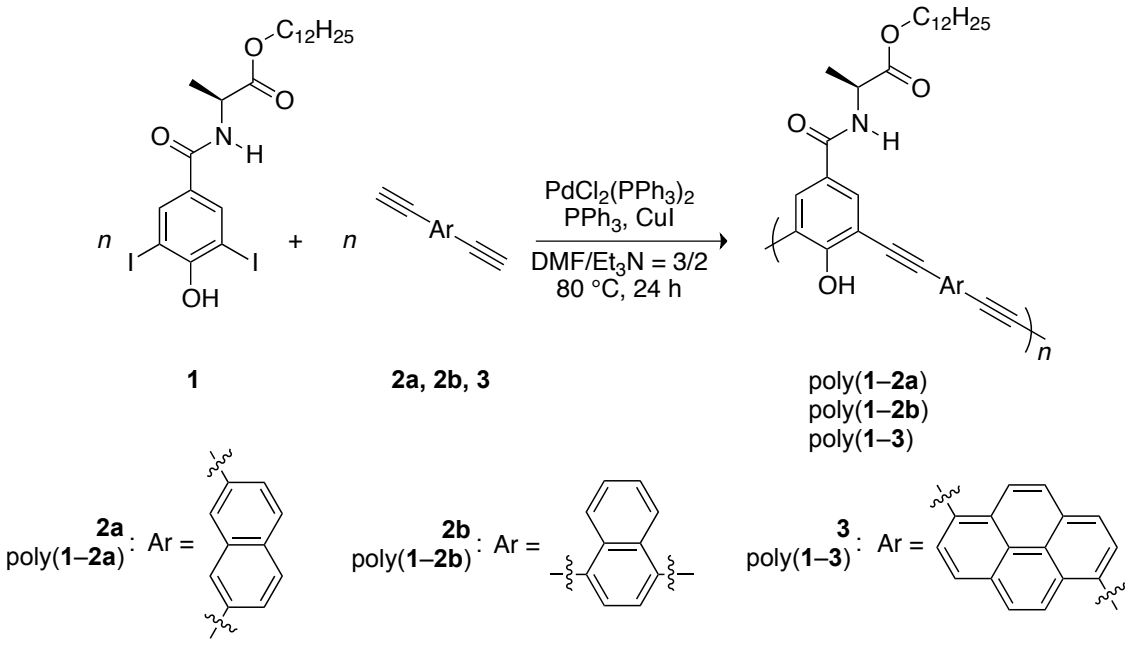

Results and Discussion

Polymerization. The Sonogashira–Hagihara coupling polymerization of diiodophenylene monomer **1** with diethynylarylene monomers **2a**, **2b** and **2c** was performed in DMF at 80 °C for 24 h to obtain the corresponding polymers [poly(**1**–**2a**), poly(**1**–**2b**) and poly(**1**–**3**)] with moderate molecular weights (M_n) in the range of 5,300–11,300 in 88–94% yields (Table 1). The M_n of poly(**1**–**2a**) was relatively low, probably due to the steric hindrance caused by the 2,7-naphthylene linkage. Poly(**1-2a**) and poly(**1-2b**) were soluble in common organic solvents such as CH_2Cl_2, $CHCl_3$, THF, DMSO and DMF. On the other hands, poly(**1-3**) was insoluble in CH_2Cl_2, and partly insoluble in $CHCl_3$, DMSO and DMF.

Table 1. Sonogashira–Hagihara coupling polymerization of **1** with **2a**, **2b** and **3**[a]

monomer	polymer			
		yield[b] (%)	M_n[c]	M_w/M_n[c]
1 + **2a**	poly(**1**–**2a**)	94	5,300	2.1
1 + **2b**	poly(**1**–**2b**)	88	7,500	1.4
1 + **3**	poly(**1**–**3**)	90	11,300	1.3
1 + **4**	poly(**1**–**4**)	90	11,300	1.3

[a] conditions: $[\mathbf{1}]_0 = [\mathbf{2a}]_0 = [\mathbf{2b}]_0 = [\mathbf{3}]_0 = [\mathbf{4}]_0 = 0.10$ M, $[PdCl_2(PPh_3)_2] = 0.0050$ M, [CuI] = 0.0025, $[PPh_3] = 0.0010$ M, DMF/Et_3N = 3/2 (v/v), 80 °C, 24 h. [b] Insoluble part in MeOH/acetone = 9/1 (v/v). [c] Estimated by SEC measured in THF, polystyrene calibration.

Chiroptical Properties of the Polymers. Figure 1 shows the CD and UV–vis spectra of the polymers measured in THF, together with 1,4-phenylene linked poly(**1**–**4**) (Chart 1) for comparison. Poly(**1**–**2a**), poly(**1**–**4**), poly(**1**–**2b**) and poly(**1**–**3**) exhibited CD signals at the absorption regions of the main chain chromophores around 250–350, 280–400, 300–450 and 350–500 nm, respectively. The CD and UV–vis signals were intact after filtering the polymer solutions using a membrane filter with a pore size of 0.45 mm. It is supposed that the CD signals do not originate from chiral aggregation but unimolecular chirality, i.e., folded helical conformations with predominantly one-handed screw sense.[36] The absorption maxima (λ_{max}) differed according to the arylene units. The λ_{max} of 2,7-naphthylene linked poly(**1**–**2a**) is the shortest (320 nm) among the four polymers, presumably due to the most kinked linkage structure. The λ_{max}'s of 1,4-naphthylene linked poly(**1**–**2b**) and 1,6-pyrenylene-linked poly(**1**–**3**) are 25 and 50 nm longer than that of poly(**1**–**4**), respectively, indicating the

longer conjugation length as predicted from the condensed aromatic rings with the linkages parallel to the main chains.

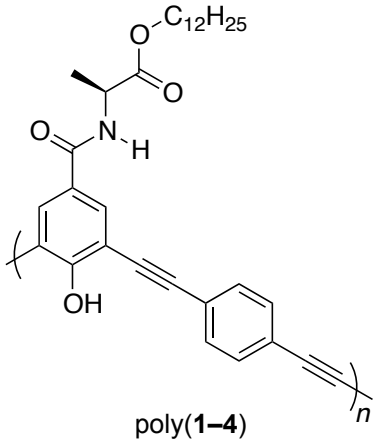

poly(**1–4**)

Chart 1. Structure of Poly(**1**–**4**).

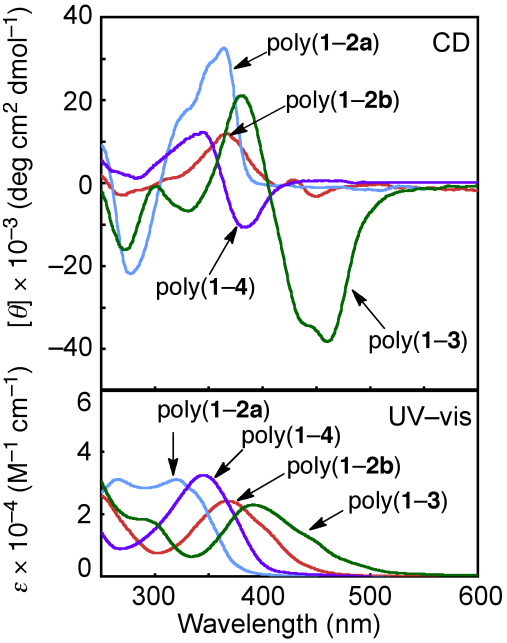

Figure 1. CD and UV–vis spectra of poly(**1**–**2a**), poly(**1**–**2b**), poly(**1**–**3**) together with poly(**1**–**4**) measured in THF (c = 0.03 mM) at 20 °C.

The author examined the thermal stability of helical conformation of the polymers. Figure 2 shows the $[\theta]_{max}$ values measured in THF at various

temperatures. The $[\theta]_{max}$ of poly(**1**–**3**) only decreased 3% by raising temperature from 0 to 60 °C, while those of poly(**1**–**2a**) and poly(**1**–**2b**) decreased 28 and 62%, respectively. The temperature-responsive change was reversible for poly(**1**–**3**), but irreversible for poly(**1**–**2a**) and poly(**1**–**2b**). The stabilities of conformations of the polymers are largely different. The UV–vis signals of poly(**1**–**2a**) and poly(**1**–**2b**) changed upon heating simultaneously with the CD change. It is likely that the folded helical structures were disrupted, and turned into different structures such as *trans*-zigzag form as increasing the temperature. Once this thermo-induced transformation occurred, refolding into helices seems to be difficult.

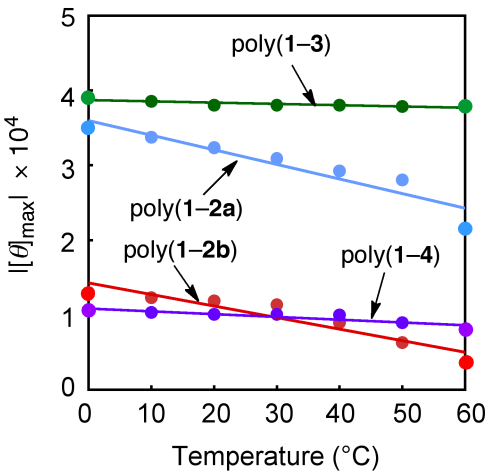

Figure 2. Plot of $|[\theta]_{max}|$ value of poly(**1**–**2a**), poly(**1**–**2b**), poly(**1**–**3**) measured in THF at various temperature (c = 0.03 mM).

The author next examined the solvent effect on the conformation of the polymers. Poly(**1**–**3**) exhibited almost the same CD signals in THF/MeOH

mixtures irrespective of the composition, though the λ_{max} was slightly blue-shifted as increasing the MeOH content. Poly(**1**–**2a**) exhibited the same trend regarding the solvent effect. On the other hands, poly(**1**–**2b**) diminished the CD signal intensity as increasing the MeOH content. The shape of the UV–vis signals of poly(**1**–**2b**) observed in THF/MeOH = 8/2 mixture almost coincided with that observed at 60 °C in THF. Poly(**1**–**2b**) seems to turn into another structure presumably *trans*-zigzag form not only by heating but also by raising MeOH content. These results indicate that all the polymers are folded into helical structures in THF, and the responsiveness to temperature and solvent depends on the structure of arylene unit and linking positions.

The fluorescence spectra of the polymers were measured in THF excited at the main chain-based absorption maxima (Figure 3). The fluorescence spectroscopic data are listed in Table 2. Poly(**1**–**2a**), poly(**1**–**4**), poly(**1**–**2b**) and poly(**1**–**3**) emitted purplish blue, blue green and yellow fluorescence (Figure 4). The emission maximum was red-shifted in consonance with the red-shift of the λ_{max}. The polymers emitted variously colored fluorescence depending on the arylene units.

Table 2. Optical data of the polymers[a]

polymer	λ_{abs} (nm)	λ_{emi} (nm)	Φ_{emi}[b]
poly(**1**–**2a**)	320	408	0.19
poly(**1**–**2b**)	367	504	–
poly(**1**–**3**)	392	535	–
poly(**1**–**4**)	342	446	0.31

[a] Measured in THF. [b] Measured using anthracene as a standard in EtOH (Φ_{emi} = 0.27).

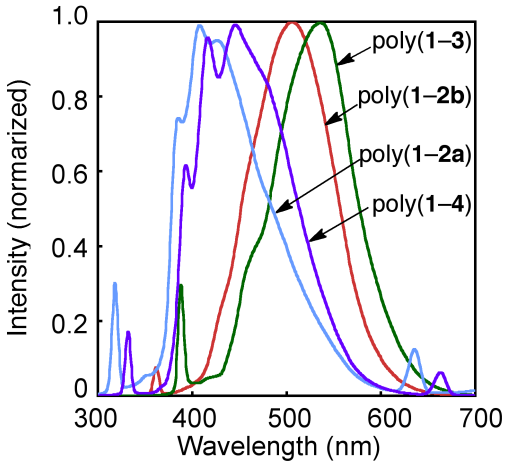

Figure 3. Fluorescence spectra of poly(**1–2a**), poly(**1–2b**), poly(**1–3**) and poly(**1–4**) measured in THF at room temperature excited at λ_{max} (c = 0.6–3.0 μM).

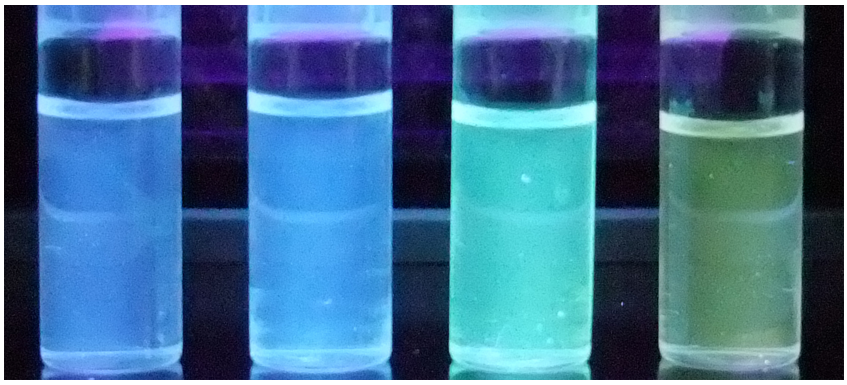

Figure 4. Photograph of THF solutions (c = 3.0 μM) of poly(**1–2a**) (left), poly(**1–4**), (second from the left), poly(**1–2b**) (third from the left), poly(**1–3**) (right) under irradiation of light (365 nm).

DFT calculation. The UV-vis spectra of the model compounds (**M1**–**M4** in Chart 2) for the polymers were simulated using the TD-DFT method at B3LYP/6–31+G* level to obtain further information about the conjugation length. Figure 5 depicts the velocity-based oscillator strength (f) values and UV–vis spectra simulated from the f values and their positions, where a half Gaussian (1/e)-bandwidth (Δ/2) was assumed to be 40 nm. The λ_{max} values

were simulated to be 338, 399, 445 and 469 nm for **M1**, **M4**, **M2** and **M3**, respectively, in harmony with the red-shifts of the observed λ_{max} of the polymers as plotted in Figure 6. The good correlation indicates the properness of TD-DFT calculation on simulating the UV-vis spectra of phenyleneethylene polymers. The experimentally observed λ_{max} values were positioned at shorter wavelengths than the simulated ones. This result is explainable from the degrees of twisting of the main chains. Tthe main chains of the polymers are twisted due to the folded helical structures. On the contrary, the main chains of model compounds **M1**–**M4** almost exist on a plane to maximize the conjugation.

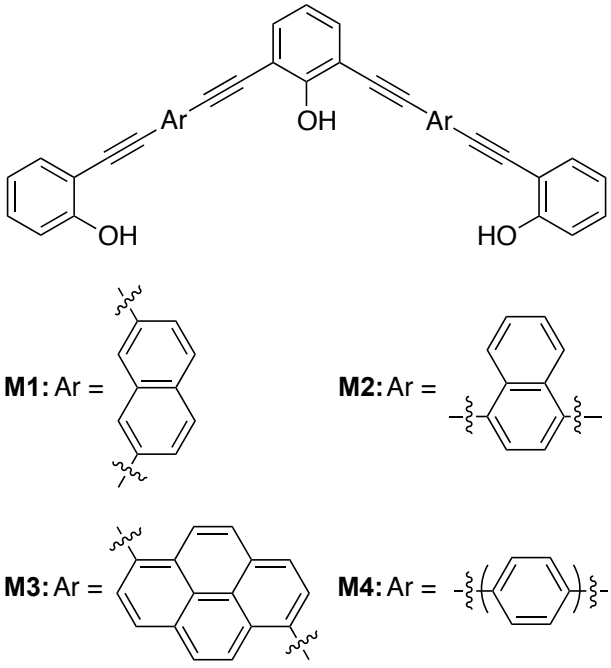

Chart 2. Structures of Model Compounds **M1**–**M4.**

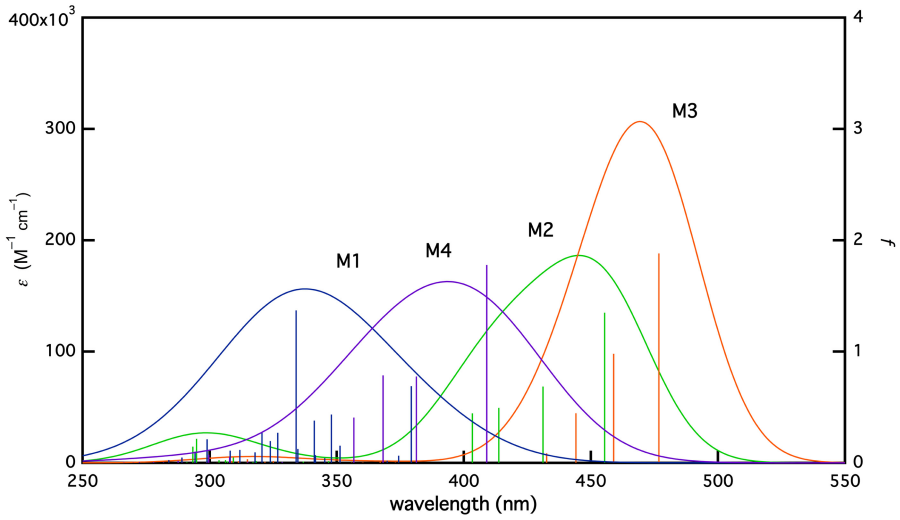

Figure 5. Excited-state parameters and UV–vis spectra simulated for **M1–M4.** The *f* values are predicted at the B3LYP/6–31+G* level in velocity form.

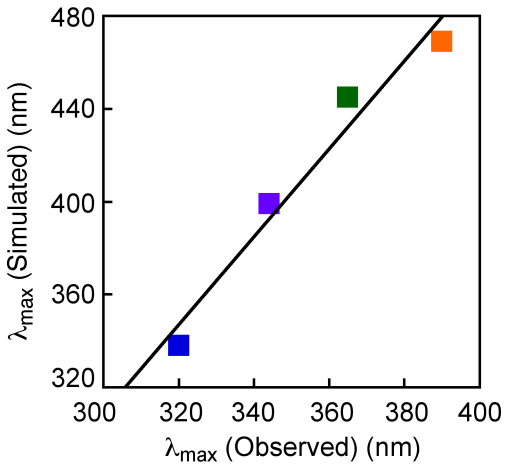

Figure 6. The plots simulated λ_{max} of **M1**–**M3** calculated by B3LYP/6–31+G* levels over the observed λ_{max} of corresponding polymers [poly(**1**–**2a**), poly(**1**–**2b**), and poly(**1**–**3**)]. The plot of poly(**1**–**4**) (purple square) was also added to improve the accuracy.

Conclusions

In this chapter, the author has synthesized novel poly(phenyleneethynylene-naphthyleneethynylene)s and

poly(phenyleneethynylene-pyrenyleneethynylene) bearing hydroxy groups [poly(**1**–**2a**), poly(**1**–**2b**), poly(**1**–**3**)] by the Sonogashira–Hagihara coupling polymerization of diiodophenylene monomer **1** with the corresponding diethynylarylene monomers **2a**, **2b** and **3**, and compared the optical properties with those of 1,4-phenylene counterpart [poly(**1**–**4**)]. CD and UV–vis spectroscopic analysis revealed that all the polymers forms predominantly one-handed folded helical structures in THF. The λ_{max} of poly(**1**–**3**) positioned at the longest wavelength among the polymers. Introduction of 1,4-naphthylene and 1,6-pyrenylene units into the polymer main chains extended the conjugated length effectively. Poly(**1**–**3**) formed a thermally stable helical structure in THF, while poly(**1**–**2a**) and poly(**1**–**2b**) lost the regulated helical structures to some extent upon heating. Poly(**1**–**2a**) and poly(**1**–**3**) kept the CD spectroscopic patterns in THF/MeOH irrespective of the MeOH content. On the other hand, poly(**1**–**2b**) remarkably diminished the CD signals upon increasing the MeOH content. Namely, the formed polymers showed different temperature- and solvent-responsiveness depending on the arylene units and linking positions. The polymers emitted variously colored fluorescence corresponding to the λ_{max}. The TD-DFT simulation for the model compounds of the polymers well agreed with the trend of conjugation length considered by UV–vis spectroscopy.

Experimental Sections

Measurements. ^{1}H (400 MHz) and ^{13}C (100 MHz) NMR spectra were

recorded on a JEOL EX-400 or a JEOL AL-400 spectrometer. IR spectra were measured on a JASCO FT/IR-4100 spectrophotometer. Melting points (mp) were measured on a Yanaco micro melting point apparatus. Mass spectra were measured on a JEOL JMS-MS700 mass spectrometer. Number- and weight-average molecular weights (M_n and M_w) of polymers were determined by SEC (Shodex columns KF805 × 3) eluted with tetrahydrofuran (THF) calibrated by polystyrene standards at 40 °C. CD, UV–vis absorption, and fluorescence spectra were recorded on a JASCO J-820 and FP-750 spectropolarimeter.

Materials. Unless stated otherwise, reagents and solvents were purchased and used without purification. 2,7-Diethynylnaphthalene (**2a**)[37] and 1,4-diethynylnaphthalene (**2b**)[38] were synthesized according to the literature. Et_3N and *N,N*-dimethylformamide (DMF) used for polymerization were distilled prior to use.

Monomer Synthesis. 1,6'-Diethynylpyrene (3). 1,6-Dibromopyrene (2.16 g, 6.00 mmol), $PdCl_2(PPh_3)_2$ (0.213 g, 0.60 mmol), PPh_3 (0.314 g, 2.40 mmol), and CuI (0.342 g, 3.60 mmol) were fed into a two-neck flask, ant it was flushed with dry nitrogen. THF (40 mL) and Et_3N (15 mL) were added to the solution, and then trimethylsilylacetylene (4.20 mL, 30.0 mmol) was added dropwise to the solution. The mixture was stirred at 50 °C for 72 h. The resulting mixture was concentrated in vacuo and the residual mass was washed with Et_2O to extract the product. The organic phase was washed with 1.0 M HCl, and saturated NaCl aq., dried over anhydrous

$MgSO_4$, and then filtered. The filtrate was concentrated, and the residual mass was purified by silica gel column chromatography eluted with hexane/EtOAc = 9/1 (v/v) and subsequently by preparative HPLC (eluent $CHCl_3$) to obtain 1,6-bis(trimethylsilylethnyl)pyrene. After that, it was dissolved in $CHCl_3$ (60 mL) and a suspension of K_2CO_3 (2.76 g, 20.0 mmol) in MeOH (30 mL) was added to the solution. The resulting mixture was concentrated in vacuo, and the residual mass was dispersed in dispersed in $CHCl_3$ and water. The organic layer was washed with 1.0 M HCl, and saturated NaCl aq., dried over anhydrous $MgSO_4$, and then filtered. The filtrate was concentrated, and the residual mass was purified by recrystallization from $CHCl_3$ and THF to obtain **3** as a brownish solid in 77%. No Mp was observed up to 172 °C (decomposition). IR (KBr): 3294, 2096, 1601, 1571, 1433, 1292, 1181, 840, 643, 597 cm^{-1}. ^1H NMR (400 MHz, $CDCl_3$): δ 3.64 (s, 2H, –C≡C*H*), 8.13–8.20 (m, 6H, Ar), 8.61–8.63 (m, 2H, Ar).[39] HRMS. (*m*/*z*): $[M]^+$ calcd for $C_{20}H_{10}$, 250.0783; found, 250.0783.

Polymerization. All the polymerizations were carried out in a glass tube equipped with a three-way stopcock under nitrogen. A typical experimental procedure for polymerization **1** with **2a** is given below. A solution of **1** (188 mg, 0.300 mmol), **2a** (52.8 mg, 0.300 mmol), $Pd(PPh_3)_2Cl_2$ (10.5 mg, 0.015 mmol), CuI (11.8 mg, 0.045 mmol), PPh_3 (5.70 mg, 0.030 mmol), and Et_3N (1.2 mL) in DMF (1.8 mL) was stirred at 80 °C for 24 h. The resulting mixture was poured into MeOH/acetone [9/1 (v/v), 300 mL] to precipitate a polymer. It was separated by filtration using a membrane filter

(ADVANTEC H100A047A) and dried under reduced pressure.

Spectroscopic Data of the Polymers. **Poly(1–2a)**: IR (KBr): 3297, 3058, 2922, 2852, 2211, 1736, 1654, 1509, 1450, 1340, 1205, 1170, 1093, 840, 800, 752, 470 cm^{-1}. ^1H NMR (400 MHz, $CDCl_3$): δ 0.80–0.94 (br, 3H, –CH_2CH_3), 1.15–1.34 [br, 21H, –$OCH_2(CH_2)_9$–, –CH_3], 1.50–1.69 (br, 2H, –CH_2CH_3), 4.21–4.30 [br, 2H, –$OCH_2(CH_2)_9$–], 4.84–4.90 (br, 1H, –C*H*–), 6.46–8.32 (br, 10H, –N*H*–, –O*H*, Ar). **Poly(1–2b)**: IR (KBr): 3328, 3058, 2923, 2852, 2200, 1736, 1654, 1509, 1451, 1189, 1161, 1092, 761 cm^{-1}. ^1H NMR (400 MHz, $CDCl_3$): δ 0.80–0.90 (br, 3H, –CH_2CH_3), 1.15–1.34 [br, 21H, –$OCH_2(CH_2)_9$–, –CH_3], 1.53–1.72 (br, 2H, –CH_2CH_3), 4.08–4.31 [br, 2H, –$OCH_2(CH_2)_9$–], 4.78–4.96 (br, 1H, –C*H*–), 6.26–8.60 (br, 10H, –N*H*–, –O*H*, Ar). **Poly(1–3)**: IR (KBr): 3423, 3040, 2921, 2851, 2195, 1735, 1654, 1509, 1457, 1341, 1091, 841, 817 cm^{-1}. ^1H NMR (400 MHz, $CDCl_3$): δ 0.72–0.88 (br, 3H, –CH_2CH_3), 1.15–1.34 [br, 21H, –$OCH_2(CH_2)_9$–, –CH_3], 1.53–1.72 (br, 2H, –CH_2CH_3), 4.26–4.41 [br, 2H, –$OCH_2(CH_2)_9$–], 4.83–5.02 (br, 1H, –C*H*–), 6.19–8.87 (br, 12H, –N*H*–, –O*H*, Ar).

Computation. All calculations were performed with the Gaussian 09 program[40] running on the supercomputer system of the Academic Center for Computing and Media Studies of Kyoto University. The density functional theory (DFT)[41] method with Becke's three- parameter hybrid functional[42] and the LYP correlation functional (B3LYP)[43] were utilized in conjunction with the 6–31+G* basis set to fully optimize geometries.

References and Notes

(1) For reviews, see: (a) Choi, S.-K.; Gal, Y.-S.; Jin, S.-H.; Kim, H. K. *Chem. Rev.* **2000**, *100*, 1645–1681; (b) Nagai, K.; Masuda, T.; Nakagawa, T.; Freeman, B. D.; Pinnau, I. *Prog. Polym. Sci.* **2001**, *26*, 721–798; (c) Masuda, T.; Sanda, F. "Polymerization of Substituted Acetylenes" in Handbook of Metathesis, Grubbs, R. H. Ed., Wiley-VCH, Weinheim, 2003, Vol. 3, Chapter 3.11, pp. 375–406; (d) Aoki, T.; Kaneko, T.; Teraguchi, M. *Polymer* **2006**, *47*, 4867–4892; (e) Masuda, T. *J. Polym. Sci., Part A: Polym. Chem.* **2007**, *45*, 165–180; (f) Masuda, T.; Sanda, F.; Shiotsuki, M. "Polymerization of Acetylenes" in *Comprehensive Organometallic Chemistry III*, Crabtree, R.; Mingos M. Eds., Elsevier, Oxford, 2007, Vol. 11, Chapter 16, pp. 557–593; (g) Yashima, E.; Maeda, K.; Iida, H.; Furusho, Y.; Nagai, K. *Chem. Rev.* **2009**, *109*, 6102–6211; (h) Akagi, K. *Chem. Rev.* **2009**, *109*, 5354–5401; (i) Liu, J.; Lam, J. W. Y.; Tang, B. Z. *Chem. Rev.* **2009**, *109*, 5799–5867; (j) Masuda, T.; Shiotsuki, M.; Sanda, F. "Product Class 31: Macromolecular Conjugated Polyenes" in Science of Synthesis. Houben-Weyl Methods of Molecular Transformations, Category 6, Volume 45b, Siegel J. S.; Tobe, Y. Eds., Georg Thieme Verlag KG, Stuttgart - New York, 2010, pp. 1421–1439; (k) Shiotsuki, M.; Sanda, F.; Masuda, T. *Polym. Chem.* **2011**, *2*, 1044–1058.

(2) Nelson, J. C.; Saven, J. G.; Moore, J. S.; Wolynes, P. G. *Science*, **1997**, *277*, 1793–1796.

(3) Prince, R. B; Saven, J. G.; Wolynes, P. G.; Moore, J. S. *J. Am. Chem. Soc.* **1999**, *121*, 3114–3121.

(4) Matsuda, K.; Stone, M. T.; Moore, J. S. *J. Am. Chem. Soc.* **2002**, *124*, 11836–11837.

(5) Abe, H.; Masuda, N.; Waki, M.; Inouye, M. *J. Am. Chem. Soc.* **2005**, *127*, 16189–16196.

(6) Jones, T. V.; Slutsky, M. M.; Laos, R.; Greef, T. F. A.; Tew, G. N. *J. Am. Chem. Soc.* **2005**, *127*, 17235–17240.

(7) Khan, A.; Hecht, S. *Chem. Eur. J.* **2006**, *12*, 4764–4774.

(8) Wackerly, J. W.; Moore, J. S. *Macromolecules* **2006**, *39*, 7269–7276.

(9) K Zhao, X.; Schanze, K. S. *Langmuir* **2006**, *22*, 4856–4862.
(10) Smaldone, R. A.; Moore, J. S. *J. Am. Chem. Soc.* **2007**, *129*, 5444–5450.
(11) Zhu, M.; Lu, W.; Zhu, N.; Che, C. *Chem. Eur. J.* **2008**, *14*, 9736–9746.
(12) Balbo Block, M. A.; Hecht, S. *Macromolecules* **2008**, *41*, 3219–3227.
(13) Zhang, Z.; Che, Y.; Smaldone, R. A.; Xu, M.; Bunes, B. R.; Moore, J. S.; Zang, L. *J. Am. Chem. Soc.* **2010**, *132*, 14113–14117.
(14) Chen, Y.; Malkovskiy, A.; Wang, X.; Lebron-Colon, M.; Sokolov, A. P.; Perry, K.; More, K.; Pang, Y. *ACS Macro Lett.* **2012**, *1*, 246–251.
(15) Banno, M.; Yamaguchi, T.; Nagai, K.; Kaiser, C.; Hecht, S.; Yashima, E. *J. Am. Chem. Soc.* **2012**, *134*, 8718–8728.
(16) Liu, R.; Shiotsuki, M.; Masuda, T.; Sanda, F. *Macromolecules* **2009**, *42*, 6115–6122.
(17) Liu, R.; Sogawa, H.; Shiotsuki, M.; Masuda, T.; Sanda, F. *Polymer* **2010**, *51*, 2255–2263.
(18) Sogawa, H.; Shiotsuki, M.; Matsuoka, H.; Sanda, F. *Macromolecules* **2011**, *44*, 3338–3345.
(19) Hashimoto, A.; Sogawa, H.; Shiotsuki, M.; Sanda, F. *Polymer* **2012**, *53*, 2559–2566.
(20) Shizuka, H. *Pure Appl. Chem.* **1997**, *69*, 825–830.
(21) Yang, F.; Akhtaruzzaman, M.; Islam, A.; Jin, T.; El-Shafei, A.; Qin, C.; Han, L.; Alamry, K. A.; Kosa, S. A.; Hussein, M. A.; Asiri, A. M.; Yamamoto, Y. *J. Mater. Chem.* **2012**, *22*, 22550–22557.
(22) Winnilk, F. M. *Chem. Rev.* **1993**, 93, 587–614.
(23) Karuppannan S.; Chambron, J. *Chem. Asian J.* **2011**, *6*, 964–984.
(24) Zhou, C.; Wang, W.; Lin, K. K.; Chen, Z.; Lai, Y. *Polymer* **2004**, *45*, 2271–2279.
(25) Kijima, M.; Mori, T. *Optical Materials* **2007**, *30*, 545–552.
(26) Zhao, Z.; Xu, X.; Jiang, Z.; Lu, P.; Yu, G.; Liu, Y. *J. Org. Chem.* **2007**, *72*, 8345–8353.
(27) Chen, H.; Hu, X.; Ng, S. *J. Polym. Sci., Part A: Polym. Chem.* **2010**, *48*, 5562–5569.
(28) Gupta, J.; Vadukumpully, S.; Valiyaveettil *Polymer* **2010**, *51*, 5078–5086.
(29) He, G.; Yan, N.; Yang, J.; Wang, H.; Ding, L.; Yin, S.; Fang, Y.

Macromolecules **2011**, *44*, 4759–4766.
(30) Shen, D.; Diele, S.; Pelzl, G.; Wirth, I.; Tschierske, C. *J. Mater. Chem.* **1999**, *9*, 661–672.
(31) Nomura, R.; Yamda, K.; Masuda, T. *Chem. Commun.* **2002**, 478–479.
(32) Ahao, H.; Sanda, F.; Masuda, T. *Macromolecules* **2004**, *37*, 8893–8896.
(33) Zhao, H.; Sanda, F.; Masuda, T. *Polymer* **2006**, *47*, 1584–1589.
(34) Yuan, W. Z.; Sun, J. Z.; Dong, Y.; Häussler, M.; Yang, F.; Xu, H. P.; Qin, A.; Lam, J. W. Y.; Zhen, Q.; Tang, B. Z. *Macromolecules* **2006**, *39*, 8011–8020.
(35) Lin, H.; Morino, K.; Yashima, E. *Chirality* **2008**, *20*, 386–392.
(36) It has been reported that membrane filtration of solutions of conjugated polymers is effective to remove aggregates. See Yamamoto, T.; Komarudin, D.; Arai, M.; Lee, B.-L.; Suganuma, H.; Asakawa, N.; Inoue, Y.; Kubota, K.; Sasaki, S.; Fukuda, T.; Matsuda, H. *J. Am. Chem. Soc.* **1998**, *120*, 2047–2058.
(37) Neenan, T. X.; Whitesides, G. M. *J. Org. Chem.* **1988**, *53*, 2489–2496.
(38) Khan, M. S.; Al-Mandhary, M. R. A.; Al-Suti, M. K.; Al-Battashi, F. R.; Al-Saadi, S.; Ahrens, B.; Bjernemose, J. K.; Mahon, M. F.; Raithby, P. R.; Younus, M.; Chawdhury, N.; Köhler, A.; Marseglia, E. A.; Tedesco, E.; Feeder, N.; Teat, S. J. *Dalton Trans.* **2004**, 2377–2385.
(39) Ji, S.; Yang, J.; Yang, Q.; Liu, S.; Chen, M.; Zhao, J. *J. Org. Chem.* **2009**, *74*, 4855–4865.
(40) Frisch, M. J.; Trucks, G. W.; Schlegel,H. B.; Scuseria, G. E.; Robb, M. A.; Cheeseman, J. R.; Scalmani, G.; Barone, V.; Mennucci, B.; Petersson, G. A.; Nakatsuji, H.; Caricato, M.; Li, X.; Hratchian, H. P; Izmaylov, A. F.; Bloino, J.; Zheng, G.; Sonnenberg, J. L.; Hada, M.; Ehara, M.; Toyota, K.; Fukuda, R.; Hasegawa, J.; Ishida, M.; Nakajima, T.; Honda, Y.; Kitao, O.; Nakai, H.; Vreven, T.; Montgomery, J. A.; Peralta, Jr., J. E.; Ogliaro, F.; Bearpark, M.; Heyd, J. J.; Brothers, E.; Kudin, K. N.; Staroverov, V. N.; Keith,T.; Kobayashi, R.; Normand, J.; Raghavachari, K.; Rendell, A.; Burant, J. C.; Iyengar, S. S.; Tomasi, J.; Cossi, M.; Rega, N.; Millam, J. M.; Klene, M.; Knox, J. E.; Cross, J. B.; Bakken, V.; Adamo, C.; Jaramillo, J.; Gomperts, R.; Stratmann, R. E.; Yazyev, O.; Austin, A. J.; Cammi, R.; Pomelli, C.;

Ochterski, J. W.; Martin, R. L.; Morokuma, K.; Zakrzewski, V. G.; Voth, G. A.; Salvador, P.; Dannenberg, J. J.; Dapprich, S.; Daniels, A. D.; Farkas, O.; Foresman, J. B.; Ortiz, J. V.; Cioslowski, J.; Fox, D. J. *Gaussian 09, Revision B.01*, Gaussian, Inc.: Wallingford CT, 2010.

(41) Parr, R. G.; Yang, W. Density-Functional Theory of Atoms and Molecules; Oxford University Press: Oxford, 1989.

(42) Becke, A. D. *J. Chem. Phys.* **1993**, *98*, 5648–5652.

(43) Lee, C. T.; Yang, W. T.; Parr, R. G. *Phys. Rev. B* **1988**, *37*, 785–789.

Chapter 3

Stabilization of Higher-Order Structures of Poly(phenyleneethynylene)s by Metathesis Polymerization at the Side Chains

Abstract

Novel poly(*m*-phenyleneethynlene-*p*-phenyleneethynylene)s bearing polymerizable diene or norbornene groups were synthesized by the Sonogashira–Hagihara coupling polymerization of the corresponding D-hydroxyphenylglycine-derived diiodo monomers with *p*-diethynylbenzene. These polymers exhibited strong Cotton effects derived from a predominantly one-handed helical conformation in $CHCl_3$ and tetrahydrofuran (THF), but exhibited weak or no Cotton effects in *N*,*N*-dimethylformamide (DMF). The metathesis polymerization of the diene and norbornene moieties was performed at the side chains of the polymers under diluted conditions in the presence of a chain-transfer agent, if necessary. The reaction took place intramolecularly, which was confirmed by size exclusion chromatography (SEC) measurements. The polymers exhibited stronger Cotton effects even in polar media after the intramolecular crosslinking, which indicated stabilization of the helical structures.

Introduction

A helix is a typical regulated secondary structure of biopolymers such as amylose, protein and DNA. Synthetic polymers also form helical structures. A helical structure in artificial polymers was first discovered in isotactic polypropylene synthesized using the Ziegler–Natta catalyst, which dates to the 1950s.[1] Since the discovery of helical poly(triphenylmethyl methacrylate) synthesized by asymmetric anionic polymerization,[2] a wide variety of synthetic helical polymers have been reported, including polyacetylenes,[3] polyisocyanates,[4] polyisocyanides,[5] polysilanes[6] and poly(phenyleneethynylene)s.[7] These polymers adopt helical conformations due to non-flexible conjugated backbones and/or steric repulsion between the side chains and garner significant attention because of their possible applications as chiral sensors, asymmetric catalysts and optical resolution materials.[8]

Novel poly(*m*-phenyleneethynlene-*p*-phenyleneethynylene)s via the Sonogashira–Hagihara coupling polymerization of D-hydroxyphenylglycine-derived diiodo monomers with *p*-diethynylbenzene have been synthesized recently.[9] The obtained polymers formed helices with a hydrophobic exterior (due to alkyl groups) and a hydrophilic interior (from phenol groups) in nonpolar solvents. This helical structure was more stable to heating than common poly(phenyleneethynylene)s (i.e., the CD and UV–vis spectroscopic signals exhibited almost no changes between 0 and 50 °C in $CHCl_3$).[10] The thermal stability was assumed to be brought about by regulated

intramolecular hydrogen bonding between the amide groups at the i^{th} and $(i+6)^{th}$ units on the side chains, as well as by amphiphilicity and *p*-stacking between the phenylene main chains. However, the helical structure was susceptible to polar solvents such as water and methanol, presumably due to collapse of the amphiphilic balance and intramolecular hydrogen-bonding strands.

Stability in polar solvents is an important property with respect to the application of D-hydroxyphenylglycine-based helical poly(phenyleneethynylene)s to functional materials. Clipping or crosslinking the side chains of the polymer is effective at stabilizing the conformation.

Hydrocarbon stapling—the ring-closing metathesis of helical peptides bearing olefinic side chains—provides a useful strategy for the experimental and therapeutic modulation of protein–protein interactions in many signaling pathways.[11] Metathesis reactions are also effective for the fixation of self-assembled supramolecules.[12] For example, a helical poly(*m*-phenyleneethynylene) bearing cinnamate groups has been covalently stabilized by [2+2] photodimerization reactions at the side chains.[13] Using this methodology, The author discusses the synthesis of novel helical poly(phenyleneethynlene)s bearing polymerizable groups at the side chains and their subsequent polymerization to obtain polymers that exhibit high helix stability in both nonpolar and polar solvents.

Results and discussion

Monomer synthesis. Monomers **1**–**3** were successfully synthesized by the condensation of *N*-a-*tert*-butoxycarbonyl-4′-hydroxy-3′,5′-diiodo-D-phenylglycine with the corresponding amines bearing diene and norbornene moieties (Scheme 1). *N*-a-*tert*-bButoxycarbonyl-4′-hydroxy-3′,5′-diiodo-D-phenylglycine was synthesized by diiodation of hydroxy-D-phenylglycine using ICl followed by *N*-*tert*-butoxycarbonylation using DIBOC. All the monomers were obtained as yellowish-white powders and were characterized by ^{1}H, ^{13}C NMR, IR and high-resolution mass spectrometry.

Scheme 1. Synthesis of Monomers **1**–**3**.

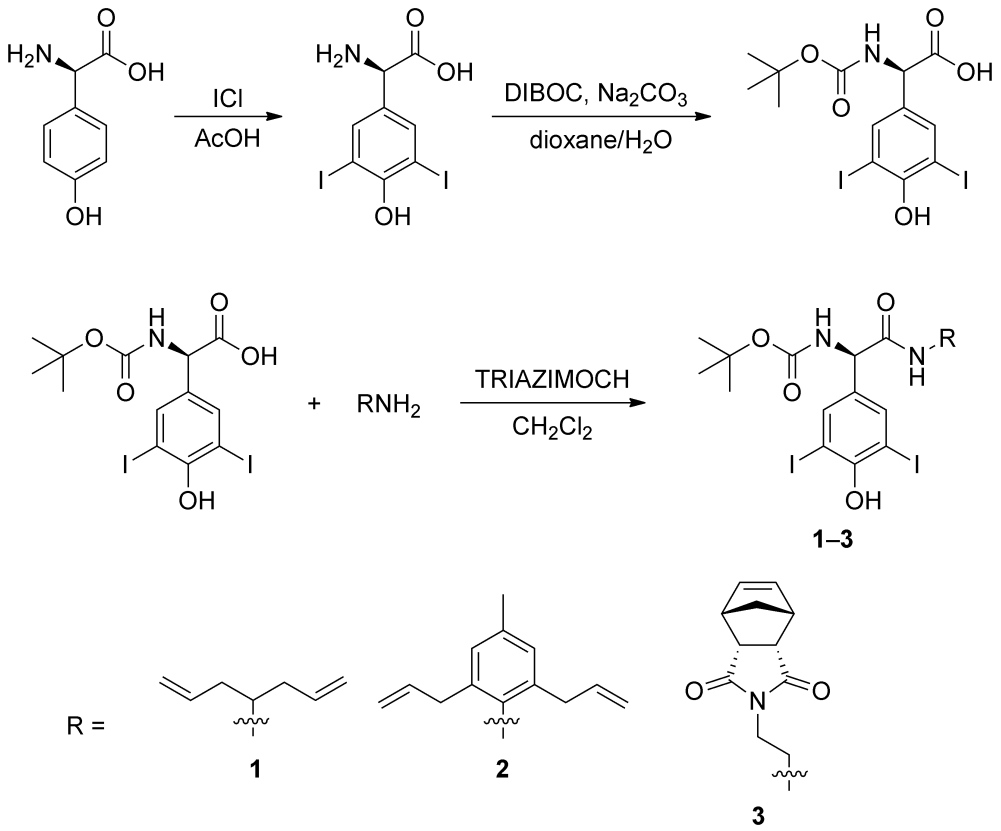

Polymerization. The Sonogashira–Hagihara coupling polymerization of **1**–**3** with *p*-diethynylbenzene afforded the corresponding poly(*m*-phenyleneethynlene-*p*-phenyleneethynlene)s **1a**–**3a** that bear polymerizable groups at the side chains with M_n values that range from 6300 to 6700 (PDI = 2.0–2.4) in 64–96% yields (Scheme 2, Table 1). The polymers were soluble in $CHCl_3$, THF, DMF and DMSO, but insoluble in hexane and MeOH.

Scheme 2. Sonogashira–Hagihara Coupling Polymerization of **1**–**3** with *p*-Diethynylbenzene.

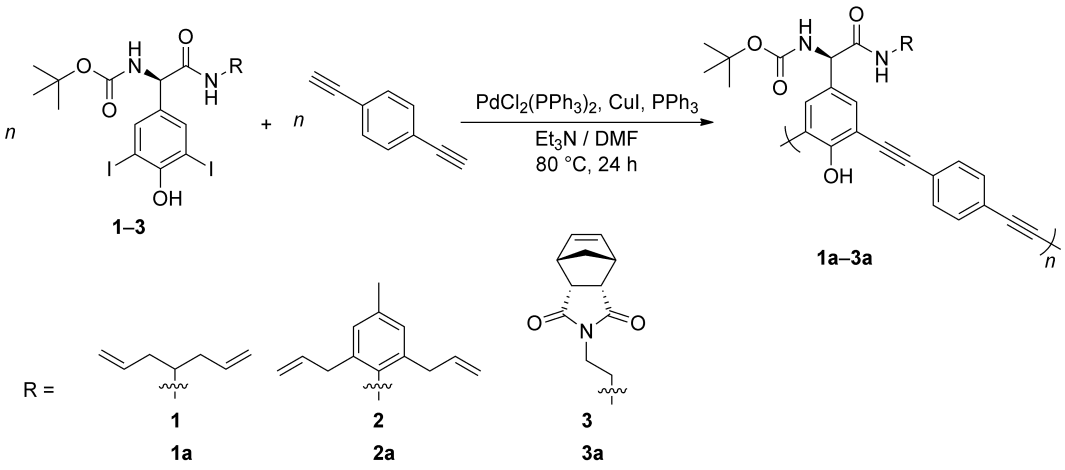

Table 1. Polymerization of **1**–**3** with *p*-diethynylbenzene.[a]

Monomer	Yield[b] (%)	M_n[c]	PDI[c]
1	72	6300	2.4
2	64	6300	2.4
3	96	6700	2.0

[a] Conditions: [**1**–**3**]$_0$ = [*p*-diethynylbenzene]$_0$ = 0.1 M, [$PdCl_2(PPh_3)_2$] = 0.012 M, [CuI] = 0.002 M, [PPh_3]=0.008 M in Et_3N/DMF (2/3,v/v), 80 °C, 24 h.
[b] MeOH/acetone = 5/1 (v/v)—insoluble fraction.
[c] Determined by SEC eluted with THF and calibrated with polystyrene standards.

Chiroptical properties. The CD and UV–vis spectra of **1a**–**3a** were measured in $CHCl_3$, THF and DMF at room temperature to obtain information on the secondary structures. All of the polymers exhibited strong split Cotton effects in $CHCl_3$ and THF (Figure 1). The CD and UV–vis signals allowed the assignment of a chirally ordered conjugated polymer main chain because the λ_{max} values of the polymers appeared at longer wavelengths than those of the monomers (**1**–**3**: λ_{max} = 224 nm) and *p*-diethynylbenzene (λ_{max} = 276 nm). The inflection point from the first positive to second negative CD sign agreed with the λ_{max} from the UV–vis absorption, which indicated the CD split was caused by exciton coupling of the chromophores.[14] The polymer solutions exhibited the same CD and UV–vis spectroscopic patterns after they were filtered using a membrane with a pore size of 0.45 mm, and patterns exhibited no concentration dependence in the range from 0.02 to 0.05 mM. Therefore, the CD signals probably originated predominantly from right-handed helical conformations instead of from chirally aggregated structures.

In DMF, **1a** and **2a** exhibited Cotton effects weaker than those in $CHCl_3$ and THF, and **3a** did not exhibit Cotton effects. In addition, the helicities of the polymers were lower in DMF than in $CHCl_3$ and THF. This fact was explainable by the higher polarity of DMF relative to the other two solvents; the higher polarity of DMF led to a collapse of regulated >N–H•••O=C< hydrogen-bonding strands between the side chains, which play an important role in helix formation.[9,15] This hypothesis was also supported by the CD and UV–

vis spectroscopic measurements of **3a** in a mixed solvent of THF/H_2O (Figure 2). Specifically, the Kuhn's dissymmetry factor (g value = $\Delta e/e$, in which Δe = $[q]/3298$) of **3a** decreased with increasing H_2O content and approached 0 when the H_2O content reached 10%. Therefore, the helicity of **3a** was highly susceptible to the polarity of solvents.

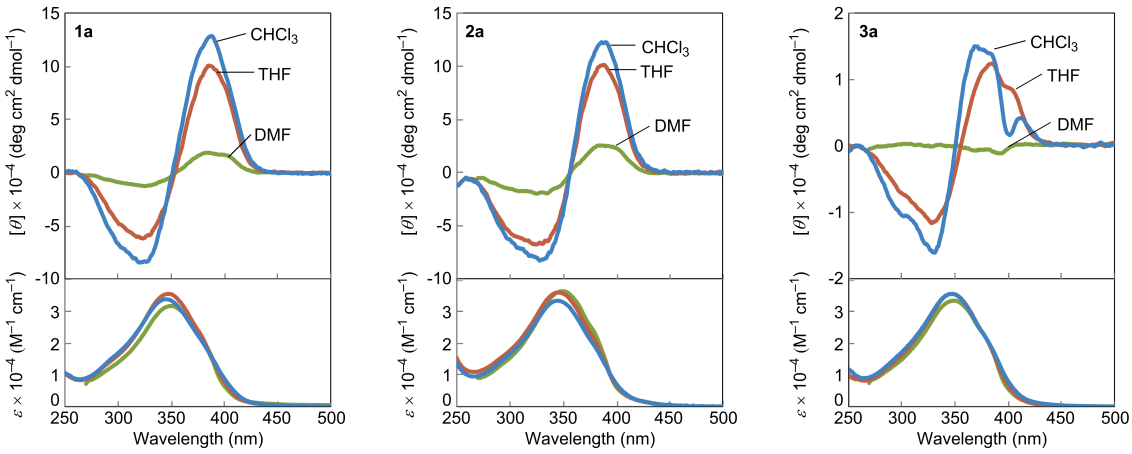

Figure 1. CD and UV–vis spectra of **1a–3a** measured in $CHCl_3$, THF and DMF at room temperature (c = 0.03 mM).

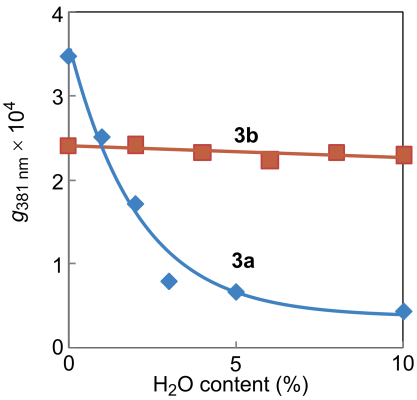

Figure 2. The relationship between g values at 381 nm and H_2O content of a solution of **3a** and **3b** in THF/H_2O (c = 0.03 mM).

Polymerization at the side chains. Polymers **1a** and **2a** were subjected to ADMET polymerization using the second-generation Grubbs' catalyst in THF and $CHCl_3$, respectively. The polymerizations were performed at high dilution [2 mM (monomer unit)] to suppress intermolecular reactions. The progress of ADMET (Scheme 3, top) was followed by the changes in the CD spectra discussed later.[16] No significant changes in M_n or PDI values (Table 2) were observed before and after ADMET, which indicates the absence of intermolecular crosslinking and side reactions, such as metathesis reactions, that involve the triple bonds of the main chain. The conjugation through the triple bonds and steric hindrance appear to effectively suppress such side reactions.

Polymer **3a** was subjected to ROMP using the second-generation Grubbs' catalyst in THF.[17] In this case, *cis*-1,4-dichloro-2-butene was added as a chain-transfer agent because the degree of polymerization at the side chains was expected to be no more than 2 based on the M_n of **3a**.[18] Based on the SEC data, the reaction did not take place intermolecularly, but intramolecularly in a fashion similar to the previously discussed ADMET of **1a** and **2a**.

Chiroptical properties of the polymers after metathesis. Figure 3 depicts the CD and UV–vis spectra of polymers **1b**–**3b** obtained from metathesis at the side chains of **1a**–**3a**. No significant difference was observed between the intensities of the Cotton effects of **1a** and **1b** measured in THF and those of **2a** and **2b** measured in $CHCl_3$, whereas the intensities of **1b** and **2b** became larger

than those of **1a** and **2a** in DMF. These results suggested that the helical structures were partly fixed by ADMET polymerization and that the stability toward DMF was partly enhanced. These results were also supported by the comparison of CD intensities of **1a** and **1b** in DMF/THF (19% and 27%) and those of **2a** and **2b** in DMF/$CHCl_3$ (21% and 44%).

Scheme 3. ADMET and ROMP at the Side Chains of **1a**–**3a**.

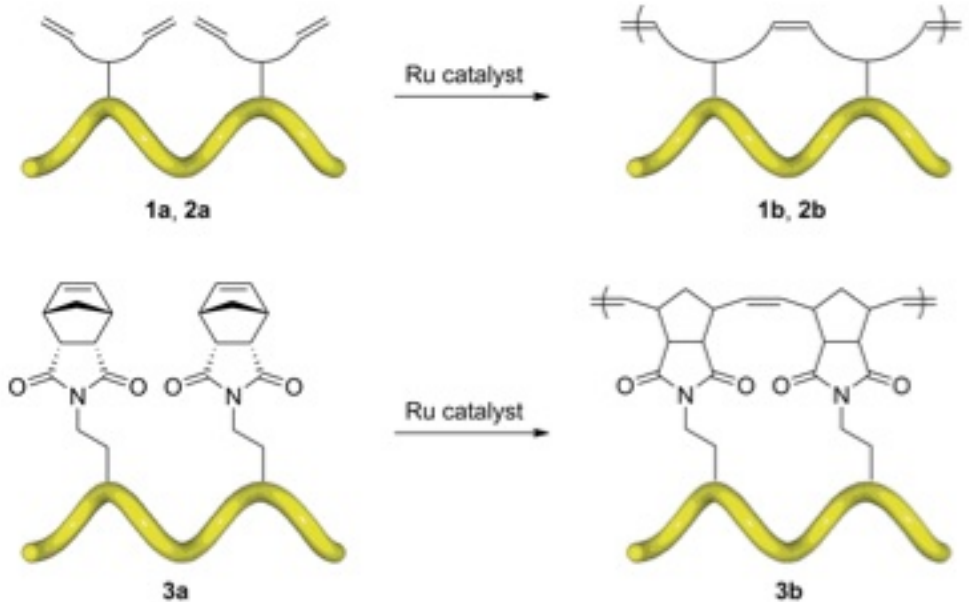

Table 2. Metathesis reactions of **1a**–**3a**.[a]

Polymer	Before metathesis		[Ru][b] (mM)	Solvent	Temp (°C)	Time (h)	After metathesis		
	M_n	PDI					Yield[c] (%)	M_n[d]	PDI[d]
1a	6300	2.4	0.06	THF	45	18	quant	5900	2.2
2a	6300	2.4	0.08	$CHCl_3$	50	24	80	6900	2.0
3a[e]	6700	2.0	0.13	THF	50	24	93	6600	1.8

[a] $[M]_0$ = 2 mM (monomer unit).
[b] Grubbs' second-generation catalyst.
[c] MeOH-insoluble fraction.
[d] Determined by SEC eluted with THF and calibrated with polystyrene standards.
[e] *cis*-1,4-Dichloro-2-butene (2 mM) was added.

The difference between **1a** → **1b** (+8%) and **2a** → **2b** (+23%) was presumably caused by the difference in degrees of ring-closing metathesis (RCM). As previously noted,[16] **1a** was more likely to induce RCM than was **2a**, which resulted in better helix stability for **1b** than for **2b**. This result was also confirmed by the CD spectroscopic analysis of films of **2a** and **2b** fabricated by solvent casting. As depicted in Figure 4, the film of **2a** exhibited a CD signal with a pattern completely different from that of the solution state (Figure 1), whereas the film of **2b** exhibited a CD pattern almost identical to that of the solution (Figure 3). This phenomenon was explainable from the difference in helix stability between **2a** and **2b**. Presumably, the helical conformation of **2a** was transformed (e.g., to a trans-zigzag structure) together with the formation of chiral aggregates upon solvent evaporation. However, the helical conformation of **2b** was intact after film casting due to the more stable helix structure. In fact, the **2a** film was more easily fabricated and tougher than the **2b** film, which supports the non-helical structure of **2a** and the presence of aggregates in the solid state.

The trend of helix stabilization was apparent in the conversion of **3a** to **3b**. In DMF, **3a** exhibited no CD signal, whereas **3b** exhibited signals comparable in intensity to that in THF. Thus, the author concluded that the helix stability of **3b** was greatly enhanced due to intramolecular cross-linking by ROMP. This conclusion was also confirmed by the CD and UV–vis spectra measured in mixed THF/H_2O solvent. The Kuhn's dissymmetry factor (*g*

value) of **3a** remarkably decreased when the H_2O content was increased from 0 to 10% (Figure 2). In contrast, the *g* value of **3b** only slightly decreased when the H_2O content was increased. These results clearly indicated that helix stability was enhanced by ROMP at the side chains.

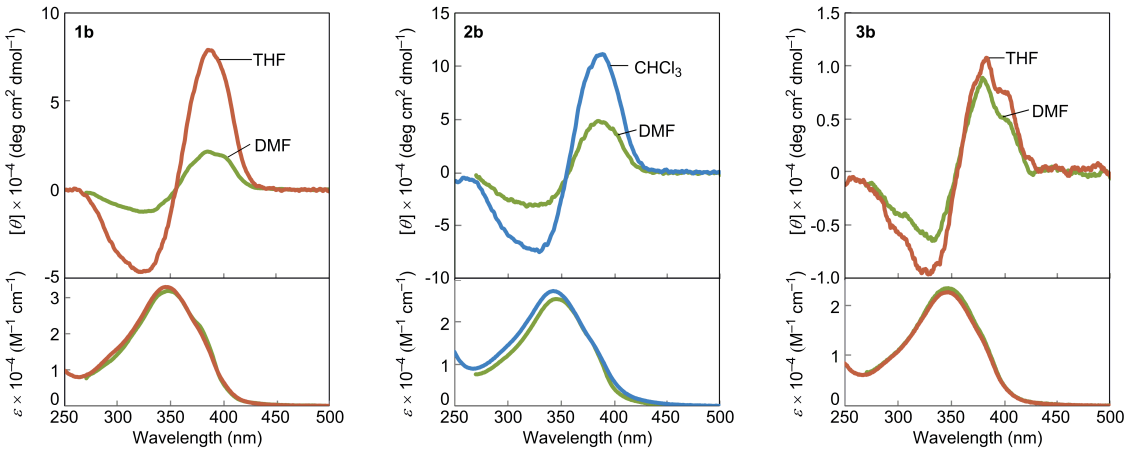

Figure 3. CD and UV–vis spectra of **1b**–**3b** measured in $CHCl_3$, THF and DMF at room temperature (c = 0.03 mM).

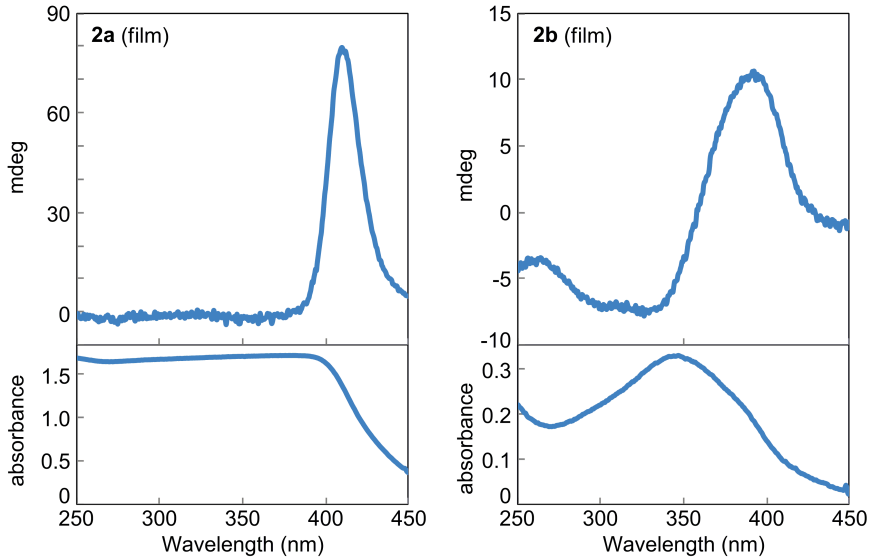

Figure 4. CD and UV–vis spectra of **2a** and **2b** films measured at room temperature. The films were fabricated on quartz glass plates by casting from THF solutions.

Conformation analysis. The conformations of **1a**–**3b** were analyzed using the MMFF94 method.[19] Based on the first positive and second negative exciton-coupled CD signals (Figures 1 and 3), the polymers adopted a predominantly right-handed helical conformation. Figure 5 depicts the top and side views of 12-mers of the polymers. In each case, the conformer formed a helically folded structure, and each turn consisted of six monomer units. The interatomic distance between the i^{th} amide carbonyl oxygen and the $(i+6)^{th}$ amide hydrogen (>C=O•••H–N<) was approximately 2 Å (i.e., the amide groups of the polymers formed $i+6 \rightarrow i$ intramolecular hydrogen bonds). The carbamate groups also formed hydrogen bonds in a similar fashion. The interatomic distances between the diagonal oxygen atoms and the pitch of the helix were 20–22 Å and 4 Å,[20] respectively. The helical structures appeared to be stabilized by hydrogen bonding and π-stacking between the aromatic rings. Intramolecular ADMET and ROMP likely occurred between the monomer units at the i^{th} and $(i+6)^{th}$ positions as well. The conformational changes were negligible before and after the metathesis reactions, which indicated smooth reactions.

Conclusions

The author has demonstrated the synthesis of novel helical poly(phenyleneethynlene)s **1a**–**3a** that bear polymerizable diene or norbornene groups at the side chains. All of the polymers exhibited first-positive and second-negative Cotton effects based on exciton coupling of the conjugated main

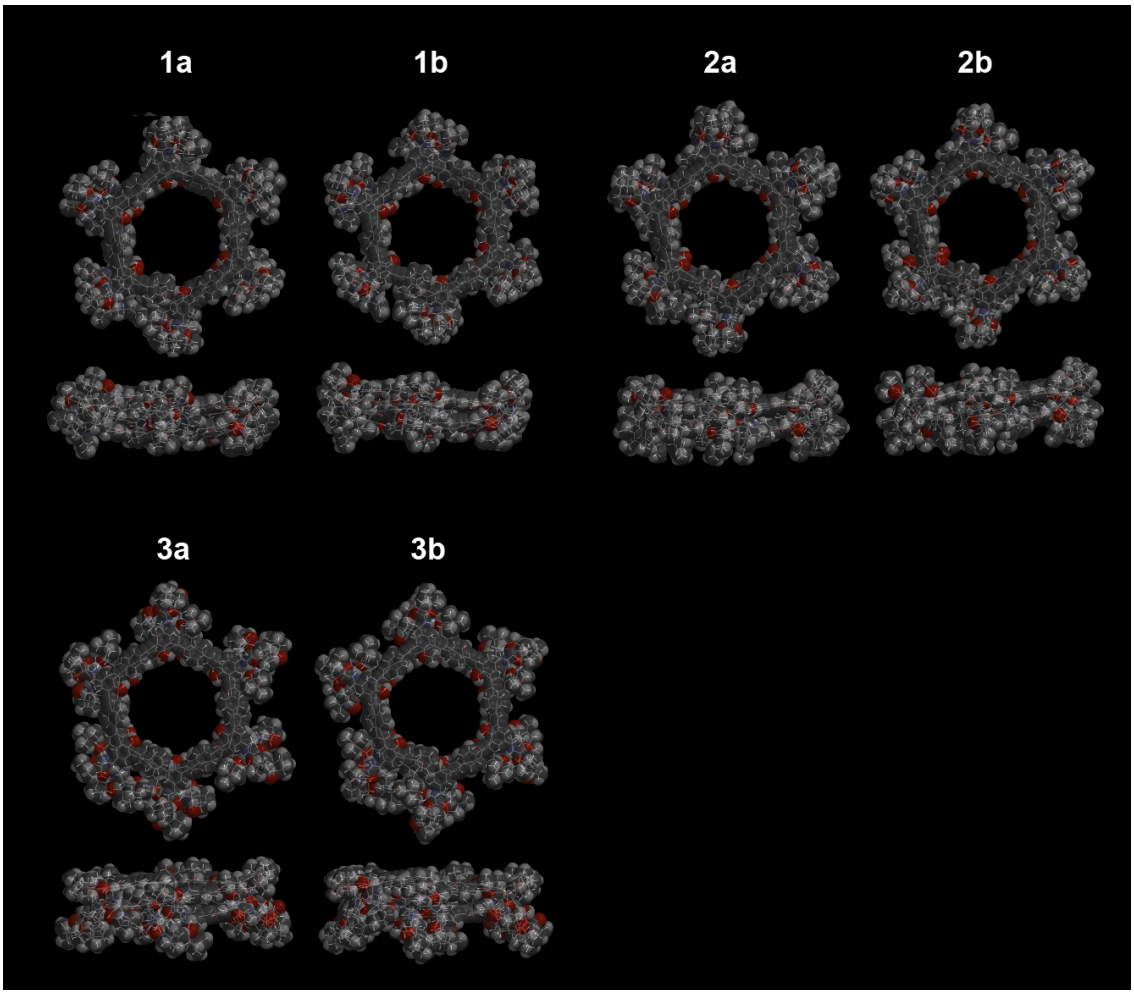

Figure 5. Top and side views of possible conformers **1a**–**3a** and **1b**–**3b** (12-mers). Geometries were fully optimized using the MMFF94 method.

chain in $CHCl_3$ and THF. The author concluded that the polymers adopted a predominantly right-handed helical conformation in these solvents. However, the polymers exhibited only weak or no Cotton effects in DMF. The author assumed that intramolecular hydrogen bonding at both the amide and carbamate groups between the side chains was effective at stabilizing the helical conformation. Polymers **1a** and **2a** bearing diene moieties were subjected to ADMET, and polymer **3a** bearing norbornene moieties was subjected to ROMP

at the side chains using the second-generation Grubbs' catalyst. After ADMET and ROMP at the side chains, the M_n values of the polymers were unchanged, which indicated that the metathesis reactions occurred intramolecularly, not intermolecularly. The synthesized polymers exhibited more intense Cotton effects in DMF than did the polymers prior to metathesis. Interestingly, **3b** exhibited CD signals in DMF comparable in intensity to those taken in THF. Moreover, the *g* value of **3b** was almost constant in a THF/H_2O mixed solvent at any composition. These results indicated that the helical conformation of **3b** was successfully fixed by intramolecular ROMP.

Experimental Sections

Measurements. ^{1}H (400 MHz) and ^{13}C (100 MHz) NMR spectra were recorded on a JEOL EX-400 or JEOL AL-400 spectrometer. IR spectra were measured on a JASCO FT/IR-4100 spectrophotometer. Melting points (mp) were measured on a Yanaco micro melting point apparatus. Mass spectra were measured on a Thermo Fisher Scientific EXACTIVE mass spectrometer. Specific rotations ($[\alpha]_D$) were measured on a JASCO DIP-1000 digital polarimeter. Number- and weight-average molecular weights (M_n and M_w) of polymers were determined by SEC (Shodex columns KF805 × 3) eluted with THF and calibrated using polystyrene standards at 40 °C. CD and UV–vis absorption spectra were recorded on a JASCO J-820 spectropolarimeter.

Materials. 1,6-Heptadienyl-4-amine, 2,6-diallyl-4-methylaniline and *N*-(2-aminoethyl)-5-norbornene-*endo,endo*-2,3-dicarboximide were synthesized according to methods reported in the literature.[21–23] DMF, Et_3N, THF and $CHCl_3$ were distilled prior to use. All other reagents were commercially obtained and used as received without purification.

Monomer synthesis. *N*-*tert*-butoxycarbonyl-4′-hydroxy-3′,5′-diiodo-D-phenylglycine. This compound was synthesized using a modified literature method.[24] Briefly, ICl (25.0 g, 154 mmol) was added dropwise to a suspension of D-*p*-hydroxyphenylglycine (12.0 g, 71.9 mmol) in AcOH (95 mL) under nitrogen. After the suspension was stirred at room temperature for 72 h, the reaction mixture was poured into ice water (1 L). The precipitated solid was collected by filtration and washed with ice water (500 mL × 2). The filtrate was dried under reduced pressure to afford 4′-hydroxy-3′,5′-diiodo-D-phenylglycine in 65% yield (19.6 g, 46.8 mmol). ^{1}H NMR (400 MHz, DMSO-d_6): δ 8.45 [br, 4H, COO*H*, NH_2, O*H*], 7.75 [s, 2H, Ar], 4.24 [s, 1H, C**H*] ppm.

A solution of di-*tert*-butyldicarbonate (DIBOC, TOKUYAMA, 6.64 g, 30.4 mmol) in 1,4-dioxane (50 mL) was added to a solution of 4′-hydroxy-3′,5′-diiodo-D-phenylglycine (10.5 g, 25.1 mmol) and Na_2CO_3 (3.30 g, 31.1 mmol) in H_2O (50 mL) at room temperature. After the resulting solution was stirred overnight, the reaction mixture was concentrated under reduced pressure. AcOEt was added to the residue, and the resulting mixture was

extracted with H_2O. The water layer was washed with AcOEt, acidified to pH = 3 by the addition of citric acid and extracted with AcOEt. The organic layer was washed with brine, dried over anhydrous $MgSO_4$ and concentrated under reduced pressure to afford *N*-α-*tert*-butoxycarbonyl-4′-hydroxy-3′,5′-diiodo-D-phenylglycine (11.6 g, 22.3 mmol) in 89% yield. The product was used in the next step without purification. ^{1}H NMR (400 MHz, $CDCl_3$): δ 8.20 [1H, N*H*], 7.75 [s, 2H, Ar], 5.81 [br, 1H, O*H*], 4.98 [d,*J* = 4.8 Hz, 1H, C**H*], 1.29 [s, 9H, C(CH_3)$_3$] ppm.

Monomer 1. 1,6-Heptadienyl-4-amine (2.35 g, 21.1 mmol) and 4-(4,6-dimethoxy-1,3,5-triazine-2-yl)-4-methylmorpholinium chloride (TRIAZIMOCH, TOKUYAMA, 4.55 g, 19.4 mmol) were added to a solution of *N*-a-*tert*-butoxycarbonyl-4′-hydroxy-3′,5′-diiodo-D-phenylglycine (13.2 g, 25.4 mmol) in THF (50 mL) at room temperature. The solution was evaporated after being stirred overnight. To the residue, CH_2Cl_2 was added and washed with 0.5 M HCl, saturated aq. $NaHCO_3$, H_2O and brine. The organic layer was dried over anhydrous $MgSO_4$ and concentrated under reduced pressure to afford a brown solid mass. The residue was purified by silica-gel column chromatography eluted with $CHCl_3$/AcOEt = 19/1 (v/v) and then hexane/AcOEt = 19/1 (v/v), followed by recrystallization to obtain **1** as a yellowish solid. Mp 163–164 °C, $[\alpha]_D$ –49.4° (*c* = 0.1 g/dL, $CHCl_3$). ^{1}H NMR (400 MHz, $CDCl_3$): δ 7.63 [s, 2H, Ar], 5.82–5.43 [m, 5H, CON*H*, OCON*H*, O*H*, CH_2=C*H*], 5.12–4.82 [m, 5H, C**H*, CH_2=CH], 4.05 [m, 1H, CH_2C*H*], 2.26–2.07 [m, 4H, CH_2], 1.42 [s,

9H, C(CH_3)$_3$] ppm. ^{13}C NMR (100 MHz, $CDCl_3$): δ 168.7, 155.0, 153.6, 138.0, 134.6, 133.8, 133.4, 118.4, 118.3, 82.5, 80.4, 56.7, 48.5, 38.5, 38.2, 28.3 ppm. IR (cm^{-1}, KBr): 3383, 3309, 2977, 2938, 1715, 1644, 1166. HR-ESI-MS (*m*/*z*): $[M+H]^+$ Calcd for $C_{20}H_{27}O_4N_2I_2$: 613.0060, found 613.0044.

Monomer 2. Monomer **2** was synthesized in a manner similar to that used for **1**, except 2,6-diallyl-4-methylaniline was used instead of 1,6-heptadienyl-4-amine. Yield: 40% (yellowish solid). Mp 197–199 °C, $[\alpha]_D$ –58.9° (*c* = 0.1 g/dL, $CHCl_3$). ^{1}H NMR (400 MHz, $CDCl_3$): δ 7.76 [s, 2H, Ar], 6.90 [s, 2H, Ar], 6.85 [br, 1H, O*H*], 5.82–5.73 [m, 4H, CON*H*, OCON*H*, CH_2=C*H*], 5.10 [br, 1H, C**H*], 5.01 and 4.81 [d, *J* = 10.2 Hz and d, *J* = 17.0Hz, 4H, CH_2=CH], 3.16–3.03 [m, 4H, CH_2], 2.28 [s, 3H, CH_3], 1.43 [s, 9H, C(CH_3)$_3$] ppm. ^{13}C NMR (100 MHz, $CDCl_3$): δ 168.2, 155.1, 153.8, 137.9, 137.8, 136.8, 136.4, 134.2, 129.8, 128.9, 115.7, 82.8, 80.6, 56.6, 36.3, 28.4, 21.1 ppm. IR (cm^{-1}, KBr): 3313, 2978, 2926, 1660, 1163. HR-ESI-MS (*m*/*z*): $[M+H]^+$ Calcd for $C_{26}H_{31}O_4N_2I_2$: 689.0373, found 689.0355.

Monomer 3. Monomer **3** was synthesized in a manner similar to that used for **1** using *N*-(2-aminoethyl)-5-norbornene-*endo*,*endo*-2,3-dicarboximide instead of 1,6-heptadienyl-4-amine. Yield: 24% (white solid). Mp: 116–118 °C. $[\alpha]_D$ –66° (*c* = 0.1 g/dL, $CHCl_3$). ^{1}H NMR (400 MHz, $CDCl_3$): δ 7.67 [s, 2H, Ar], 6.36–5.78 [m, 5H, CON*H*, OCON*H*, O*H*, C*H*=C*H*], 4.92 [1H, C**H*], 3.54–3.20 [m, 8H, CONHCH_2CH_2N, C*H*CONCOC*H*, C*H*-CH=CH-C*H*], 1.73 [d, *J* = 9.04 Hz, 1H, bridge position], 1.54 [d, *J* = 8.80 Hz, 1H, bridge position], 1.42

[s, 9H, C(CH_3)$_3$] ppm. ^{13}C NMR (100 MHz, $CDCl_3$): δ 178.0, 169.5, 154.9, 153.6, 137.9, 134.4, 134.3, 82.7, 80.4, 56.6, 52.3, 45.8, 44.9, 39.8, 37.2, 28.3 ppm. IR (cm^{-1}, KBr): 3311, 2978, 2941, 1693, 1185, 1161. HR-APCI-MS (*m*/*z*): $[M+H]^+$ Calcd for $C_{24}H_{28}O_6N_3I_2$: 708.0067, found 708.0058.

Polymerization. Sonogashira–Hagihara coupling polymerization.[9] Typical procedure: A solution of **1** (1.22 g, 1.99 mmol), *p*-diethynylbenzene (0.251 g, 1.99 mmol), $PdCl_2(PPh_3)_2$ (44.7 mg, 0.235 mmol), CuI (25.7 mg, 0.0366 mmol) and PPh_3 (44.7 mg, 0.170 mmol) in Et_3N (8 mL) and DMF (12 mL) was stirred at 80 °C for 24 h. The reaction mixture was poured into MeOH/acetone [5/1 (v/v), 600 mL]. The precipitate was separated by filtration using a membrane filter (ADVANTEC H100A047A) and then dried under reduced pressure.

Spectroscopic data for polymers. **1a**: ^{1}H NMR (400 MHz, $CDCl_3$): δ 7.89–7.33 [br, 2H, Ar], 6.08–5.43 [br, 5H, CON*H*, OCON*H*, O*H*, CH_2=C*H*], 5.31–4.58 [br, 5H, C**H*, CH_2=CH], 4.18–3.91 [br, 1H, CH_2C*H*], 2.59–1.98 [br, 4H, CH_2], 1.84–1.09 [br, 9H, C(CH_3)$_3$] ppm. **2a**: ^{1}H NMR (400 MHz, $CDCl_3$): δ 7.82–7.40 [br, 2H, Ar], 6.98–6.47 [br, 3H, Ar, O*H*], 5.86–5.50 [br, 4H, CON*H*, OCON*H*, CH_2=C*H*], 5.08–4.53 [br, 5H, C**H*, CH_2=CH], 3.22–2.86 [br, 4H, CH_2], 2.37–2.10 [br, 3H, CH_3], 1.84–1.11 [br, 9H, C(CH_3)$_3$] ppm. **3a**: ^{1}H NMR (400 MHz, $CDCl_3$): δ 7.80–7.32 [br, 2H, Ar], 6.23–5.69 [br, 5H, CON*H*, OCON*H*, O*H*, C*H*=C*H*], 5.35–5.10 [br, 1H, C**H*], 3.88–2.84 [br, 8H, CONHCH_2CH_2N, C*H*CONCOC*H*, C*H*-CH=CH-C*H*], 2.01–1.12 [br, 11H, bridge

position, C(CH_3)$_3$] ppm.

Metathesis polymerization at the side chains; Acyclic diene metathesis (ADMET) polymerization at the side chains of 1a and 2a. A solution of **1a** [26.0 mg, 0.0539 mmol (monomer unit)] and the second-generation Grubbs' catalyst (1.3 mg, 1.5 μmol) in THF (26 mL) was stirred at 45 °C for 18 h. Excess ethyl vinyl ether was added, and the solution was concentrated to a volume of approximately 2 mL. The residual solution was poured into MeOH (100 mL) to precipitate the polymer. The precipitate was filtered using a membrane filter (ADVANTEC H100A047A) and dried under reduced pressure. The yield was quantitative. ^{1}H NMR (400 MHz, $CDCl_3$): δ 8.00–6.48 [br, 2H, Ar], 5.92–5.35 [br, 4H, Ar, CON*H*, OCON*H*, C*H*=C*H*], 5.18–4.82 [br, 1H, C**H*], 4.09–3.77 [br, 1H, CH_2C*H*], 2.46–1.85 [br, 4H, CH_2], 1.83–0.87 [br, 9H, C(CH_3)$_3$] ppm.

The ADMET reaction for the preparation of **2a** was performed in a manner analogous to that used for **1a** in $CHCl_3$ at 50 °C for 24 h. Yield: 80%. ^{1}H NMR (400 MHz, $CDCl_3$): δ7.88–7.39 [br, 2H, Ar], 6.97–6.61 [br, 3H, Ar, O*H*], 5.90–5.47 [br, 4H, Ar, CON*H*, OCON*H*, C*H*=C*H*], 5.04–4.54 [br, 1H, C**H*], 3.24–2.95 [br, 4H, CH_2], 2.46–2.05 [br, 3H, CH_3], 2.03–0.92 [br, 9H, C(CH_3)$_3$] ppm.

Metathesis polymerization at the side chains; Ring-opening metathesis polymerization (ROMP) at the side chains of 3a. A solution of **3a** [116 mg, 0.200 mmol (monomer unit)], second-generation Grubbs' catalyst

(11.1 mg, 13.1 μmol) and *cis*-1,4-dichloro-2-butene (20 μL, 0.19 mmol) as a chain-transfer agent in THF (100 mL) was stirred at 50 °C for 24 h.[25] The solution was then concentrated to a volume of approximately 2 mL. The residue was poured into MeOH (100 mL) to precipitate the polymer, which was collected using a membrane filter (ADVANTEC H100A047A) and dried under reduced pressure. Yield: 93%. ^{1}H NMR (400 MHz, $CDCl_3$): δ 8.53–6.87 [br, 2H, Ar], 6.36–5.59 [br, 3H, CON*H*, OCON*H*, O*H*], 5.51–5.00 [br, 3H, C*H*=C*H*, C**H*], 4.41–2.90 [br, 8H, CONHCH_2CH_2N, C*H*CONCOC*H*, C*H*-CH=CH], 2.58–0.86 [br, 11H, CH-CH_2-CH, C(CH_3)$_3$] ppm.

References and Notes

(1) Natta, G.; Pino, P.; Corradini, P.; Danusso, F.; Mantitca, E.; Nazzanti, G.; Moraglio, G. *J. Am. Chem. Soc.* **1955**, *77*, 1708–1710.

(2) Okamoto, Y.; Suzuki, K.; Ohta, K.; Hatada, K.; Yuki, H. *J. Am. Chem. Soc.* **1979**, *101*, 4763–4765.

(3) Reviews: (a) Aoki, T.; Kaneko, T.; Teraguchi, M. *Polymer* **2006**, *47*, 4867–4892. (b) Yashima, E.; Maeda, K.; Iida, H.; Furusho, Y.; Nagai, K. *Chem. Rev.* **2009**, *109*, 6102–6211. (c) Akagi, K. *Chem. Rev.* **2009**, *109*, 5354–5401. (d) Liu, J.; Lam, J. W. Y.; Tang, B. Z. *Chem. Rev.* **2009**, *109*, 5799–5867. (e) Shiotsuki, M.; Sanda, F.; Masuda, T. *Polym. Chem.* **2011**, *2*, 1044–1058.

(4) Review: Green, M. M.; Park, J.-W.; Sato, T.; Teramoto, A.; Lifson, S.; Selinger, R. L. B.; Selinger, J. V. *Angew. Chem. Int. Ed.* **1999**, *38*, 3138–3154.

(5) Reviews: (a) Cornelissen, J. J. L. M.; Rowan, A. E.; Nolte, R. J. M.; Sommerdijk, N. A. J. M. *Chem. Rev.* **2001**, *101*, 4039–4070. (b) Suginome, M.; Ito, Y. *Adv. Polym. Sci.* **2004**, *171*, 77–136. (c) David, B.

A.; Serrano, J.; Sierra, T.; Veciana, J. *J. Polym. Sci., Part A: Polym. Chem.* **2006**, *44*, 3161–3174.

(6) Reviews: (a) Fujiki, M. *J. Organomet. Chem*. **2003**, *685*, 15–34. (b) Fujiki, M.; Koe, J. R.; Terao, K.; Sato, T.; Teramoto, A.; Watanabe, J. *Polym. J.* **2003**, *35*, 297–344. (c) Sato, T.; Terao, K.; Teramoto, A.; Fujiki, M. *Polymer* **2003**, *44*, 5477–5495.

(7) Reviews: (a) Bunz U. H. F. *Adv. Polym. Sci.* **2005**, *177*, 1–52. (b) Smaldone, R. A.; Moore, J. S. *Chem. Eur. J.* **2008**, *14*, 2650–2657. (c) Bunz U. H. F. *Macromol. Rapid. Commun.* **2009**, *30*, 772–805.

(8) Nakano, T.; Okamoto, Y. *Chem. Rev.* **2001**, *101*, 4013–4038.

(9) Liu, R.; Shiotsuki, M.; Masuda, T.; Sanda, F. *Macromolecules* **2009**, *42*, 6115–6122.

(10) (a) Prince, R. B.; Saven, J. G.; Wolynes, P. G.; Moore, J. S. *J. Am. Chem. Soc.* **1999**, *121*, 3114–3121. (b) Prince, R. B.; Brunsveld, L.; Meijer, E. W.; Moore, J. S. *Angew. Chem. Int. Ed.* **2000**, *39*, 228–230.

(11) Walensky, L. D.; Kung, A. L.; Escher, I.; Malia, T. J.; Wright, R. D.; Wagner, G.: Verdine, G. L.; Korsmeyer, S. J. *Science* **2004**, *305*, 1466–1470.

(12) Jin, W.; Fukushima, T.; Kosaka, A.; Niki, M.; Ishii, N.; Aida, T. *J. Am. Chem. Soc.* **2005**, *127*, 8284–8285.

(13) Hecht, S.; Khan, A. *Angew. Chem. Int. Ed.* **2003**, *42*, 6021–6024.

(14) Circular Dichroism: Principles and Applications, 2nd ed.; Berova, N., Nakanishi, K., Woody, R. W., *Eds.; Wiley-VCH: New York*, **2000** (Chapter 12).

(15) Sogawa, H.; Shiotsuki, M.; Matsuoka, H.; Sanda, F. *Macromolecules* **2011**, *44*, 3338–3345.

(16) The ADMET polymerization of monomers **1** and **2** was performed to examine the reactivity of the diene groups. Monomer **1** afforded no polymer, but rather a compound that contained a cyclopentene unit, an RCM product of 1,6-heptadiene. ADMET was also observed at the side chains of polymer **1a** in addition to RCM, likely because of the higher local concentration of 1,6-heptadiene units in the side chains of **1a** than in **1**. Meanwhile, monomer **2** afforded no RCM product, but rather

oligomers with M_n = 1000, which indicated the high selectivity of ADMET at the side chains of **2a**.

(17) An *exo*,*exo*-isomer (M_n = 7500, PDI = 2.2) of **3a** was also synthesized and subjected to ROMP under the same conditions. The obtained polymer was only partly soluble in THF, presumably due to the occurrence of intermolecular crosslinking reactions. Because *exo*,*exo*-norbornene monomers are commonly more reactive than their *endo,endo*-counterparts, the *exo,exo*-isomer of **3a** likely also underwent ROMP intermolecularly.

(18) This value was calculated based on molecular modeling and indicated that one turn of the helix of the present polymers consisted of six monomer units. Consequently, the maximum degree of polymerization (*DP*) at the side chains was estimated by the following equation:
$DP = M_n$ of polymer/(MW of monomer unit × 6)
When the reaction was performed in the absence of *cis*-1,4-dichloro-2-butene, the intensity change of the CD signal was small in DMF. The addition of 0.5 and 1.5 equivalents of *cis*-1,4-dichloro-2-butene were also examined, but the CD intensities were smaller than the case of 1.0 equivalents.

(19) Halgren, T. A. *J. Comput. Chem.* **1996**, *17*, 490–519.

(20) The pitch of helical poly(*m*-phenyleneethynylene) was estimated to be 3.9 Å based on a molecular dynamics simulation. Lee, O. S.; Saven, J. G. *J. Phys. Chem. B* **2004**, *108*, 11988–11994.

(21) Ma, S.; Ni, B. *Chem. Eur. J.* **2004**, *10*, 3286–3300.

(22) (a) Li, L.; Jones, W. D. *J. Am. Chem. Soc.* **2007**, *129*, 10707–10713. (b) Gonazález, I.; Souto, A.; Rodoríguez, R.; Cruces, J. *Tetrahedron Lett.* **2008**, *49*, 2002–2004.

(23) Lu, H.; Cheng, J. *J. Am. Chem. Soc.* **2008**, *130*, 12562–12563.

(24) Yamada, Y.; Akiba, A.; Arima, S.; Okada, C.; Yoshida, K.; Itou, F.; Kai, T.; Satou, T.; Takeda, K.; Harigaya, Y. *Chem. Pharm. Bull.* **2005**, *53*, 1277–1290.

(25) Vargas, J.; Fomine, S.; Fomina, L.; Tienkopatchev, M. A. *The Open Macromolecules Journal* **2008**, *2*, 32–37.

Part II

Synthesis and Properties of Poly(phenyleneethynylene)s containing Azobenzene Moieties

Chapter 4

Synthesis, Chiroptical Properties, and Photo-responsiveness of Optically Active Poly(*m*-phenyleneethynylene)s Containing Azobenzene Moieties

Abstract

The Sonogashira–Hagihara coupling polymerization of 3',5'-diiodo-4'-hydroxy-*N*-α-*tert*-butoxycarbonyl-D-phenylglycine ethyl-, hexyl-, and laurylamides **1a**–**c** with *p*-non-substituted, cyano, hexyl, and methoxy 3,5-diethynylazobenzenes **2a**–**d** was carried out to obtain optically active novel poly(*m*-phenyleneethynylene) with M_w's in the range from 6,900 to15,400 in 62–84% yields. CD and UV–vis spectroscopic data indicated that the polymers adopted thermally stable helical conformations in CH_2Cl_2 and *N,N*-dimethylformamide. Poly(**1b**–**2a**) further formed a chirally aggregated structure. The azobenzene moieties of the polymers underwent reversible photo-isomerization upon UV- and visible-light irradiation, accompanying the changes of the higher-order structures.

Introduction

Biomacromolecules such as proteins and DNA commonly have one-handed helical structures based on the homochirality of the components. Their functions and biological activities are generated by their well-defined higher-order structures. Artificial helical polymers have been extensively synthesized by imitating naturally derived helices.[1] Development of artificial helical polymers may encourage better understanding of the mechanisms for complicated and elegant functions of biopolymers. π-Conjugated helical polymers such as polyisocyanides,[2] polyacetylenes,[3] polythiophenes,[4] poly(phenylenevinylene)s,[5] and poly(phenyleneethynylene)s[6] have attracted much attention because of their potential of practical applications including molecular recognition materials,[7–12] chiral catalysts,[13–15] and chemical sensors[16–18] using their unique electronic and optical properties based on the secondary structures. Among them, poly(*m*-phenyleneethynylene)s substituted with polar groups tend to folded into helical structures in polar solvents based on the amphiphilic property between the hydrophilic side chains and hydrophobic main chain.[1b, 19–21] On the other hand, new examples of hydroxyphenylglycine- and tyrosine-based poly(*m*-phenyleneethynylene-*p*-phenyleneethynylene)s that adopt helical conformations consisting of hydrophobic exterior (alkyl groups and phenyleneethynylene main chain) and hydrophilic interior (hydroxy groups) in nonpolar solvents have been found recently.[22,23] The helix formation of these polymers is based on the amphiphilic balance opposite from that of

poly(*m*-phenyleneethynylene) derivatives reported so far.

Meanwhile, azobenzene is one of the best-known photo-responsive molecules undergoing reversible photo-isomerization between *trans*- and *cis*-forms upon UV- and visible-light irradiation.[24] This conformational change triggers not only geometric change but also chemical properties such as dipole moment. Among various kinds of external stimuli, photo-irradiation is practically useful for constructing sensing materials because of easy control over the irradiation wavelength, time and intensity.[25–30] Azobenzene-containing π-conjugated helical polymers are applicable to intelligent materials that possess photo-responsiveness in addition to the electronic and optical properties as mentioned above.[31–34]

In this chapter, the author wishes to discuss the synthesis of novel hydroxyphenylglycine-derived poly(*m*-phenyleneethynylene)s containing azobenzene moieties (Scheme 1), and investigation of the effects of the alkyl chain lengths or substituent of azobenzene moieties on the higher-order structure, together with the solvent effect. The author also discusses the reversible photo-responsive conformational changes of the polymers.

Results and Discussion

Monomer Synthesis and Sonogashira–Hagihara Coupling Polymerization. 3,5-Diethynylazobenzene monomers **2a–d** were synthesized by the route illustrated in Scheme 2. First, 3,5-diiodoazobenzene derivatives

3a–**c** were synthesized by the condensation of 3,5-diiodoaniline with the corresponding nitrosobenzene derivatives in condensation of 3,5-diiodoaniline with the corresponding nitrosobenzene derivatives in CH_3COOH. Compound **3d** was synthesized by the diazo coupling reaction of 3,5-diiodoaniline with phenol, followed by methyl etherification of 4-(3,5-diiodophenylazo)phenol formed, because the reaction using 4-nitrosoanisole was unsatisfactory. Subsequently, the Sonogashira–Hagihara coupling reaction of **3a**–**d** with trimethylsilylacetylene and desilylation from the ethynyl group were carried out to obtain monomers **2a**–**d**. All the monomers were characterized by ^1H, ^{13}C NMR, and IR spectroscopies besides elemental analysis or high-resolution mass spectrometry.

Scheme 1. Sonogashira–Hagihara Coupling Polymerization of Monomers **1a**–**c** with **2a**–**d**

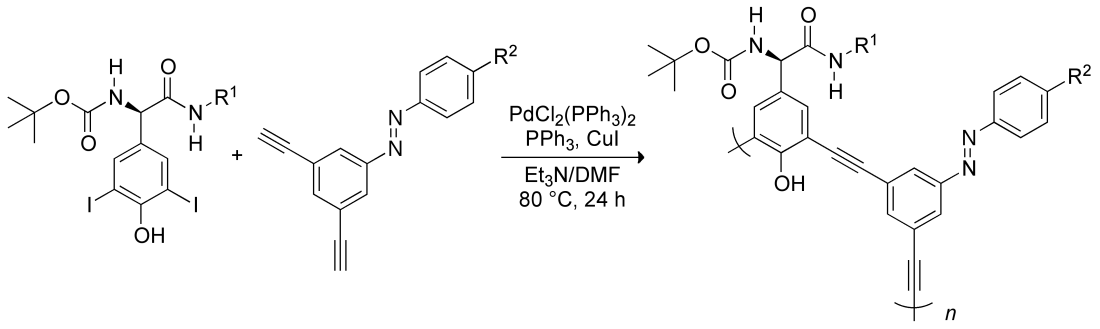

1a–c
1a: $R^1 = C_2H_5$
1b: C_6H_{13}
1c: $C_{12}H_{25}$

2a–d
2a: R^2 = H
2b: CN
2c: C_6H_{13}
2d: OCH_3

poly(**1a–2a**)–poly(**1c–2a**)
poly(**1a–2a**): $R^1 = C_2H_5$ R^2 = H
poly(**1b–2a**): C_6H_{13} H
poly(**1b–2b**): CN
poly(**1b–2c**): C_6H_{13}
poly(**1b–2d**): OCH_3
poly(**1c–2a**): $C_{12}H_{25}$ H

Scheme 2. Synthesis of Monomers **2a–d**

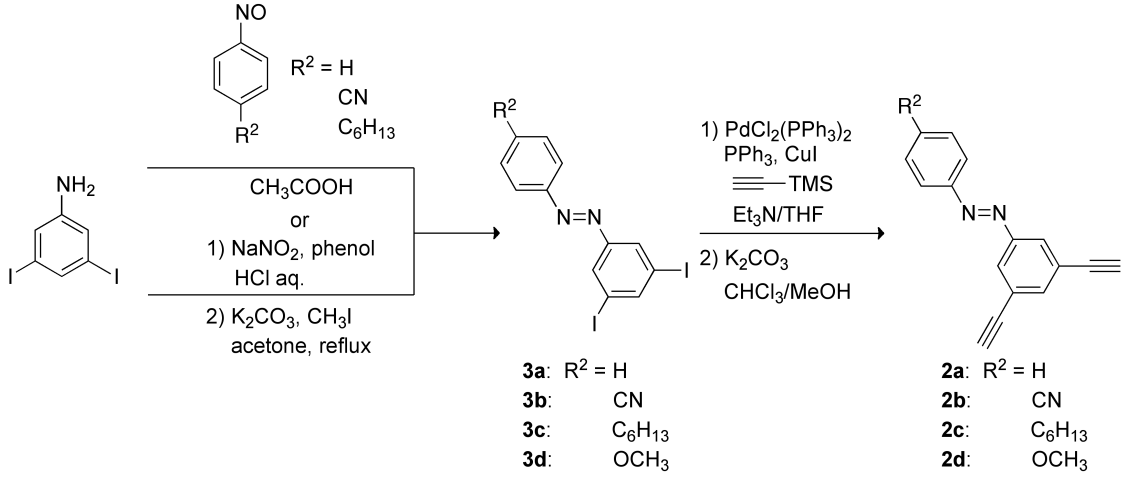

The Sonogashira–Hagihara coupling polymerization of **1a** with **2a**, **1b** with **2a–d**, and **1c** with **2a** was carried out in DMF at 80 °C for 24 h to obtain the corresponding polymers [poly(**1a**–**2a**)–poly(**1c**–**2a**)] with M_w's in the range of 6,900–15,400 in 62–84% yields as listed in Table 1. Except for poly(**1b**–**2b**), the polymers were soluble in common organic solvents such as CH_2Cl_2, $CHCl_3$, THF, DMSO, and DMF. Poly(**1b**–**2b**) was insoluble in CH_2Cl_2 and $CHCl_3$, partly soluble in THF, DMSO, and DMF.

Table 1. Sonogashira–Hagihara Coupling Polymerization of **1a**–**c** with **2a**–**d**[a]

monomer	polymer			
		yield[b] (%)	M_w[c]	M_w/M_n[c]
1a+2a	poly(**1a**–**2a**)	83	11,900	1.9
1b+2a	poly(**1b**–**2a**)	62	15,400	1.8
1b+2b	poly(**1b**–**2b**)	65	8,800[d]	1.5[d]
1b+2c	poly(**1b**–**2c**)	68	6,900	1.8
1b+2d	poly(**1b**–**2d**)	84	14,000	1.9
1c+2a	poly(**1c**–**2a**)	72	10,900	1.6

[a] Conditions: [**1a–c**] = [**2a–d**] = 0.20 M, [$PdCl_2(PPh_3)_2$] = 0.0040 M, [CuI] = 0.024 M, [PPh_3] = 0.016 M, Et_3N/DMF = 2/3 (v/v), 80 °C, 24 h. [b] MeOH/acetone = 4/1 (v/v)-insoluble part. [c] Determined by GPC eluted with $CHCl_3$, polystyrene calibration. [d] Eluted with THF.

Chiroptical Properties of the Polymers. The CD and UV–vis spectra of the polymers in CH_2Cl_2 at 20 °C were measured to obtain information on the secondary structures. Poly(**1a**–**2a**), poly(**1b**–**2a**), and poly(**1c**–**2a**) exhibited CD signals at 250–450 nm as shown Figure 1. They showed UV–vis absorption at the same region (λ_{max} around 315 nm) as the CD signals. The λ_{max}'s of the polymers appeared blue-shifted by 76–79 nm comparing to those of **1a**–**c**. It is considered that these CD and UV–vis absorption peaks come from the conjugated *m*-phenyleneethynylene backbone. The absorption derived from the azobenzene moieties seems to overlap with that of the main chains, because the λ_{max} of **2a** was 320 nm as well. Hence, it is considered that poly(**1a**–**2a**), poly(**1b**–**2a**), and poly(**1c**–**2a**) adopt helical conformations with predominantly one-handed screw sense in CH_2Cl_2 in a manner similar to the analogous poly(*m*-phenyleneethynylene-*p*-phenyleneethynylene)s.[23] The CD intensity of poly(**1c**–**2a**) was higher than that of poly(**1a**–**2a**) probably due to the longer alkyl chains, which are effective to stabilize the helical structure by enhancing the hydrophobicity of the helix exterior, and/or hydrophobic interaction between the side chains.

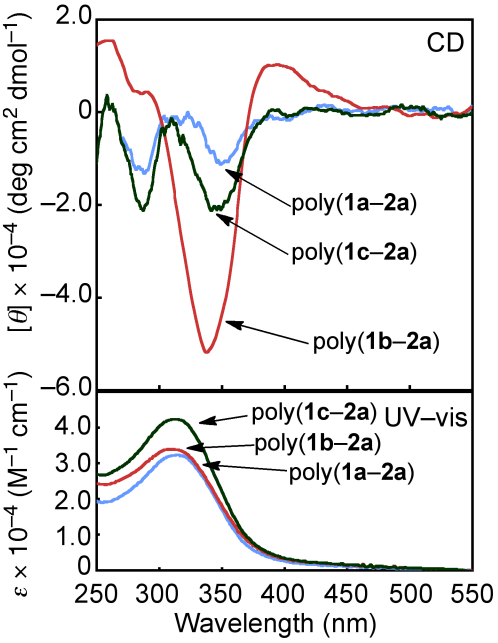

Figure 1. CD and UV–vis spectra of poly(**1a**–**2a**), poly(**1b**–**2a**), and poly(**1c**–**2a**) measured in CH_2Cl_2 (c = 0.030 mM) at 20 °C.

It should be noted that the CD spectrum of poly(**1b**–**2a**) was different from those of poly(**1a**–**2a**) and poly(**1c**–**2a**). The author filtered the sample solution using a membrane with a pore size of 0.45 mm, and then measured the CD and UV–vis spectra of the sample again. Interestingly, the CD signal of poly(**1b**–**2a**) became nearly identical to those of the other two polymers, poly(**1a**–**2a**) and poly(**1c**–**2a**), as shown Figure 2. This result suggests that poly(**1b**–**2a**) formed the chiral aggregates exhibiting the different CD signals from those of non-aggregated states. Since the UV–vis intensities of the sample before and after filtration were almost the same, it is likely that the population of the aggregates is very small. The CD and UV–vis spectra of poly(**1a**–**2a**) and poly(**1c**–**2a**) samples did not change at all before and after filtration.

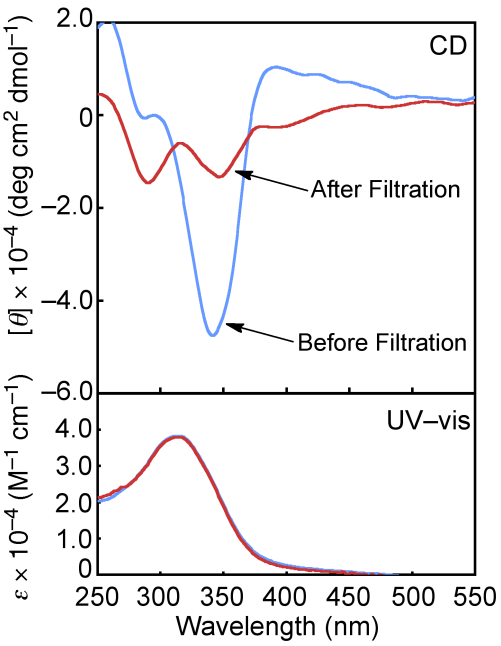

Figure 2. CD and UV–vis spectra of poly(**1b**–**2a**) measured in CH_2Cl_2 (c = 0.030 mM) at 20 °C before and after filtration using a membrane with 0.45 μm pore size.

The author measured the dynamic light scattering (DLS) of a CH_2Cl_2 solution of poly(**1b**–**2a**) to elucidate the formation of aggregates. From the correlation functions depicted in Figure 3, a hydrodynamic radius (R_h) could be evaluated both from fast and slow modes. From the fast mode, the presence of aggregated particles with an R_h around 385 nm was confirmed. The slow mode indicates the presence of very large aggregates whose size is about 2000 nm, which is larger by the order of magnitude. According to the scattering principle, the scattering intensity is proportional to the volume of the scatter, hence the number population of the large aggregates should be 10^{-3} or less, which leads us to the conclusion that the fast mode is main component, about which the author should discuss. The filtration of the sample solution resulted in disappearance

of the DLS modes assignable to aggregated particles (fast mode) in addition to the large aggregates (slow mode). It is concluded that the aggregated particles have chirality, showing the intense CD signals.[35]

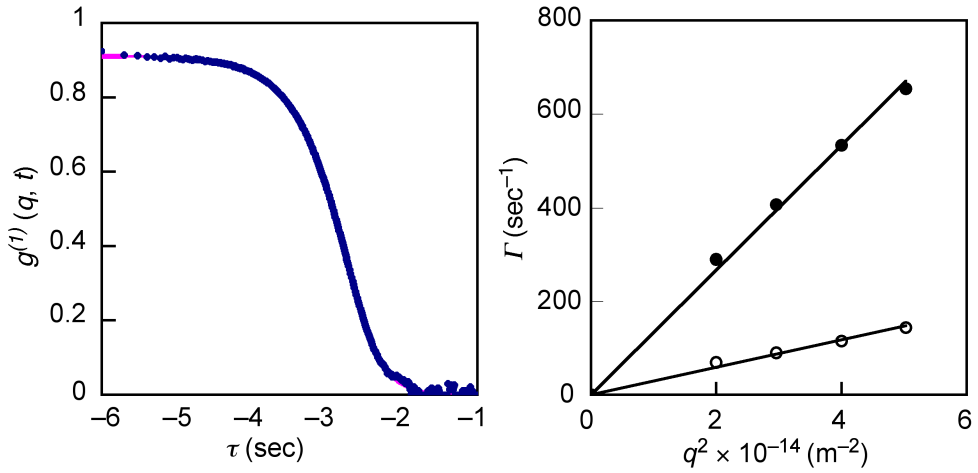

Figure 3. DLS results for solutions of poly(**1b**–**2a**) 0.10 wt% in CH_2Cl_2 measured at a scattering angle of 90° at 25 °C. Left: Time correlation functions for the scattered filed. Solid lines are double-exponential fits. Right: Decay rate Γ vs q^2 plot for poly(**1b**–**2a**) for the fast mode (●) and slow mode (○). The excellent linearity in this plot guarantees that both of these two modes correspond to the translational diffusion. The diffusion coefficients of the particles were evaluated from the slopes of the straight lines for the fast mode.

Figure 4 shows the CD and UV–vis spectra of poly(**1b**–**2a**) measured in THF and DMF. The previously reported hydroxyphenylglycine-based poly(*m*-phenyleneethynylene-*p*-phenyleneethynylene)s exhibited Cotton effect on the CD spectrum indicating the formation of predominantly one-handed helical conformation in THF, while no CD signal was observed in DMF.[32] Poly(**1b**-**2a**), on the contrary, exhibited intense CD signals in either of the

solvents. Poly(**1b**-**2a**) seems to have a high ability to form a chiral higher-order structure compared to the reported hydroxyphenylglycine-based poly(*m*-phenyleneethynylene-*p*-phenyleneethynylene)s. The all *meta*-linked structure of poly(**1b**-**2a**) may be preferable for the polymer to adopt a folded structure. In addition, the azobenzene moieties of poly(**1b**-**2a**) may participate in intramolecular *p*-stacking between the phenylene groups of the main chain, resulting in the high ability of helix formation. Poly(**1a**–**2a**) and poly(**1c**–**2a**) also exhibited CD signals in CH_2Cl_2, THF, and DMF.

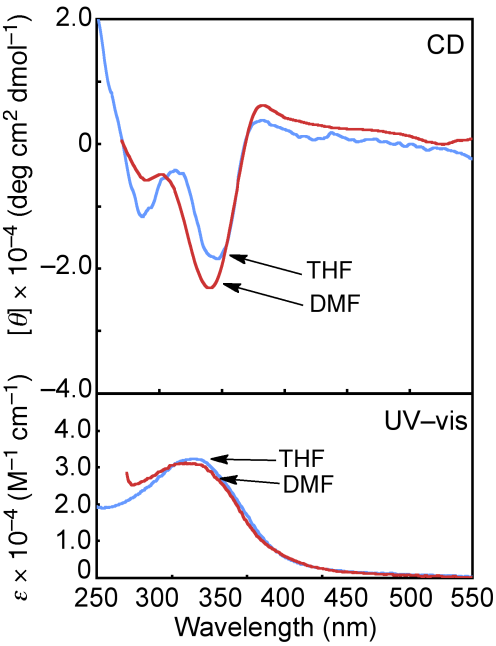

Figure 4. CD and UV–vis spectra of poly(**1b**–**2a**) measured in THF and DMF (c = 0.030 mM) at 20 °C.

As mentioned above, poly(**1b**–**2a**) formed chiral aggregates in CH_2Cl_2, while poly(**1a**–**2a**) and poly(**1c**–**2a**) did not. It is presumed that the chain length of alkyl groups of poly(**1b**–**2a**) match the requirement for inducing aggregation.

The CD intensity slightly increased as the sample concentration was increased in CH_2Cl_2 as shown in Figure 5, left. An interesting phenomenon was observed in DMF as shown in Figure 5, right. At a concentration of 0.010 mM, a non-aggregated CD pattern was observed. On the other hand at 0.025 mM, an aggregated CD pattern appeared, and the intensity increased as the concentration was increased to 0.035 mM. It was confirmed that the critical aggregation concentration of poly(**1b**–**2a**) exists between 0.010 and 0.025 mM in DMF.

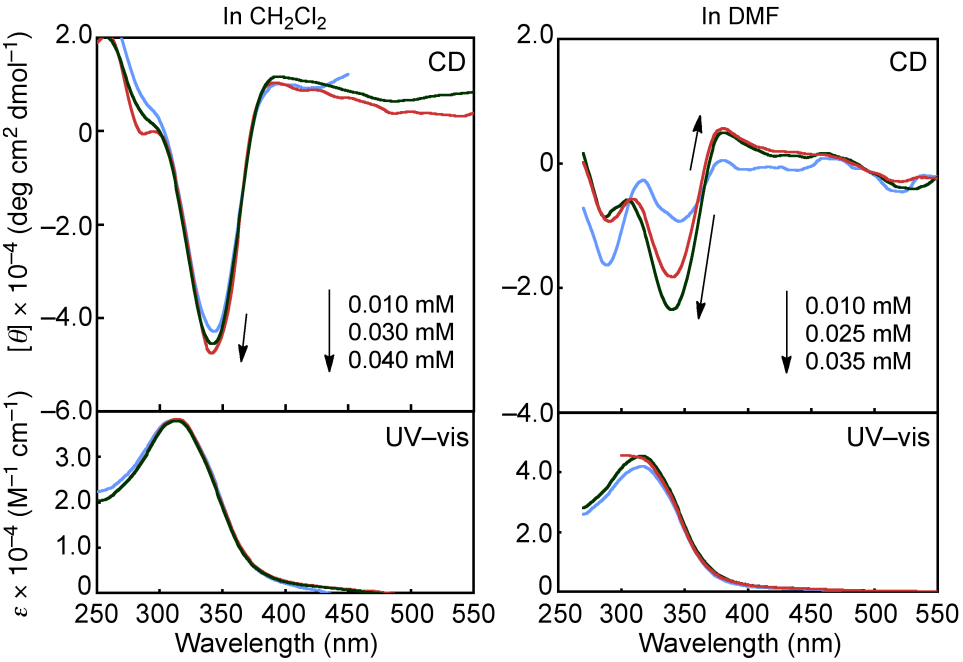

Figure 5. CD and UV–vis spectra of poly(**1b**–**2a**) measured in CH_2Cl_2 (left) and DMF (right) at various concentrations at 20 °C.

The helical structures of poly(*m*-phenyleneethynylene)s are commonly susceptible to temperature.[36,37] The author measured the CD spectra of poly(**1a**–**2a**), poly(**1b**–**2a**), and poly(**1c**–**2a**) in CH_2Cl_2 at 0–40 °C to find

negligibly small changes. The Kuhn's dissymmetry factors ($g = \Delta\varepsilon/\varepsilon$, in which $\Delta\varepsilon = [\theta]/3298$) of poly(**1a**–**2a**) and poly(**1c**–**2a**) decreased only 6% and 5% by raising temperature from 20 to 40 °C, and that of poly(**1b**–**2a**) did not decreased at this temperature range.[38] The *g* values gives quantitative information associated with the degree of preferential screw sense.[39] The temperature dependence of *g* values of the present polymers is very small compared to that of the previously reported poly(*m*-phenyleneethynylene) derivatives. For example, the *g* value of a poly(phenyleneethynylene) tethering tetraethylene glycol decreases 17% by from 20 to 40 °C.[36]

Thus, the higher-order structures of the polymers are thermally stable compared to the poly(*m*-phenyleneethynylene)s reported so far. This is explainable by the presence of intramolecular hydrogen bonding between the amide and carbamate groups at the side chains, which was confirmed by the solution state IR spectra of the polymers measured in CH_2Cl_2 at diluted concentrations (Table 2). The carbonyl absorption peaks of amide and carbamate groups of the polymers were observed at 28–29 and 5–6 cm^{-1} lower than those of the monomers **1a**–**c**, respectively.

Poly(**1b**–**2c**) and poly(**1b**–**2d**) also exhibited CD signals as shown Figure 6, indicating that they also formed chiral higher-order structures. On the other hand, poly(**1b**–**2b**) exhibited no CD signal in THF and DMF. The electron-withdrawing character of the CN groups seems to affect the amphiphilic balance, preventing from the polymer to adopt a helical conformation with

predominantly one-handed screw sense.

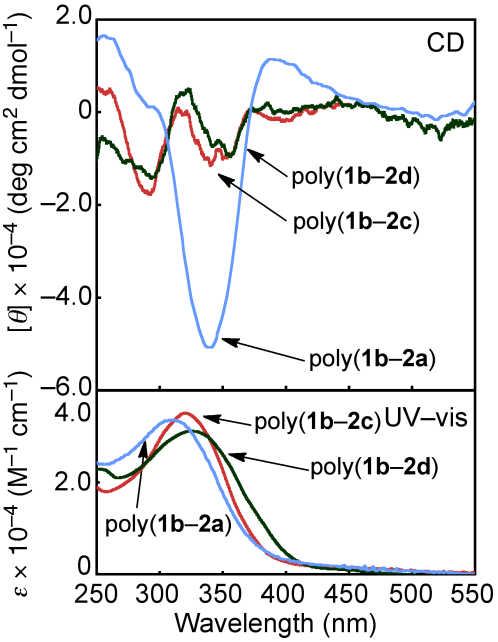

Figure 6. CD and UV–vis spectra of poly(**1b**–**2a**), poly(**1b**–**2c**), and poly(**1b**–**2d**) measured in CH_2Cl_2 (c = 0.030 mM) at 20 °C. Poly(**1b**–**2b**) was insoluble in CH_2Cl_2.

Only poly(**1b**–**2a**) formed a chirally aggregated structure in CH_2Cl_2 among the polymers containing of monomer **1b** unit. This is probably because the affinity of poly(**1b**–**2a**) to CH_2Cl_2 is smaller than that of poly(**1b**–**2c**) and poly(**1b**–**2d**) having hexyl and methoxy groups, respectively. Poly(**1b**–**2c**) and poly(**1b**–**2d**) showed λ_{max}'s longer than that of poly(**1b**–**2a**) as shown in Figure 6. Poly(**1b**–**2d**) showed the longest λ_{max}, corresponding to the λ_{max} order of the monomers (**2a**: 320 nm, **2c**: 335 nm, **2d**: 354 nm). This is quite reasonable because the π–π^* transition band of azobenzene is shifted to a longer wavelength region by introducing electron-donating groups.[40]

Figure 7 depicts the changes of CD and UV–vis spectra of poly(**1b**–**2a**),

poly(**1b**–**2c**), and poly(**1b**–**2d**) with UV-light irradiation. The polymer solutions in CH_2Cl_2 were irradiated with a 400-W high-pressure mercury lamp through a suitable filter to exclude the light of the wavelength below 300 nm and above 400 nm. The UV–vis absorption of poly(**1b**–**2a**) at 320 nm decreased as UV-light irradiation, accompanying a decrease of CD intensity at 340 nm, and took photo-stationary state after 8 min. These spectroscopic changes indicate that the *trans*-azobenzene moieties isomerized into *cis*-form, resulting in partial collapse of a chirally aggregated structure. It seems that the bended main chain of photo-irradiated poly(**1b**–**2a**) due to the *cis*-azobenzene moieties is unfavorable for aggregation compared to the more linear main chain before irradiation. No absorption attributable to n–π* transition of *cis*-azobenzene unit was observed around 440 nm probably due to the low photo-isomerization ratio, which was estimated to be 7% based on change of the UV–vis absorption.[41] The low degree of photo-isomerization is attributable to the overlap of π–π* transition band of the phenyleneethynylene main chain with that of the *trans*-azobenzene units.[19] It is considered that the UV-light was absorbed not only by the azobenzene units but also by the conjugated main chain, preventing the effective photo-isomerization. This assumption seems reasonable from the photo-isomerization data of poly(**1b**–**2c**) and poly(**1b**–**2d**). Namely, it was calculated that the *trans* → *cis* isomerization ratios of azobenzene units of poly(**1b**–**2c**) and poly(**1b**–**2d**) were 17% and 31%, respectively, which were higher than that of poly(**1b**–**2a**). As mentioned above, the π–π* transition

bands of azobenzene moieties of poly(**1b**–**2c**) and poly(**1b**–**2d**) are positioned at longer wavelength regions than that of poly(**1b**–**2a**). It is considered that the azobenzene moieties of the former two polymers can absorb UV-light with higher efficiencies, because the overlaps of the absorption bands with those of phenyleneethynylene backbones are smaller. Interestingly, the CD signals of poly(**1b**–**2c**) and poly(**1b**–**2d**) around 450 nm increased with UV-light irradiation. This result suggests that the polymers induced a certain regulated structure according to the photo-isomerization of the azobenzene moieties. Visible-light irradiation to the UV-light irradiated samples resulted in complete recovery of the initial CD and UV–vis spectroscopic patterns. Reversible conformational changes were confirmed in all the polymers.

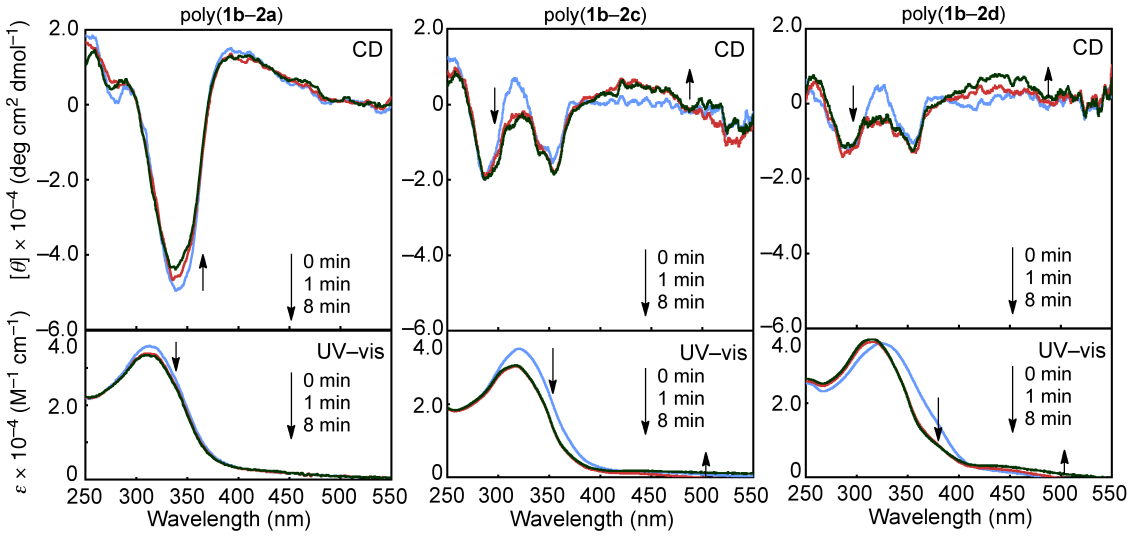

Figure 7. CD and UV–vis spectra of poly(**1b**–**2a**) (left), poly(**1b**–**2c**) (center), and poly(**1b**–**2d**) (right) measured in CH_2Cl_2 (c = 0.030 mM) with irradiation at 300 < λ < 400 nm at 20 °C.

Conformational Analysis. The conformations of poly(*m*-phenyleneethynylene)s have been analyzed by several methods since they have been found to fold into helices under certain conditions. Amine-[42,43] and ester-functionalized[44] poly(*m*-phenyleneethynylene)s energetically prefer helical conformations to coiled and extended ones in water, wherein surrounding water molecules play an important role to fold the polymer chains according to the molecular dynamics simulations. When the molecule adopts a helical conformation, the interaction between the polar side chains and solvents becomes maximum, and *p*-stacking interaction between phenylene units as well. The unfavorable contact between the hydrocarbon backbone and polar solvents becomes minimum simultaneously.[1b]

Judging from the nature of poly(*m*-phenyleneethynylene)s, it is likely that the polymers in the present chapter also adopt folded helical structures with stacked phenylene moieties. The author examined the conformation of the polymers based on the molecular mechanics method (MMFF94).[45] The author first constructed helical 18-mers of poly(**1a**–**2a**), whose both chain ends were terminated with hydrogen atoms as illustrated in Chart 1. The torsional angles of main chains of left- and right-handed helices were set to –6° and +6° per phenylene unit at the initial geometries, respectively. Chart 2 illustrates the eight possible regulated conformers. Symbols *a* and *b* in the pattern column represent the two ways of directions (+180° and –180°) of the carbamate/amide and azobenzene moieties along the conjugated plane of the main chain.

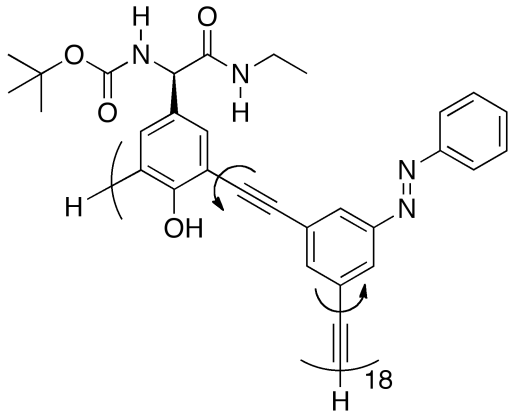

Chart 1. Structure of 18-mers of poly(**1a**–**2a**). The arrows indicate a torsional angle per phenylene unit.

After geometry optimization, the right-handed helical 18-mers became 3.2–6.3 kJ/mol•unit more stable than the left-handed counterparts of patterns *a*–*a*, *a*–*b*, *b*–*a*, and *b*–*b*. Among the eight conformers, the right-handed *b*–*a* in Chart 2 was the most stable. As shown in Figure 8, the amide and carbamate N–H groups of a monomer unit formed regulated intramolecular hydrogen bonds with the C=O groups of the amide and carbamate groups three units earlier ($i + 3 \rightarrow i$ N–H•••O=C hydrogen bonding), respectively. Accordingly, the conformer is surrounded by regulated three hydrogen-bonding strands formed at the amide groups, and the other three hydrogen-bonding strands formed at the carbamate groups. The interatomic distances of the hydrogen and oxygen (N–H•••O=C) participating in hydrogen bonding between the (i + 3) th and i th units at the amide and carbamate moieties were 1.76 Å and 1.79 Å in average, respectively. The shorter interatomic distance between the amide groups may explain the larger shift of carbonyl absorption of the solution state IR from the monomer to

pattern	helical sense	
	left-handed	right-handed
a – *a*	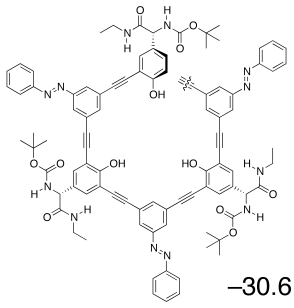 –30.6	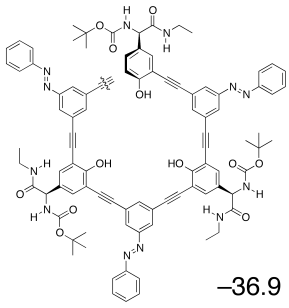 –36.9
a – *b*	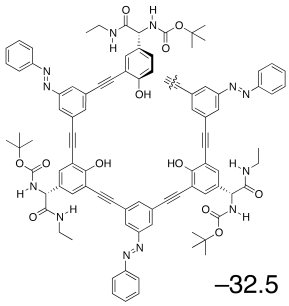 –32.5	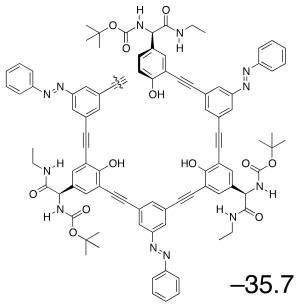 –35.7
b – *a*	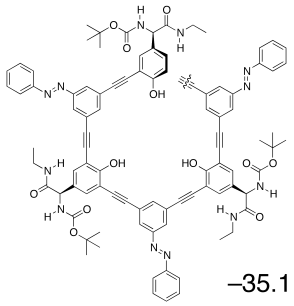 –35.1	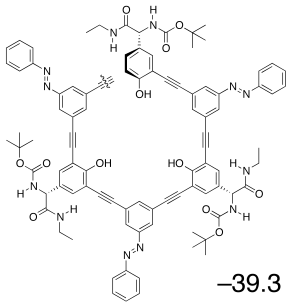 –39.3
b – *b*	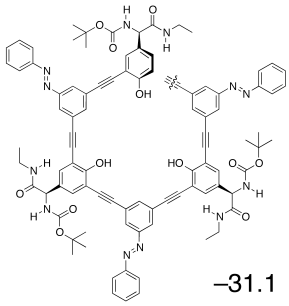 –31.1	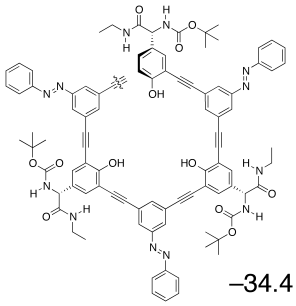 –34.4

Chart 2. Possible regulated conformers of poly(**1a**–**2a**)-18-mer. Fifteen monomer units are omitted at the wavy lines. The values are the energies in kJ/mol•unit of the conformers after geometry optimization by the MMFF94 method.

polymer, than that of carbamate as listed in Table 2. The hydroxy groups inside of the helix cannot form hydrogen bonding each other, because the distance is too long (3–4 Å). The helical pitch after geometry optimization was 3.8 Å, which was same as the value before optimization. This value is consistent with the turns of the helix being near van der Waals contact, and comparable to *p*-stacking between aromatic rings.[47]

Table 2. Solution-State IR Spectroscopic Data (Amide and Carbamate C=O Absorption Peaks) of the Monomers and Polymers[a]

compound	wavenumber (cm^{-1}) amide C=O	carbamate C=O
1a	1683	1707
poly(**1a**–**2a**)	1654	1701
1b	1682	1707
poly(**1b**–**2a**)	1653	1701
1c	1682	1706
poly(**1c**–**2a**)	1654	1701

[a] Measured in CH_2Cl_2 (c = 10–20 mM).

Conclusions

The author has demonstrated the synthesis of novel photo-responsive optically active poly(*m*-phenyleneethynylene)s by the Sonogashira–Hagihara coupling polymerization of D-phenylglycine-derived *m*-diiodobenzenes with 3,5-diethynylazobenzene derivatives. CD and UV–vis spectroscopic studies revealed that the polymers except for poly(**1b**–**2b**) formed thermally stable chiral

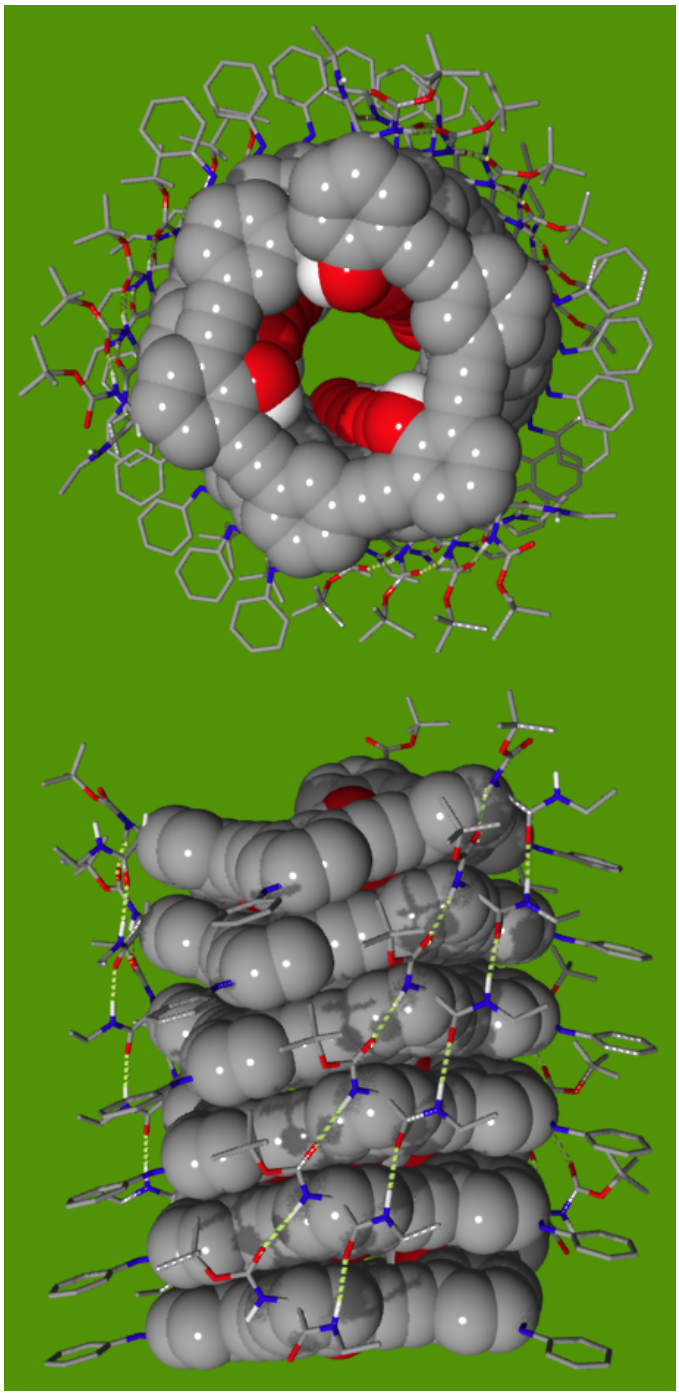

Figure 8. Top and side views of a possible conformation (right-handed *b*–*a* in Chart 2) of poly(**1a**–**2a**)-18-mer. The phenyleneethynylene main chain and O–H groups are illustrated by the space filling models, and the hydrogen atoms other than N–H and O–H moieties are omitted for enhancement of visibility. The green dotted lines represent hydrogen bonds (N–H•••O=C) between the amide groups and carbamate groups. Geometries were optimized by the MMFF94 method.

higher-order structures in CH_2Cl_2, THF, and DMF. Unlike the reported poly(*m*-phenyleneethynylene)s, the present polymers could form chiral higher-order structures in nonpolar CH_2Cl_2, and in polar DMF as well. The presence of intramolecular hydrogen bonds between the amide and carbamate groups at the side chains seems to be effective to stabilize the higher-order structures. The *trans*-azobenzene moieties of the polymers isomerized into *cis*-forms upon UV-light irradiation, accompanying the conformational changes of the polymers. Poly(**1b**–**2a**) formed a chirally aggregated structure in CH_2Cl_2, which partly collapsed according to *trans* → *cis* photo-isomerization. Poly(**1b**–**2c**) and poly(**1b**–**2d**) showed other CD signals at regions of n–π* transition band of *cis*-azobenzene moieties after UV-light irradiation, indicating the formation of chiral structures different from those before photo-irradiation. The degree of photo-isomerization was improved by introducing a *para*-substituent in the azobenzene. The azobenzene moieties of the polymers reversibly isomerized from *cis* to *trans* upon visible-light irradiation, recovering the initial higher-order structures.

Experimental Section

Measurements. ^{1}H (400 MHz) and ^{13}C (100 MHz) NMR spectra were recorded on a JEOL EX-400 or a JEOL AL-400 spectrometer. IR spectra were measured on a JASCO FT/IR-4100 spectrophotometer. Melting points (mp) were measured on a Yanaco micro melting point apparatus. Elemental analysis

was done at the Microanalytical Center of Kyoto University. Mass spectra were measured on an Applied Biosystems Voyager Elite MALDI mass spectrometer or a JEOL JMS-SX102A mass spectrometer. Number- and weight-average molecular weights (M_n and M_w) of polymers were determined by GPC (Shodex columns K803, K804, K805) eluted with $CHCl_3$ or (Shodex columns KF805 × 3) eluted with THF calibrated by polystyrene standards at 40 °C. CD and UV–vis absorption spectra were recorded on a JASCO J-820 spectropolarimeter. Dynamic light scattering (DLS) measurements were carried out with an Otsuka Electronic SLS-7000 goniometer with a GC-1000 correlator. The time-correlation functions were analyzed by double exponential methods. The measurements were performed at four different scattering angles, and the diffusion coefficient D was calculated from the slope of the straight line in the decay rate Γ vs q^2 plot, with q as the scattering vector. The hydrodynamic radii of scatterers were evaluated by the Stokes-Einstein equation.

Photo-irradiation. Photo-irradiation was carried out with a 400 W high-pressure mercury lamp equipped with a power source (HB-400, Fuji Glass Work) at room temperature. The appropriate wavelengths were selected either with a Pyrex glass and a UV-D33S filter (Toshiba) for irradiation at 300 nm < λ < 400 nm or with an L-42 filter (Toshiba) for irradiation at 420 nm < λ. Sample solutions were fed in a quartz cell, and it was placed 20 cm apart from the lamp. The photo-isomerization was monitored by UV–vis absorption spectroscopy.

Materials. 3',5'-Diiodo-4'-hydroxy-*N*-α-*tert*-butoxycarbonyl-D-phenylglycine ethylamide (**1a**), 3',5'-diiodo-4'-hydroxy-*N*-α-*tert*-butoxycarbonyl-D-phenylglycine hexylamide (**1b**), 3',5'-diiodo-4'-hydroxy-*N*-α-*tert*-butoxycarbonyl-D-phenylglycine laurylamide (**1c**), 3,5-diiodoaniline, 4-nitrosobenzonitrile, and 4-nitrosohexylbenzene were prepared according to the literature.[23,46–48] *N,N*-dimethylformamide (DMF) and Et_3N used for polymerization were distilled prior to use.

Monomer Synthesis. 3,5-Diiodoazobenzene (3a). Nitrosobenzene (1.29 g, 12.0 mmol) was added to a solution of 3,5-diiodoaniline (3.49 g, 10.0 mmol) in CH_3COOH, and the resulting mixture was stirred at room temperature overnight. The orange precipitated was collected by filtration and washed with CH_3COOH and with water to obtain **3a** as orange solid in 71% yield; Mp 127–128 °C. ^{1}H NMR (400 MHz, $CDCl_3$): δ 7.51–7.56 (m, 3H, Ar), 7.90 (d, J = 8.0 Hz, 2H, Ar), 8.12 (s, 1H, Ar), 8.21 (d, J = 1.6 Hz, 2H, Ar). ^{13}C NMR (100 MHz, $CDCl_3$): δ 94.84, 123.19, 129.21, 131.34, 131.95, 146.74, 152.08, 153.71. Anal. Calcd for $C_{12}H_8I_2N_2$: C, 33.21; H, 1.86; N, 6.45. Found: C, 33.41; H, 1.89; N, 6.50.

4-(3,5-Diiodophenylazo)benzonitrile (3b). The title compound was synthesized 4-nitrosobenzonitrile and 3,5-diiodoaniline in a manner similar to **3a**. Yield 58%; Mp 189–191 °C. ^{1}H NMR (400 MHz, $CDCl_3$): δ 7.83 (d, J = 8.4 Hz, 2H, Ar), 7.98 (d, J = 8.8 Hz, 2H, Ar), 8.20 (s, 1H, Ar), 8.25 (d, J = 2.0 Hz, 2H, Ar). ^{13}C NMR (100 MHz, $CDCl_3$): δ 94.94, 114.88, 118.17 (–*C*≡N),

123.61, 131.68, 133.32, 147.87, 152.23, 153.74. HRMS. (*m*/*z*): $[M]^+$ Calcd for $C_{13}H_7I_2N_3$ 458.8729. Found: 458.8732.

4-(3,5-Diiodophenylazo)hexylbenzene (3c). The title compound was synthesized 4-nitrosohexylbenzene and 3,5-diiodoaniline in a manner similar to **3a**. Yield 30%; Mp 67–69 °C. ^{1}H NMR (400 MHz, $CDCl_3$): δ 0.88 (t, *J* = 6.8 Hz, 3H, C*H*$_3$), 1.37 [m, 6H, (C*H*$_2$)$_3$CH$_3$], 1.63 [m, 2H, CH$_2$C*H*$_2$(CH$_2$)$_3$CH$_3$], 2.67 [t, *J* = 8.0 Hz, 2H, C*H*$_2$CH$_2$(CH$_2$)$_3$CH$_3$], 7.30 (d, *J* = 8.4 Hz, 2H, Ar), 7.98 (d, *J* = 8.4 Hz, 2H, Ar), 8.08 (s, 1H, Ar), 8.17 (s, 2H, Ar). ^{13}C NMR (100 MHz, $CDCl_3$): δ 14.17 [CH$_2$CH$_2$(CH$_2$)$_3$*C*H$_3$], 22.65, 29.01, 31.22, 31.75 [CH$_2$*C*H$_2$(*C*H$_2$)$_3$CH$_3$], 36.02 [*C*H$_2$CH$_2$(CH$_2$)$_3$CH$_3$], 94.81, 123.18, 129.13, 131.15, 146.29, 147.68, 150.28, 153.72. HRMS. (*m*/*z*): $[M + H]^+$ Calcd for $C_{18}H_{21}I_2N_2$ 518.9794. Found: 518.9782.

4-(3,5-Diiodophenylazo)anisole (3d). $NaNO_2$ (0.76 g, 11 mmol) was added to a solution of 3,5-diiodoaniline (3.45 g, 10 mmol) in HCl aq. at 0 °C, and the resulting solution was stirred for 2 h at this temperature. Then, the viscous solution was added to dropwise into a solution of phenol (1.03 g, 11 mmol) in 2 M NaOH aq. (100 mL) at 0 °C while the pH of the reaction mixture was kept just under 7 by the addition of appropriate amount of Na_2CO_3. The reaction was carried out at this temperature for 3 h, then excessive HCl was added to the mixture. The precipitate formed was collected by filtration and washed with water to obtain 4-(3,5-diiodophenylazo)phenol. After that, it was dissolved in acetone (25 mL), and K_2CO_3 (1.66 g, 12 mmol) and CH_3I (0.75 mL, 12 mmol)

were added to the solution. The resulting mixture was heated under reflux for 12 h. After the reaction mixture was cooled, the precipitate formed was removed by filtration. After evaporation of the solvent, it was purified by silica gel column chromatography eluted with hexane/CH_2Cl_2 = 2/1 (v/v) to obtain **3d** as an orange solid in 31% yield; Mp 127–128 °C. ^{1}H NMR (400 MHz, $CDCl_3$): δ 3.90 (s, 3H, –OC*H*$_3$), 7.01 (d, *J* = 8.8 Hz, 2H, Ar), 7.90 (d, *J* = 9.2 Hz, 2H, Ar), 8.09 (d, *J* = 1.2 Hz, 1H, Ar), 8.17 (d, *J* = 1.2 Hz, 2H, Ar). ^{13}C NMR (100 MHz, $CDCl_3$): δ 55.67 (–O*C*H$_3$), 94.82, 114.38, 125.29, 131.11, 146.07, 146.56, 153.97, 162.87. HRMS. (*m*/*z*): $[M + H]^+$ Calcd for $C_{13}H_{11}I_2N_2O$ 464.8961. Found: 464.8943.

3,5-Diethynylazobenzene (2a). Compound **3a** (2.17 g, 5.00 mmol), $PdCl_2(PPh_3)_2$ (84 mg, 0.12 mmol), CuI (137 mg, 0.720 mmol), PPh_3 (126 mg, 0.480 mmol) were added into a two-neck flask, and it was flushed with nitrogen. THF (10 mL) and Et_3N (20 mL) were fed into the flask, and then trimethylsilylacetylene (1.70 mL, 12.2 mmol) was added dropwise to the solution. The resulting mixture was stirred at room temperature overnight. The mixture was concentrated in vacuo and the residual mass was washed with Et_2O to extract the product. The Et_2O solution was washed with 1.0 M HCl and saturated NaCl aq. The organic layer was dried over anhydrous $MgSO_4$ and concentrated on a rotary evaporator. The residual mass was purified by silica gel column chromatography eluted with hexane/$CHCl_3$ = 9/1 (v/v) to obtain 3,5-di(trimethylsilylethynyl)azobenzene as an orange solid. After that, it was

dissolved in $CHCl_3$ (10 mL) and a suspension of K_2CO_3 (1.66 g, 12.00 mmol) in MeOH (15 mL) was added to the solution. The resulting mixture was concentrated in vacuo, and the residual mass was dispersed in $CHCl_3$ and water. The organic layer was washed with NaCl aq. subsequently, dried over anhydrous $MgSO_4$, and concentrated on a rotary evaporator. The residual mass was purified by silica gel column chromatography eluted with hexane/CH_2Cl_2 = 4/1 (v/v) and recrystallization from hexane/CH_2Cl_2 to give **2a** as an orange solid in 58% yield; Mp 105–106 °C. IR (KBr): 3440, 3292, 3064, 2103, 1446, 1139, 890 cm^{-1}. ^1H NMR (400 MHz, $CDCl_3$): δ 3.13 (s, 2H, –C≡C*H*), 7.48–7.53 (m, 3H, Ar), 7.68 (t, *J* = 1.6 Hz, 1H, Ar), 7.89–7.92 (m, 2H, Ar), 7.99 (d, *J* = 1.5 Hz, 2H, Ar). ^{13}C NMR (100 MHz, $CDCl_3$): δ 78.62 (–C≡*C*H), 81.97 (–*C*≡CH), 123.10, 123.43, 126.72, 129.17, 131.68, 137.30, 152.25, 152.31. Anal. Calcd for $C_{16}H_{10}N_2$: C, 83.46; H, 4.38; N, 12.17. Found: C, 83.16; H, 4.45; N, 11.88.

4-(3,5-Diethynylphenylazo)benzonitrile (2b). The title compound was synthesized from **3b** in a manner similar to **2a** in 58% yield; Mp 192–194 °C. IR (KBr): 3855, 3404, 3291, 3088, 2922, 2225, 2112, 1591, 1468, 1279, 1246, 888 cm^{-1}. ^1H NMR (400 MHz, $CDCl_3$): δ 3.16 (s, 2H, –C≡C*H*), 7.72 (t, *J* = 1.5 Hz, 1H, Ar), 7.80–7.83 (m, 2H, Ar), 7.96–7.98 (m, 2H, Ar), 8.01 (d, *J* = 1.5 Hz, 2H, Ar). ^{13}C NMR (100 MHz, $CDCl_3$): δ 79.09 (–C≡*C*H), 81.61 (–*C*≡CH), 114.65, 118.26 (–*C*≡N), 125.55, 123.71, 126.99, 133.29, 138.32, 151.88, 154.02. HRMS. (*m*/*z*): $[M]^+$ Calcd for $C_{17}H_9N_3$ 255.0796. Found: 255.0797.

4-(3,5-Diethynylphenylazo)hexylbenzene (2c). The title compound

was synthesized from **3c** in a manner similar to **2a** in 28% yield; Mp 67–68 °C. IR (KBr): 3278, 2954, 2927, 2852, 2108, 1603, 1465, 1150, 889 cm^{-1}. ^1H NMR (400 MHz, $CDCl_3$): δ 0.89 (t, *J* = 6.8 Hz, 3H, C*H*$_3$), 1.31 [m, 6H, (C*H*$_2$)$_3$CH$_3$], 1.63 [m, 2H, –CH$_2$C*H*$_2$(CH$_2$)$_3$CH$_3$], 2.67 [t, *J* = 7.6 Hz, 2H, –C*H*$_2$CH$_2$(CH$_2$)$_3$CH$_3$], 3.14 (s, 2H, –C≡C*H*), 7.30 (d, *J* = 8.4 Hz, 2H, Ar), 7.67 (t, *J* = 1.2 Hz, 1H, Ar), 7.83 (d, *J* = 8.4 Hz, 2H, Ar), 7.90 (d, *J* = 1.6 Hz, 1H, Ar). ^{13}C NMR (100 MHz, $CDCl_3$): δ 14.07 [CH$_2$CH$_2$(CH$_2$)$_3$*C*H$_3$], 22.57, 28.94, 31.17, 31.66 [CH$_2$*C*H$_2$(*C*H$_2$)$_3$CH$_3$], 35.92 [*C*H$_2$CH$_2$(CH$_2$)$_3$CH$_3$], 78.53 (–C≡*C*H), 82.06 (–*C*≡CH), 123.12, 123.33, 126.61, 129.13, 136.98, 147.40, 150.55, 152.31. HRMS. (*m*/*z*): $[M + H]^+$ Calcd for $C_{22}H_{23}N_2$ 315.1861. Found: 315.1853.

4-(3,5-Diethynylphenylazo)anisole (2d). The title compound was synthesized from **3d** in a manner to **2a**. Yield 31%; Mp 104–105 °C. IR (KBr): 3430, 3287, 3068, 2108, 2049, 1602, 1502, 1256, 1147, 1029, 887 cm^{-1}. ^1H NMR (400 MHz, $CDCl_3$): δ 3.14 (s, 2H, –C≡C*H*), 3.90 (s, 3H, –OC*H*$_3$), 7.01 (d, *J* = 9.2 Hz, 2H, Ar), 7.66 (s, 1H, Ar), 7.92 (d, *J* = 8.8 Hz, 2H, Ar), 7.97 (d, *J* = 1.2 Hz, 2H, Ar). ^{13}C NMR (100 MHz, $CDCl_3$): δ 55.63 (–O*C*H$_3$), 78.40 (–C≡*C*H), 82.12 (–*C*≡CH), 114.33, 123.31, 125.15, 126.49, 136.70, 146.72, 153.77, 162.65. HRMS. (*m*/*z*): $[M + H]^+$ Calcd for $C_{17}H_{13}N_2O$ 261.1028. Found: 261.1018.

Polymerization. All the polymerizations were carried out in a glass tube equipped with a three-way stopcock under nitrogen. A typical experimental procedure for polymerization **1a** with **2a** is given below.

A solution of **1a** (164 mg, 0.30 mmol), **2a** (69.1 mg, 0.30 mmol), $Pd(PPh_3)_2Cl_2$ (4.2 mg, 6.0 μmol), CuI (6.9 mg, 36 μmol), PPh_3 (6.3 mg, 24 μmol), and Et_3N (0.6 mL) in DMF (0.9 mL) was stirred at 80 °C for 24 h. The resulting mixture was poured into MeOH/acetone [4/1 (v/v), 150 mL] to precipitate a polymer. It was separated by filtration using a membrane filter (ADVANTEC H020A047A) and dried under reduced pressure.

Spectroscopic Data of the Polymers. **Poly(1a–2a)**: IR (KBr): 3423, 3068, 2924, 2853, 1685, 1489, 1366, 1163, 884 cm^{-1}. ^1H NMR (400 MHz, $CDCl_3$): δ 0.82–1.72 [br, 12H, –$CONHCH_2CH_3$, –$NHCOOC(CH_3)_3$], 3.12–3.57 (br, 2H, –$CONHCH_2CH_3$), 5.11–5.36 (br, 1H, –C*H*CONH–), 5.76–6.81 (br, 3H, –CON*H*CH_2CH_3, –N*H*$COOC(CH_3)_3$, –O*H*), 7.10–8.32 (br, 10H, Ar). **Poly(1b–2a)**: IR (KBr): 3423, 3060, 2924, 2853, 1677, 1488, 1366, 1165, 884 cm^{-1}. ^1H NMR (400 MHz, $CDCl_3$): δ 0.82–1.79 [br, 20H, –$CONHCH_2(CH_2)_4CH_3$, –$NHCOOC(CH_3)_3$], 3.08–3.53 [br, 2H, –$CONHCH_2(CH_2)_4CH_3$], 5.03–5.38 (br, 1H, –C*H*CONH–), 5.52–6.88 [br, 3H, –CON*H*$CH_2(CH_2)_4CH_3$, –N*H*$COOC(CH_3)_3$, –O*H*], 7.10–8.38 (br, 10H, Ar). **Poly(1b–2b)**: IR (KBr): 3339, 3068, 2928, 2860, 2224, 1677, 1607, 1508, 1165, 848 cm^{-1}. ^1H NMR (400 MHz, DMSO-d_6): δ 0.72–1.60 [br, 20H, –$CONHCH_2(CH_2)_4CH_3$, –$NHCOOC(CH_3)_3$], 5.02–5.28 (br, 1H, –C*H*CONH–), 7.19–8.34 (br, 9H, Ar). **Poly(1b–2c)**: IR (KBr): 3418, 3324, 3068, 2927, 2855, 1685, 1499, 1366, 1159 cm^{-1}. ^1H NMR (400 MHz, $CDCl_3$): δ 0.82–1.79 [br, 31H, –$CONHCH_2(CH_2)_4CH_3$, –$CH_2(CH_2)_4CH_3$, –$NHCOOC(CH_3)_3$], 2.31–2.72 [br, 2H,

–C*H*$_2$(CH$_2$)$_4$CH$_3$], 3.08–3.53 [br, 2H, –CONHC*H*$_2$(CH$_2$)$_4$CH$_3$], 5.03–5.38 (br, 1H, –C*H*CONH–), 5.52–6.88 [br, 3H, –CON*H*CH$_2$(CH$_2$)$_4$CH$_3$, –N*H*COOC(CH$_3$)$_3$, –O*H*], 7.10–8.38 (br, 9H, Ar). **Poly(1b–2d)**: IR (KBr): 3339, 3068, 2929, 2857, 1677, 1600, 1503, 1253, 1148, 1028, 837 cm^{-1}. ^{1}H NMR (400 MHz, CDCl$_3$): δ 0.80–1.78 [br, 20H, –CONHCH$_2$(C*H*$_2$)$_4$C*H*$_3$, –NHCOOC(C*H*$_3$)$_3$], 3.08–3.98 [br, 5H, –CONHC*H*$_2$(CH$_2$)$_4$CH$_3$, –OC*H*$_3$], 5.08–5.29 (br, 1H, –C*H*CONH–), 5.50–6.82 [br, 3H, –CON*H*CH$_2$(CH$_2$)$_4$CH$_3$, –N*H*COOC(CH$_3$)$_3$, –O*H*], 7.08–8.42 (br, 9H, Ar). **Poly(1c–2a)**: IR (KBr): 3422, 3060, 2923, 2853, 1685, 1488, 1466, 1164, 690 cm^{-1}. ^{1}H NMR (400 MHz, CDCl$_3$): δ 0.79–1.77 [br, 32H, –CONHCH$_2$(C*H*$_2$)$_{10}$C*H*$_3$, –NHCOOC(C*H*$_3$)$_3$], 3.08–3.56 [br, 2H, –CONHC*H*$_2$(CH$_2$)$_{10}$CH$_3$], 5.12–5.44 (br, 1H, –C*H*CONH–), 5.51–6.78 [br, 3H, –CON*H*CH$_2$(CH$_2$)$_{10}$CH$_3$–, –N*H*COOC(CH$_3$)$_3$, –O*H*], 7.02–8.28 (br, 10H, Ar).

References and Notes

(1) Reviews: (a) Yashima, E.; Maeda, K.; Iida, H.; Furusho, Y.; Nagai, K. *Chem. Rev.* **2009**, *109*, 6102–6211. (b) Hill, D. J.; Mio, M. J.; Prince, R. B.; Hughes, T. S.; Moore, J. S. *Chem. Rev.* **2001**, *101*, 3893–4011. (c) Nakano, T.; Okamoto, Y. *Chem. Rev.* **2001**, *101*, 4013–4038.

(2) Reviews: (a) David, B. A.; Serrano, J.; Sierra, T.; Veciana, J. *J. Polym. Sci., Part A: Polym. Chem.* **2006**, *44*, 3161–3174. (b) Suginome, M.; Ito, Y. *Adv. Polym. Sci.* **2004**, *171*, 77–136. (c) Cornelissen, J. J. L. M.; Rowan, A. E.; Nolte, R. J. M.; Sommerdijk, N. A. J. M. *Chem. Rev.* **2001**, *101*, 4039–4070.

(3) Reviews: (a) Shiotsuki, M.; Sanda, F.; Masuda, T. *Polym. Chem.* in press (DOI: 10.1039/c0py00333f). (b) Masuda, T. *J. Polym. Sci., Part A: Polym. Chem.* **2007**, *45*, 165–180. (c) Aoki, T.; Kaneko, T.; Teraguchi, M. *Polymer* **2006**, *47*, 4867–4892.

(4) Reviews: (a) Kane-Maguire, L. A. P.; Wallace, G. G. *Chem. Soc. Rev.* **2010**, *39*, 2545–2576. (b) Hoeben, F. J. M.; Jonkheijim, P.; Meijer, E. W.; Schenning, A. P. H. J. *Chem. Rev.* **2005**, *105*, 1491–1546.

(5) Review: Ajayaghosh, A.; Praveen, V. K. *Acc. Chem. Res.* **2007**, *40*, 644–656.

(6) Reviews: (a) Bunz U. H. F. *Macromol. Rapid Commun.* **2009**, *30*, 772–805. (b) Smaldone, R. A.; Moore, J. S. *Chem. Eur. J.* **2008**, *14*, 2650–2657. (c) Bunz U. H. F. *Adv. Polym. Sci.* **2005**, *177*, 1–52.

(7) Fukuhara, G.; Inoue, Y. *J. Am. Chem. Soc.* in press (DOI: 10.1021/ja110075p).

(8) Tamura, K.; Miyabe, T.; Iida, H.; Yashima, E. *Polym. Chem.* **2011**, *2*, 91–98.

(9) Fukuhara, G.; Inoue, Y. *Chem. Eur. J.* **2010**, *16*, 7859–7864.

(10) Smaldone, R. A.; Moore, J. S. *J. Am. Chem. Soc.* **2007**, *129*, 5444–5450.

(11) Ikeda, M.; Furusho, Y.; Okoshi, K.; Tanahara, S.; Maeda, K.; Nishio, S.; Mori T.; Yashima, E. *Angew. Chem. Int. Ed.* **2006**, *45*, 6491–6495.

(12) Abe, H.; Masuda, N.; Waki, M.; Inouye, M. *J. Am. Chem. Soc.* **2005**, *127*, 16189–16196.

(13) Yamamoto, T.; Yamada, T.; Nagata, Y.; Suginome, M. *J. Am. Chem. Soc.* **2010**, *132*, 7889–7901.

(14) Terada, K.; Masuda, T.; Sanda, F. *J. Polym. Sci., Part A: Polym. Chem.* **2009**, *47*, 2596–2602.

(15) Maeda, K.; Tanaka, K.; Morino, K.; Yashima, E. *Macromolecules* **2007**, *40*, 6783–6785.

(16) Kakuchi, R.; Shimada, R.; Tago, Y.; Sakai, R.; Satoh, T.; Kakuchi, T. *J. Polym. Sci., Part A: Polym. Chem.* **2010**, *48*, 1683–1689.

(17) Kakuchi, R.; Kodama, T.; Shimada, R.; Tago, Y.; Sakai, R.; Satoh, T.; Kakuchi, T. *Macromolecules* **2009**, *42*, 3892–3897.

(18) McQuade, D. T.; Pullen, A. E.; Swager, T. M. *Chem. Rev.* **2000**, *100*, 2537–2574.

(19) Li, C.; Guo, Y.; Lv, J.; Xu, J.; Li, Y.; Wang, S.; Liu, H.; Zhu, D. *J. Polym. Sci., Part A: Polym. Chem.* **2007**, *45*, 1403–1412.

(20) Zhao, X.; Schanze, K. S. *Langmuir* **2006**, *22*, 4856–4862.

(21) Arnt, L.; Tew, G. N. *Macromolecules* **2004**, 37, 1283–1288.
(22) Liu, R.; Sogawa, H.; Shiotsuki, M.; Masuda, T.; Sanda, F. *Polymer* **2010**, *51*, 2255–2263.
(23) Liu, R.; Shiotsuki, M.; Masuda, T.; Sanda, F. *Macromolecules* **2009**, *42*, 6115–6122.
(24) Reviews: (a) Seki, T. *Bull. Chem. Soc. Jpn.* **2007**, *80*, 2084–2109. (b) Natansohn, A.; Ronchon, P. *Chem. Rev.* **2002**, *102*, 4139–4175. (c) Tamai, N.; Miyasaka, H. *Chem. Rev.* **2000**, *100*, 1875–1890.
(25) Ercole, F.; Davis, T. P.; Evans, R. A. *Polym. Chem.* **2010**, *1*, 37–54.
(26) Stoll, R. S.; Peters, M. V.; Kuhn, A.; Helices, S.; Goddard, R.; Buhl, M.; Thiele, C. M.; Hecht, S. *J. Am. Chem. Soc.* **2009**, *131*, 357–367.
(27) Masiero, S.; Lena, S.; Pieraccini, S.; Spada, G. P. *Angew. Chem. Int. Ed.* **2008**, *47*, 3184–3187.
(28) Yamada, M.; Kondo, M.; Mamiya, J.; Yu, Y.; Kinoshita, M.; Barrett, C. J.; Ikeda, T. *Angew. Chem. Int. Ed.* **2008**, *47*, 4986–4988.
(29) Koumura, N.; Kudo, M.; Tamoki, N. *Langmuir* **2004**, *20*, 9897–9990.
(30) Furusho, Y.; Tanaka, Y.; Maeda, T.; Ikeda, M.; Yashima, E. *Chem. Commun.* **2007**, *3174*–3176.
(31) Fujii, T.; Shiotsuki, M.; Inai, Y.; Sanda, F.; Masuda, T. *Macromolecules* **2007**, *40*, 7079–7088.
(32) Khan, A.; Hecht, S. *Chem. Eur. J.* **2006**, *12*, 4764–4774.
(33) Zhao, H.; Sanda, F.; Masuda, T. *Polymer* **2006**, *47*, 2596–2602.
(34) Mayer, S.; Zentel, R. *Prog. Polym. Sci.* **2001**, *26*, 1973–2013.
(35) The DLS measurements were also performed for CH_2Cl_2 solutions (0.1 wt%) of poly(**1a**–**2a**) and poly(**1c**–**2a**). Particles with R_h's of 585 nm and 477 nm were detected, respectively. These two polymers also seem to form aggregates at this concentration. On the contrary, these two polymers did not show the CD signals in CH_2Cl_2 [c = 0.030 mM (1.24–1.56 × 10^{-3} wt%)] attributable to the aggregates. It is presumed that this is due to the difference in sample concentrations between DLS and CD measurements. The concentrations of the DLS samples were 65–80 times higher than those of the CD samples. Because of the different requirements of sample concentrations, we could not obtain the data of DLS and CD at the same

concentration.
(36) Prince, R. B.; Brunsyeld, L.; Meijer, E. W.; Moore, J. S. *Angew. Chem. Int. Ed.* **2000**, *39*, 228–230.
(37) Prince, R. Saven, J. G.; Wolynens, P. G.; Moore, J. S. *J. Am. Chem. Soc.* **1999**, *121*, 3114–3121.
(38) Aggregation also seems to contribute to the thermal stability in the case of poly(**1b**–**2a**).
(39) Fujiki, M. *Macromol. Rapid Commun.* **2001**, *22*, 539–563.
(40) Gore, P. R.; Wheeler, O. H. *J. Org. Chem.* **1961**, *26*, 3295–3298.
(41) Moniruzzaman, M.; Talbot, J. D. R.; Sabey, C. J.; Fernando, G. F. *J. Appl. Polym. Sci.* **2006**, *100*, 1103–1112.
(42) Adisa, B.; Bruce, D. A. *J. Phys. Chem. B* **2005**, *109*, 7548–7556.
(43) Adisa, B.; Bruce, D. A. *J. Phys. Chem. B* **2005**, *109*, 19952–19959.
(44) Lee, O. S.; Saven, J. G. *J. Phys. Chem. B* **2004**, *108*, 11988–11994.
(45) Halgren, T. A. *J. Comput. Chem.* **1996**, *17,* 490–519. The molecular mechanics calculation was carried out with Wavefunction Inc., Spartan ’08 Macintosh.
(46) Bérubé, M.; Poirier, D. *Org. Lett.* **2004**, *6*, 3127–3130.
(47) ten Brink, G.; Vis, J. M.; Arends, I. W. C. E.; Sheldon, R. A. *Tetrahedron* **2002**, *58*, 3977–3983.
(48) *Org. Synth., Coll.* **1955**, *3*, 711–712.

Chapter 5

Synthesis and Photo-responsive Chiroptical Properties of Optically Active Poly(phenyleneethynylene)s Bearing Azobenzene Moieties at the Main Chains

Abstract

Novel optically active poly(phenyleneethynylene)s bearing azobenzene moieties at the main chains [poly(**1**–**2m)**, poly(**1**–**2p**)] were synthesized by the Sonogashira–Hagihara coupling polymerization of 3',5'-diiodo-4'-hydroxy-*N*-α-*tert*-butoxycarbonyl-D-phenylglycine hexylamide (**1**) with 3,3'-diethynylazobenzene (**2m**) and 4,4'-diethynylazobenzene (**2p**). The corresponding polymers [poly(**1**–**2m**), poly(**1**–**2p**)] with number-average molecular weights of 10,700 and 9,400 were obtained in 70 and 86% yields, respectively. CD and UV–vis spectroscopic analyses revealed that poly(**1**–**2m**) and poly(**1**–**2p**) formed predominantly one-handed helically folded structures in $CHCl_3$/THF mixtures. Poly(**1**–**2m**) underwent reversible conformational change between folded and unfolded structures upon UV-and visible-light irradiation accompanying *trans-cis* isomerization of the azobenzene moieties. On the other hand, poly(**1**–**2p**) hardly underwent such transformation of conformation as well as isomerization of the azobenzene moieties.

Introduction

Photo-responsive materials gather much interest because of their applicability to optical memories,[1–4] molecular machines,[5,6] recognition matrials,[7–11] catalysts,[12–14] actuators[15–18] and so on. Azobenzene is the most widely used photo-responsive molecules due to its highly efficient reversible photo-isomerization property between *trans*- and *cis*-forms.[19] Namely, *trans*-azobenzene undergoes isomerization upon UV-light irradiation into *cis*-azobenzene, and the isomerization occurs in a reverse way upon visible-light irradiation or heating. This photo-isomerization between *trans*- and *cis*-forms occurs reversibly with high quantum yields, accompanying the changes of dipole moments between 0 and 3 debye, and molecular shapes between extended coplanar and twisted forms. Meanwhile, control over higher order structures of conjugated polymers by external stimuli gathers considerable attention, because it possibly leads to the development of stimuli-responsive photoelectrically functional materials.[20] There are various reports about the synthesis of conjugated polymers containing azobenzene moieties either at the side chains[21–28] or main chains,[29–32] whose higher order structures are controllable by photo-irradiation. Recently, a series of D-hydroxyphenylglycine-/ L-tyrosine-derived poly(*m*-phenyleneethynylene-*p*-phenyleneethynylene)s have been synthesized,[28,33–35] and examined the secondary structures. These polymers forms folded helical structures in nonpolar solvents such as $CHCl_3$ based on the amphiphilicity caused by hydrophobic exterior (alkyl chains and

phenyleneethynylene main chain) and hydrophilic interior (hydroxy groups). It should be noted that the amphiphilic balance is opposite from that of typical poly(phenyleneethynylene) derivatives reported so far.[36] The author synthesized poly(*m*-phenyleneethynylene)s containing azobenzene moieties at the side chains that are helically folded in nonpolar solvents.[28] The higher order structures of the polymers collapsed to some extent by UV-light irradiation and reconstructed by visible-light irradiation, which were caused by photo-isomerization of the azobenzene moieties. The degree of change of higher order structure was not large probably because the *cis*-*trans* isomerization of the azobenzene units does not directly twist the main chain.

In this chapter, the author discusses the synthesis of D-hydroxyphenylglycine-derived novel optically active poly(pheyleneethynylene)s containing azobenzene moieties at the main chains with *m,m'*- and *p,p'*-linkages by the Sonogashira–Hagihara coupling polymerization of the corresponding monomers (Scheme 1). Photo-induced large conformational changes are expected because the azobenzene units are completely contained in the main chains, differently from previous polymers. The author also discusses the chiroptical and photo-responsive properties of the formed polymers based on CD, UV–vis spectroscopic analysis together with MM and DFT calculations.

Scheme 1. Sonogashira–Hagihara Coupling Polymerization of D-Hydroxyphenylglycine-derived Diiodophenylene Monomer **1** with 3,3'- and 4,4'-Diethynylazobenzene Monomers **2m** and **2p**

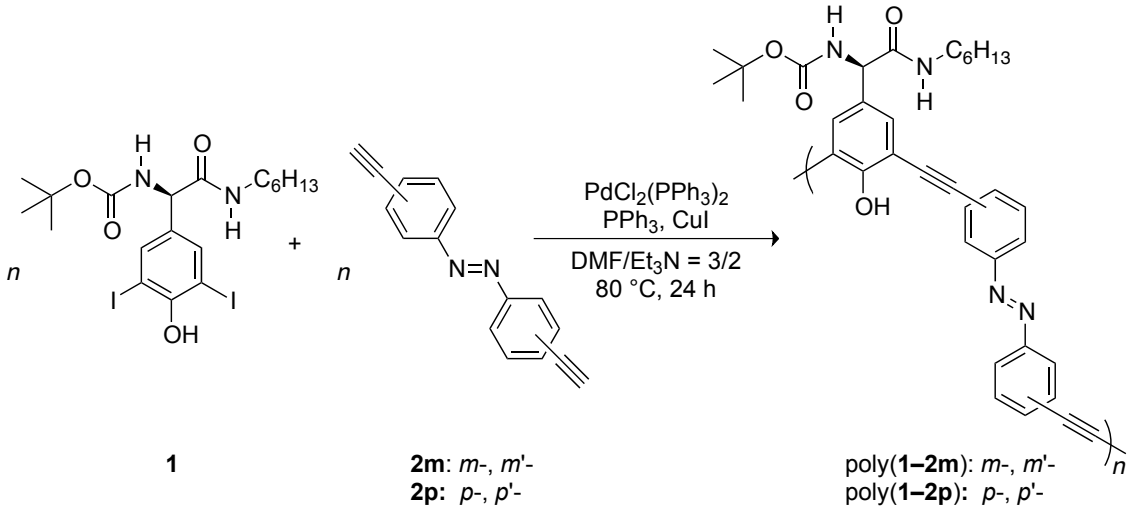

Results and Discussion

Polymerization. The Sonogashira–Hagihara coupling polymerization of **1** with diethynylazobenzenes **2m** and **2p** were performed in DMF at 80 °C for 24 h. The formed polymers were isolated as insoluble parts in MeOH/acetone = 9/1 (v/v) mixture. Poly(**1**–**2m**) and poly(**1**–**2p**) with M_n's of 10,700 and 9,400 were obtained in 70 and 86% yields, respectively (Table 1). Poly(**1**-**2m**) and poly(**1**-**2p**) were soluble in $CHCl_3$, THF and DMF. Poly(**1**–**2m**) was soluble in CH_2Cl_2 and toluene as well, while poly(**1**–**2p**) was not. The solubility of poly(**1**–**2m**) was comparatively higher than that of poly(**1**–**2p**), presumably the main chain of poly(**1**–**2m**) is less stiff than that of poly(**1**–**2p**). This will be discussed later.

Table 1. Sonogashira–Hagihara coupling polymerization of **1** with **2m** and **2p**[a]

monomer	polymer			
		yield[b] (%)	M_n[c]	M_w/M_n[c]
1 + **2m**	poly(**1**–**2m**)	70	10,700	1.7
1 + **2p**	poly(**1**–**2p**)	86	9,400	1.8

[a] conditions: $[\mathbf{1}]_0 = [\mathbf{2m}]_0 = [\mathbf{2p}]_0 = 0.20$ M, $[PdCl_2(PPh_3)_2] = 0.010$ M, $[PPh_3] = 0.020$ M, [CuI] = 0.030 M, DMF/Et_3N = 3/2 (v/v), 80 °C, 24 h. [b] Insoluble part in MeOH/acetone = 9/1 (v/v). [c] Estimated by SEC measured in THF, polystyrene calibration.

Chiroptical Properties of the Polymers. The CD and UV–vis spectroscopic analysis was performed to obtain the information of the higher order structures of the polymers. As shown in Figure 1, poly(**1**–**2m**) showed intense split type CD signals at the absorption region of main chain chromophore in $CHCl_3$/THF = 7/3 mixture, while the polymer did not show such intense peaks either in $CHCl_3$ or THF. On the other hand, poly(**1**–**2p**) exhibited intense CD signals both in $CHCl_3$ and THF, and in $CHCl_3$/THF mixtures with various compositions as well (Figure 2). The CD and UV–vis signals of the polymers did not change by the concentration change at a range of 0.03–0.3 mM, and after filtration using a membrane filter with a pore size of 0.45 mm.[37] Furthermore, no particle was observed by DLS measurement. These results indicate that the CD signals do not originate from chiral aggregation but unimolecularly folded helical structures of the polymers with predominantly one-handed screw sense. The λ_{max} of poly(**1**–**2p**) lied on 390 nm, which is 76 nm longer than that of poly(**1**–**2m**), indicating that poly(**1**–**2p**) possesses more conjugated main chain

through the *p,p'*-linked azobenzene units. The CD intensities of poly(**1**–**2m**) varied according to the compositions of $CHCl_3$/THF mixtures. Figure 3 shows the plot of the Kuhn dissymmetry factor g (= $\Delta\varepsilon/\varepsilon$, in which $\Delta\varepsilon = [\theta]/3{,}298$) of poly(**1**–**2m**) observed in $CHCl_3$/THF with various compositions at the $[\theta]_{max}$ wavelengths. *G*-values give quantitative information associated with the degree of preferential screw sense.[38] The *g*-value became the maximum at a ratio of $CHCl_3$/THF = 7/3. Poly(**1**–**2p**) exhibited the similar trend, though it showed intense CD signals either in $CHCl_3$ or THF. As listed in Table 2, the *g*-values of poly(**1**–**2p**) were almost five times larger than those of poly(**1**–**2m**) both at the wavelengths of the first and second Cotton effects. It is considered that the predominance of one-handedness of poly(**1**–**2p**) helix is larger than that of poly(**1**–**2m**) helix.

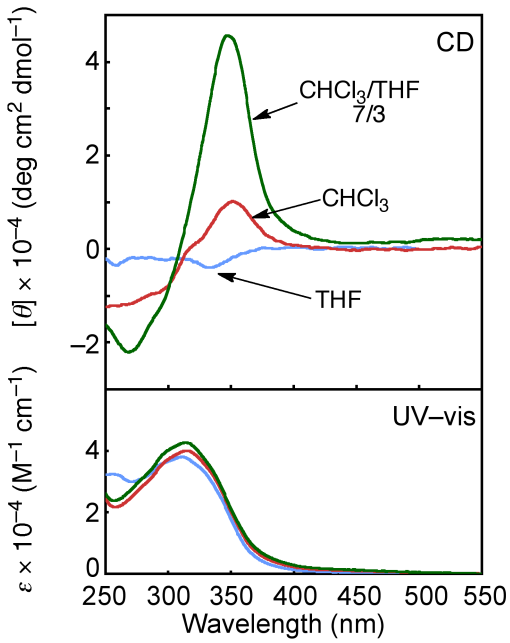

Figure 1. CD and UV–vis spectra of poly(**1**–**2m**) measured in $CHCl_3$, THF and $CHCl_3$/THF = 7/3 (c = 0.03 mM) at 20 °C.

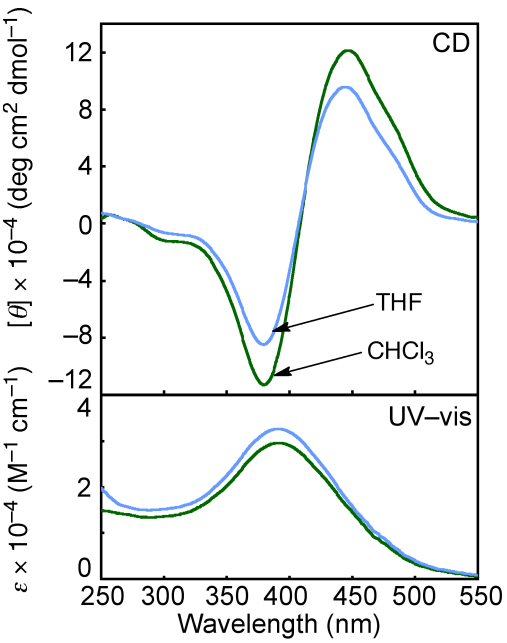

Figure 2. CD and UV–vis spectra of poly(**1**–**2p**) measured in $CHCl_3$ and THF (c = 0.03 mM) at 20 °C.

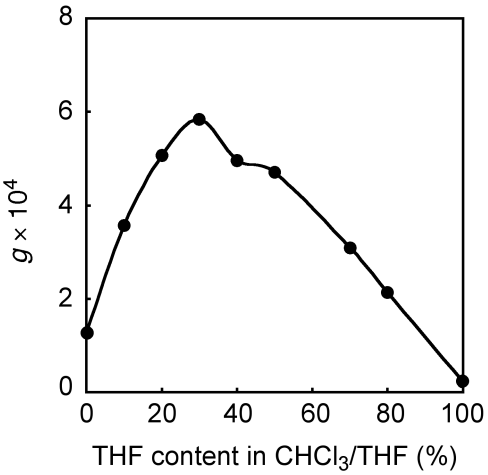

Figure 3. Plot of g-values of poly(**1**–**2m**) at the $[\theta]_{max}$ wavelengths measured in $CHCl_3$/THF mixtures with various compositions (c = 0.03 mM) at 20 °C.

Table 2. Absolute g-values of poly(**1**–**2m**) and poly(**1**–**2p**)

polymer	$\lvert g \rvert \times 10^4$	
	first Cotton	second Cotton
poly(**1**–**2m**)[a]	5.07	2.49
poly(**1**–**2p**)[b]	25.1	11.7

[a] Measured in $CHCl_3$/THF = 7/3 (c = 0.03 mM). [b] Measured in $CHCl_3$/THF = 8/2 (c = 0.03 mM).

Intramolecular hydrogen bonds as well as π-stacking are the key factors for stabilizing helically folded structures of some poly(phenyleneethnylene)s in a fashion similar to the other artificial helical polymers including polyisocyanide, polyisocyanate, polyacetylene and so on.[28,33,39–41] Solution-state IR spectra of poly(**1**–**2m**), poly(**1**–**2p**) and monomer **1** were measured in $CHCl_3$/THF =7/3 and $CHCl_3$ under diluted conditions (20 mM) to determine the presence/absence of intramolecular hydrogen bonding (Table 3). All the compounds exhibited two strong absorption peaks assignable to C=O stretching vibrations of amide and carbamate groups. Poly(**1**–**2m**) exhibited the carbamate and amide C=O peaks at 1703 cm^{-1} and 1671 cm^{-1}, which were lower by 6 and 7 cm^{-1} compared with those of **1**, respectively. On the other hand, the carbamate C=O peak of poly(**1**–**2p**) was observed only at 1 cm^{-1} lower wavenumber position than that of **1**, while the amide C=O peak was observed at 25 cm^{-1} lower position than that of **1**. The sample solutions were diluted enough to avoid intermolecular interaction as mentioned above. Thus, it is indicated that poly(**1**–**2m**) forms intramolecular hydrogen bonds not so strongly between the carbamate and amide groups in $CHCl_3$/THF = 7/3 mixture, while poly(**1**–**2p**) does between the amide groups strongly in $CHCl_3$. As the result, it is assumed that poly(**1**–**2p**) is folded into a helix with a bias higher than poly(**1**–**2m**).

Table 3. Solution-state IR spectroscopic data (C=O absorption peaks) of the monomer and polymers[a]

solvent	compound	wavenumber (cm^{-1}) C=O	
		carbamate	amide
$CHCl_3$/THF	**1**	1709	1678
7/3	poly(**1**–**2m**)	1703	1671
$CHCl_3$	**1**	1701	1677
	poly(**1**–**2p**)	1700	1652

[a] c = 20 mM.

The CD and UV–vis spectra of the polymers was measured upon photo-irradiation to examine the photo-isomerization behavior. A solution of poly(**1**–**2m**) in $CHCl_3$/THF = 7/3 [the composition that poly(**1**–**2m**) exhibited the largest CD intensities] was irradiated with UV-light through a suitable transmission filter using a high pressure mercury lamp. The intensities of the CD signals gradually decreased upon UV-light irradiation, and almost saturated after 16 min (Figure 4). The intensity of the UV–vis signal around 315 nm also decreased, apparently due to the decrease of absorption based on the π–π* transition band of *trans*-azobenzene units. Although no increase was observed corresponding to the n–π* of *cis*-azobenzene, it seems that *trans*-azobenzene moieties isomerized into *cis*-azobenzene, weakening the chirality of the polymer molecule. In helical polymers, the decrease of CD intensity represents the transformation of a helix into a random structure and/or loss of predominance of one-handedness keeping the total helix content constant. In the present case, it is likely that the decrease of CD intensities is caused by the collapse of helically

folded structures. It has been reported that the *trans*-to-*cis* photo-isomerization of azobenzene units at the main chains of oligo(phenyleneethynylene) derivatives disorders the helically folded structures due to the loss of π–stacking interactions between the folded main chains induced by loss of planarity.[29,31,32] This is predictable from the fact that *trans*-azobenzene is linear and planar, while *cis*-azobenzene is bended. In the present chapter, the CD intensities of poly(**1**–**2m**) decreased as large as 71% by UV-light irradiation for 16 min, which is much larger than those of the analogous polymer (10%) that possess azobenzene moieties at the side chains under the same conditions.[28] This remarkable difference is caused by introducing the azobenzene moieties at the main chain. The further visible-light irradiation to the UV-light irradiated samples resulted in almost full recovery of the initial CD and UV–vis spectra, indicating that poly(**1**–**2m**) was refolded into a helix accompanying the isomerization of azobenzene units from *cis* to *trans*. Further reversibility was confirmed upon repeated UV- and visible-light irradiation. As shown in Figure 5, the CD and UV–vis intensities showed good reversible responsiveness upon alternating UV- and visible-light irradiation for 16 min intervals without remarkable decomposition. It indicates that the folded helical structure was repeatedly deformed and reformed even after 8 cycles of alternating UV- and visible-light irradiation. On the contrary, the UV-light irradiation induced no CD and UV–vis spectra change to poly(**1**–**2p**) (Figure 6). After UV-light irradiation for 16 min, the intensity decreases of CD and UV–vis signals were as small as 17 and 1%, respectively.

Monomer **2p** was photo-isomerized upon UV- and visible-light irradiation; the UV–vis absorption at the λ_{max} decreased 51% upon UV-light irradiation for 8 min compared with its initial state. The large difference in photo-responsiveness between poly(**1**–**2p**) and **2p** is explained by conjugation. When azobenzene is incorporated at *p,p'*-positions into the main chain of a conjugated polymer, π-electrons of azobenzene are delocalized through the conjugated main chain. As a result, the efficiency of UV-induced π–π* transition localized at azobenzene is decreased in conjunction with the enhanced stiffness of the main chain by extension of conjugation involving azobenzene.[42–44] Azobenzene-containing oligo(phenyleneethynylene)s undergo photo-isomerization more efficiently when they form random coil structures compared with helically folded structures.[32] As mentioned above, poly(**1**–**2p**) possesses more conjugated main chains and higher helix bias than those of poly(**1**–**2m**). Consequently, poly(**1**–**2p**) hardly undergoes photo-isomerization, while poly(**1**–**2m**) easily does. It is possible to estimate the photo-isomerization ratio of *trans*-azobenzene moieties from the decrease in the ratio of π–π* absorption.[45] In the present paper, however, it was difficult to do that due to the overlap of absorption peaks of the azobenzene units and conjugated main chain. The author tried to determine the isomerization ratio by ^{1}H NMR spectroscopy and SEC measurement but failed to obtain clear information, unfortunately.

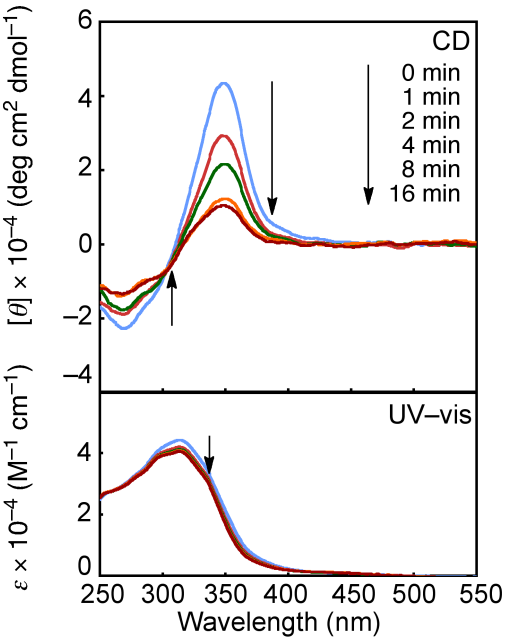

Figure 4. CD and UV–vis spectra of poly(**1**–**2m**) upon UV-light irradiation (300 < λ < 400 nm) for 16 min measured in $CHCl_3$/THF = 7/3 (c = 0.03 mM) at 20 °C.

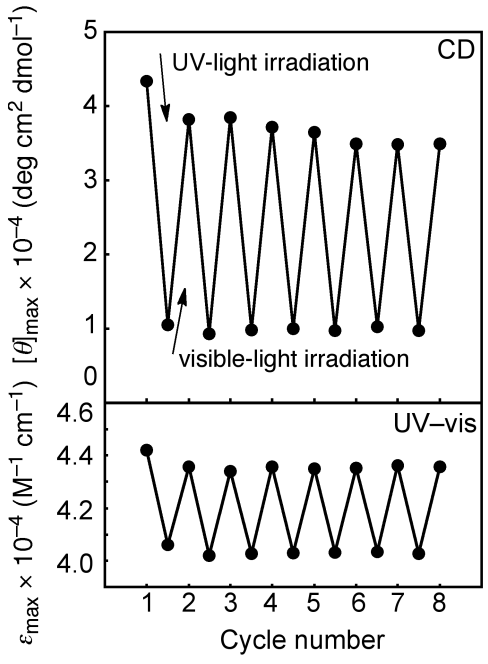

Figure 5. The plot of $[\theta]_{max}$ and ε_{max} upon alternating photo-irradiation cycle upon UV-light (300 < λ < 400 nm) and visible-light (420 nm < λ) irradiation for 16 min measured in $CHCl_3$/THF = 7/3 (c = 0.03 mM) at 20 °C.

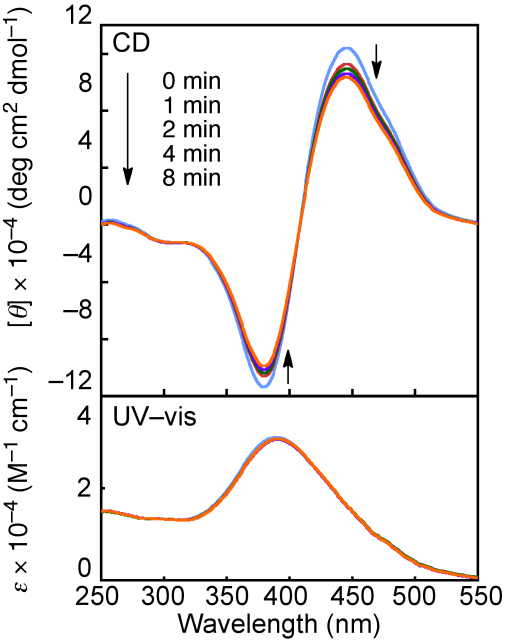

Figure 6. CD and UV–vis spectra of poly(**1**–**2p**) upon UV-light irradiation ($300 < \lambda < 400$ nm) for 16 min measured in $CHCl_3$ (c = 0.03 mM) at 20 °C.

Conformational Analysis. There are several reports regarding the conformation analysis of poly(phenyleneethynylene)s using the molecular mechanics[28,33] and molecular dynamics simulations.[46–48] In the present chapter, the geometries were optimized first with the molecular mechanics method using the MMFF94,[49] second with the semi-empirical molecular orbital method using the PM6 hamiltonian, and finally with the DFT method at the M06-2X/6-31G* level for selected conformers. The M06-2X functional was employed because it is superior compared with commonly used B3LYP functional in estimating noncovalent interactions including *p*-stacking and hydrogen bonding,[50,51] both of which are essential for stabilizing the helically folded structures of the present poly(phenyleneethynylene) derivatives. Charts 1–3 summarize the possible

regulated right- and left-handed helical conformers of 12-mers of poly(**1**–**2m**) and poly(**1**–**2p**), whose both chain ends are terminated with hydrogen atoms. The hexyl groups are replaced with methyl groups to save the CPU time. Trans zigzag conformers (Chart 4) were also calculated for comparison.

As shown in Chart 1, poly(**1**–**2m**) forms helices with short diameters when the two ethynylene groups at the 3,3'-positions of the azobenzene moiety adopt "*cis*" geometry. One turn consists of two monomer units (2-1 helices). In the chart, symbols "R" and "L" represent right- and left-handed helices, respectively. Four regulated conformers are possible as right-handed helices considering the directions of the azobenzene and amide/carbamate moieties. Symbols "O" and "I" represent the directions of the azobenzene moieties along the conjugated plane of the main chain, bending outside and inside viewed from the top positions. Symbols "A" and "B" represent the two ways of directions of the amide/carbamate moieties. In a similar way, four regulated conformers are possible as left-handed helices. The torsional angles of main chains of right- and left-handed helices are set to +6° and –6° per phenylene unit, respectively, and the azobenzene units are set to a planar structure in the initial geometries. After geometry optimization by the MMFF94 method using those constraints, the amide and carbamate N–H groups of a monomer unit formed regulated intramolecular hydrogen bonds with the C=O groups of the amide and carbamate groups two units earlier ($i + 2 \rightarrow i$ N–H•••O=C hydrogen bonding), respectively. Next, the geometries were fully optimized without any constraints by the PM6

method. In every case, the regulated $i + 2 \rightarrow i$ N–H•••O=C hydrogen bonding strands were intact after the semi-empirical calculations.

On the other hand, poly(**1**–**2m**) forms helices with long diameters when the two ethynylene groups at the 3,3'-positions of the azobenzene adopt "*trans*" geometry as shown in Chart 2. One turn consists of six monomer units (6-1 helices). There are four possible regulated conformers according to the directions of the azobenzene and amide/carbamate moieties in right-handed helices, and four left-handed helices as well. The symbols "R/L", "O/I" and "A/B" are employed in the same manner as the 2-1 helices mentioned above. The torsional angles of main chains of right- and left-handed helices are set to +1° and –1° per phenylene unit, respectively, and the azobenzene units are set to a planar structure at the initial geometries. Regulated hydrogen-bonding strands were formed after geometry optimization with these constraints by the MMFF94 method; the amide and carbamate N–H groups of a monomer unit formed regulated intramolecular hydrogen bonds with the C=O groups of the amide and carbamate groups six units earlier ($i + 6 \rightarrow i$ N–H•••O=C hydrogen bonding), respectively. The hydrogen bonding strands were intact after full geometry optimization without any constraints by the PM6 method in a fashion similar to the 2-1 helices mentioned above. Judging from the relative energy values calculated by the PM6 (Table 4), 2-1 helical conformer ***m*-2-1-R-I-A** is most likely among the possible regulated 16 conformers for poly(**1**–**2m**). The geometries of stable conformers were further optimized by the DFT method at

the M06-2X/6-31G* level to confirm the similar trend with the PM6 method. Though PM6 is a semi empirical method, and therefore it is exempt from long CPU time compared with DFT, PM6 is reliable enough for preliminarily estimating the stable conformers of the present polymers involving p-stacking and hydrogen bonding,[52] The right-handed helical structure of ***m*-2-1-R-I-A** coincides with the first-positive and second-negative exciton coupling observed in the CD spectra of poly(**1**–**2m**) shown in Figure 1. The helical pitch after full optimization with DFT was 3.8 Å, which is consistent with the turns of the helix being near van der Waals contact and comparable to p-stacking between aromatic rings.[53] The trans zigzag conformer was unstable compared with ***m*-2-1-R-I-A** as large as 132.6 kJ/(mol•unit) at the M06-2X/6-31G* level, definitely due to the absence of p-stacking and hydrogen bonding.

Differently from poly(**1**–**2m**), poly(**1**–**2p**) cannot form 2-1 helices because of the geometrical restriction. Poly(**1**–**2p**) possibly forms 6-1 helices listed in Chart 3. The symbols "R/L", "O/I" and "A/B" are used in a similar fashion with the cases of poly(**1**–**2m**) helices mentioned above. Among the possible eight helical structures, ***p*-L-I-B** seems to be most stable based on the relative energies calculated by the PM6 and M06-2X/6-31G* method. However, the left-handed helical structure does not coincide with the exciton coupling of the CD spectra shown in Figure 2. The CD and UV–vis spectra of the polymers were theoretically simulated by the ZINDO/S method to obtain more structural information. Among the conformers listed in Table 4, ***p*-R-I-A**

successfully gave theoretical CD and UV–vis spectra (Figure 7) that well simulate to the observed ones. The theoretical CD spectrum shows the positive first and negative second CD signals assignable to exciton coupling based on the main chain chromophore twisted in right-handed

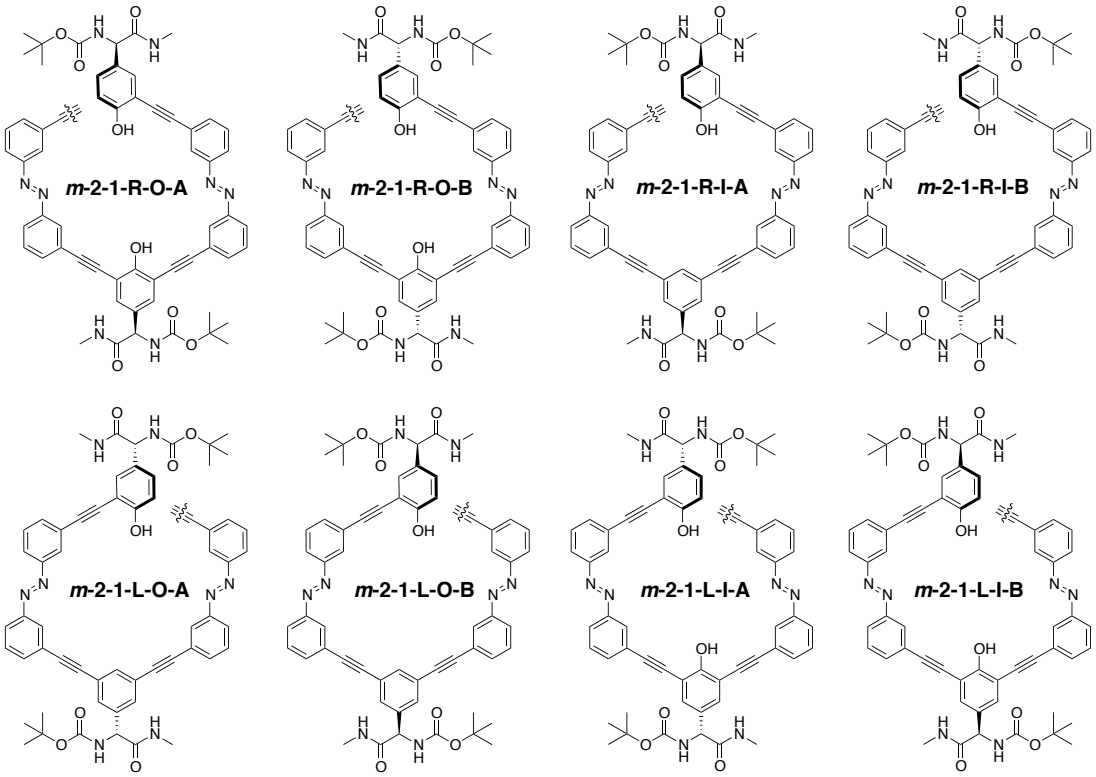

Chart 1. Possible regulated 2-1 helical conformers of 12-mers of poly(**1**–**2m**). Ten monomer units are omitted at the wavy lines.

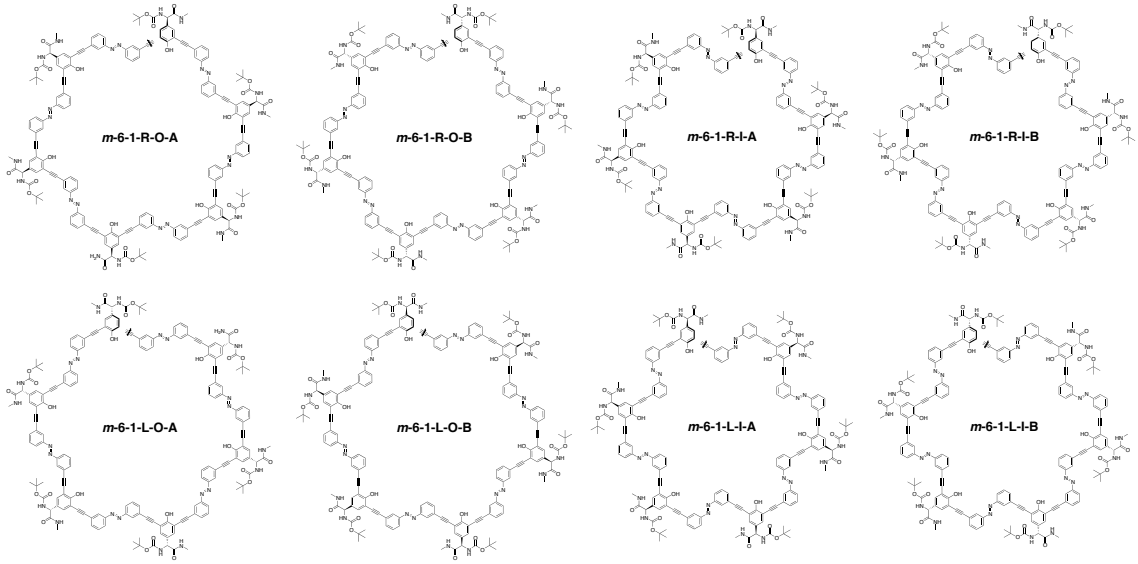

Chart 2. Possible regulated 6-1 helical conformers of 12-mers of poly(**1**–**2m**). Six monomer units are omitted at the wavy lines.

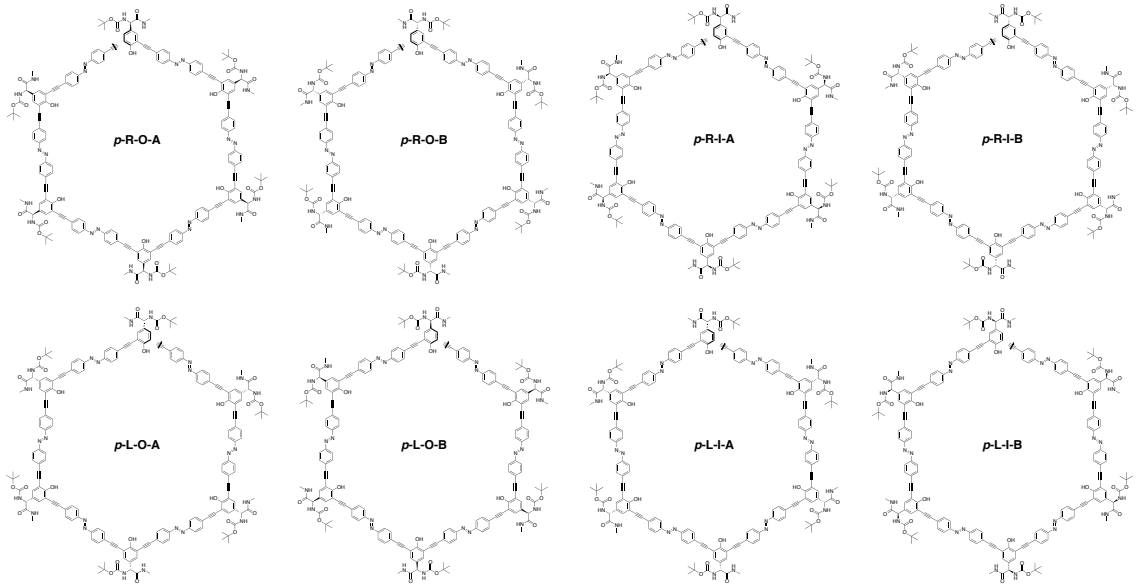

Chart 3. Possible regulated 6-1 helical conformers of 12-mers of poly(**1**–**2p**). Six monomer units are omitted at the wavy lines.

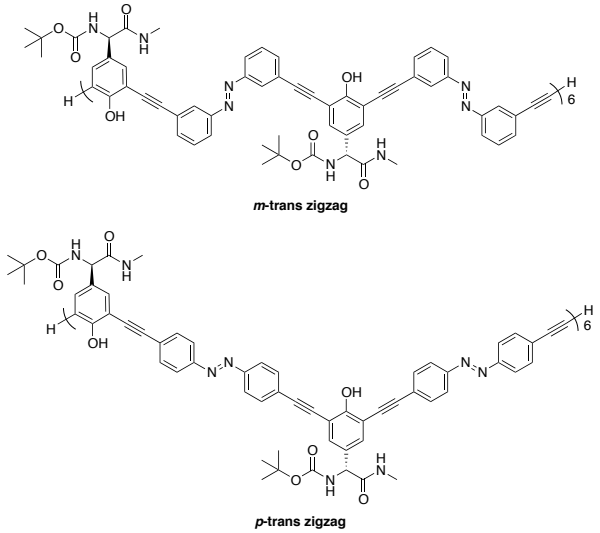

Chart 4. Trans zigzag conformers of 12-mers of poly(**1**–**2m**) and poly(**1**–**2p**).

Table 4. Relative Energies for the Possible Conformers of 12-mers of Poly(**1**–**2m**) and Poly(**1**–**2p**)

conformer of poly(**1**–**2m**)	relative energy [kJ/(mol•unit)]		conformer of poly(**1**–**2m**)	relative energy [kJ/(mol•unit)]		conformer of poly(**1**–**2p**)	relative energy [kJ/(mol•unit)]	
	PM6 [a]	M06-2X /6-31G* [b]		PM6 [a]	M06-2X /6-31G* [b]		PM6 [a]	M06-2X /6-31G* [b]
***m*-trans zigzag**	40.2	132.6	–	–	–	***p*-trans zigzag**	59.1	153.9
***m*-2-1-R-O-A**	4.6	–	***m*-6-1-R-O-A**	14.8	–	***p*-R-O-A**	32.7	80.7
***m*-2-1-R-O-B**	2.2	6.4	***m*-6-1-R-O-B**	11.7	44.0	***p*-R-O-B**	33.9	–
***m*-2-1-R-I-A**	0.0	0.0	***m*-6-1-R-I-A**	13.2	–	***p*-R-I-A**	33.2	81.8
***m*-2-1-R-I-B**	6.2	–	***m*-6-1-R-I-B**	10.7	47.4	***p*-R-I-B**	33.7	–
***m*-2-1-L-O-A**	11.8	–	***m*-6-1-L-O-A**	15.4	–	***p*-L-O-A**	47.5	101.0
***m*-2-1-L-O-B**	4.1	13.1	***m*-6-1-L-O-B**	9.6	44.7	***p*-L-O-B**	50.6	–
***m*-2-1-L-I-A**	10.1	–	***m*-6-1-L-I-A**	13.2	41.8	***p*-L-I-A**	50.1	–
***m*-2-1-L-I-B**	5.7	13.9	***m*-6-1-L-I-B**	15.5	–	***p*-L-I-B**	28.7	72.3

[a] Converted using the value of ***m*-2-1-R-I-A** [66.6 kJ/(mol•unit)] as zero.

[b] Converted using the value of ***m*-2-1-R-I-A** [–4405952.4 kJ/(mol•unit)] as zero.

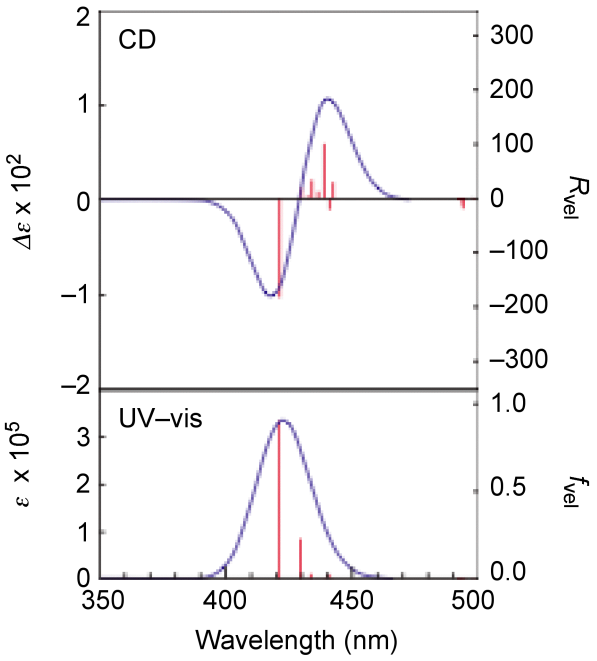

Figure 7. CD and UV–vis spectra of ***p*-R-I-A** simulated by the ZINDO/S (nstates = 20) method using the geometries optimized by the M06-2X/6-31G*. ε, $\Delta\varepsilon$, R_{vel} and f_{vel} of the polymer molecule are divided by 12 as the values per monomer unit.

Conclusions

In the present chapter, the author has synthesized novel optically active poly(phenyleneethynylene)s containing azobenzene moieties at the main chains [poly(**1**–**2m**) and poly(**1**–**2p**)] by the Sonogashira–Hagihara coupling polymerization of D-hydroxyphenylglycine-derived monomer **1** with 3,3'- and 4,4'-diethynylazobenzenes (**2m**, **2p**). Poly(**1**–**2m**) was folded into a predominantly one-handed helix in $CHCl_3$/THF = 7/3 but not so much either in $CHCl_3$ and THF. On the other hand, poly(**1**–**2p**) was folded into a helix both in $CHCl_3$ and THF, and their mixtures. The λ_{max} of poly(**1**–**2p**) positioned at a

longer wavelength than that of poly(**1**–**2m**) due to the expansion of main chain conjugation through the azobenzene units. The solution state IR measurement revealed the existence of intramolecular hydrogen bonds between the carbamate/amide groups at the side chains, and higher hydrogen-bonding strength in poly(**1**–**2p**) than that in poly(**1**–**2m**), which well explains the higher helicity of poly(**1**–**2p**). The folded structure of poly(**1**–**2m**) was disrupted upon UV-light irradiation, which was induced by the photo-isomerization of the azobenzene units from planar *trans*-form to bended *cis*-form. The deformed poly(**1**–**2m**) was refolded into a helix upon visible-light irradiation accompanying isomerization of the azobenzene units from *cis*-form to *trans*-form. This reversible photo-induced conformational change of poly(**1**–**2m**) was further confirmed by the cycles of alternating UV- and visible-light irradiation. Thus, incorporation of *m,m'*-linked azobenzene units at the main chain is effective to achieve reversible photo-responsive conformational changes of poly(phenyeleneethynylene)s. Interestingly, poly(**1**–**2p**) was almost irresponsive to photo-irradiation regarding the *cis*-*trans* isomerization of the azobenzene units and polymer conformation. This is explainable from the stiff main chain more strongly stabilized by hydrogen bonding and longer conjugation through *p,p'*-linked azobenzene units compared with the *m,m'*-counterpart [poly(**1**–**2m**)]. The conformation analysis of the polymers using the MM, semiempirical MO and DFT methods confirmed that the folded helical structures are energetically more stable than the extended trans zigzag structures due to the

contribution of p-stacking and hydrogen bonding.

Experimental Sections

Measurements. ^{1}H (400 MHz) and ^{13}C (100 MHz) NMR spectra were recorded on a JEOL EX-400 or a JEOL AL-400 spectrometer. IR spectra were measured on a JASCO FT/IR-4100 spectrophotometer. Melting points (mp) were measured on a Yanaco micro melting point apparatus. Mass spectra were measured on a JEOL JMS-MS700 mass spectrometer. Specific rotations ($[a]_D$) were measured on a JASCO DIP-1000 digital polarimeter. Number- and weight-average molecular weights (M_n and M_w) of polymers were determined by SEC (Shodex columns KF805 × 3) eluted with tetrahydrofuran (THF) calibrated by polystyrene standards at 40 °C. CD, UV–vis absorption, and fluorescence spectra were recorded on a JASCO J-820 and FP-750 spectropolarimeter. Dynamic light scattering (DLS) measurements were performed using a Malvern Instruments Zetasizer Nano ZS at 25°C. The measured autocorrelation function was analyzed using a cumulant method. The hydrodynamic radii (R_h) of the polymers were calculated from the Stokes-Einstein equations.

Materials. Unless stated otherwise, reagents and solvents were purchased and used without purification. 3,3'-Dibromoazobenzene[54] and 4,4'-diethynylazobenzene[55] (**2p**) were synthesized according to the literature. Et_3N and *N,N*-dimethylformamide (DMF) used for polymerization were distilled prior to use.

Photo-irradiation. Photo-irradiation was carried out with a 400 W high-pressure mercury lamp with a power source (HB-400, Fuji Glass Work) at room temperature. The appropriate wavelengths were selected either with a Pyrex glass and a UV-D33S filter (Toshiba) for irradiation at $300 < \lambda < 400$ nm or with an L-42 filter (Toshiba) filter for irradiation at $420 \text{ nm} < \lambda$. A sample solution was fed in a quartz cell, and it was placed 20 cm apart from the lamp. The photo-isomerization was monitored by UV–vis absorption spectroscopy.

Synthesis of 3,3'-Diethynylazobenzene (3). 3,3'-Dibromoazobenzene (3.40 g, 10.00 mmol), $PdCl_2(PPh_3)_2$ (0.168 g, 0.24 mmol), PPh_3 (0.252 g, 0.96 mmol) and CuI (0.274 g, 1.44 mmol) were fed into a two-neck flask, ant it was flushed with dry nitrogen. THF (20 mL) and Et_3N (15 mL) were added to the solution, and then trimethylsilylacetylene (3.30 mL, 23.9 mmol) was added dropwise to the solution. The mixture was stirred at 50 °C for 72 h. The resulting mixture was concentrated in vacuo and the residual mass was washed with Et_2O to extract the product. The organic phase was washed with 1.0 M HCl, and saturated NaCl aq., dried over anhydrous $MgSO_4$, and then filtered. The filtrate was concentrated, and the residual mass was purified by silica gel column chromatography eluted with hexane/EtOAc = 9/1 (v/v) to obtain crude 3,3'-bis(trimethylsilylethynyl)azobenzene. After that, it was dissolved in THF (5 mL), and 1.0 M solution of tetrabutylammonium fluoride (TBAF) in THF (25 mL) was added to the solution. The resulting mixture was concentrated in vacuo, and the residual mass was dispersed in $CHCl_3$ and water. The organic

layer was washed with 1.0 M HCl and saturated NaCl aq., dried over anhydrous $MgSO_4$, and then filtered. The filtrate was concentrated, and the residual mass was purified by silica gel column chromatography eluted with hexane/$CHCl_3$ = 19/1 (v/v) to obtain **3** as an orange solid in 28%. ^{1}H NMR (400 MHz, $CDCl_3$): δ 3.13 (s, 2H, –C≡C*H*), 7.47 (t, *J* = 7.2 Hz, 2H, Ar), 7.59 (d, *J* = 7.6 Hz, 2H, Ar), 7.89 (d, *J* = 7.6 Hz, 2H, Ar), 8.03 (s, 2H, Ar). ^{13}C NMR (100 MHz, $CDCl_3$): δ 78.06 (–C≡*C*H), 82.83 (–*C*≡CH), 123.1, 123.5, 126.3, 129.1, 134.5, 152.1 (Ar).[56]

Polymerization. All the polymerizations were carried out in a glass tube equipped with a three-way stopcock under nitrogen. A typical experimental procedure for polymerization **1** with **2m** is given below. A solution of **1** (218 mg, 0.400 mmol), **2m** (92.0 mg, 0.400 mmol), $Pd(PPh_3)_2Cl_2$ (14.4 mg, 0.020 mmol), PPh_3 (10.4 mg, 0.040 mmol), CuI (11.4 mg, 0.060 mmol), and Et_3N (0.8 mL) in DMF (1.2 mL) was stirred at 80 °C for 24 h. The resulting mixture was poured into MeOH/acetone [9/1 (v/v), 300 mL] to precipitate a polymer. It was separated by filtration using a membrane filter (ADVANTEC H100A047A) and dried under reduced pressure.

Spectroscopic Data of the Polymers. Poly(1–2m): IR (KBr): 3421, 3331, 3064, 2952, 2926, 2857, 2215, 1671, 1476, 1366, 1160, 798, 687, 519. ^{1}H NMR (400 MHz, $CDCl_3$): δ 0.82–1.79 [br, 20H, –CONHCH$_2$(C*H*$_2$)$_4$C*H*$_3$, –NHCOOC(C*H*$_3$)$_3$], 3.08–3.53 [br, 2H, –CONHC*H*$_2$(CH$_2$)$_4$CH$_3$], 5.03–5.38 (br, 1H, –C*H*CONH–), 5.52–6.88 [br, 3H, –CON*H*CH$_2$(CH$_2$)$_4$CH$_3$, –N*H*COOC(CH$_3$)$_3$, –O*H*], 7.10–8.38 (br, 10H, Ar). **Poly(1–2p)**: IR (KBr): 3422,

3339, 3060, 2956, 2928, 2857, 2204, 1676, 1491, 1366, 1260, 1228, 1161, 849, 804, 490 cm^{-1}. ^1H NMR (400 MHz, $CDCl_3$): δ 0.82–1.79 [br, 20H, –$CONHCH_2(CH_2)_4CH_3$, –$NHCOOC(CH_3)_3$], 3.08–3.53 [br, 2H, –$CONHCH_2(CH_2)_4CH_3$], 5.03–5.38 (br, 1H, –C*H*CONH–), 5.52–6.88 [br, 3H, –$CONHCH_2(CH_2)_4CH_3$, –N*H*$COOC(CH_3)_3$, –O*H*], 7.10–8.38 (br, 10H, Ar).

Computation. The molecular mechanics calculations (MMFF94)[57] were carried out with Wavefunction, Inc., Spartan '10 version 1.1.0, Macintosh. The semi-empirical molecular orbital calculations (PM6,[58] ZINDO) and DFT[59] calculations were performed with the GAUSSIAN 09 program,[60] EM64L-G09 Rev C.01 running on the supercomputer system, Academic Center for Computing and Media Studies, Kyoto University. Theoretical CD and UV-vis spectra were simulated by the ZINDO/S method in the GAUSSIAN 09 program. The low-energy transition states of 20 were predicted under the condition of a CI number of 20 × 20, including each oscillator strength (f_{vel}) and rotatory strength (R_{vel}) in velocity form. The simulated CD and UV-vis spectra were produced by using the R_{vel}– and f_{vel}–wavelength data with a wavelength-based Gaussian function of 14 nm tentatively used for a half of 1/e-bandwidth, respectively.

References

(1) Kawata, S.; Kawata, Y. *Chem. Rev.* **2000**, *100*, 1777–1788.
(2) Irie, M. *Bull. Chem. Soc. Jpn.* **2008**, *277*, 1793–1796.
(3) Russew, M.; Hecht, S. *Adv. Mater.* **2010**, *22*, 3348–3360.
(4) Lee, S.; Kang, H. S.; Park, J. *Adv. Mater.* **2012**, *24*, 2069–2103.

(5) Mal, N. K.; Fujiwara, M.; Tanaka, Y.; Taguchi, T.; Matsukata, M. *Chem. Mater.* **2005**, *127*, 16189–16196.
(6) Wells, L. A.; Furukawa, S.; Sheardown, H. *Biomacromolecules* **2011**, *12*, 923–932.
(7) Tomatsu, I.; Hashidzume, A.; Harada, A. *Macromolecules* **2005**, *38*, 5223–5227.
(8) Yamauchi, K.; Takashima, Y.; Hashidzume, A.; Yamaguchi, H.; Harada, A. *J. Am. Chem. Soc.* **2008**, *130*, 5024–5025.
(9) Liao, X.; Chen, G.; Liu , X.; Chen, W.; Chen, F.; Jiang, M. *Angew. Chem. Int. Ed.* **2010**, *49*, 4409–4413.
(10) Yamaguchi, H.; Kobayashi, Y.; Kobayashi, R.; Takashima, Y.; Hashidzume, A.; Harada, A. *Nat. Commun.* **2012**, *3*, 603.
(11) Natali, M.; Giordani, S. *Chem. Soc. Rev.* **2012**, *41*, 4010–4029.
(12) Peters, M. V.; Stoll, R. S.; Kühn, A.; Hecht, S. *Angew. Chem. Int. Ed.* **2008**, *47*, 5968–5972.
(13) Stoll, R. S.; Peters, M. V.; Kuhn, A.; Heiles, S.; Goddard, R.; Buhl, M.; Thiele, C. M.; Hecht, S. *J. Am. Chem. Soc.* **2009**, *131*, 357–367.
(14) Neilson, B. M.; Bielawski, C. W. *J. Am. Chem. Soc.* **2012**, *134*, 12693–12699.
(15) Jiang, H.; Kelch, S.; Lendlein, A. *Adv. Mater.* **2006**, *18*, 1471–1475.
(16) Yamada, M.; Kondo, M.; Mamiya, J.; Yu, Y.; Kinoshita, M.; Barrett, C. J.; Ikeda, T. *Angew. Chem. Int. Ed.* **2008**, *47*, 4986–4988.
(17) Priimagi, A.; Shimamura, A.; Kondo, M; Hiraoka, T.; Kubo, S.; Mamiya, J.; Kinoshita, M.; Ikeda, T.; Shishido, A. *ACS Macro. Lett.* **2012**, *1*, 96–99.
(18) Lee, K. M.; White, T. *Macromolecules* **2012**, *45*, 7163–7170.
(19) For a review, see: Bandara, H. M. D.; Burdette, S. C. *Chem. Soc. Rev.* **2012**, *41*, 1809–1825.
(20) For a review, see: Yashima, E.; Maeda, K.; Iida, K.; Furusho, Y.; Nagai, K. *Chem. Rev.* **2009**, *109*, 6102–6211.
(21) Mayer, S.; Maxein, G.; Zentel, R. *Macromolecules* **1998**, *31*, 8522–8525.
(22) Mruk, R.; Zentel, R. *Macromolecules* **2002**, *35*, 185–192.
(23) Sanda, F.; Teraura, T.; Masuda, T. *J. Polym. Sci., Part A: Polym. Chem.* **2004**, 42, 4641–4647.

(24) Horiuchi, H.; Fukushima, T.; Zhao, C.; Okutsu, T.; Hiratsuka, H. *Chem. Lett.* **2005**, *34*, 1292–1293.
(25) Zhao, H.; Sanda, F.; Masuda, T. *Polymer* **2006**, *47*, 2596–2602.
(26) Fujii, T.; Shiotsuki, M.; Inai, Y.; Sanda, F.; Masuda, T. *Macromolecules* **2007**, *40*, 7079–7088.
(27) Qu, J.; Jiang, F.; Chen, H.; Sanda, F.; Masuda, T. *J. Polym. Sci., Part A: Polym. Chem.* **2009**, *47*, 4749–4761.
(28) Sogawa, H.; Shiotsuki, M.; Matsuoka, H.; Sanda, F. *Macromolecules* **2011**, *44*, 3338–3345.
(29) Khan, A.; Hecht, S. *Chem. Eur. J.* **2006**, *12*, 4764–4774.
(30) Zhang, W.; Yoshida, K.; Fujiki, M.; Zhu, X. *Macromolecules* **2011**, *44*, 5105–5111.
(31) Yu, Z.; Hecht, S. *Angew. Chem. Int. Ed.* **2011**, *50*, 1640–1643.
(32) Yu, Z.; Hecht, S. *Chem. Eur. J.* **2012**, *18*, 10519–10524.
(33) Liu, R.; Shiotsuki, M.; Masuda, T.; Sanda, F. *Macromolecules* **2009**, *42*, 6115–6122.
(34) Liu, R.; Sogawa, H.; Shiotsuki, M.; Masuda, T.; Sanda, F. *Polymer* **2010**, *51*, 2255–2263.
(35) Hashimoto, A.; Sogawa, H.; Shiotsuki, M.; Sanda, F. *Polymer* **2012**, *53*, 2559–2566.
(36) For a review, see: Hill, D. J.; Mio, M. J.; Prince, R. B.; Hughes, T. S.; Moore, J. S. *Chem. Rev.* **2001**, *101*, 3893–4011.
(37) Yamamoto, T.; Komarudin, D.; Arai, M.; Lee, B.-L.; Suganuma, H.; Asakawa, N.; Inoue, Y.; Kubota, K.; Sasaki, S.; Fukuda, T.; Matsuda, H. *J. Am. Chem. Soc.* **1998**, *120*, 2047–2058.
(38) Fujiki, M. *Macromol. Rapid Commun.* **2001**, *22*, 539–563.
(39) Cary, J. M.; Moore, J. S. *Org. Lett.* **2002**, *4*, 4663–4666.
(40) Yang, X.; Brown, A. L.; Furukawa, M.; Li, S.; Gardinier, W. E.; Bukowski, E. J.; Bright, F. V.; Zheng, C.; Zeng, X. C.; Gong, B. *Chem. Commun.* **2003**, 56–57.
(41) Banno, M.; Yamaguchi, T.; Nagai, K.; Kaiser, C.; Hecht, S.; Yashima, E. *J. Am. Chem. Soc.* **2012**, *134*, 8718–8728.
(42) Izumi, A.; Nomura, R.; Masuda, T. *Macromolecules*, **2000**, *33,* 8918–8920.

(43) Izumi, A.; Nomura, R.; Masuda, T. *Macromolecules*, **2001**, *34*, 4342–4347.
(44) Humphrey, J. L.; Lott, K. M.; Wright, M. E.; Kuciauskas, D. *J. Phys. Chem. B* **2005**, *109*, 21496–21498.
(45) Moniruzzaman, M.; Talbot, J. D. R.; Sabey, J.; Fernando, F. *J. Appl. Polym. Sci.* **2006**, *100*, 1103.
(46) Adisa, B.; Bruce, D. A. *J. Phys. Chem. B* **2005**, *109*, 7548–7556.
(47) Adisa, B.; Bruce, D. A. *J. Phys. Chem. B* **2005**, *109*, 19952–19959.
(48) Lee, O. S.; Saven, J. G. *J. Phys. Chem. B* **2004**, *108*, 11988–11994.
(49) Halgre, T. A. *J. Comput. Chem.* **1996**, *17*, 490–519. The molecular mechanics calculations were carried out with Wavefunction, Inc., Spartan ’10 Macintosh.
(50) Zhao, Y.; Truhlar, D. G. *Theor. Chem. Account* **2008**, *120*, 215–241.
(51) Zhao, Y.; Truhlar, D. G. *Acc. Chem. Res.* **2008**, *41*, 157–167.
(52) Řezáč, J.; Fanfrlík, J.; Salahub, D.; Hobza, P. *J. Chem. Theory Comput.* **2009**, *5,* 1749–1760.
(53) Lee, O. S.; Saven, J. G. *J. Phys. Chem. B* **2004**, *108*, 11988.
(54) Priewisch, B.; Braun, K. *J. Org. Chem.* **2005**, *70*, 2350–2352.
(55) Zeitouny, J.; Aurisicchio, C.; Bonifazi, D.; Zorzi, R. D.; Geremia, S.; Bonini, M.; Palma, C.; Samori, P.; Listorti, A.; Belbakra, A.; Armaroli, N. *J. Mater. Chem.* **2009**, *19*, 4715–4724.
(56) Ma, H.; Li, W.; Wang, J.; Xiao, G.; Gong, Y.; Qi, C.; Feng, Y.; Li, X.; Bao, Z.; Cao, W.; Sun, Q.; Veaceslav, C.; Wang, F.; Lei, Z. *Tetrahedron* **2012**, *68*, 8358–8356.
(57) Halgren, T. A. *J. Comput. Chem.* **1996**, *17*, 490–519.
(58) Stewart, J. J. P. *J. Mol. Model.* **2007**, *13*, 1173–1213.
(59) Parr, R. G.; Yang, W. Density-Functional Theory of Atoms and Molecules; Oxford University Press: Oxford, 1989.
(60) Frisch, M. J.; Trucks, G. W.; Schlegel, H. B.; Scuseria, G. E.; Robb, M. A.; Cheeseman, J. R.; Scalmani, G.; Barone, V.; Mennucci, B.; Petersson, G. A.; Nakatsuji, H.; Caricato, M.; Li, X.; Hratchian, H. P.; Izmaylov, A. F.; Bloino, J.; Zheng, G.; Sonnenberg, J. L.; Hada, M.; Ehara, M.; Toyota, K.; Fukuda, R.; Hasegawa, J.; Ishida, M.; Nakajima, T.; Honda, Y.; Kitao, O.; Nakai, H.; Vreven, T.; Montgomery, J. A.; Peralta, Jr., J. E.; Ogliaro, F.; Bearpark, M.;

Heyd, J. J.; Brothers, E.; Kudin, K. N.; Staroverov, V. N.; Keith,T.; Kobayashi, R.; Normand, J.; Raghavachari, K.; Rendell, A.; Burant, J. C.; Iyengar, S. S.; Tomasi, J.; Cossi, M.; Rega, N.; Millam, J. M.; Klene, M.; Knox, J. E.; Cross, J. B.; Bakken, V.; Adamo, C.; Jaramillo, J.; Gomperts, R.; Stratmann, R. E.; Yazyev, O.; Austin, A. J.; Cammi, R.; Pomelli, C.; Ochterski, J. W.; Martin, R. L.; Morokuma, K.; Zakrzewski, V. G.; Voth, G. A.; Salvador, P.; Dannenberg, J. J.; Dapprich, S.; Daniels, A. D.; Farkas, O.; Foresman, J. B.; Ortiz, J. V.; Cioslowski, J.; Fox, D. J. Gaussian 09, Revision C.01, Gaussian, Inc.: Wallingford CT, 2010.

Part III

Synthesis and Properties of α-Propargyl Amino Acid-derived Optically Active Substituted Polyacetylenes

Chapter 6

α-Propargyl Amino Acid-derived Optically Active Novel Substituted Polyacetylenes: Synthesis, Secondary Structures, and Responsiveness to Ions

Abstract

Novel optically active substituted acetylenes $HC{\equiv}CCH_2CR^1(CO_2CH_3)NHR^2$ [(*S*)-/(*R*)-**1**: R^1 = H, R^2 = Boc, (*S*)-**2**: R^1 = CH_3, R^2 = Boc, (*S*)-**3**: R^1 = H, R^2 = Fmoc, (*S*)-**4**: R^1 = CH_3, R^2 = Fmoc (Boc = *tert*-butoxycarbonyl, Fmoc = 9-fluorenylmethoxycarbonyl)] were synthesized from α-propargylglycine and α-propargylalanine, and polymerized with a rhodium catalyst to provide the polymers with number-average molecular weights of 2400–38 900 in good yields. Polarimetric, CD and UV–vis spectroscopic analyses indicated that poly[(*S*)-**1**], poly[(*R*)-**1**], and poly[(*S*)-**4**] formed predominantly one-handed helical structures both in polar and nonpolar solvents. The plus CD signal of poly[(*S*)-**1a**] turned into minus one upon addition of alkali hydroxide (LiOH, NaOH, KOH) and tetrabutylammonium fluoride (TBAF), accompanying the red-shift of λ_{max}. The degree of λ_{max} shift became large as the size of cation of the additive.

Introduction

The helix is one of the most common higher-order structures of macromolecules. Many sophisticated and intricate functions of biomacromolecules such as proteins and DNA largely depend on their well-defined helical structures. Various types of helical polymers have been synthesized so far including polymethacrylates,[1] polyisocyanides,[2] polysilanes,[3] poly(phenyleneethynylene)s[4] and polyacetylenes,[5] dating back to the discovery of isotactic polypropylene by Natta and co-workers.[6] Monosubstituted polyacetylenes synthesized by the polymerization with rhodium catalysts feature a highly *cis*-stereoregurlar structure.[7–9] Introduction of appropriated chiral substituents into the side chain leads to the formation of a helical structure with predominantly one-handed screw sense. There have been reported that rhodium-based *cis*-stereoregular polyacetylene derivatives such as poly(*N*-propargylamide)s,[10–12] poly(*N*-propargylcarbamate)s,[13,14] poly(*N*-butynylamide)s,[15,16] poly(1-methylpropargyl- *N*-alkylcarbamate)s[17] form helical structures with predominantly one-handed screw sense, which are stabilized by intramolecular hydrogen bonds together with the steric repulsion between the side chains in the biomimetically same way as peptides and proteins. They undergo reversible helix-helix or helix-coil transitions by external stimuli such as heat and the addition of polar solvents, wherein the formation and deformation of hydrogen bonds are key factors for the conformational transition.

Amino acid is a useful chiral building block for synthetic helical

polymers, because the amino and carboxy groups are transformable into wide variety of functional groups, making versatile molecular design possible. When amide groups are introduced in amino acid based helical polymers, they are usable for stabilizing the helical structure due to the strong nature forming hydrogen bonding in a manner similar to α-helix of peptide. Various helical polyacetylenes functionalized with amino acids have been also synthesized so far,[18–42] some of which change the conformation according to external stimuli such as temperature,[18,19] solvent,[20–23] acid/base,[24–27] electricity,[28] and photo-irradiation.[29,30] Amino acid based helical polymers also show useful properties including chemical sensing,[31–34] chiral recognition,[35] and asymmetric induction[36–39] originated from the conjugated backbone and regularly ordered functional groups at the side chain strands.

Recently, the synthesis of highly optically pure non-natural amino acids becomes possible by the enantioselective alkylation of a prochiral protected glycine derivative utilizing a chiral phase transfer catalyst (Maruoka Catalyst) having binaphthyl group.[43] Various optically active amino acids bearing olefinic pendants are now commercially synthesized with Maruoka Catalyst, and find application to hydrocarbon stapling (ring-closing metathesis reaction) of helical peptides, which provides a useful strategy for experimental and therapeutic modulation of protein-protein interactions in many signaling pathways.[44] Non-natural optically active amino acids bearing acetylenic pendants such as α-propargylglycine are synthesized by Maruoka Catalyst as

well. In the course of the study on amino acid based helical polyacetylenes, the author has decided to utilize α-propargyl amino acid derivatives as the monomers. The present article deals with the synthesis of novel polyacetylenes from α-propargylglycine and alanine (Scheme 1), and examination of the secondary structures. As far as the author knows, this is the first example regarding the synthesis of α-propargyl amino acid derived helical polyacetylenes. The author further discloses the removal of protecting groups from the amino and carboxy groups, and ion-responsiveness of the polymers having unprotected amino/carboxy groups.

Scheme 1. Polymerization of Monomers (*S*)- / (*R*)-**1**–**4**.

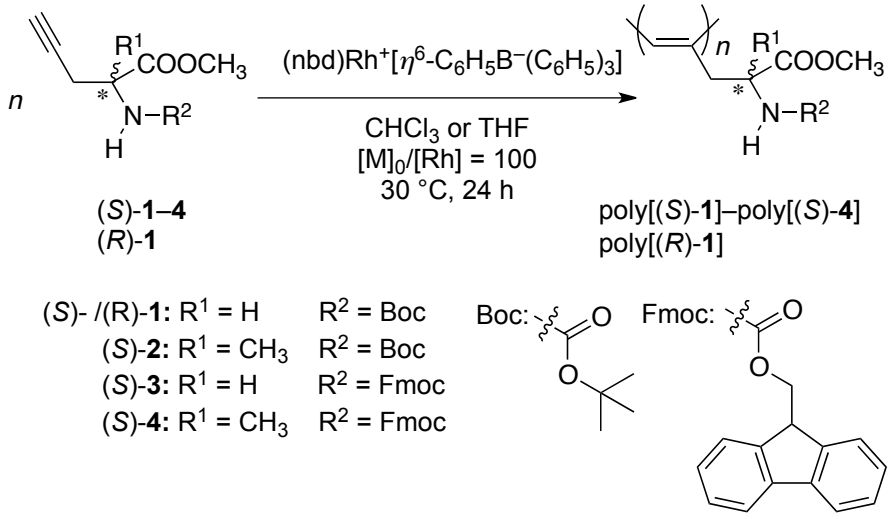

Results and Discussion

Polymerization. Rhodium catalysts tolerate a wide variety of functional groups including carbamate and ester, and polymerize monosubstituted acetylenes to afford the corresponding *cis*-stereoregular

polymers.[7,8] Thus, the polymerization of monomers (*S*)-/(*R*)-**1**–(*S*)-**4** was carried out using (nbd)$Rh^+[\eta^6\text{-}C_6H_5B^-(C_6H_5)_3]$ in $CHCl_3$ and THF at 30 °C for 24 h (Scheme 1). The formed polymers were isolated as hexane- or Et_2O-insoluble parts. The polymerization of (*S*)-**1**, (*R*)-**1**, and (*S*)-**4** proceeded homogeneously to give polymers with M_n's of 2400–38 900 in good yields (Table 1). These polymers were soluble in common organic solvents such as $CHCl_3$ and THF. On the other hand, yellow polymeric masses precipitated out of the solution onto the sides of the glass tube in a little while after initiating the polymerization of (*S*)-**2** and (*S*)-**3**. The molecular weights of isolated poly[(*S*)-**2**] and poly[(*S*)-**3**] could not be determined by SEC because they were insoluble in $CHCl_3$, THF, DMF, and H_2O. The author further tried the polymerization of (*S*)-**2** and (*S*)-**3** under the conditions different from those in Table 1, but failed to obtain solvent-soluble polymers.

Chiroptical Properties of the Polymers. As shown in Table 1, poly[(*S*)-**1**], poly[(*R*)-**1**], and poly[(*S*)-**4**] displayed $|[\alpha]_D|$ values 5–14 times larger than those of the corresponding monomers, indicating the presence of chirally regulated higher order structures. The signs of $[\alpha]_D$ of poly[(*S*)-**1**] and poly[(*R*)-**1**], enantiomerically isomeric polymers, were opposite, and the absolute values were almost the same as predicted. The polymers exhibited intense CD signals at the absorption region of the main chain chromophore around 320–360 nm in $CHCl_3$, THF, THF/MeOH = 1/1, THF/DMF = 1/1, and DMF as shown in

Table 1. Polymerization of (*S*)- / (*R*)-**1**–**4**[a]

Run	Monomer	Polymer			
		Yield[c] (%)	M_n[e]	M_w/M_n[e]	$[\alpha]_D$[f] (°)
1	(*S*)-**1**	83	38 900	1.9	+113
2	(*R*)-**1**	76	30 700	1.8	–106
3	(*S*)-**2**	–[d]	–[d]	–[d]	–[d]
4	(*S*)-**3**	–[d]	–[d]	–[d]	–[d]
5	(*S*)-**4**	61	2400	1.6	–[g]
6[b]	(*S*)-**4**	83	7900	1.7	+662

[a] Conditions: catalyst (nbd)$Rh^+[\eta^6$-$C_6H_5B^-(C_6H_5)_3]$, nbd = 2,5-norbornadiene, $[M]_0$ = 0.20 M, $[M]_0/[Rh]$ = 100, in $CHCl_3$, at 30 °C for 24 h. [b] $[M]_0$ = 0.50 M, in THF. Gelation occurred at this concentration in $CHCl_3$. [c] Hexane-insoluble part {poly[(*S*)-**1**] and poly[(*R*)-**1**]} and Et_2O-insoluble part {poly[(*S*)-**4**]}. [d] Not determined due to insolubility. [e] Determined by SEC eluted with THF, polystyrene calibration. [f] Measured by polarimetry at room temperature, *c* = 0.09−0.14 g/dL in THF. $[\alpha]_D$ of monomers: (*S*)-**1**, +23°; (*R*)-**1**, –22°; (*S*)-**4**, –45°. [g] Not determined.

Figures 1 and 2. The wavelengths of the CD and UV–vis absorption peaks coinciding with each other imply that the CD signals originate from the conjugated polyacetylene main chain. Fluorine-derived CD signals are negligibly small, presumably because the fluorene moieties are positioned apart from the main chain, which makes their regulated arrangement difficult.[45]

After membrane filtration (pore size = 0.45 mm) of the sample solutions, the CD and UV–vis signals were still observed with the same intensities as those before filtration,[46] and the sample concentration did not affect the signal intensity at a range of 0.25–1.00 mM. These results indicate that the CD signals do not originate from chiral aggregates like the case of poly(thiophene)s[47,48] and poly(*p*-phenylenevinylene)s[48,49] bearing chiral substituents but unimolecular

helical conformations of the polymers with predominantly one-handed screw sense.

Poly(*N*-butynylamide)s[15,16] and poly(*N*-propargylamide)s[10,15] efficiently form helices stabilized by intramolecular >N–H ••• O=C< hydrogen bonds between the amide groups at the side chains in nonpolar solvents such as $CHCl_3$. On the other hand, the polymers hardly form helices in polar solvents such as MeOH and DMF, because these solvents disturb the formation of the intramolecular hydrogen bonding. Interestingly, poly[(*S*)-**1**] showed intense CD signals even in THF/MeOH = 1/1 and THF/DMF = 1/1,[50] and the CD intensity of poly[(*S*)-**1**] was larger in THF/DMF = 1/1 than that in less polar THF. Poly[(*S*)-**1**] has high helix-forming ability even in these polar solvents unlike poly(*N*-butynylamide)s and poly(*N*-propargylamide)s. The remarkable helix induction is probably due to the location of stereogenic centers close to the main chain. Namely, it is considered that the presence of chiral groups in close proximities to the main chain is quite effective to induce a helix stabilized by steric repulsion between the side chains, in a fashion similar to poly(1-methylpropargyl alcohol)s,[51] poly(1-methylpropargyl ester)s,[51,52] and poly(1-methylpropargyl-*N*-alkylcarbamate)s.[17] Poly[(*S*)-**1**] and poly[(*R*)-**1**], having side chains with different absolute configurations, exhibited mirror-image CD spectra at 250–500 nm. Together with the results of optical rotations listed in Table 1 {poly[(*S*)-**1**] +113°, poly[(*R*)-**1**] –106°}, it is concluded that these polymers form helical structures with opposite screw sense mutually, and the

helix sense is determined by the amino acid chirality. As depicted in Figure 2, poly[(*S*)-**4**] also showed intense CD signals in both nonpolar and polar solvents, $CHCl_3$, THF, and DMF. The UV–vis absorption maximum at the region of main chain chromophore was 33 nm shorter in DMF than those in THF and $CHCl_3$. It is presumed that poly[(*S*)-**4**] form a tightly twisted helix (i.e., smaller pitch/diameter) in DMF than the latter two solvents, causing blue shift due to the reduced conjugation.[53]

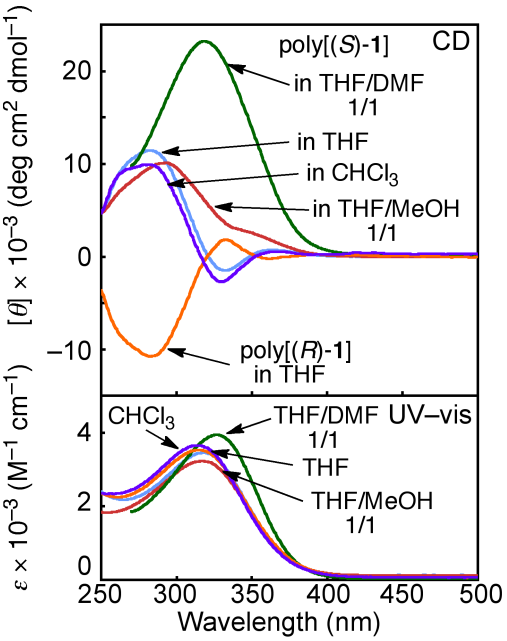

Figure 1. CD and UV–vis spectra of poly[(*S*)-**1**] and poly[(*R*)-**1**] measured in $CHCl_3$, THF, THF/MeOH = 1/1, and THF/DMF = 1/1 (c = 0.50 mM) at 20 °C.

The author further examined the thermal stability of helical conformation of the polymers. Figure 3 shows the Kuhn dissymmetry factor ($g = \Delta\varepsilon/\varepsilon$, in which $\Delta\varepsilon = [\theta]/3298$) at $[\theta]_{max}$ of poly[(*S*)-**1**] and poly[(*S*)-**4**] in $CHCl_3$, THF, and DMF at various temperatures. The g value of poly[(*S*)-**1**] decreased 24% by

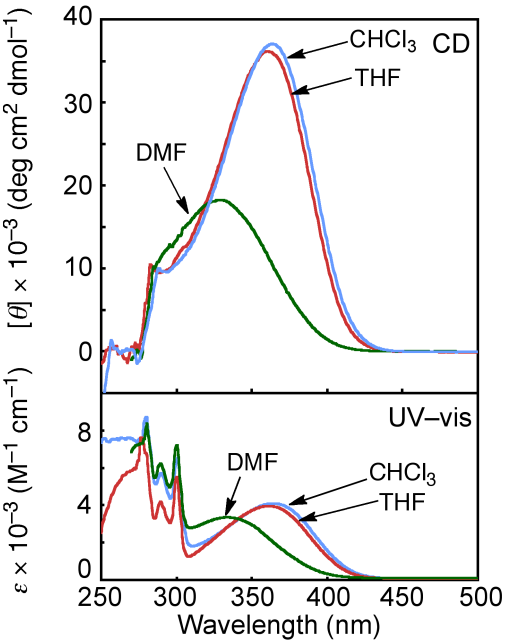

Figure 2. CD and UV–vis spectra of poly[(*S*)-**4**] measured in $CHCl_3$, THF, and DMF (*c* = 0.50 mM) at 20 °C.

raising temperature from 0 °C to 60 °C in THF, while that of poly[(*S*)-**4**] decreased only 2% under the same temperature range. Since the *g* values give quantitative information associated with the degree of preferential screw sense,[54] the present results indicate that the helical structure of poly[(*S*)-**4**] is more stable than that of poly[(*S*)-**1**] to thermo-driven screw sense reversal probably due to the larger steric repulsion between the side chains originated from the methyl groups at the chiral centers. The *g* values of poly[(*S*)-**4**] were smaller and more temperature-sensitive in DMF than those in $CHCl_3$ and THF. In DMF, poly[(*S*)-**4**] may be more flexible than in the latter two solvents, because of the less conjugated main chain as mentioned above. Compared to $CHCl_3$ and THF, it seems that the solvation ability of DMF with poly[(*S*)-**4**] is high because

dipole–dipole interaction between the carbonyl moieties of DMF and the polymer is possibly present along with hydrogen-bonding interaction, resulting in high flexibility of conformation as well.

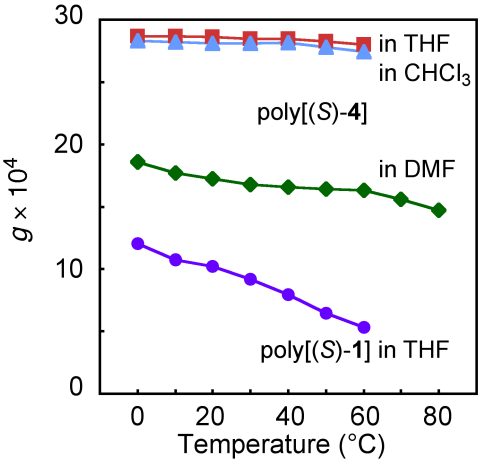

Figure 3. Plots of g values of poly[(*S*)-**1**] and poly[(*S*)-**4**] at $[\theta]_{max}$ versus temperature measured in $CHCl_3$, THF, and DMF (c = 0.50 mM).

Removal of Protecting Groups of Poly[(*S*)-1] and Poly[(*S*)-4]. The ester groups of poly[(*S*)-**1**] were hydrolyzed using NaOH aq. to obtain the corresponding polymer {poly[(*S*)-**1a**]} bearing unprotected carboxy groups (Scheme 2).[55] The proceeding of the reaction was confirmed by ^{1}H NMR spectroscopy, i.e., a signal around 3.6–3.8 ppm corresponding to the methyl groups mostly disappeared after hydrolysis. The M_n and M_w/M_n of poly[(*S*)-**1a**] were determined as 30 500 and 1.9 by SEC,[56] respectively, which were almost the same as those of poly[(*S*)-**1**] listed in Table 1. Decomposition during hydrolysis seems to be negligibly small.

Further, removal of the Fmoc groups from poly[(*S*)-**4**] was attempted to

obtain poly[(*S*)-**4b**] bearing unprotected amino groups according to Scheme 3. The reaction successfully proceeded, which was evident from the disappearance of the ^{1}H NMR signals assignable to the Fmoc proton signals.

Figures 4 and 5 depict the CD and UV–vis spectra of poly[(*S*)-**1a**] and poly[(*S*)-**4b**] measured in THF, MeOH, and DMF. Poly[(*S*)-**1a**] exhibited intense Cotton effects around 300 nm in THF, while only small peaks in MeOH and DMF as shown in Figure 4. Meanwhile, poly[(*S*)-**4b**] exhibited a large minus CD signal around 280 nm both in THF and DMF as shown Figure 5. It is concluded that these polymers bearing unprotected carboxy and amino groups also adopt helical conformations with an excess of predominantly one-handed screw sense in the solvents. It should be noted that CD and UV–vis spectroscopic patterns of poly[(*S*)-**1a**] and poly[(*S*)-**4b**] were totally different from those of the precursors, poly[(*S*)-**1**] and poly[(*S*)-**4**] bearing protected carboxy and amino groups, implying that these polymers form different helical structures before and after removal of the protecting groups. This is predictable because it is likely that the carboxy groups interact with the functional groups at the side chains strongly and intramolecularly, and also with solvent molecules by hydrogen bonding, both of which largely affect the conformation and helicity. This is also the case for amino groups. Specifically, poly[(*S*)-**4b**] exhibited the λ_{max} at a wavelength 30–60 nm shorter than that of poly[(*S*)-**4**]. Removal of bulky Fmoc groups probably reduced the steric repulsion between the side chains, leading to tightening the helix accompanying the inversion of screw sense as a

more stable conformation.

As mentioned above, intramolecular hydrogen bonds possibly exist between the pendent side chains and stabilize the helical structures in a fashion similar to poly(*N*-propargylcarbamate)s[13] and poly(*N*-butynylamide)s.[15,16] Solution-state IR spectroscopic study was carried out under diluted conditions to determine the presence/absence of intramolecular hydrogen bonding. Table 2 summarizes the results of IR measurement for solutions (40 mM)[57] of poly[(*S*)-**1**] and poly[(*S*)-**1a**], and the corresponding monomers (*S*)-**1** and (*S*)-**1a**. Monomer (*S*)-**1** and poly[(*S*)-**1**] exhibited two strong absorption peaks assignable to C=O stretching of ester and carbamate groups, and a peak assignable to N–H bending of the carbamate groups. Monomer (*S*)-**1a** and poly[(*S*)-**1a**] exhibited C=O peaks of carboxy groups instead of ester groups. The carbamate C=O peaks of poly[(*S*)-**1**] were observed at 11 cm^{-1} lower, and N–H peaks at 12 cm^{-1} higher wavenumber regions than those of (*S*)-**1**. Compared to the difference of the carbamate C=O peak positions between the monomer and polymer, the difference of ester C=O peak positions was smaller, i.e., 4 cm^{-1}. On the other hand, the difference of carboxy C=O peak positions between (*S*)-**1a** and poly[(*S*)-**1a**] was as large as 16 cm^{-1}. The difference of carbamate C=O peak was 1 cm^{-1} between the monomer and polymer, and that of N–H was 16 cm^{-1}. These results confirm the presence of intramolecular hydrogen bonds in the both polymers, but the patterns seem to be largely different. Namely, it is assumed that poly[(*S*)-**1**] forms intramolecular hydrogen bonds between the C=O and N–H

of carbamate groups. The participation of the ester groups in hydrogen bonding of poly[(*S*)-**1**] seems to be negligibly small judging from the trace difference of the ester C=O absorption from that of (*S*)-**1** as mentioned above.

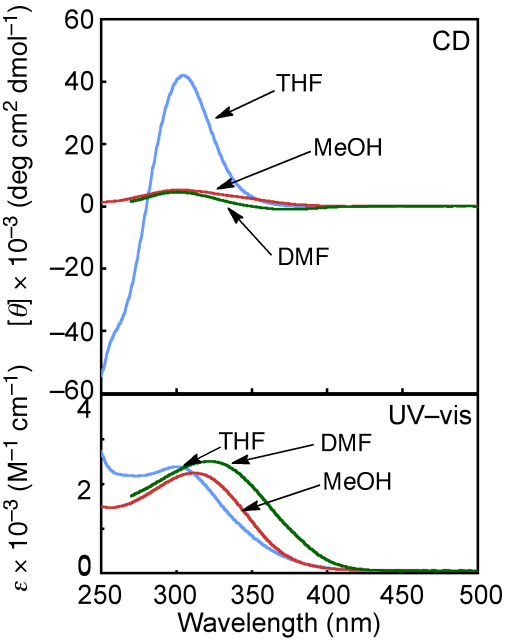

Figure 4. CD and UV–vis spectra of poly[(*S*)-**1a**] measured in THF, MeOH, and DMF (c = 0.50 mM) at 20 °C.

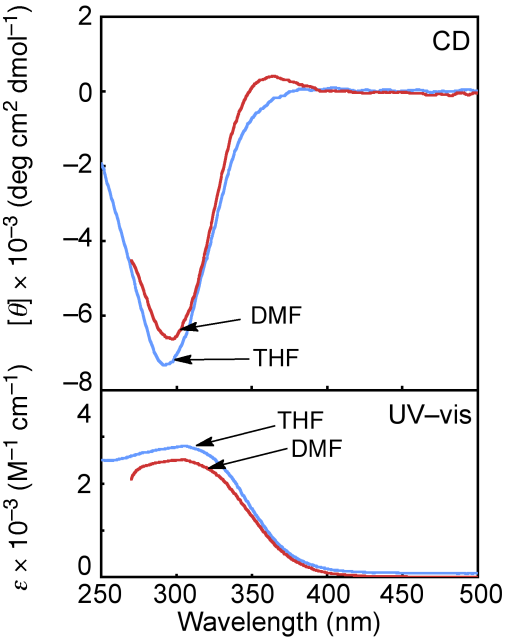

Figure 5. CD and UV–vis spectra of poly[(*S*)-**4b**] measured in THF and DMF (c = 0.50 mM) at 20 °C.

Meanwhile, poly[(*S*)-**1a**] presumably forms hydrogen bonds between the C=O of unprotected carboxy and N–H of carbamate groups. It is considered that this difference of hydrogen-bonding patterns causes the different helical structures between poly[(*S*)-**1**] and poly[(*S*)-**1a**].

Table 2. Solution-State IR Spectroscopic Data (C=O and N–H Absorption Peaks) of the Monomers and Polymers

Compound	Wavenumber (cm^{-1})		
	C=O		
	Ester or Carboxy	Carbamate	N–H
(*S*)-**1** [a]	1746	1709	1506
poly[(*S*)-**1**] [a]	1742	1698	1518
(*S*)-**1a** [b]	1747	1718	1506
poly[(*S*)-**1a**] [b]	1731	1717	1522

[a] Measured in $CHCl_3$ (c = 40 mM). [b] Measured in THF (c = 40 mM).

Ion Sensing Properties of Poly[(*S*)-1a]. Figure 6 shows the change of CD and UV–vis spectra of poly[(*S*)-**1a**] upon addition of KOH measured in THF/MeOH = 1/1. The CD signal around 250–350 nm gradually decreased by raising the amount of KOH up to 0.75 equiv, and disappeared at 1.00 equiv. Further addition of KOH induced a minus peak around 312 nm at 1.50 equiv, and a red-shift to 330 nm at 4.00 equiv. The analogous spectral change was also observed in MeOH. It is suggested that poly[(*S*)-**1a**] varied its helical conformation (preference of screw sense and pitch/diameter) in response to KOH in these solvents. The other alkali metal hydroxides were also added to a solution of poly[(*S*)-**1a**]. Figure 7 depicts the CD and UV–vis spectra of

poly[(*S*)-**1a**] in the absence and presence of 4 equiv of LiOH and NaOH in THF/MeOH = 1/1, along with the data of KOH. A plus-signed CD signal was observed at 304 nm without an alkali hydroxide, while minus-signed ones were observed around 310–330 nm with all alkali hydroxides. The λ_{max} order was non < LiOH (+23 nm) < NaOH (+2 nm) < KOH (+5 nm).[58] The λ_{max} was more shifted as the size of alkali metal became larger.[59] These results suggest that poly[(*S*)-**1a**] changes the structure by the addition of an alkali metal hydroxide due to the ionic interactions between the carboxy groups and cationic species. Since the cations seem to exist close to the carboxy groups of the polymer in THF/MeOH, it is likely that the ionic repulsion between the side chains gets larger, resulting in a loosely twisted helix (larger pitch/diameter and enhanced conjugation) showing the λ_{max} at a longer wavelength region. Addition of TBAF,[60] which has larger cationic species than the alkali metals,[61,62] was examined in THF. As shown in Figure 8, the CD and UV–vis spectra of poly[(*S*)-**1a**] showed trends similar to those of the case of KOH addition (Figure 6). The λ_{max} was red-shifted largely by TBAF (51 nm) compared to those by the alkali metal hydroxides (25–30 nm), which supports the assumption of helix-loosening induced by ionic repulsion as mentioned above.[63] After the addition of 4 equiv of alkali metal or TBAF to a polymer solution, excess equivalents of HCl was added to the resulting solution. Then the CD and UV–vis spectral patterns completely returned to the original ones. It was confirmed that poly[(*S*)-**1a**] recovered the original helical structure without an alkali metal

or TBAF reversibly.

Figure 9 shows the pictures of poly[(*S*)-**1a**] solutions before and after addition of 4 equiv of alkali metal hydroxides and TBAF. Since the color of each polymer solution is distinguishable by the naked eye, the present system may be applicable to an ionic sensor. It is apparent that the ionic interaction between unprotected carboxy groups and additives is the key importance to induce such sensing abilities, because no spectral change was observed upon addition of TBAF to a solution of poly[(*S*)-**1**] bearing protected carboxy groups.

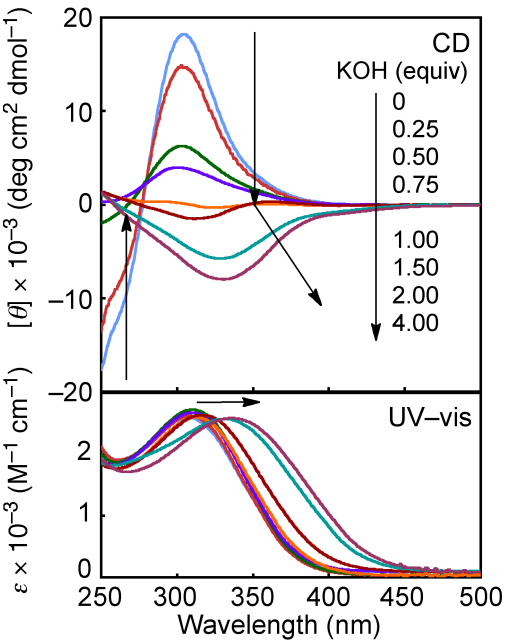

Figure 6. CD and UV–vis spectra of poly[(*S*)-**1a**] upon addition of KOH measured in THF/MeOH = 1/1 (*c* = 0.50 mM) at 20 °C.

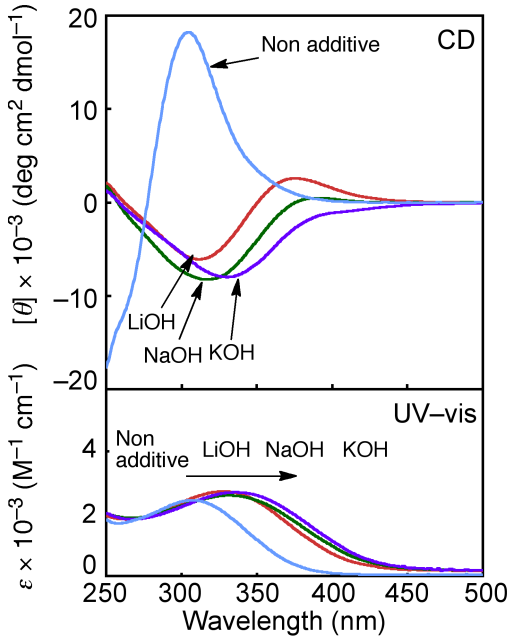

Figure 7. CD and UV–vis spectra of poly[(*S*)-**1a**] in the absence and presence of 4 equiv of LiOH, NaOH, and KOH measured in THF/MeOH = 1/1 (c = 0.50 mM) at 20 °C.

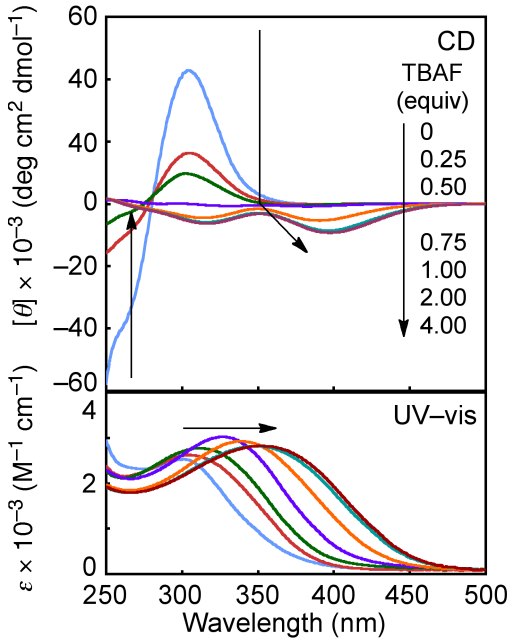

Figure 8. CD and UV–vis spectra of poly[(*S*)-**1a**] upon addition of TBAF measured in THF (c = 0.50 mM) at 20 °C.

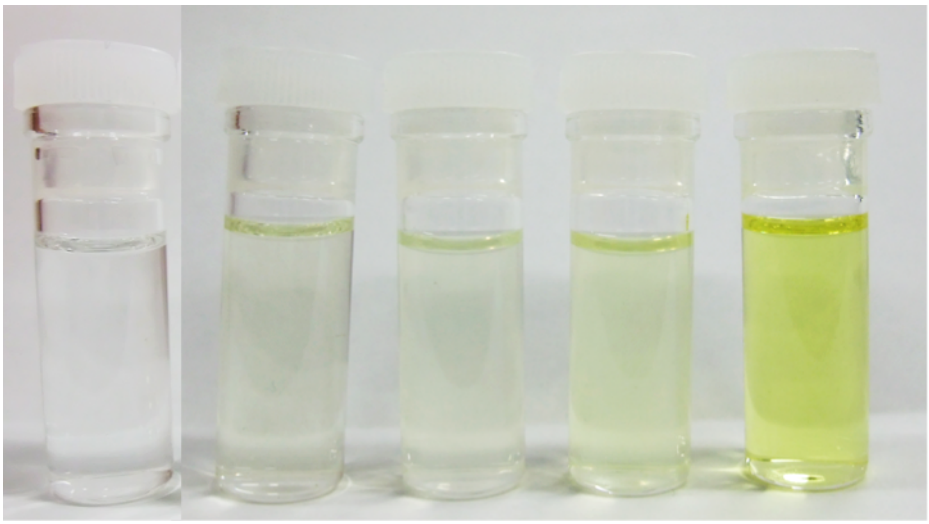

Figure 9. Photograph of solutions of poly[(*S*)-**1a**]. From left to right: without additive, with 4 equiv of LiOH, NaOH, KOH measured in THF/MeOH = 1/1, and TBAF measured in THF (c = 0.50 mM).

Conformational Analysis. As described above, it is considered that the present polymers take predominantly one-handed helical structures. The molecular mechanics calculation (MMFF94[64]) was carried out to gain knowledge on the conformation of the polymers. The conformers of poly[(*S*)-**1**] (18-mer) were optimized with the dihedral angles ϕ at the single bonds in the main chain varying by the increment of 10°. The polymer formed two different patterns of hydrogen bonding according to the value of ϕ, intramolecular hydrogen bonding between i th and (i+2) th units, and that between i th and (i+3) th units. As shown in Figure 10, a left-handed helical conformer with ϕ = –80° was the most stable one. The right-handed counterpart with ϕ = +80° was 11.7 kJ/mol•unit less stable than the left-handed one. This energy difference between the left- and right-handed helical conformers is explainable by the steric factor. Namely,

the van der Waals surface areas of the left- and right-handed conformers with f = –80° and +80° are 4663 and 4639 Å^2, and volumes are 3813 and 3813 Å^3, respectively.[65] These data indicate that the left-handed one is more extended, and therefore sterically more favorable than the right-handed one, resulting in the higher stability. The most stable conformer with ϕ = –80° forms regulated intramolecular hydrogen-bonding strands between the carbamate groups at i th and (i+3) th monomer units as depicted in Figure 11. The existence of this pattern of intramolecular hydrogen bonds is supported by the solution state IR spectroscopic data listed in Table 2.

The conformers of poly[(*S*)-**4**] and poly[(*S*)-**4b**] were also analyzed in a similar fashion to those of poly[(*S*)-**1**]. It is revealed that the most stable conformers of poly[(*S*)-**4**] and poly[(*S*)-**4b**] are left- (ϕ = –80°) and right-handed (ϕ = +80°) helices. These molecular mechanics calculation results well explain the CD signals with opposite sign of these two polymers.

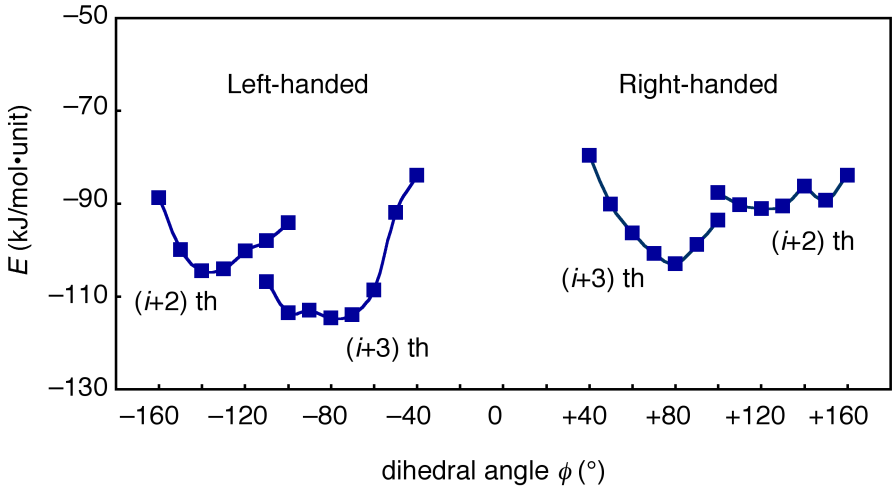

Figure 10. Relationship between the dihedral angle at the single bond in the main chain of poly[(*S*)-**1**] (18-mer) and the energy calculated by MMFF94.

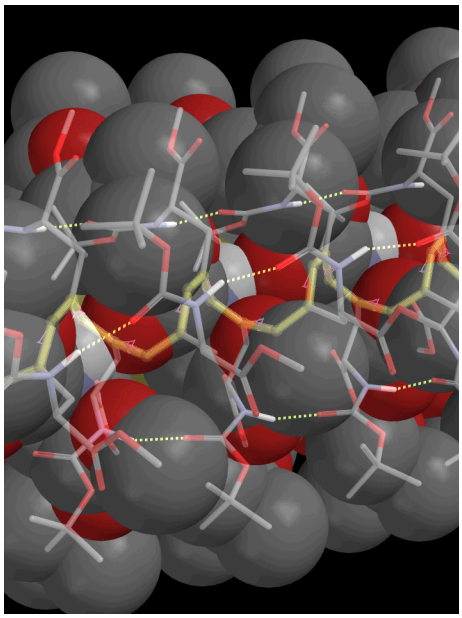

Figure 11. The most stable conformer of poly[(*S*)-**1**] optimized by MMFF94. The dihedral angles ϕ at the single bonds in the main chain are –80°. The green dotted lines represent hydrogen bonds between the carbamate groups at *i* th and (*i*+3) th monomer units. The polyacetylene backbone is colored in yellow.

Conclusions

In the present chapter, the author has demonstrated the synthesis and polymerization of novel optically active substituted acetylenes (*S*)-/(*R*)-**1**–(*S*)-**4** derived from α-propargylglycine and α-propargylalanine using a rhodium zwitterionic catalyst. Poly[(*S*)-**1**], poly[(*R*)-**1**] and poly[(*S*)-**4**] exhibited optical rotations 5–14 times larger than those of the corresponding monomers. These polymers showed intense CD signals at the absorption region of the conjugated polyacetylene backbone. Since the CD patterns and intensities were not affected by membrane filtration and sample concentration, the chiroptical properties are not explainable by the formation of chiral aggregates but

predominantly one-handed helical structures. As far as the author knows, this is the first example regarding the synthesis of α-propargyl amino acid derived helical polyacetylenes. Removal of the protecting groups from poly[(*S*)-**1**] and poly[(*S*)-**4**] provided poly[(*S*)-**1a**] and poly[(*S*)-**4b**] bearing unprotected carboxy and amino groups, respectively. The helical natures of poly[(*S*)-**1a**] and poly[(*S*)-**4b**] were largely different from those of the precursor polymers, presumably due to the participation of carboxy and amino groups into intramolecular hydrogen-bonding strands at the side chains, which play an important role for helix formation and stabilization. The presence of intramolecular hydrogen bonding is supported by the shifts of C=O and N–H IR absorption to lower and higher wavenumber regions from monomers to polymers. The different patterns of hydrogen bonding of poly[(*S*)-**1**] and poly[(*S*)-**1a**] is also suggested by IR spectroscopy. The helical structure of poly[(*S*)-**1a**] became extended upon addition of alkali hydroxides (LiOH, NaOH, KOH) and TBAF, and the degree of extension agreed with the order of the cation size, which were confirmed by the red λ_{max} shift of the CD and UV–vis peaks. A conceivable idea for explaining this phenomenon is the change of ionic and steric repulsion between the side chains. Namely, the repulsion becomes large due to the cations existing close to the carboxylate moieties, resulting in helix loosening accompanying the extension of conjugation of the polyacetylene backbone, and the order of the red shift agrees with that of cation size. Poly[(*S*)-**1a**] has potential as a cation sensor since the ion-responsive conformational transition is

reversible and causes the color change of the polymer solution detectable by the naked eye. Molecular mechanics calculation suggested that the most stable conformer of poly[(*S*)-**1**] was a left-handed helix stabilized by intramolecular hydrogen bonds between the carbamate groups, whose presence was confirmed by IR spectroscopy as mentioned. Further investigation on the mechanistic aspects of conformational change of poly[(*S*)-**1a**] upon addition of alkali metal and TBAF with considering solvent effect, and responsiveness of poly[(S)-**4b**] bearing unprotected amino groups to various acids are now under progress.

Experimental Sections

Measurements. ^{1}H (400 MHz) and ^{13}C (100 MHz) NMR spectra were recorded on a JEOL EX-400 or a JEOL AL-400 spectrometer. IR spectra were measured on a JASCO FT/IR-4100 spectrophotometer. Melting points (mp) were measured on a Yanaco micro melting point apparatus. Mass spectra were measured on a Thermo Scientific Exactive mass spectrometer. Specific rotations ($[\alpha]_D$) were measured on a JASCO DIP-1000 digital polarimeter. Number- and weight-average molecular weights (M_n and M_w) of polymers were determined by SEC (Shodex columns KF805 × 3) eluted with tetrahydrofuran (THF) calibrated by polystyrene standards at 40 °C. CD and UV–vis absorption spectra were recorded on a JASCO J-820 spectropolarimeter.

Materials. Unless stated otherwise, reagents and solvents were purchased and used without purification. (nbd)Rh^{+}[η^6-$C_6H_5B^{-}(C_6H_5)_3$] (nbd =

2,5-norbornadiene) was prepared according to the literature.[66] α-Propargyl amino acid derivatives [(*S*)-α-propargylglycine, (*R*)-α-propargylglycine, (*S*)-α-propargylalanine, (*S*)-*N*-Fmoc-α-propargylalanine (*ee* ≥ 99%)], and di-*tert*-butylcarbonate [$(Boc)_2O$] were gifted from Nagase & Co., LTD. and Tokuyama. $CHCl_3$, THF, and *N,N*-dimethylformamide (DMF) used for polymerization were distilled prior to use.

Monomer Synthesis. (*S*)-*N*-Boc-α-propargylglycine Methyl Ester [(*S*)-1]. $(Boc)_2O$ (3.72 g, 15.0 mmol) and K_2CO_3 (1.59 g, 15.0 mmol) were added to a solution of (*S*)-α-propargylglycine (1.13 g, 10.0 mmol) in 1,4-dioxane/H_2O (30 mL/50 mL) at 0 °C, and the resulting mixture was stirred at room temperature overnight. 1,4-Dioxane was evaporated off, and the residual solution was carefully acidified with 0.5 M HCl to pH = 3. The resulting solution was extracted with CH_2Cl_2. The organic layer was washed with water and saturated NaCl aq., dried over anhydrous $MgSO_4$, and then filtered. The filtrate was concentrated to obtain (*S*)-*N*-Boc-α-propargylglycine [(*S*)-**1a**] as a viscosity liquid. After that, 1-(3-dimethylaminopropyl)-3-ethylcarbodiimide hydrochloride (EDC•HCl, 2.30 g, 12.0 mmol), *N,N*-dimethyl-4-aminopyridine (DMAP, 0.140 g, 1.20 mmol), and MeOH (2.00 mL, 49.4 mmol) were added to a solution of (*S*)-**1a** in CH_2Cl_2 (40 mL) at 0 °C, and then the resulting mixture was stirred at room temperature overnight. It was washed with 1.0 M HCl, saturated $NaHCO_3$ aq., and saturated NaCl aq., dried over anhydrous $MgSO_4$, and then filtered. The filtrate was concentrated, and the residual mass was purified by

preparative HPLC to obtain (*S*)-**1** as a viscous liquid in 44%. $[\alpha]_D$ +23° (*c* = 0.14 g/dL, THF). IR (in $CHCl_3$): 3436, 3308, 2982, 1746, 1709, 1502, 1368, 1222, 1162, 1064, 655 cm^{-1}. ^1H NMR (400 MHz, $CDCl_3$): δ 1.45 [s, 9H, –C(C*H*$_3$)$_3$], 2.07 (t, *J* = 2.4 Hz, 1H, –C≡C*H*), 2.71–2.74 (m, 2H, –C*H*$_2$–), 3.78 (s, 3H, –OC*H*$_3$), 4.45–4.50 (m, 1H, –C*H*–), 5.45 (d, *J* = 8.4 Hz, 1H, –N*H*–). ^{13}C NMR (100 MHz, $CDCl_3$): δ 22.56 (–*C*H$_2$–), 28.06 [–C(*C*H$_3$)$_3$], 51.76 (–O*C*H$_3$), 52.38 (–*C*H–), 71.46 (–C≡*C*H), 78.38 (–*C*≡CH), 79.89 [–*C*(CH$_3$)$_3$], 154.89 (–NH*C*O–), 170.93 (–*C*OOCH$_3$). HRMS. (*m*/*z*): $[M + Na]^+$ calcd for $C_{11}H_{17}NO_4Na$, 250.1055; found, 250.1042.

(*R*)-*N*-Boc-α-propargylgylcine Methyl Ester [(*R*)-1]. The title compound was synthesized from (*R*)-α-propargylglycine in a manner similar to (*S*)-**1**. Yield 43% (viscous liquid). $[\alpha]_D$ –21° (*c* = 0.09 g/dL, THF). IR (in $CHCl_3$): 3436, 3308, 3019, 2981, 2123, 1747, 1709, 1503, 1368, 1215, 1162, 1064, 668 cm^{-1}. ^1H NMR (400 MHz, $CDCl_3$): δ 1.45 [s, 9H, –C(C*H*$_3$)$_3$], 2.07 (t, *J* = 2.8 Hz, 1H, –C≡C*H*), 2.71–2.74 (m, 2H, –C*H*$_2$–), 3.78 (s, 3H, –OC*H*$_3$), 4.44–4.50 (m, 1H, –C*H*–), 5.44 (d, *J* = 8.4 Hz, 1H, –N*H*–). ^{13}C NMR (100 MHz, $CDCl_3$): δ 22.56 (–*C*H$_2$–), 28.07 [–C(*C*H$_3$)$_3$], 51.78 (–O*C*H$_3$), 52.37 (–*C*H–), 71.45 (–C≡*C*H), 78.39 (–*C*≡CH), 79.89 [–*C*(CH$_3$)$_3$], 154.89 (–NH*C*O–), 170.92 (–*C*OOCH$_3$). HRMS. (*m*/*z*): $[M + Na]^+$ calcd for $C_{11}H_{17}NO_4Na$, 250.1055; found, 250.1050.

(*S*)-*N*-Boc-α-propargylalanine Methyl Ester [(*S*)-2]. The title compound was synthesized from (*S*)-α-propargylalanine in a manner similar to

(*S*)-**1.** Yield 38% (white solid). Mp 72–73 °C. $[\alpha]_D$ –63° (*c* = 0.10 g/dL, THF). IR (KBr): 3382, 3331, 3318, 2985, 2937, 2120, 1732, 1711, 1666, 1517, 1457, 1385, 1251, 1174, 1064, 624 cm^{-1}. ^1H NMR (400 MHz, $CDCl_3$): δ 1.43 [s, 9H, –C(C*H*$_3$)$_3$], 1.54 [s, 3H, –C*H*$_3$], 2.06 (t, *J* = 2.4 Hz, 1H, –C≡C*H*), 2.88–2.96 (m, 2H, –C*H*$_2$–), 3.76 (s, 3H, –OC*H*$_3$), 5.37 (br, 1H, –N*H*–). ^{13}C NMR (100 MHz, $CDCl_3$): δ 22.93 (–*C*H$_3$), 26.69 (–*C*H$_2$–), 28.04 [–C(*C*H$_3$)$_3$], 52.45 (–O*C*H$_3$), 57.97 (–*C*H–), 71.08 (–C≡*C*H), 79.20 [–*C*(CH$_3$)$_3$], 79.66 (–*C*≡CH), 154.16 (–NH*C*O–), 173.41 (–*C*OOCH$_3$). HRMS. (*m*/*z*): $[M + H]^+$ calcd for $C_{12}H_{20}NO_4$, 242.1392; found, 242.1386.

(*S*)-*N*-Fmoc-α-propargylglycine Methyl Ester [(*S*)-3]. A solution of *N*-Fmoc-succinimide (1.01 g, 3.00 mmol) in 1,2-dimethoxyethane (DME) (10 mL) was added to a solution of (*S*)-α-propargylglycine (0.226 g, 2.00 mmol) in 10 wt% Na_2CO_3 aq. (10 mL) at 0 °C, and the resulting mixture was stirred at room temperature overnight. Precipitates formed were filtered off, and then DME was removed from the filtrate by evaporation. The residual solution was carefully acidified by 0.1 M HCl to adjust the pH neutral, and then extracted with EtOAc. The organic phase was washed with 0.1 M HCl, and saturated NaCl aq., dried over anhydrous $MgSO_4$, and then filtered. The filtrate was concentrated to obtain (*S*)-*N*-Fmoc-α-propargylglycine [(*S*)-**3a**]. After that, (*S*)-**3** was synthesized from (*S*)-**3a** and MeOH in a manner similar to (*S*)-**1**, and purified by silica gel column chromatography eluted with hexane/$CHCl_3$ = 1/1 (v/v). Yield 32% (white solid). Mp 136–137 °C. $[\alpha]_D$ –9° (*c* = 0.08 g/dL, THF). IR

(KBr): 3320, 3273, 3065, 3020, 2951, 2116, 1734, 1691, 1543, 1450, 1296, 1014, 746 cm^{-1}. ^1H NMR (400 MHz, $CDCl_3$): δ 2.05 (s, 1H, –C≡C*H*), 2.75–2.78 (m, 2H, –CH_2–), 3.75 (s, 3H, –OCH_3), 4.21 (t, *J* = 6.8 Hz, 1H, >C*H*–), 4.38 (d, *J* = 7.2 Hz, 2H, –CH_2O–), 4.53–4.55 (m, 1H, –C*H*–), 5.74 (d, *J* = 6.8 Hz, 1H, –N*H*–), 7.28 (t, *J* = 7.6 Hz, 2H, Ar), 7.37 (t, *J* = 7.6 Hz, 2H, Ar), 7.59 (d, *J* = 6.8 Hz, 2H, Ar), 7.73 (d, *J* = 7.6 Hz, 2H, Ar). ^{13}C NMR (100 MHz, $CDCl_3$): δ 22.56 (–*C*H_2–), 46.93 (>*C*H–), 52.23 (–O*C*H_3), 52.26 (–*C*H–), 67.08 (–*C*H_2O–), 71.74 (–C≡*C*H), 78.21 (–*C*≡CH), 119.86, 124.97, 126.93, 127.59, 141.13, 143.57 (Ar), 155.50 (–NH*C*O–), 170.64 (–*C*OOCH_3). HRMS. (*m*/*z*): $[M + Na]^+$ calcd for $C_{21}H_{19}NO_4Na$, 372.1212; found, 372.1207.

(*S*)-*N*-Fmoc-α-propargylalanine Methyl Ester [(*S*)-4]. The title compound was synthesized from (*S*)-*N*-Fmoc-α-propargylalanine containing 27% of methyl *tert*-butyl ether and MeOH in a manner similar to (*S*)-**1**, and purified by silica gel column chromatography eluted with hexane/$CHCl_3$ = 1/1 (v/v). Yield 53% (white solid). Mp 54–56 °C. $[\alpha]_D$ –45° (*c* = 0.09 g/dL, THF). IR (KBr): 3357, 3292, 3065, 3040, 2951, 2120, 1719, 1524, 1509, 1450, 1276, 1231, 1118, 1077, 974, 739 cm^{-1}. ^1H NMR (400 MHz, $CDCl_3$): δ 1.57 (s, 3H, –CH_3), 2.01 (s, 1H, –C≡C*H*), 2.89–3.05 (m, 2H, –CH_2–), 3.73 (s, 3H, –OCH_3), 4.20 (t, *J* = 6.8 Hz, 1H, >C*H*–), 4.38 (br, 2H, –CH_2O–), 5.76 (br, 1H, –N*H*–), 7.27 (t, *J* = 7.6 Hz, 2H, Ar), 7.35 (t, *J* = 7.2 Hz, 2H, Ar), 7.57 (d, *J* = 7.2 Hz, 2H, Ar), 7.71 (d, *J* = 7.6 Hz, 2H, Ar). ^{13}C NMR (100 MHz, $CDCl_3$): δ 23.03 (–*C*H_3), 26.73 (–*C*H_2–), 47.02 (>*C*H–), 52.78 (–O*C*H_3), 58.52 (–*C*H–),

66.57 (–*C*H_2O–), 71.25 (–C≡*C*H), 79.08 (–*C*≡CH), 119.74, 124.85, 126.81, 127.44, 141.04, 143.56 (Ar), 154.46 (–NH*C*O–), 172.96 (–*C*$OOCH_3$). HRMS. (*m*/*z*): $[M + H]^+$ calcd for $C_{22}H_{22}NO_4$, 364.1549; found, 364.1532.

Polymerization. All the polymerizations were carried out in a glass tube equipped with a three-way stopcock under nitrogen. A typical experimental procedure for polymerization is given below.

A solution of (nbd)$Rh^+[\eta^6$-$C_6H_5B^-(C_6H_5)_3]$ (5.1 mg, 10 μmol) in $CHCl_3$ (2.5 mL) was added to a solution of a monomer (1.0 mmol) in $CHCl_3$ (2.5 mL) under dry nitrogen, and the resulting solution was kept at 30 °C for 24 h. The reaction mixture was poured into a large amount of hexane to precipitate a polymer. It was separated by filtration using a membrane filter (ADVANTEC H100A047A) and dried under reduced pressure.

Alkaline Hydrolysis of Ester Groups of Poly[(*S*)-1]. Aqueous NaOH (1.00 M, 1.00 mL) was added to a solution of poly[(*S*)-**1**] (0.113 g, 0.500 unit mmol) in THF/MeOH/H_2O (5 mL/5 mL/10 mL) at room temperature, and then the resulting mixture was stirred at 60 °C for 8 h. THF and MeOH were evaporated from the mixture, and the residual solution was carefully acidified by citric acid, and then extracted with EtOAc. The organic phase was washed with saturated NaCl aq., and then dried over anhydrous $MgSO_4$. EtOAc was evaporated off to obtain poly[(*S*)-**1a**] as a yellow solid in 76%.

Removal of Fmoc Groups from Poly[(*S*)-4]. Piperidine (2.00 mL) was added to a solution of poly[(*S*)-**4**] (0.108 g, 0.300 unit mmol) in $CHCl_3$ (10.0

mL). The resulting mixture was stirred at room temperature for 8 h, and then poured into hexane to precipitate the produced polymer. It was collected by filtration using a membrane filter (ADVANTECH H100A047A) and dried under reduced pressure to obtain poly[(*S*)-**4b**] as a yellow solid in 83 %.

Spectroscopic Data of the Polymers. **Poly[(*S*)-1]**: IR (KBr): 3368, 2978, 2933, 1747, 1717, 1509, 1367, 1166, 1057, 1024, 860, 781 cm^{-1}. ^1H NMR (400 MHz, $CDCl_3$): δ 1.42 [br, 9H, $(CH_3)_3C$–], 2.71 (br, 2H, –CH_2–), 3.70 (br, 3H, –OCH_3), 4.30 (br, 1H, –C*H*–), 5.50–6.64 (br, 2H, –C=C*H*–, –N*H*–). **Poly[(*R*)-1]**: IR (KBr): 3368, 2978, 2933, 1746, 1718, 1509, 1366, 1167, 1057, 1024, 856, 781 cm^{-1}. ^1H NMR (400 MHz, $CDCl_3$): δ 1.42 [br, 9H, $(CH_3)_3C$–], 2.82 (br, 2H, –CH_2–), 3.70 (br, 3H, –OCH_3), 4.33 (br, 1H, –C*H*–), 5.60–6.42 (br, 2H, –C=C*H*–, –N*H*–). **Poly[(*S*)-1a]**: IR (KBr): 3412, 2980, 2935, 2623, 1704, 1509, 1395, 1369, 1251, 1163, 855 cm^{-1}. ^1H NMR (400 MHz, CD_3OD): δ 1.45 [br, 9H, $(CH_3)_3C$–], 2.68 (br, 2H, –CH_2–), 4.23 (br, 1H, –C*H*–), 6.02–6.48 (br, *2*H, –C=C*H*–, –N*H*–). **Poly[(*S*)-4]**: IR (KBr): 3407, 3017, 2949, 1721, 1500, 1450, 1233, 1107, 1075, 739 cm^{-1}. ^1H NMR (400 MHz, $CDCl_3$): δ 1.46 (br, 3H, –CH_3), 2.26 (br, 2H, –CH_2–), 3.56 (br, 3H, –OCH_3), 4.01–4.38 (br, 3H, >C*H*–, –CH_2O–), 5.71–5.91 (br, 1H, –N*H*–), 6.29 (br, 1H, –C=C*H*–), 7.12–7.72 (br, 8H, Ar). **Poly[(*S*)-4b]**: IR (in $CHCl_3$): 3438, 3308, 1747, 1714, 1610, 1508, 1424, 1046, 928 cm^{-1}. ^1H NMR (400 MHz, $CDCl_3$): δ 1.66 [br, 3H, CH_3–], 2.32 (br, 2H, –CH_2–), 3.75 (br, 3H, –OCH_3), 6.11 (br, 1H, –C=C*H*–).

References and Notes

(1) For a review, see: Nakano, T.; Okamoto, Y. *Chem. Rev.* **2001**, *101*, 4013–4038.

(2) For a review, see: Amabilino, D. B.; Serrano, J.; Sierra, T.; Veciana, J. *J. Polym. Sci., Part A: Polym. Chem.* **2006**, *44*, 3161–3174.

(3) For a review, see: Sato, T.; Terao, K.; Teramoto, A.; Fujiki, M. *Polymer* **2003**, *44*, 5477–5495.

(4) For a review, see: Hill, D. J.; Mio, M. J.; Prince, R. B.; Hughes, T. S.; Moore, J. S. *Chem. Rev.* **2001**, *101*, 4013–4018.

(5) For a review, see: Masuda, T. *J. Polym. Sci., Part A: Polym. Chem.* **2007**, *45*, 165–180.

(6) Natta, G.; Pino, P.; Corradini, P.; Danusso, F.; Manititca, E.; Nazzanti, G.; Moraglio, G. *J. Am. Chem. Soc.* **1955**, *77*, 1708–1710.

(7) Tabata, M.; Yang, W.; Yokota, K. *Polym. J.* **1990**, *22*, 1105–1107.

(8) Kishimoto, Y.; Eckerle, P.; Miyatake, T.; Kainosho, M.; Ono, A.; Ikariya, T.; Noyori, R. *J. Am. Chem. Soc.* **1999**, *121*, 12035–12044.

(9) Ke, Z.; Abe, S.; Ueno, T.; Morokuma, K. *J. Am. Chem. Soc.* **2011**, *133*, 7926–7941.

(10) Nomura, R.; Tabei, J.; Masuda, T. *J. Am. Chem. Soc.* **2001**, *123*, 8430–8431.

(11) Tabei, J.; Nomura, R.; Masuda, T. *Macromolecules* **2002**, *35*, 5405–5409.

(12) Tabei, J.; Nomura, R.; Masuda, T. *Macromolecules* **2003**, *36*, 573–577.

(13) Nomura, R.; Nishiura, S.; Tabei, J.; Sanda, F.; Masuda, T. *Macromolecules* **2003**, *36*, 5076–5080.

(14) Sanda, F.; Nishiura, S.; Shiotsuki, M.; Masuda, T. *Macromolecules* **2005**, *38*, 3705–3078.

(15) Tabei, J.; Shiotsuki, M.; Sanda, F.; Masuda, T. *Macromolecules* **2005**, *38*, 5860–5867.

(16) Suzuki, Y.; Tabei, J.; Shiotsuki, M.; Inai, Y.; Sanda, F.; Masuda, T. *Macromolecules* **2008**, *41*, 1086–1093.

(17) Shirakawa, Y.; Suzuki, Y.; Terada, K.; Shiotsuki, M.; Masuda, T. *Macromolecules* **2010**, *43*, 5575–5581.

(18) Sanda, F.; Araki, H.; Masuda, T. *Macromolecules* **2004**, *37*, 8510–8516.

(19) Zhao, H.; Sanda, F.; Masuda, T. *Macromolecules* **2004**, *37*, 8888–8892.
(20) Gao, G.; Sanda, F.; Masuda, T. *Macromolecules* **2003**, *36*, 3932–3937.
(21) Zhao, H.; Sanda, F.; Masuda, T. *Macromolecules* **2004**, *37*, 8893–8896.
(22) Sanda, F.; Araki, H.; Masuda, T. *Macromolecules* **2005**, *38*, 10605–10608.
(23) Cheuk, K. K. L.; Li, B. S.; Lam, J. W. Y.; Xie, Y.; Tang, B. Z. *Macromolecules* **2008**, *41*, 5997–6005.
(24) Maeda, K.; Kamiya, N.; Yashima, E. *Chem. Eur. J.* **2004**, *10*, 4000–4010.
(25) Sanda, F.; Terada, K.; Masuda, T. *Macromolecules* **2005**, *38*, 8419–8154.
(26) Liu, R.; Sanda, F.; Masuda, T. *Polymer* **2007**, *48*, 6510–6518.
(27) Chan, K. H.; Lam, J. W.; Wong, K. M.; Tang, B. Z.; Yam, V. W. *Chem. Eur. J.* **2009**, *15*, 2328–2334.
(28) Zheng, Y.; Cui, J.; Zheng, J.; Wan, X. *J. Mater. Chem.* **2010**, *20*, 5915–5922.
(29) Sanda, F.; Teraura, T.; Masuda, T. *J. Polym. Sci., Part A: Polym. Chem.* **2004**, *42*, 4641–4647.
(30) Zhao, H.; Sanda, F.; Masuda, T. *Polymer* **2006**, *47*, 2596–2602.
(31) Kakuchi, R.; Nagata, S.; Tago, Y.; Sakai, R.; Otsuka, I.; Satoh, T.; Kakuchi, T. *Macromolecules* **2009**, *42*, 1476–1481.
(32) Kakuchi, R.; Tago, Y.; Sakai, R.; Satoh, T.; Kakuchi, T. *Macromolecules* **2009**, *42*, 4430–4435.
(33) Louzao, I.; Seco, J. M.; Quiñoá, E.; Riguera, R. *Angew. Chem. Int. Ed.* **2010**, *49*, 1430–1433.
(34) Sakai, R.; Sakai, N.; Satoh, T.; Li, W.; Zhang, A.; Kakuchi, T. *Macromolecules* **2011**, *44*, 4249–4257.
(35) Liu, R.; Sanda, F.; Masuda, T. *J. Polym. Sci., Part A: Polym. Chem.* **2008**, *46*, 4175–4182.
(36) Sanda, F.; Araki, H.; Masuda, T. *Chem. Lett.* **2005**, *34*, 1642–1643.
(37) Maeda, K.; Tanaka, K.; Morino, K.; Yashima, E. *Macromolecules* **2007**, *40*, 6783–6785.
(38) Terada, K.; Masuda, T.; Sanda, F. *J. Polym. Sci., Part A: Polym. Chem.* **2009**, *47*, 4971–4981.
(39) Ikeda, A.; Terada, K.; Shiotsuki, M.; Sanda, F. *J. Polym. Sci., Part A: Polym. Chem.* **2011**, *49*, 3783–3796.

(40) Sanda, F.; Gao, G.; Masuda, T. *Macromol. Biosci.* **2004**, *4*, 570–574.
(41) Terada, K.; Masuda, T.; Sanda, F. *Macromolecules* **2009**, *42*, 913–920.
(42) Ohsawa, S.; Sakurai, S.; Nagai, K.; Banno, M.; Maeda, K.; Kumaki, J.; Yashima, E. *J. Am. Chem. Soc.* **2011**, *133*, 108–114.
(43) For a review, see: Maruoka, K. *Bull. Chem. Soc. Jpn.* **2009**, *82*, 917–930.
(44) Walensky, L. D.; Kung, A. L.; Escher, I.; Malia, T. J.; Wright, R. D.; Wagnew, G.: Verdine, G. L.; Korsmeyer, S. J. *Science* **2004**, *305*, 1466–1470.
(45) In the case of poly[(*S*)-**4**], fluorine-derived absorption peaks exist at 250–300 nm, shorter than the wavelength region of polyacetylene backbone.
(46) It has been reported that membrane filtration of solutions of conjugated polymers is effective to remove aggregates. See Yamamoto, T.; Komarudin, D.; Arai, M.; Lee, B.-L.; Suganuma, H.; Asakawa, N.; Inoue, Y.; Kubota, K.; Sasaki, S.; Fukuda, T.; Matsuda, H. *J. Am. Chem. Soc.* **1998**, *120*, 2047–2058.
(47) Yue, S.; Berry, G. C.; McCullough, R. D. *Macromolecules* **1996**, *29,* 933–939.
(48) Langeveld-Voss, B. M. W.; Peeters, E.; Janssen, R. A. J.; Meijer, E. W. *Synth. Met.* **1997**, *84*, 611–614.
(49) Peeters, E.; Janssen, R. A. J.; Meijer, E. W. *Synth. Met.* **1999**, *102*, 1105–1106.
(50) Poly[(*S*)-**1**] and poly[(*R*)-**1**] were insoluble in MeOH and DMF.
(51) Suzuki, Y.; Shiotsuki, M.; Sanda, F.; Masuda, T. *Macromolecules* **2007**, *40*, 1864–1867.
(52) Suzuki, Y.; Shiotsuki, M.; Sanda, F.; Masuda, T. *Chem. Asian J.* **2008**, *3*, 2075–2081.
(53) Percec, V.; Obata, M.; Rudick, J. G.; De, B. B.; Glodde, M.; Bera, T. K.; Magonov, S. N.; Balagurusamy, V. S. K.; Heiney, P. A. *J. Polym. Sci., Part A: Polym. Chem.* **2002,** *40,* 3509-3533.
(54) Fujiki, M. *Macromol. Rapid Commun.* **2001**, *22*, 539–563.
(55) The also tried to obtain poly[(*S*)-**1a**] by the polymerization of (*S*)-**1a** bearing unprotected carboxy groups, but failed under the conditions in Table 1, presumably due to the deactivation of the rhodium catalyst by the carboxy

groups. See Saito, M. A.; Maeda, K.; Onouchi, H.; Yashima, E. *Macromolecules* **2000**, *33*, 4616.

(56) The carboxy groups were transformed into methyl ester groups using trimethylsilyldiazomethane, because poly[(*S*)-**1a**] was not eluted out.

(57) This concentration is low enough to eliminate the effect of intermolecular hydrogen bonding.

(58) RbOH was hardly soluble in THF/MeOH = 1/1. CsOH (4 equiv) shifted the λ_{max} but induced no clear CD signal unlike the others.

(59) Ionic radius (Å): Li^+ 0.9, Na^+ 1.2, K^+ 1.5. See Shannon, R. D. *Acta Cryst.* **1976**, *A32*, 751–767.

(60) Addition of tetrabutylammonium hydroxide was also examined but the trends of CD and UV-vis spectra were different from those with alkali metal hydroxides.

(61) The ionic radius of Bu_4N^+ = 4.8 Å. See Watanabe, Y.; Ohnaka, K.; Fujita, S.; Kishi, M.; Yuchi, A. *Anal. Chem.* **2011**, *83*, 7480–7485.

(62) Mo, H.; Pochapsky, T. C. *J. Phys. Chem. B* **1997**, *101*, 4485–4486.

(63) No red-shift of λ_{max} was observed upon TBAF addition in THF/MeOH = 1/1 and THF/H_2O= 1/1. The ionic interaction between unprotected carboxy groups and TBAF does not seem preferable in highly polar solvents, presumably due to the presence of hydrophobic alkyl groups.

(64) Halgren, T. A. *J. Comput. Chem.* **1996**, *17,* 490–519. The molecular mechanics calculation was carried out with Wavefunction Inc., Spartan ’10 Macintosh.

(65) Calculated by Winmostar Ver. 3.8. http://winmostar.com/; Senda, N. *Idemitsu Tech. Rep.* **2006**, *49*, 106–111.

(66) Schrock, R. R.; Osborn, J. A. *Inorg. Chem.* **1970**, *9*, 2339–2343.

List of Publications

Chapter 1

"Synthesis of Optically Active Poly(*m*-phenyleneethynylene-aryleneethynylene)s Bearing Hydroxy Groups and Examination of the Higher Order Structures"
Sogawa, H.; Shiotuki, M.; Sanda, F.
under preparation

Chapter 2

"Synthesis of Optically Active Poly(*m*-phenyleneethynylene-aryleneethynylene)s Bearing Hydroxy Groups with Various Conjugation Lengths and Examination of the Higher Order Structure"
Sogawa, H.; Shiotuki, M.; Sanda, F.
under preparation

Chapter 3

"Stabilization of Higher-Order Structure of Poly(phenyleneethynylene)s by Metathesis Polymerization at the Side Chains"
Hashimoto, A.; Sogawa, H.; Shiotuki, M.; Sanda, F.
Polymer **2012**, *53*, 2559–2556.

Chapter 4

"Synthesis, Chiroptical Properties, and Photo-responsiveness of Optically Active Poly(*m*-phenyleneethynylene)s Containing Azobenzene Moieties"
Sogawa, H.; Shiotsuki, M.; Matsuoka, H.; Sanda, F.
Macromolecules **2011**, *44*, 3338–3345.

Chapter 5

"Synthesis and Photo-responsive Chiroptical Properties of Optically Active Poly(phenyleneethynylene)s Bearing Azobenzene Moieties at the Main Chains"
Sogawa, H.; Shiotsuki, M.; Sanda, F.
under Preparation

Chapter 6

"α-Propargyl Amino Acid-derived Optically Active Novel Substituted Polyacetylenes: Synthesis, Secondary Structures, and Responsiveness to Ions"
Sogawa, H.; Shiotsuki, M.; Sanda, F.
J. Polym. Sci., Part A: Polym. Chem. **2012**, *50*, 2008–2018.

Other Publications Not Included in This Thesis

"Synthesis and Properties of Amino Acid-derived Optically Active Photo-responsive Polymers"
Sogawa, H.; Terada, K.; Masuda, T.; Sanda, F.
Polym. Bull. **2009**, *63*, 803–813.

"Tyrosine-based Poly(*m*-phenyleneethynylene-*p*-phenyleneethynylene)s. Helix Folding and Responsiveness to a Base"
Liu, R.; Sogawa, H.; Shiotsuki, M.; Masuda, T.; Sanda, F.
Polymer **2010**, *51*, 2255–2263.

"Synthesis and Properties of Conjugated Polymers Containing 3,9-Carbazolylene and Silylenevinylene Moieties in the Main Chain"
Sasano, T.; Sogawa, H.; Tamura, K.; Shiotsuki, M.; Masuda, T.; Sanda, F.
J. Polym. Sci., Part A: Polym. Chem. **2010**, *48*, 1815–1821.

Acknowledgments

This thesis presents the studies that the author carried out at the Department of Polymer Chemistry, Kyoto University, during the years from 2008 to 2013 under the supervision of Professor Fumio Sanda.

The author would like to express his sincerest gratitude to Professor Fumio Sanda for his continuous guidance, valuable suggestions, and encouragement throughout the present thesis. The author is also grateful to Professor Yoshiki Chujo and Professor Hirokazu Hasegawa for their helpful suggestions.

The author would like to thank Professor Hideki Matsuoka for his collaboration and helpful suggestions in the present works.

The author wishes to express his gratitude to Professor Toshio Masuda and Professor Masashi Shiotsuki for their helpful advice and discussion during this research. Sincere thanks are due to all colleagues in the Sanda Laboratory for their discussion, and particularly, to Mr. Akinori Hashimoto for his collaborations in this thesis, and Dr. Kayo Terada for her fruitful advice and discussion for this research.

The author is grateful to the Research Fellowship of the Japan Society for the Promotion of Science for Young Scientists.

Finally, the author would like to give his greatest thanks to his family, especially his parents, Mr. Atsushi Sogawa and Mrs. Michiyo Sogawa for their constant assistance and kind-hearted encouragement.

Hiromitsu Sogawa

January 2013